



LOUISIANA
POWER & LIGHT

142 DELARONDE STREET
P. O. BOX 6008 • NEW ORLEANS, LOUISIANA 70174 • (504) 386-2345

October 10, 1985

W3P85-3218
A4.05
QA

Robert D. Martin
Regional Administrator, Region IV
U.S. Nuclear Regulatory Commission
611 Ryan Plaza Drive, Suite 1000
Arlington, TX 76011

Dear Mr. Martin:

Subject: Waterford 3 SES
Docket No. 50-382
License No. NPF-38
STARTUP REPORT

Enclosed are two copies of the Waterford 3 Startup Report which provides the results of the recently completed startup test program conducted under the subject license. This report is submitted pursuant to Section 6.9.1.1 in the Waterford 3 Technical Specifications (NUREG-1117) of Appendix A to Facility Operating License No. NPF-38.

Very truly yours,

K.W. Cook
Nuclear Support & Licensing Manager

KWC:GEW:sms

Enclosure

cc (w/enclosure): NRC Director, Office of I&E (Document Control Desk) (6)
NRC Resident Inspectors Office

cc (w/o enclosure): G.W. Knighton, NRC-NRR
J.H. Wilson, NRC-NRR
B.W. Churchill
W.M. Stevenson

*IE26
1/6*

8510170010 851010
PDR ADOCK 05000382
P PDR

LOUISIANA POWER & LIGHT COMPANY

WATERFORD STEAM ELECTRIC STATION UNIT 3

STARTUP REPORT

TO THE

UNITED STATES

NUCLEAR REGULATORY COMMISSION

LICENSE NUMBER NPF-38

DOCKET NUMBER 50-382

October 10, 1985

APPROVAL FOR ISSUE

The Waterford Steam Electric Station Unit 3 Startup Report has been approved for issue by the members of the Plant Operations Review Committee (PORC) and the Plant Manager-Nuclear.

<u>PORC MEMBER</u>	<u>SIGNATURE</u>	<u>DATE</u>
Maintenance Superintendent	<u>V. Smith</u>	<u>10/10/85</u>
Operations Superintendent	<u>W. Smith</u>	<u>10-10-85</u>
Radiation Protection Superintendent	<u>Ronald H. Egan</u>	<u>10/10/85</u>
Plant Quality Manager	<u>J. Woods</u>	<u>10/10/85</u>
Technical Support Superintendent	<u>J. Santoro</u>	<u>10/10/85</u>
Assistant Plant Manager	<u>M. S. Carr</u>	<u>10/10/85</u>
PORC Chairman	<u>A. Allen</u>	<u>10-10-85</u>
PLANT MANAGER-NUCLEAR	<u>R. Barkhurst</u>	<u>10/10/85</u>

ACKNOWLEDGEMENTS

The Phase III Test Program was conducted and contributions were made to this Startup Report by the following individuals. Louisiana Power & Light Company appreciates the professional manner in which the test program was conducted and hereby expresses its gratitude to the contributing members of the program.

Tom Andrews	Hamid Mahdavy
Dennis Barr	Steve Matlock
Russ Brian	John McCauley
Marcia Brisson	Glenn McCloskey
Howard Brodt	Matt Melancon
Roger Carr	George Miller
Mark Constable	Jack Mosely
Charles DeDeaux	Jerry Moyers
Tom Earle	Chuck Mitchell
Jim Edwards	Rudy Poulos
Dave Evans	Bob Ryan
Ed Fiegler	Dave Shannon
Tom Firestone	Rob Starkey
Steve Johnson	Rick Thomas
Roger Ju	Bernie vonKutzleben
William Karras	Carl Whitaker
Mark Konya	Reid Wolf
John Lewis	

TABLE OF CONTENTS

	<u>PAGE</u>
1.0 <u>INTRODUCTION AND SUMMARY</u>	17
1.1 INTRODUCTION	18
1.1.1 The Startup Report	18
1.1.2 The Facility	18
1.1.3 The Test Program	29
1.2 SUMMARY	50
1.2.1 Initial Fuel Load	50
1.2.2 Post Core Hot Functional Testing	50
1.2.3 Initial Criticality	51
1.2.4 Low Power Physics Testing	51
1.2.5 Power Ascension Testing Through 20% Power	51
1.2.6 Power Ascension Testing From 20% Through 50% Power	52
1.2.7 Power Ascension Testing From 50% Through 80% Power	53
1.2.8 Power Ascension Testing From 80% Through 100% Power	53
2.0 <u>INITIAL FUEL LOADING</u>	55
2.1 Preparations	56
2.2 Reactivity Monitoring	60
2.3 The Fuel Loading Sequence	63
2.4 Fuel Movement	65
2.5 Fuel Load Verification	67
2.6 Delays, Problems and Resolutions	71

TABLE OF CONTENTS
(continued)

	<u>PAGE</u>
3.0 <u>POST-CORE HOT FUNCTIONAL TESTING</u>	74
3.1 INSTRUMENTATION TESTING/CALIBRATION	75
3.1.1 Intercomparison of Plant Protection System (PPS), Core Protection Calculator (CPC), and Plant Monitoring Computer (PMC) Inputs	75
3.1.2 Incore Instrumentation Baseline Data	79
3.1.3 Moveable Incore Instrumentation Operation Verification	81
3.1.4 Post Core Vibration and Loose Parts Monitoring System	85
3.2 REACTOR COOLANT SYSTEM TESTING	87
3.2.1 Reactor Coolant System Flow and Flow Coastdown Measurement	87
3.2.2 Reactor Coolant System Leak Rate Measurement	118
3.2.3 Reactor Coolant System Heat Loss	121
3.2.4 Reactor Coolant System Expansion Measurement	125
3.2.5 Control Element Drive Mechanism (CEDM) and Control Element Assembly (CEA) Tests (CEDM Performance)	133
3.2.6 Pressurizer Spray Valve and Control Adjustment	140
3.3 OTHER TESTING	145
3.3.1 Post-Core Test Data Record	145
3.3.2 Heated Junction Thermocouple Operation Verification	147
3.3.3 RCS and Steam Generator Parameters	150
3.3.4 Determination of Auxiliary Spray Flow Split	152
3.3.5 Post-Core Thermal Expansion Testing	154
 4.0 <u>INITIAL CRITICALITY</u>	
4.1 CEA Withdrawal	158
4.2 RCS Dilution	159

TABLE OF CONTENTS
(continued)

	<u>PAGE</u>
5.0 <u>LOW POWER PHYSICS TESTING</u>	169
5.1 CEA Symmetry Checks	171
5.2 Shutdown CEA and Regulating CEA Worth Measurements	174
5.3 Isothermal Temperature Coefficient	174
5.4 Critical Boron Concentration Measurement	179
5.5 Boron Worth Measurements	180
6.0 <u>POWER ASCENSION TESTING</u>	182
6.1 POWER LEVEL DETERMINATION	183
6.1.1 RCS ΔT Power Determination	183
6.1.2 NSSS Calorimetric	185
6.2 INSTRUMENTATION TESTING/CALIBRATION	191
6.2.1 Nuclear and Thermal Power Calibration	191
6.2.2 Process Variable Intercomparison	195
6.2.3 Linear Power Subchannel Calibration	203
6.2.4 Vibration and Loose Parts Monitoring System	209
6.2.5 Control Systems Checkout	212
6.2.6 Incore Detector Signal Verification	218
6.3 CPC/COLSS TESTING	224
6.3.1 COLSS Power/Flow Verification Data Record	224
6.3.2 Adjustment of COLSS Secondary Pressure Loss Terms	229
6.3.3 CPC/COLSS Verification	241
6.3.4 Radial Peaking Factor and CEA Shadowing Factor Verification	247
6.3.5 Temperature Decalibration Verification	254
6.3.6 Shape Annealing Matrix Measurement	263

	<u>PAGE</u>
6.4 PHYSICS TESTING	289
6.4.1 Core Performance Record	289
6.4.2 Variable Tavg	310
6.5 REACTOR COOLANT SYSTEM TESTING	318
6.5.1 RCS Calorimetric Flow Measurement	318
6.5.2 Natural Circulation Demonstration Testing	329
6.6 TRANSIENT TESTING	337
6.6.1 Remote Reactor Trip With Subsequent Remote Cooldown	337
6.6.2 Load Changes	348
6.6.3 Loss of Offsite Power Trip	350
6.6.4 80% Total Loss of Flow Test/Natural Circulation	356
6.6.5 100% Turbine Trip	373
6.7 PLANT TESTING	381
6.7.1 NSSS Plant Data Record	381
6.7.2 Transient Data Record	383
6.7.3 Biological Shield Effectiveness Survey	385
6.7.4 Power Ascension Testing Ventilation Capability	388
6.7.5 Atmospheric Steam Dump and Turbine Bypass Valve Capacity Checks	392
6.7.6 Initial Turbine Startup	401
6.7.7 BOP Data Record	405
6.7.8 Level 2 Piping Vibration Testing	407
6.7.9 Pipe Whip Restraint Monitoring	409
6.7.10 Inspection of Mechanical Snubbers and Spring Supports	411
7.0 APPENDIX A - List of Acronyms	414

LIST OF TABLES

	<u>PAGE</u>
1.1 Design Parameters of Waterford 3 SES	26
1.2 List of Startup Test Procedures and FSAR Chapter 14 Test Commitments Filled	32
1.3 Power Ascension Milestones	34
1.4 Post-Core Hot Functional Test Plateaus and Tests Performed at Each Plateau	35
1.5 Power Ascension Test Plateaus and Tests Performed at Each Plateau	36
2.2.1 Detector Count Rates (Uncorrected for Background)	62
3.2.1.1 4-RCP Steady State PCHFT RCS Flow Rate Measurement Test Results	94
3.2.1.2 As-Left PCHFT CPC Flow Constants	95
3.2.1.3 As-Left PCHFT COLSS Flow Constants	95
3.2.2.1 RCS Leak Rate Test Results (Gallons per Minute)	120
3.2.3.1 Final RCS Heat Loss Test Results	123
3.2.5.1 CEA Drop Times to 90% Inserted	136
3.2.5.2 Average Drop Times to 90% Inserted of Three Drops of CEAs Outside 2σ	138
3.3.3.1 RCS and Steam Generator Parameters	151
4.1 1/M Summary for the Approach to Initial Criticality	162
4.2 Verification of Startup and Log Power Channel Overlap	164
5.0.1 Waterford 3 SES LPPT Results	181
6.1.1.1 RCS Delta-T Power Determination Test Results	184
6.1.2.1 NSSS Calorimetric Results	189
6.2.1.1 Nuclear and Thermal Power Calibration	194
6.2.3.1 As-Left Signals and Signal Fractions at 20%	206
6.2.3.2 As-Left Signals and Signal Fractions at 50%	207
6.3.1.1 Calibrated Turbine First Stage Pressure (BTFSP) and Secondary Calorimetric Power (BSCAL) for all Power Plateaus	226
6.3.2.1 Adjustment of COLSS Secondary Pressure Loss Terms, 20% Power Test Results	232

LIST OF TABLES

(continued)

	<u>PAGE</u>
6.3.2.2 Adjustment of COLSS Secondary Pressure Loss Terms, 50% Power Test Results	232
6.3.2.3 Adjustment of COLSS Secondary Pressure Loss Terms, 80% Power Test Results	232
6.3.2.4 Adjustment of COLSS Secondary Pressure Loss Terms, 100% Power Test Results	233
6.3.2.5 Adjustment of COLSS Secondary Pressure Loss Terms, Installed COLSS Constant Values	234
6.3.2.6 Verification of Installed COLSS Secondary Pressure Loss Constants' Adequacy	235
6.3.3.1 CPC/CEDIPS Comparisons	244
6.3.4.1 CPC Planar Radial Peaking Factors	252
6.3.4.2 COLSS Planar Radial Peaking Factors	253
6.3.4.3 CEA Shadowing Correction Factors	253
6.3.5.1 Summary of Temperature Decalibration Verification Test Results	256
6.3.6.1 Comparison of Measured and Design SAM and BPPCC Values	271
6.4.1.1 20% Peaking Factors	296
6.4.1.2 50% Peaking Factors	297
6.4.1.3 80% Peaking Factors	297
6.4.1.4 100% Peaking Factors	297
6.4.2.1 50% Variable Tav _g Test Results	317
6.4.2.2 95% Variable Tav _g Test Results	317
6.5.1.1 20% Plateau Results, RCS Calorimetric Flow	323
6.5.1.2 50% Plateau Results, RCS Calorimetric Flow	324
6.5.1.3 80% Plateau Results, RCS Calorimetric Flow	325
6.5.1.4 100% Plateau (First Run) Results, RCS Calorimetric Flow	326
6.5.1.5 100% Plateau (Second Run) Results, RCS Calorimetric Flow	327
6.6.4.1 CESE Single Value Acceptance Criteria Parameters During the First 60 Seconds Following Loss of Flow	361
6.6.5.1 Turbine Trip Single Value Acceptance Criteria and Results	375

LIST OF TABLES

(continued)

	<u>PAGE</u>
6.7.4.1 Summary of HVAC Test Results	391
6.7.5.1 Measured ADV and TBV Capacities	399

LIST OF FIGURES

	<u>PAGE</u>	
1.1	The Facility	19
1.2	The Region Within 50 Miles of WSES-3	21
1.3	The Region Within 5 Miles of WSES-3	22
1.4	Isometric View of the NSSS	23
1.5	Reactor Coolant System Arrangement Elevations	24
1.6	WSES-3 Cycle 1 Power History Through Completion of Test Program	38
1.7-1	Major Events During Power Ascension (March 22 - 31, 1985)	39
1.7-2	Major Events During Power Ascension (April 1 - 10, 1985)	40
1.7-3	Major Events During Power Ascension (April 11 - 20, 1985)	41
1.7-4	Major Events During Power Ascension (April 21 - 30, 1985)	42
1.7-5	Major Events During Power Ascension (May 1 - 10, 1985)	43
1.7-6	Major Events During Power Ascension (May 11 - 20, 1985)	44
1.7-7	Major Events During Power Ascension (May 21 - 30, 1985)	45
1.7-8	Major Events During Power Ascension (May 31 - June 9, 1985)	46
1.7-9	Major Events During Power Ascension (June 20 - 29, 1985)	47
1.7-10	Major Events During Power Ascension (June 30 - July 9, 1985)	48
1.7-11	Major Events During Power Ascension (July 10 - 19, 1985)	49
2.1.1	Location of Temporary Fuel Loading Neutron Detectors 'A' and 'B'	58
2.1.2	Schematics of Temporary Neutron Counting Station Setup	59
2.3.1	Fuel Loading Sequence	64
2.4.1	Elapsed Time Between Fuel Assemblies Placed in Core	66
2.5.1	WSES-3 Cycle 1 Core Map (Fuel)	68
2.5.2	WSES-3 Cycle 1 Core Map (CEAs)	69
2.5.3	WSES-3 Cycle 1 Core Map (Neutron Sources)	70
3.2.1.1	RCS Flow and Flow Coastdown Measurement Test Sequence	89
3.2.1.2	RCP 1A Differential Pressure Transmitter PDT-0110 Calibration Curves	96
3.2.1.3	RCP 1A Differential Pressure Transmitter PDT-0111 Calibration Curves	97

LIST OF FIGURES

(continued)

	<u>PAGE</u>
3.2.1.4 RCP 1B Differential Pressure Transmitter PDT-0112 Calibration Curves	98
3.2.1.5 RCP 1B Differential Pressure Transmitter PDT-0113 Calibration Curves	99
3.2.1.6 RCP 2A Differential Pressure Transmitter PDT-0120 Calibration Curves	100
3.2.1.7 RCP 2A Differential Pressure Transmitter PDT-0121 Calibration Curves	101
3.2.1.8 RCP 2B Differential Pressure Transmitter PDT-0122 Calibration Curves	102
3.2.1.9 RCP 2B Differential Pressure Transmitter PDT-0123 Calibration Curves	103
3.2.1.10 Reactor Vessel 1A Differential Pressure Transmitter PDT-0124W Calibration Curves	104
3.2.1.11 Reactor Vessel 1B Differential Pressure Transmitter PDT-0124X Calibration Curves	105
3.2.1.12 Reactor Vessel 2A Differential Pressure Transmitter PDT-0124Y Calibration Curves	106
3.2.1.13 Reactor Vessel 2B Differential Pressure Transmitter PDT-0124Z Calibration Curves	107
3.2.1.14 SG #1 Differential Pressure Transmitter PDT-9116-SMA Calibration Curves	108
3.2.1.15 SG #1 Differential Pressure Transmitter PDT-9116-SMB Calibration Curves	109
3.2.1.16 SG #1 Differential Pressure Transmitter PDT-9116-SMC Calibration Curves	110
3.2.1.17 SG #1 Differential Pressure Transmitter PDT-9116-SMD Calibration Curves	111
3.2.1.18 SG #2 Differential Pressure Transmitter PDT-9126-SMA Calibration Curves	112

LIST OF FIGURES

(continued)

	<u>PAGE</u>
3.2.1.19 SG #2 Differential Pressure Transmitter PDT-9126-SMB Calibration Curves	113
3.2.1.20 SG #2 Differential Pressure Transmitter PDT-9126-SMC Calibration Curves	114
3.2.1.21 SG #2 Differential Pressure Transmitter PDT-9126-SMD Calibration Curves	115
3.2.1.22 Measured Flow Coastdown vs. FSAR Assumed Flow Coastdown	116
3.2.4.1 Reactor Vessel Support Lateral Restraint Gaps	129
3.2.4.2 Steam Generator Sliding Base X-Direction Gaps	130
3.2.4.3 Reactor Vessel Support Anchor Bolt Grillage-to-Washer Gaps	131
3.2.4.4 Steam Generator Anchor Bolt Nut-to-Washer Gaps	132
3.2.5.1 Histogram of CEA Drop Times to 90% Inserted at 545°F and 2250 psia	139
3.2.6.1 Location of Temporary Thermocouples	143
3.2.6.2 Pressurizer/Reactor Coolant System Depressurization versus Time Curve	144
3.3.2.1 Approximate Location of Heated Junction Thermocouple Levels	148
4.1 W3 Initial Criticality - Inverse Multiplication	165
4.2 W3 Initial Criticality - Boron Concentration	166
4.3 W3 Initial Criticality - 1/M versus Boron	167
4.4 W3 Initial Criticality - Overlap Verification	168
5.1.1 CEA Symmetry Test	173
5.2.1 Integral CEA Group Worth Regulating Groups 6 and 5, No Overlap BOL, HZP (measured values)	175
5.2.2 Integral CEA Group Worth Regulating Groups 4 and 3, No Overlap BOL, HZP (measured values)	176
5.2.3 Integral CEA Group Worth Regulating Groups 2 and 1, No Overlap BOL, HZP (measured values)	177
5.2.4 Integral CEA Group Worth Part Length CEAs (Group P) BOL, HZP (measured values)	178

LIST OF FIGURES

(continued)

	<u>PAGE</u>
6.2.3.1 Excore Signal Paths	204
6.2.6.1 Incore Detector System Layout	219
6.2.6.2 Incore Detector Test Circuits (TS-3 and TS-4)	221
6.3.1.1 Calibrated Turbine Power	227
6.3.2.1 SG1 Feedwater to Steam Header Pressure Loss versus Steam Flow	236
6.3.2.2 SG2 Feedwater to Steam Header Pressure Loss versus Steam Flow	237
6.3.2.3 SG1 Generator Steam Header Pressure Loss versus Steam Flow	238
6.3.2.4 SG2 Generator Steam Header Pressure Loss versus Steam Flow	239
6.3.5.1 CPC Temperature Decalibration, Channel A	258
6.3.5.2 CPC Temperature Decalibration, Channel B	259
6.3.5.3 CPC Temperature Decalibration, Channel C	260
6.3.5.4 CPC Temperature Decalibration, Channel D	261
6.3.6.1 W3 Cycle 1 Shape Annealing, Axial Shape Index	272
6.3.6.2 W3 Cycle 1 Shape Annealing, Upper Excore Responses	273
6.3.6.3 W3 Cycle 1 Shape Annealing, Upper Peripheral Powers	274
6.3.6.4 W3 Cycle 1 Shape Annealing, Middle Excore Responses	275
6.3.6.5 W3 Cycle 1 Shape Annealing, Middle Excore Response - Expanded Scale	276
6.3.6.6 W3 Cycle 1 Shape Annealing, Middle Peripheral Powers	277
6.3.6.7 W3 Cycle 1 Shape Annealing, Middle Peripheral Powers - Expanded Scale	278
6.3.6.8 W3 Cycle 1 Shape Annealing, Lower Excore Responses	279
6.3.6.9 W3 Cycle 1 Shape Annealing, Lower Peripheral Powers	280
6.3.6.10 W3 Cycle 1 Shape Annealing, Channel A Excore Values	281
6.3.6.11 W3 Cycle 1 Shape Annealing, Channel A Peripheral Powers	282

LIST OF FIGURES

(continued)

	<u>PAGE</u>
6.3.6.12 W3 Cycle 1 Shape Annealing, Channel B Excore Values	283
6.3.6.13 W3 Cycle 1 Shape Annealing, Channel B Peripheral Powers	284
6.3.6.14 W3 Cycle 1 Shape Annealing, Channel C Excore Values	285
6.3.6.15 W3 Cycle 1 Shape Annealing, Channel C Peripheral Powers	286
6.3.6.16 W3 Cycle 1 Shape Annealing, Channel D Excore Values	287
6.3.6.17 W3 Cycle 1 Shape Annealing, Channel D Peripheral Powers	288
6.4.1.1 Waterford -3 SES, 20% Axial Power Comparison (CECOR vs CPC A)	298
6.4.1.2 Waterford -3 SES, 20% Axial Power Comparison (CECOR vs CPC B)	299
6.4.1.3 Waterford -3 SES, 20% Axial Power Comparison (CECOR vs CPC C)	300
6.4.1.4 Waterford -3 SES, 20% Axial Power Comparison (CECOR vs CPC D)	301
6.4.1.5 Waterford -3, Radial Power Distribution Comparison, 20% Rated Thermal Power	302
6.4.1.6 Waterford -3, Radial Power Distribution Comparison, 50% Rated Thermal Power	303
6.4.1.7 Waterford -3, Radial Power Distribution Comparison, 80% Rated Thermal Power	304
6.4.1.8 Waterford -3, Radial Power Distribution Comparison, 100% Rated Thermal Power	305
6.4.1.9 Waterford -3, Axial Power Distribution Comparison, 20% Rated Thermal Power	306
6.4.1.10 Waterford -3, Axial Power Distribution Comparison, 50% Rated Thermal Power	307
6.4.1.11 Waterford -3, Axial Power Distribution Comparison, 80% Rated Thermal Power	308
6.4.1.12 Waterford -3, Axial Power Distribution Comparison, 100% Rated Thermal Power	309

LIST OF FIGURES

(continued)

	<u>PAGE</u>
6.4.2.1 Variable Tavg Test Sequence	314
6.5.1.1 Adjustment Flowchart During Calorimetric Flow Measurement	319
6.5.2.1 Natural Circulation Demonstration, Reactor Coolant Hot and Cold Leg Temperatures	334
6.5.2.2 Natural Circulation Demonstration, Steam Generator Pressures	335
6.5.2.3 Natural Circulation Demonstration, Pressurizer Pressure	336
6.6.1.1 WSES-3 Remote Reactor Trip, RCS Cold Leg Temperatures	341
6.6.1.2 WSES-3 Remote Reactor Trip, RCS Hot Leg Temperatures	342
6.6.1.3 WSES-3 Remote Reactor Trip, Pressurizer Pressure	343
6.6.1.4 WSES-3 Remote Reactor Trip, Pressurizer Level	344
6.6.1.5 WSES-3 Remote Reactor Trip, Steam Generator Pressures	345
6.6.1.6 WSES-3 Remote Reactor Trip, Steam Generator Levels	346
6.6.3.1 Loss of Off-Site Power Test, Reactor Coolant Hot and Cold Leg Temperatures	353
6.6.3.2 Loss of Off-Site Power Test, Steam Generator Levels	354
6.6.4.1 W3 Loss of Flow Test, Steam Generator Average Pressure	364
6.6.4.2 W3 Loss of Flow Test, RCS Temperatures	365
6.6.4.3 W3 Loss of Flow Test, Pressurizer Pressures	366
6.6.4.4 W3 Loss of Flow Test, Pressurizer Level	367
6.6.4.5 W3 Loss of Flow Test, Steam Generator	368
6.6.4.6 W3 Loss of Flow Test, RCS Temperatures	369
6.6.4.7 W3 Loss of Flow Test, Pressurizer Pressures	370
6.6.4.8 W3 Loss of Flow Test, Pressurizer Level	371
6.6.4.9 Natural Circulation Demonstration, Reactor Coolant Hot and Cold Leg Temperatures	372
6.6.5.1 W3 Turbine Trip Test - Hot Leg Temperatures	377
6.6.5.2 W3 Turbine Trip Test - Pressurizer Pressures	378
6.6.5.3 W3 Turbine Trip Test - Pressurizer Levels	379
6.6.5.4 W3 Turbine Trip Test - Steam Generator Pressures	380

SECTION 1.0

INTRODUCTION AND SUMMARY

1.1 INTRODUCTION

1.1.1 The Startup Report

The issuance of this Startup Report for the Waterford Steam Electric Station Unit 3 (WSES-3) is in compliance with the United States Nuclear Regulatory Commission's (US NRC's) Regulatory Guide 1.16, Revision 4 (Reporting of Operating Information - Appendix A, Technical Specifications), as outlined in, and required by Sections 6.9.1.1 through 6.9.1.3 of the Station Technical Specifications.

The report describes the initial fuel load, the postcore hot functional testing, the initial criticality, the low power physics testing and the power ascension testing performed following the receipt of a Low Power Operating License (NPF-26) on December 18, 1984, and an Operating License (NPF-38) on March 16, 1985. It addresses each of the post core-load tests described in the FSAR, and includes a description of the measured values of the operating conditions or characteristics obtained during the test program and a comparison of these values with design predictions and specifications. Any corrective actions that were required to achieve satisfactory operation of the plant are also described, as are all other specific details required in license conditions based on other commitments (e.g. the Safety Evaluation Report (SER) NUREG-0787).

1.1.2 The Facility

WSES-3 (Figure 1-1) is a nuclear generating station utilizing a Combustion Engineering (C-E) 3410 MWth (including 20 MWth reactor coolant pump (RCP) heat) pressurized water nuclear steam supply system (NSSS) and a Westinghouse Electric



FIGURE 1.1
THE FACILITY



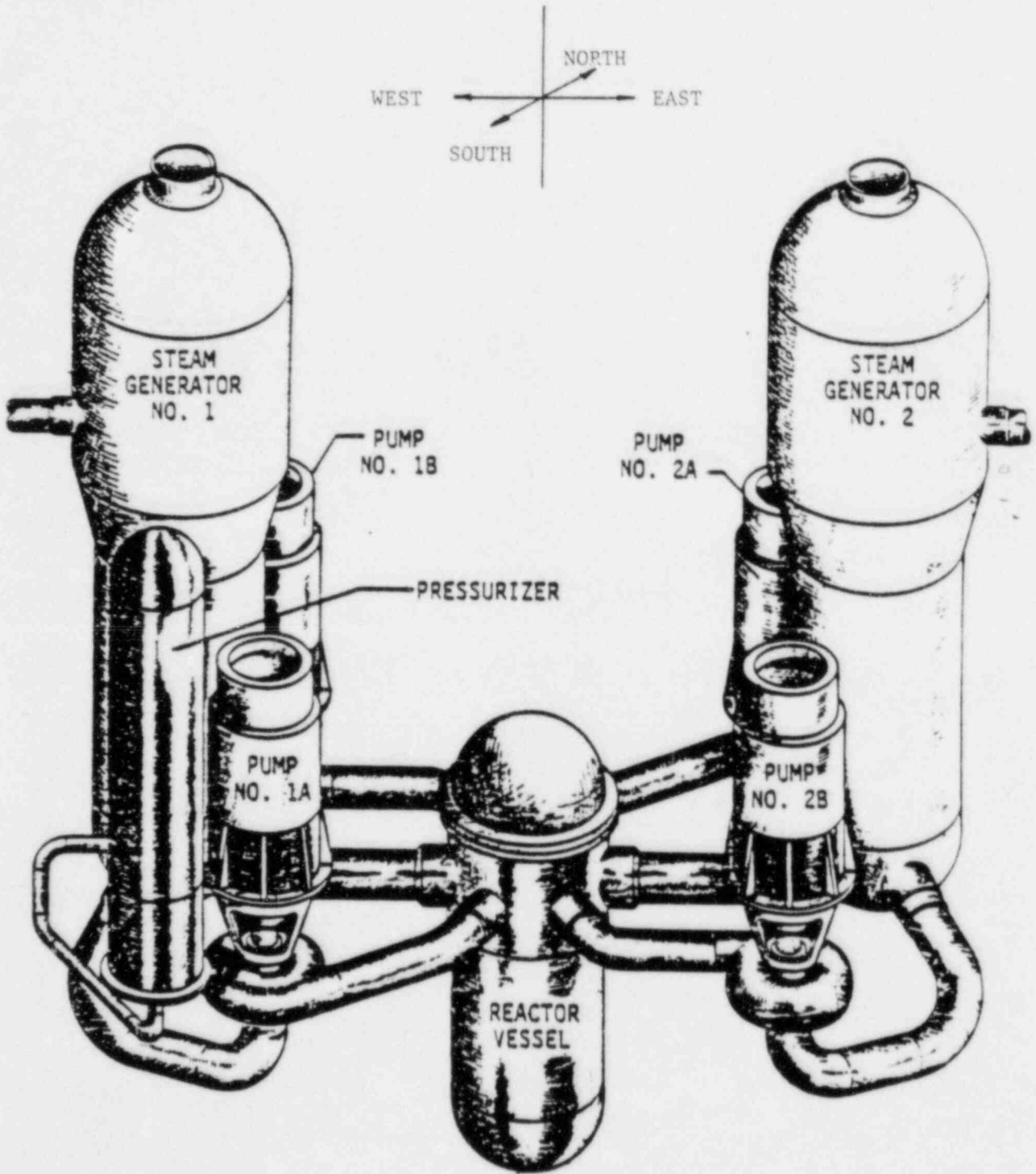
LOOKING NORTH

Corporation turbine-generator outputting 1153 MWE gross (1104 MWE net). Ebasco Services was the architect-engineer and managed construction services.

The unit is located adjacent to two fossil fueled generating units, Waterford SES-1 and -2, on the west bank of the Mississippi River between Baton Rouge and New Orleans, Louisiana. The site is in the northwestern section of St. Charles Parish, near the towns of Killona and Taft (Figures 1.2 and 1.3). The Louisiana Power & Light (LP&L) Company is its owner-operator, and was responsible for the design and construction of the facility. Construction commenced on November 19, 1974, and was essentially completed by May 1984.

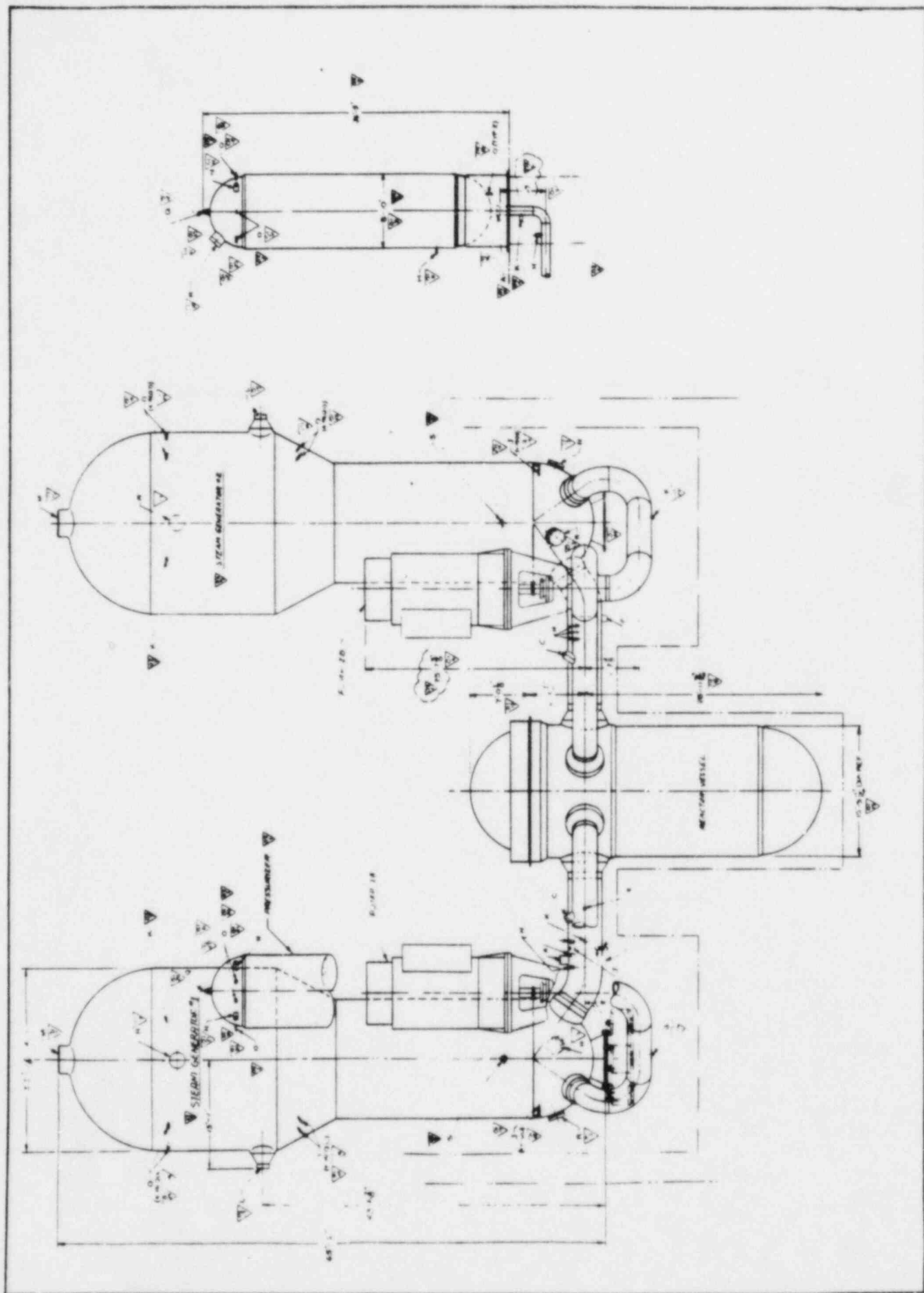
The NSSS is a closed cycle, two loop system consisting of a reactor vessel, two steam generators, four reactor coolant pumps and a pressurizer (Figures 1.4 and 1.5). It is similar to the systems utilized at the San Onofre Nuclear Generating Station (SONGS) Units 2 and 3. The nuclear core consists of 217 fuel assemblies each containing 236 fuel rods. The fuel rods contain slightly enriched uranium dioxide pellets (1.87 - 2.91 wt % U235 for cycle 1) clad in zircaloy tubes with welded end caps. Ninety-one control element assemblies (CEAs), consisting of NiCrFe alloy-clad boron carbide neutron absorber rods, are located in select fuel assemblies throughout the core.

The turbine-generator consists of a tandem compound, six flow exhaust, 1800 rpm turbine using steam at 526.6°F and 860 psia. The generator is an 1800 rpm, three phase, 60 cycle hydrogen and water cooled unit, rated at 1,333,200 KW. The generator output feeds LP&L's 230 KV transmission system. Condensate cooling is provided by the Mississippi River, and will be pumped through the plant at a rate of 1,400,000,000 gallons



ISOMETRIC VIEW OF THE NSSS

FIGURE 1.4



REACTOR COOLANT SYSTEM ARRANGEMENT ELEVATIONS
FIGURE 1.5

per day (this represents about half of one percent of the mean daily river flow). All cooling water is returned to the river.

Table 1.1 lists some of the major design parameters of WSES-3.

TABLE 1.1
Part 1 of 3

DESIGN PARAMETERS OF WATERFORD-3 SES

Hydraulic and Thermal Design Parameters, RCS

Rated core heat output	3,390 MWTh
RCP heat input to RCS	20 MWTh
Total thermal power	3,410 MWTh
System pressure (nominal)	2,250 psia
Reactor coolant flow rate	148×10^6 lb/hr
Average coolant flow velocity along fuel rods	16.4 ft/sec
Nominal core inlet temperature	553 °F
Nominal core exit temperature	611 °F
Average operating temperature (100% power)	582 °F
Fuel center temperature (maximum at 100% power)	3,420 °F
Total reactor coolant system volume (without pressurizer)	10,300 ft ³

Core Mechanical Design Parameters

Number of fuel assemblies	217
Fuel weight (as UO ₂)	223,900 lb
Total weight	310,744 lb
Number of fuel rods	49,580
Number of control element assemblies (full/part length)	83/8

TABLE 1.1
 (Continued)
 Part 2 of 3

DESIGN PARAMETERS OF WATERFORD-3 SES

Nuclear Design Data

Core diameter (equivalent)	136 in
Core height (active fuel)	150 in
Fuel enrichment Region 1 (cycle 1)	1.87 wt%
Fuel enrichment Region 2 (cycle 1)	2.38 wt%
Fuel enrichment Region 3 (cycle 1)	2.88 wt%
Total control element assembly worth (net)	11.35 % Δ k/k

Steam Generator Design Data (Each Generator, Full Power)

Heat transfer rate	5.819×10^9 BTU/hr
Steam pressure	900 psia
Steam flow rate	7.565×10^6 lb/hr
Steam temperature	532 °F
Feedwater temperature	445 °F
Blowdown flow (maximum)	250 gpm

Reactor Coolant Pump Design Data

Flow	99,000 gpm
Head	310 ft
Motor rating	9,700 hp

TABLE 1.1
 (Continued)
 Part 3 of 3

DESIGN PARAMETERS OF WATERFORD-3 SES

Pressurizer Design Data

Operating temperature	653 °F
Operating pressure	2,250 psia
Internal free volume	1,500 ft ³
Normal operating water volume (100% power)	800 ft ³
Normal operating steam volume (100% power)	700 ft ³
Installed heater capacity	1,500 KW
Maximum spray flow	375 gpm
Continuous spray flow	1.5 gpm

Containment Design Data

Inside diameter	140 ft
Height	240.5 ft
Free volume	2,677,000 ft ³
Reference accident pressure	44 psig

Electrical Design Data

Electrical power (gross)	1,153 MWE
Electrical power (net)	1,104 MWE
Diesel generator rating (each)	4,400 KW

NOTE: The above are all design values only and do not necessarily reflect actual as-built values.

1.1.3 The Test Program

The power ascension test program at WSES-3 was developed by LP&L and designed to fulfill the requirements of the NRC's Regulatory Guide 1.68, Revision 2, as detailed in Chapter 14 of the WSES-3 Final Safety Analysis Report (FSAR). The objective of the test program was to determine the as-built plant characteristics during steady state and transient operation from cold shutdown conditions to 100% power, to confirm certain design bases, and to demonstrate the plants' ability to withstand those anticipated transients and postulated failures analyzed in the FSAR.

The test program commenced with the initial fuel loading, and continued through the 100% power test plateau. It culminated with the satisfactory completion of testing at 100% power. The program was divided into three categories, each of which is described below:

a) Precritical (Post-Core Hot Functional) Testing

This consisted of a series of tests performed after the fuel had been loaded, but before the reactor sustained its first critical operation, to allow a final evaluation of those systems requiring the core to be in place (Examples are: i) CEA testing; ii) RCS flow and flow coastdown measurement). The plant was brought to hot standby conditions (545°F, 2250 psia, $k_{eff} < 0.99$, and 0% of rated thermal power) using RCP heat. Testing was performed at various plateaus of increasing temperature and pressure, with the bulk of the testing occurring at hot standby.

The Post-Core Hot Functional phase of the test program is summarized in Section 1.2.2, and detailed in Section 3.0 of this report.

b) Low Power Physics Testing

This consisted of a series of tests performed after the reactor was taken critical and sustained critical operation without producing measurable nuclear heat. Core physics parameters were measured, and similarity between the WSES-3 and SONGS-2 cores was demonstrated. Based in part on this similarity (additional similarity was demonstrated during the power ascension test program), WSES-3 qualified as a follow-on plant to SONGS-2 (the C-E 3410 class reactor prototype plant), and was able to eliminate the following tests from its test program:

- Pseudo-ejected CEA
- Dropped CEA
- PLCEA Xenon Control

The Low Power Physics phase of the test program is summarized in Section 1.2.4, and detailed in Section 5.0 of this report.

c) Power Ascension Testing

This consisted of a series of test performed at increasing power levels to make final adjustments/calibrations to equipment, to demonstrate satisfactory at-power operation of the plant, and to verify its ability to withstand operational transients. This phase of the test program demonstrated satisfactory operation of all plant systems as an integral unit, and verified adequacy of plant operating and off-normal procedures.

The Power Ascension phase of the test program is summarized in Sections 1.2.5 through 1.2.8, and detailed in Section 6.0 of this report.

The test program was conducted under strict adherence to test procedures, which directed the individual tests and documented all test data and results. Table 1.2 lists by title and number the test procedures used during the test program, and identifies the FSAR Chapter 14 commitments satisfied by a given procedure. The testing function fulfilled by the individual procedures is described in detail in the individual test descriptions of Sections 2.0 through 6.0 of this report.

Table 1.3 lists major milestones of the power ascension test program, and Tables 1.4 and 1.5 list the PCHFT and the power ascension tests and the plant conditions/power levels, respectively, at which each test was performed. Figure 1.6 shows the WSES-3 Cycle 1 power history from initial criticality through completion of the test program, while Figures 1.7-1 through 1.7-11 show significant events that affected the test program.

TABLE 1.2
Part 1 of 2
LIST OF STARTUP TEST PROCEDURES AND FSAR CHAPTER 14 TEST COMMITMENTS FILLED

Seq. No.	Procedure Number	Procedure Title	FSAR Ch. 14 Commitment
1.	SIT-TP-400	Initial Fuel Load	14.2.10.1
2.	SIT-TP-500	Post-Core Hot Functional Controlling Document	14.2.10.1.3
3.	SIT-TP-501	Intercomparison of PPS, CPC, and PMC Inputs	14.2.12.3.4
4.	SIT-TP-502	RCS Flow and Coastdown Measurement	14.2.12.3.2
5.	SIT-TP-503	CEDM Performance	14.2.12.3.1
6.	SIT-TP-505	Pressurizer Spray Valve and Control Adjustment	14.2.12.3.5
7.	SIT-TP-506	RCS Leak Rate Measurement	N/A
8.	SIT-TP-507	Incore Instrumentation Baseline Data	14.2.12.3.3
9.	SIT-TP-508	RCS Heat Loss	14.2.12.3.6
10.	SIT-TP-509	RCS Expansion Measurements	14.2.12.3.17
11.	SIT-TP-511	Post-Core Test Data Record	N/A
12.	SIT-TP-512	Moveable Incore Instrumentation Operation Verification	14.2.12.3.3
13.	SIT-TP-513	Post-Core Vibration and Loose Parts Monitoring System	14.2.12.3.40
14.	SIT-TP-600	Initial Criticality	14.2.10.2
15.	SIT-TP-650	Low Power Physics Test	14.2.12.3.10/11/12/13/14
16.	SIT-TP-700	Power Ascension Test Controlling Document	14.2.12.3
17.	SIT-TP-701	NSSS Plant Data Record	N/A
18.	SIT-TP-702	Transient Data Record	N/A
19.	SIT-TP-704	RCS ΔT Power Determination	14.2.12.3.27
20.	SIT-TP-705	Nuclear and Thermal Power Calibration	14.2.12.3.27
21.	SIT-TP-707	SBCS Capacity Check	14.2.12.3.29
22.	SIT-TP-708	Initial Turbine Startup	N/A
23.	SIT-TP-709	NSSS Calorimetric	14.2.12.3.27
24.	SIT-TP-710	RCS Calorimetric Flow Measurement	14.2.12.3.2
25.	SIT-TP-711	Linear Power Subchannel Calibration	14.2.12.3.28
26.	SIT-TP-712	Process Variable Intercomparison	14.2.12.3.30
27.	SIT-TP-714	Vibration and Loose Parts Monitoring System	14.2.12.3.40
28.	SIT-TP-715	Biological Shield Effectiveness Survey	14.2.12.3.15
29.	SIT-TP-716	Core Performance Record	14.2.12.3.27
30.	SIT-TP-717	CPC/COLSS Verification	14.2.12.3.27
31.	SIT-TP-718	Variable Tav _g	14.2.12.3.26
32.	SIT-TP-721	Load Changes (Control Systems Checkout)	14.2.12.3.31/39
33.	SIT-TP-723	Shape Annealing Matrix Measurement	14.2.12.3.28
34.	SIT-TP-724	Temperature Decalibration Verification	14.2.12.3.28
35.	SIT-TP-725	Radial Peaking Factor Verification	14.2.12.3.28
36.	SIT-TP-726	Remote Reactor Trip with Subsequent Remote Cooldown	14.2.12.3.33

TABLE 1.2
 (continued)
 Part 2 of 2

LIST OF STARTUP TEST PRECEDURES AND FSAR CHAPTER 14 TEST COMMITMENTS FILLED

<u>Seq. No.</u>	<u>Procedure Number</u>	<u>Procedure Title</u>	<u>FSAR Ch. 14 Commitment</u>
37.	SIT-TP-727	80% Total Loss of Flow Test/Natural Circulation	14.2.12.3.34
38.	SIT-TP-728	Loss of Offsite Power Trip	14.2.12.3.35/41
39.	SIT-TP-735	Incore Detector Signal Verification	14.2.12.3.3
40.	SIT-TP-739	COLSS Power/Flow Verification Data Record	N/A
41.	SIT-TP-740	100% Turbine Trip	14.2.12.3.37
42.	SIT-TP-741	Adjustment of COLSS Secondary Pressure Loss Terms	N/A
43.	SIT-TP-743	Ventilation Capability	14.2.12.3.32
44.	SIT-TP-748	BOP Data Record	N/A
45.	SIT-TP-749	RPCS 50% Loss of Load Test	14.2.12.3.38
46.	SIT-TP-750	RPCS 70% Loss of Feed Test	14.2.12.3.42
47.	SIT-TP-751	RPCS 80% Loss of Load Test	14.2.12.3.38
48.	SIT-TP-752	RPCS 100% Loss of Load Test	14.2.12.3.38
49.	SIT-TP-753	RPCS 100% Loss of Feed Test	14.2.12.3.42
50.	SIT-TP-755	Natural Circulation Demonstration	14.2.12.3.25
51.	SIT-TP-900	Pipe Whip Restraint Monitoring	14.2.12.3.17

TABLE 1.3
POWER ASCENSION MILESTONES

<u>EVENT</u>	<u>TIME</u>	<u>DATE</u>
Received Low Power Operating License NPF-26	1300	12.18.84
Commence Initial Core Load	2140	12.18.84
Mode 6 Declared for First Time	2155	12.18.84
Completed Initial Core Load	1400	12.24.84
Mode 5 Declared for First Time	2100	12.30.84
Commenced Post Core Hot Functional Testing	~1500	12.31.84
Mode 4 Declared for First Time	0226	1.23.85
Mode 3 Declared for First Time	1847	2.1.85
Completed Post Core Hot Functional Testing	1800	2.20.85
Mode 2 Declared for First Time	2013	3.4.85
Initial Criticality Achieved	2148	3.4.85
Commenced Low Power Physics Testing	0145	3.5.85
Completed Low Power Physics Testing	1215	3.10.85
Received Operating License NPF-38	--	3.16.85
Commenced Initial Power Ascension	0345	3.17.85
Mode 1 Declared for First Time	1748	3.17.85
Initial Synchronization to Grid (@ ~10% power)	1813	3.18.85
20% Power Attained for First Time	~0750	4.12.85
50% Power Attained for First Time	2337	4.19.85
80% Power Attained for First Time	1845	5.7.85
100% Power Attained for First Time	1844	7.1.85
Declared Commercial Operation	0001	9.24.85

TABLE 1.4

POST-CORE HOT FUNCTIONAL TEST PLATEAUS AND TESTS PERFORMED AT EACH PLATEAU

SEQ. NO.	TEST (PROCEDURE NUMBER)	TEST PLATEAU						
		FILL AND VENT	PRE-RCS	DURING RCS FILL AND VENT	120 F/ 150 psia	260 F/ 350 psia	345 F/ 392 psia	545 F/ 2250 psia
1	Intercomparison of PPS,CPC and PMC Inputs (SIT-TP-501)				X		X	X
2	RCS Flow and Coastdown Measurement (SIT-TP-502)							X
3	CEDM Performance (SIT-TP-503)					X		X
4	Pressurizer Spray Valve and Control Adjustment (SIT-TP-505)							X
5	RCS Leak Rate Measurement (SIT-TP-506)							X
6	Incore Instrumentation Baseline Data (SIT-TP-507)				X	X	X	X
7	RCS Heat Loss (SIT-TP-508)				X	X	X	X
8	RCS Expansion Measurements (SIT-TP-509)	X			X	X	X	X
9	Postcore Test Data Record (SIT-TP-511)				X	X	X	X
10	Movable Incore Instrumentation Operation Verif.(SIT-TP-512)							X
11	Post-Core Vibration and Loose Parts Monit. Sys.(SIT-TP-513)							X
12	Heated Junction Thermocouple Operation Verif. (SIT-TP-500)			X				
13	RCS and Steam Generator Parameters (SIT-TP-500)					X	X	X
14	Determination of Auxiliary Spray Flow Split (SIT-TP-500)							X
15	Postcore Thermal Expansion Testing (SPO-99P-003)				X	X	X	X
16	Adjustment of COLSS Second. Press. Loss Terms (SIT-TP-741)							X
17	Ventilation Capability (SIT-TP-743)							X

NOTE: An RCS Heatup/Cooldown and Pressurization History (per SIT-TP-500) was recorded during plant heatup and pressurization.

TABLE 1.5
Part 1 of 2
POWER ASCENSION TEST PLATEAUS AND TESTS PERFORMED AT EACH PLATEAU

SEQ. NO.	TEST (PROCEDURE NUMBER)	TEST PLATEAU													
		0%	5%	10%	15%	20% Non-Eq. Xe Eq. Xe	30%	40%	50% Non-Eq. Xe Eq. Xe	60%	70%	80% Non-Eq. Xe Eq. Xe	90%	95%	100% Non-Eq. Xe Eq. Xe
1	Low Power Physics Test (SIT-TP-650)	X													
2	NSSS Plant Data Record (SIT-TP-701)	X	X		X	X	X	X	X	X	X	X	X	X	X
3	KCS Delta-T Power Determination (SIT-TP-704)		X		X	X	X								
4	Nuclear and Thermal Power Calibration (SIT-TP-705)		X		X	X	X	X	X	X	X	X	X	X	X
5	SBCS Capacity Checks (SIT-TP-707)									X					
6	Initial Turbine Startup (SIT-TP-708)					X		X	X	X		X	X		
7	NSSS Calorimetric (SIT-TP-709)					X	X	X	X	X	X	X	X	X	X
8	RCS Calorimetric Flow Measurement (SIT-TP-710)						X			X					X
9	Linear Power Subchannel Calibration (SIT-TP-711)						X			X					
10	Process Variable Intercomparison (SIT-TP-712)					X			X						X
11	Vibration and Loose Parts Monit. Sys. (SIT-TP-714)	X				X			X			X			X
12	Biological Shield Effectiveness Survey (SIT-TP-715)		X			X			X						X
13	Core Performance Record (SIT-TP-716)						X			X			X		X
14	CPC/COLSS Verification (SIT-TP-717)	X					X			X			X		X
15	Variable Tavg (SIT-TP-718)									X					X
16	Load Changes (Control Systems Checkout) (SIT-TP-721)									X					X
17	Shape Annealing Matrix Measurement (SIT-TP-723)								X	X		X			X
18	Temperature Decalibration Verification (SIT-TP-724)									X					
19	Radial Peaking Factor Verification (SIT-TP-725)									X					
20	Remote Reactor Trip with Subsequent Remote Cooldown (SIT-TP-726)														
21	80% Total Loss of Flow/Natural Circ. (SIT-TP-727)					X							X		
22	Loss of Offsite Power Trip (SIT-TP-728)					X									
23	Incore Detector Signal Verification (SIT-TP-735)					X			X			X			X
24	COLSS Power/Flow Verif. Data Record (SIT-TP-739)	X				X		X	X		X	X	X	X	X
25	100% Turbine Trip (SIT-TP-740)														X

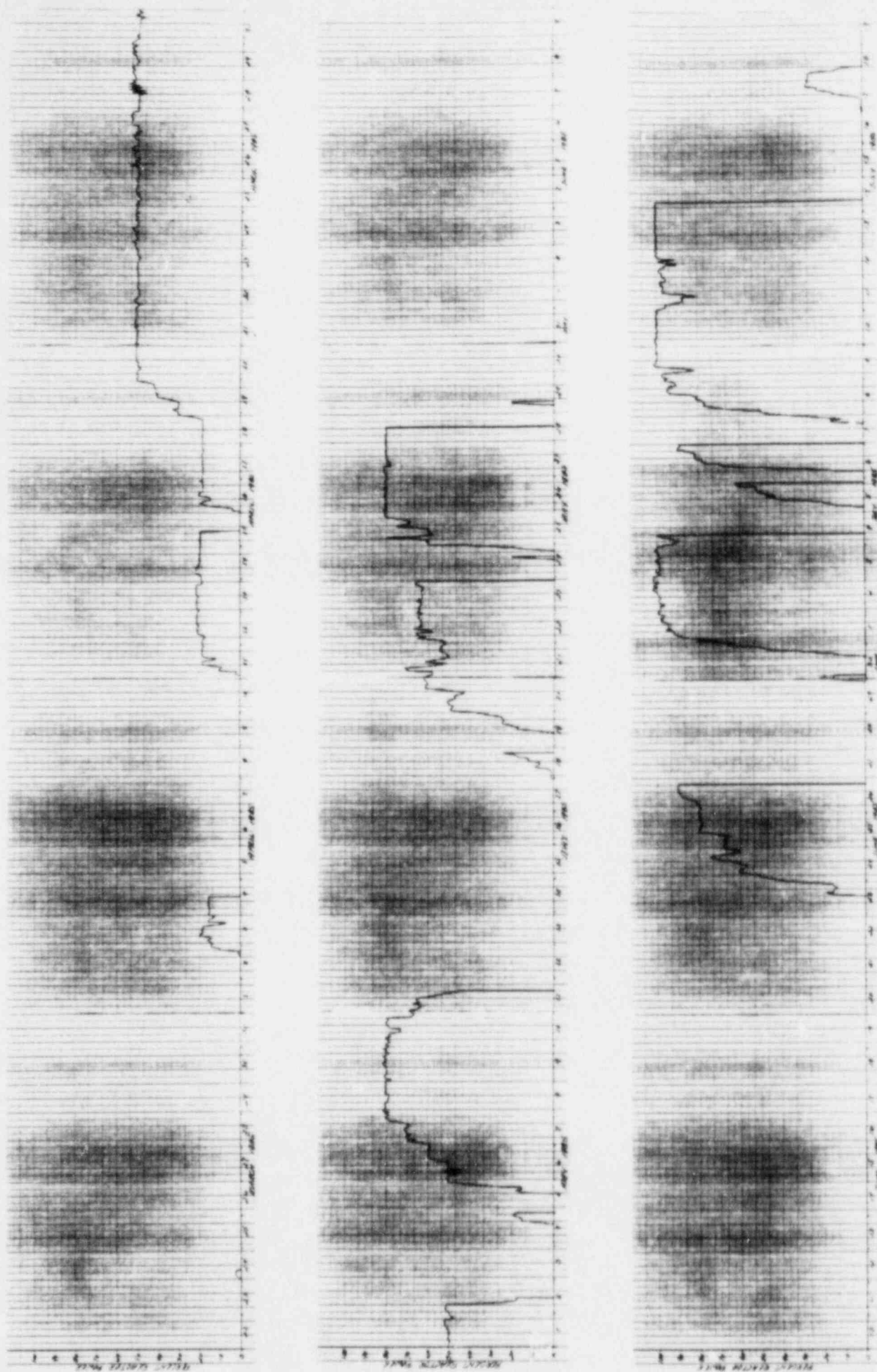
TABLE 1.5
(continued)
Part 2 of 2

POWER ASCENSION TEST PLATEAUS AND TEST PERFORMED AT EACH PLATEAU

SEQ. NO.	TEST (PROCEDURE NUMBER) Load Changes (Control Systems Checkout (SIT-TP-721))	TEST PLATEAU														
		0%	5%	10%	15%	20%	30%	40%	50%	60%	70%	80%	90%	95%	100%	
						Eq. Xe Non-Eq. Xe		Eq. Xe Non-Eq. Xe		Eq. Xe Non-Eq. Xe				Eq. Xe Non-Eq. Xe		
26	Adjustment of COLSS Secondary Pressure Loss Terms (SIT-TP-741)	X				X		X				X			X	
27	Ventilation Capability (SIT-TP-743)	X				X		X							X	
28	BOP Data Record (SIT-TP-748)	X	X		X	X		X	X		X	X		X	X	
29	Natural Circulation Demonstration (SIT-TP-755)											X				
30	Pipe Whip Restraint Measurements (SIT-TP-900)727)					X		X				X			X	
31	Thermal Expansion (SPO-99P-003)					X		X				X			X	

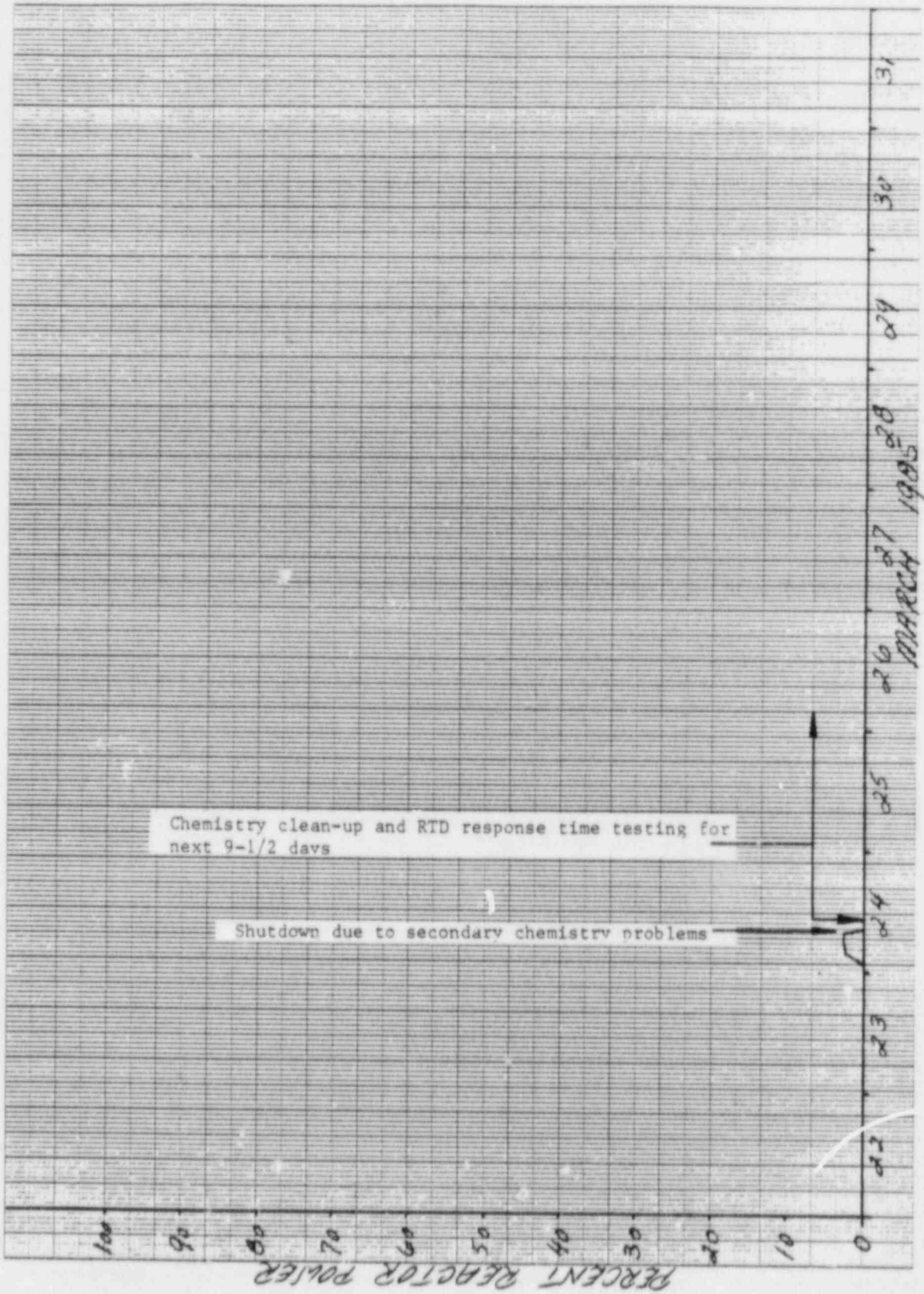
NOTES:

- a) Transient Data Record (SIT-TP-702) performed during every initial power increase.



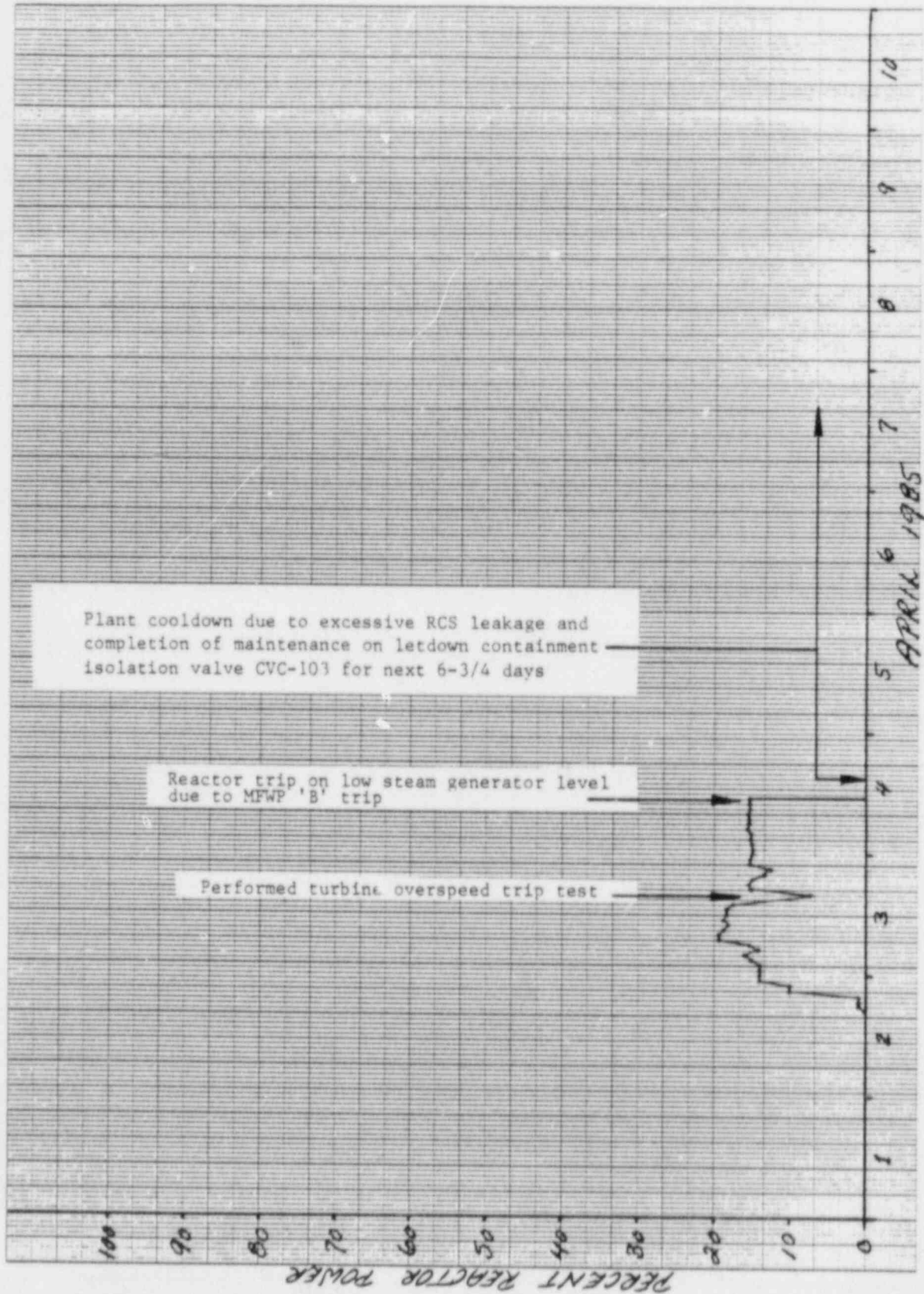
WSES-3 CYCLE 1 POWER HISTORY THROUGH COMPLETION OF TEST PROGRAM

FIGURE 1.6



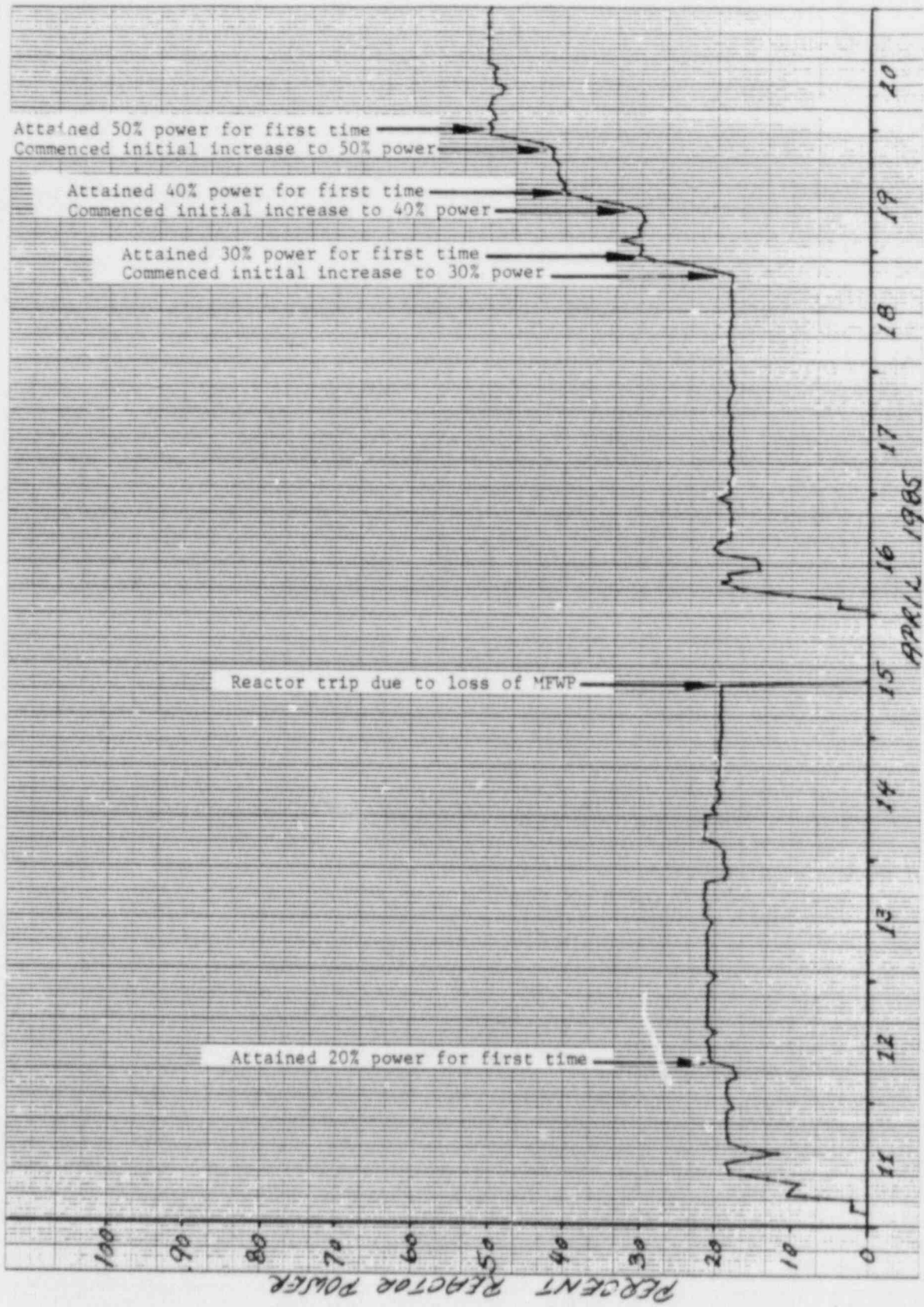
MAJOR EVENTS DURING POWER ASCENSION (MARCH 22-31, 1985)

FIGURE 1.7-1



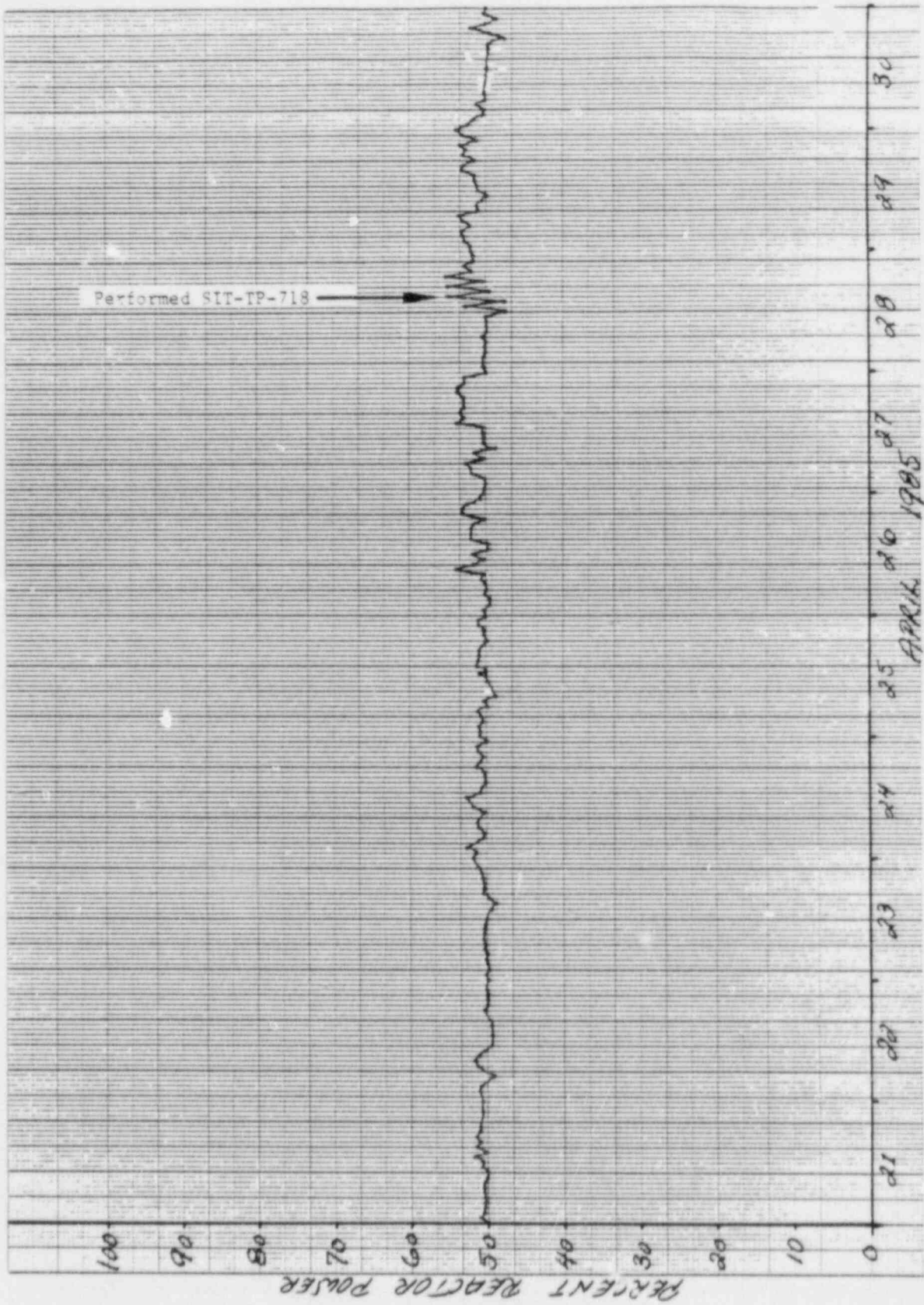
MAJOR EVENTS DURING POWER ASCENSION (APRIL 1-10, 1985)

FIGURE 1.7-2



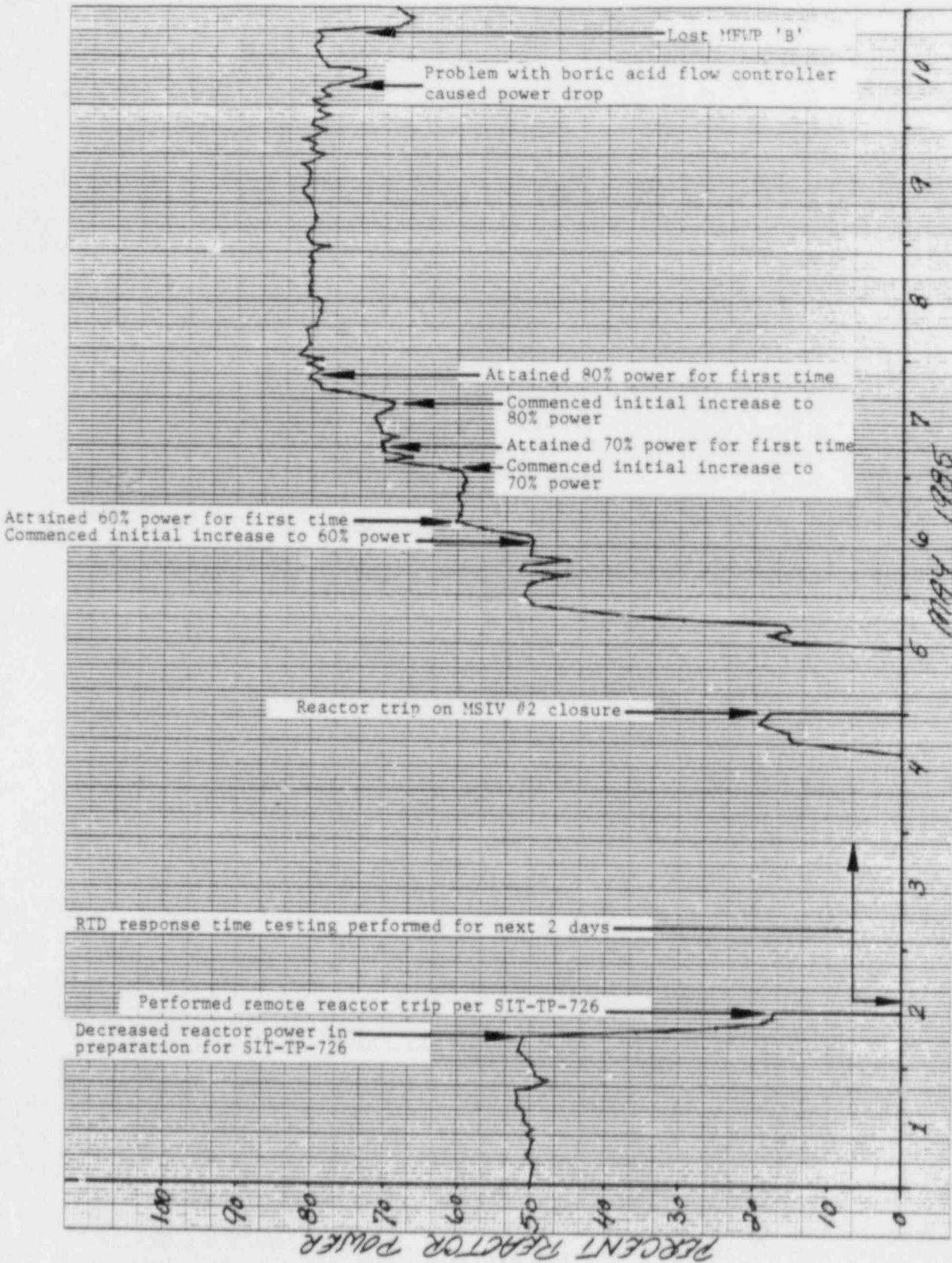
MAJOR EVENTS DURING POWER ASCENSION (APRIL 11-20, 1985)

FIGURE 1.7-3



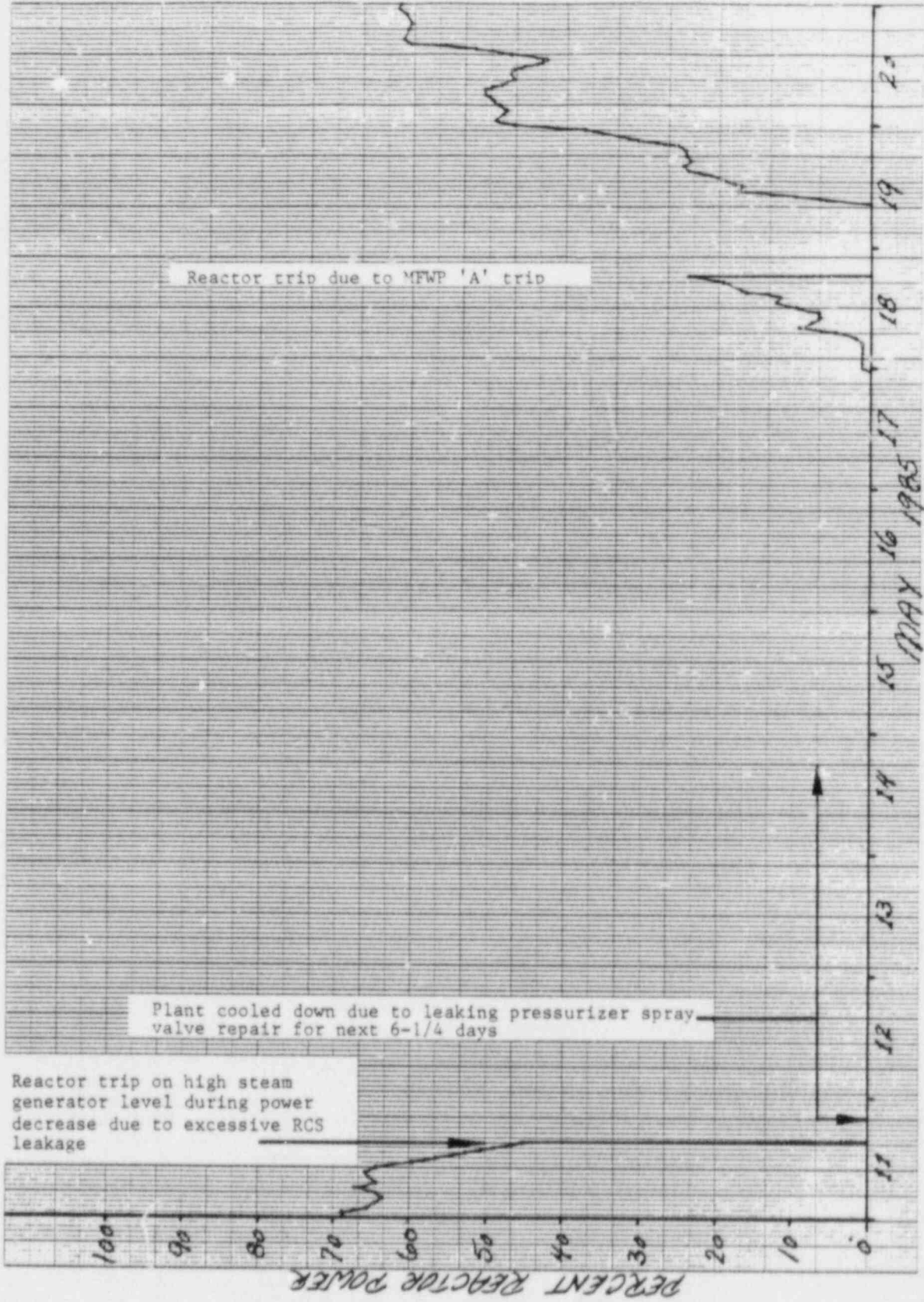
MAJOR EVENTS DURING POWER ASCENSION (APRIL 21-30, 1985)

FIGURE 1.7-4



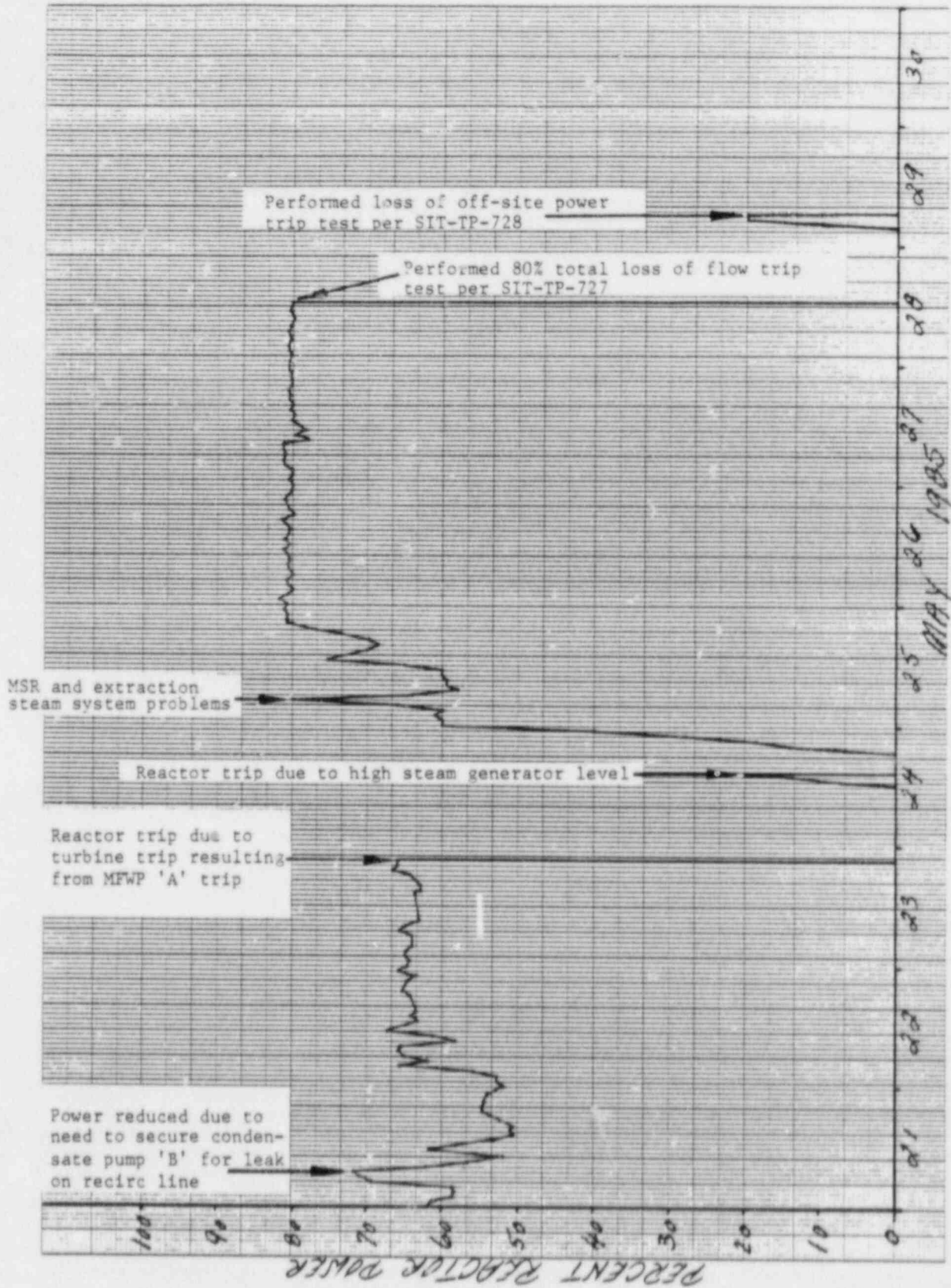
MAJOR EVENTS DURING POWER ASCENSION (MAY 1-10, 1985)

FIGURE 1.7-5



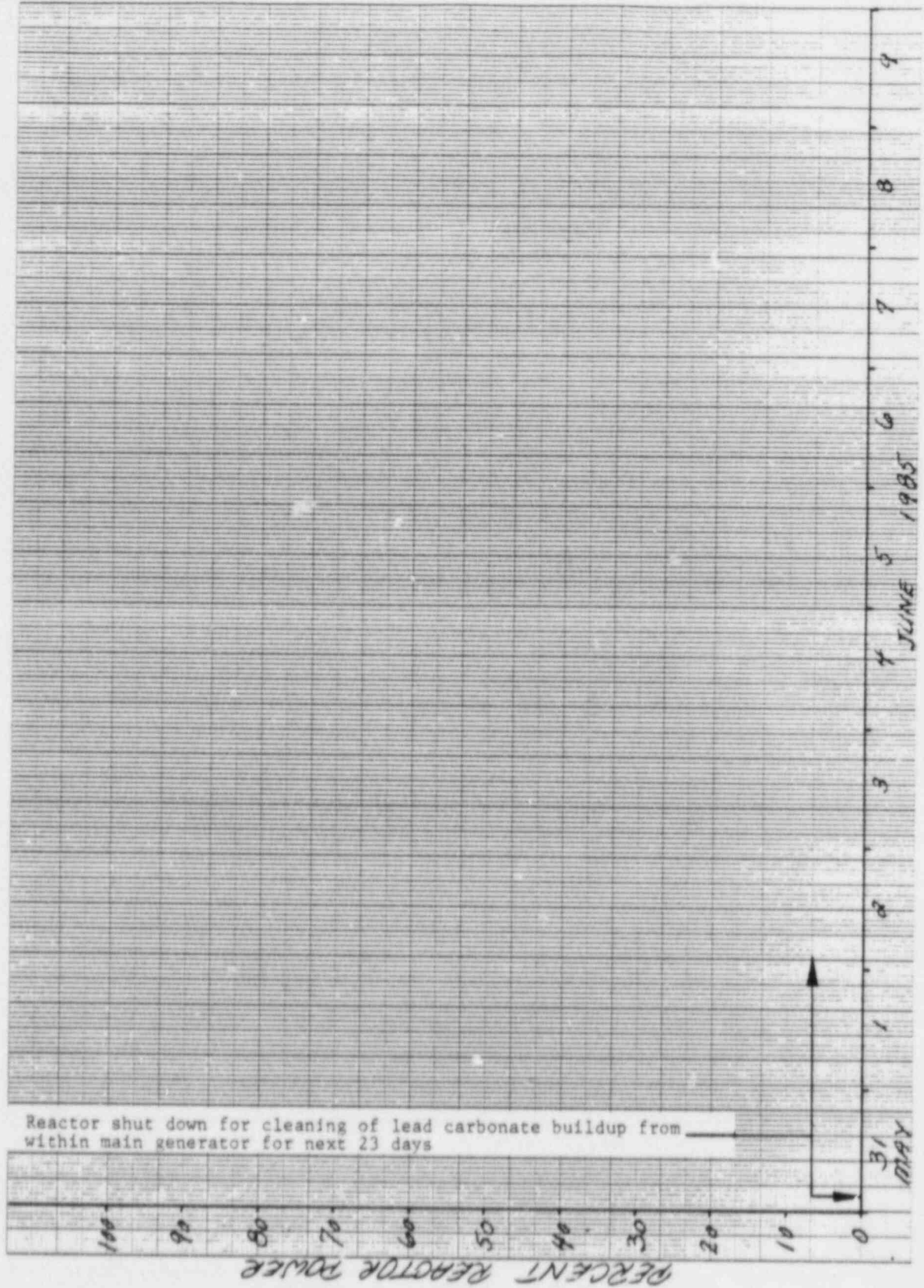
MAJOR EVENTS DURING POWER ASCENSION (MAY 11-20, 1985)

FIGURE 1.7-6



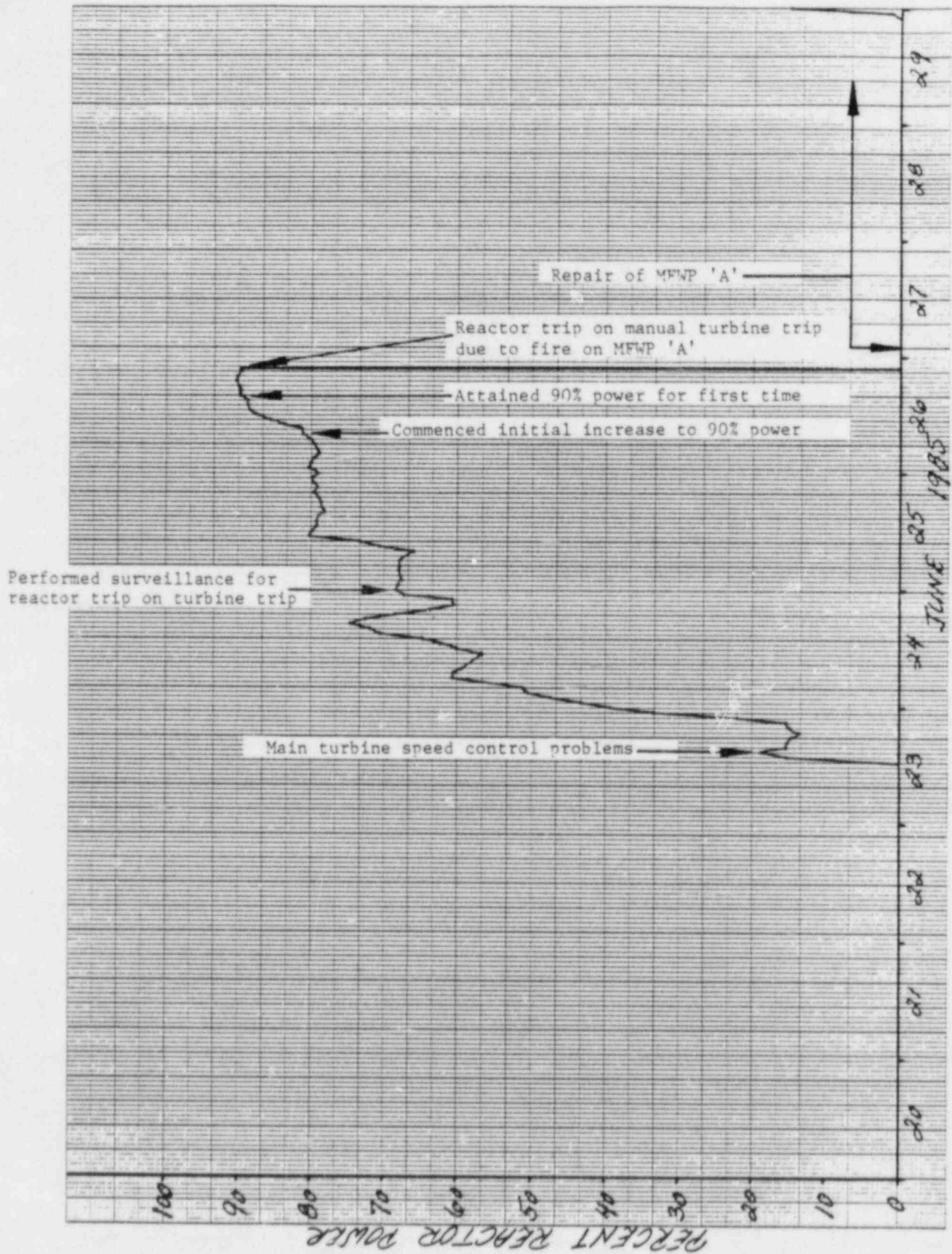
MAJOR EVENTS DURING POWER ASCENSION (MAY 21-30, 1985)

FIGURE 1.7-7



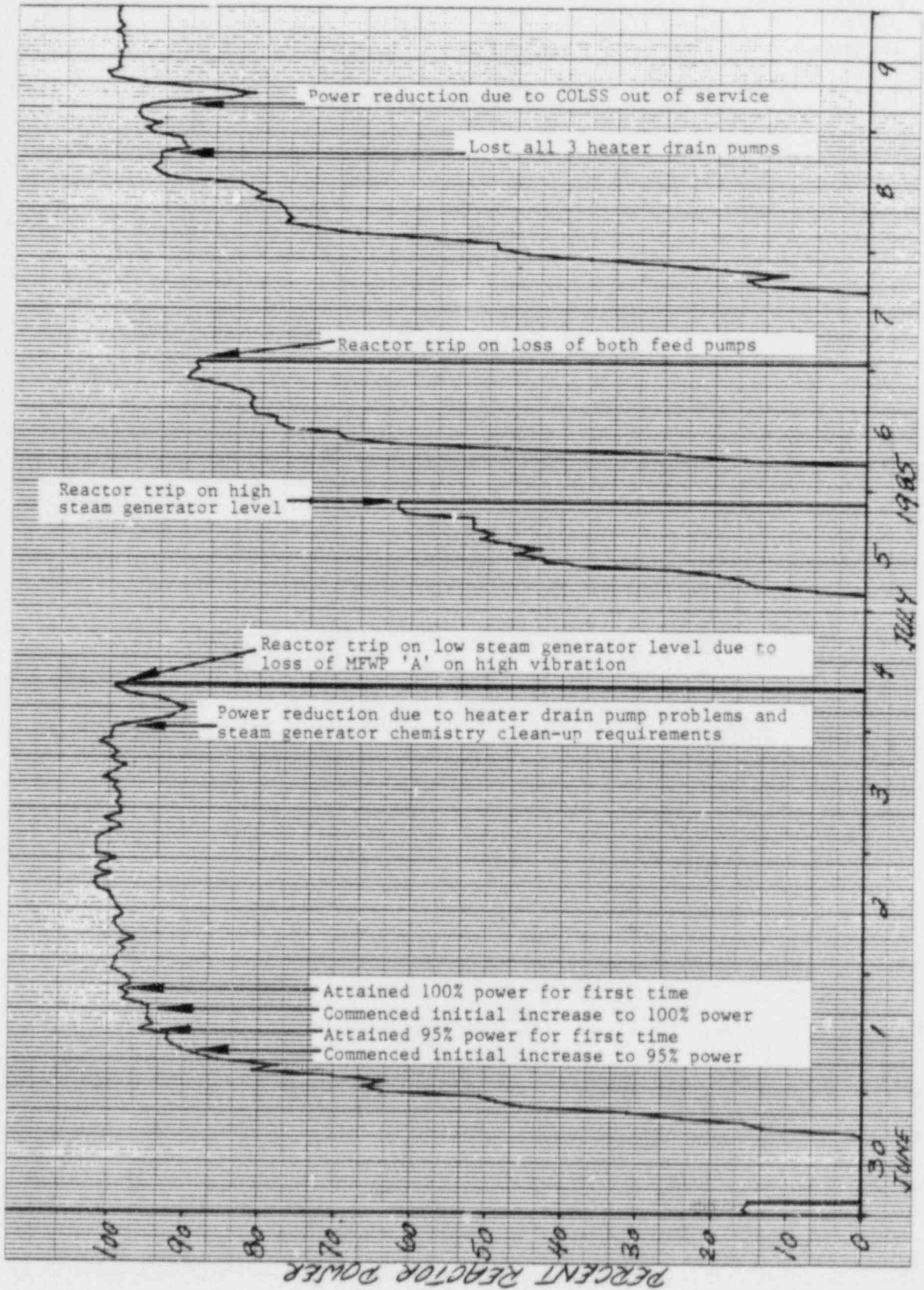
MAJOR EVENTS DURING POWER ASCENSION (MAY 31 - JUNE 9, 1985)

FIGURE 1.7-8



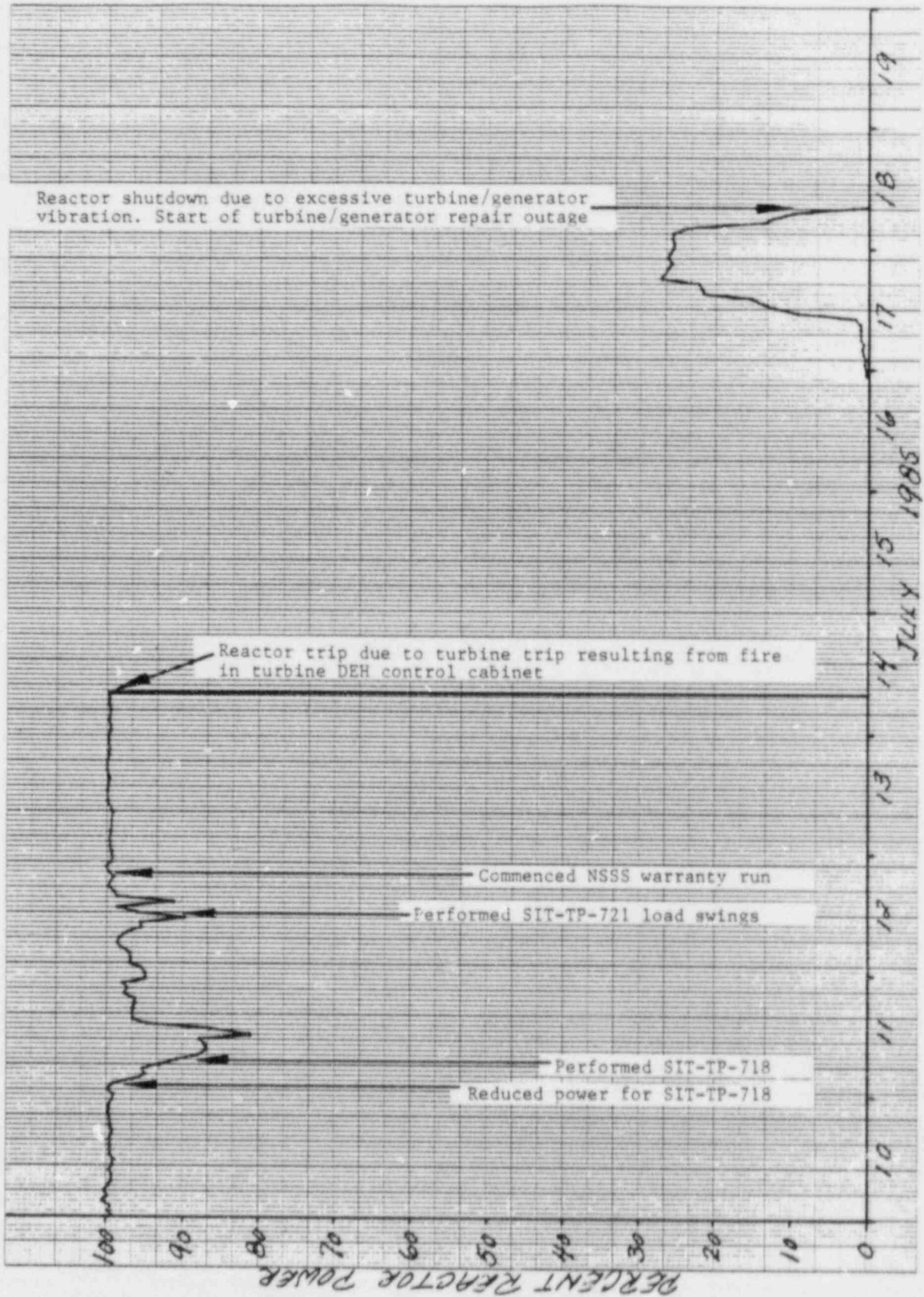
MAJOR EVENTS DURING POWER ASCENSION (JUNE 20-29, 1985)

FIGURE 1.7-9



MAJOR EVENTS DURING POWER ASCENSION (June 30 - JULY 9, 1985)

FIGURE 1.7-10



MAJOR EVENTS DURING POWER ASCENSION (JULY 10-19, 1985)

FIGURE 1.7-11

1.2 SUMMARY

1.2.1 Initial Fuel Load

The initial fuel loading of WSES-3 was performed in accordance with test procedure SIT-TP-400, "Initial Fuel Load". Fuel loading commenced on December 18, 1984, at 2140 (CST), approximately 8 hours after the facility received its low power license from the NRC. The first fuel assembly (B077), containing the first of two neutron sources, was seated at core location X-11 at 2331. Fueling operations lasted 4 days, 17 hours and 20 minutes. The last fuel assembly was placed in the core at 1500 on December 23, 1985. The subsequent fuel loading verification took until 1400 on December 24, 1984; its satisfactory completion marked the end of the fuel loading operation.

The initial fuel loading is further discussed in detail in Section 2.0 of this report.

1.2.2 Post Core Hot Functional Testing

The post-core hot functional test program was performed in accordance with test procedure SIT-TP-500, "Post Core Hot Functional Test Controlling Document", and other test procedures of the SIT-TP-500 series, as listed in Tables 1.2 and 1.4. Testing commenced on December 31, 1985, and lasted approximately 52 days, until February 20, 1985.

Post-core hot functional testing is further discussed in detail in Section 3.0 of this report.

1.2.3 Initial Criticality

The approach to initial criticality was performed in accordance with test procedure SIT-TP-600, "Initial Criticality". Withdrawal of the CEA's commenced at 0328 on March 4, 1985. RCS dilution followed the CEA withdrawal until initial criticality was satisfactorily achieved at 2148 on the same day.

Initial criticality is further discussed in detail in Section 4.0 of this report.

1.2.4 Low Power Physics Testing

Low power physics testing was performed in accordance with test procedure SIT-TP-650, "Low Power Physics Test". Testing commenced, after initial criticality had been achieved, at 0145 on March 5, 1984, and lasted approximately 5.4 days, until 1215 on March 10, 1985.

Low power physics testing is further discussed in detail in Section 5.0 of this report.

1.2.5 Power Ascension Testing Through 20% Power

Power ascension testing through 20% power was performed in accordance with test procedure SIT-TP-700, "Power Ascension Test Controlling Document", and other test procedures of the SIT-TP-700 series, as shown in Tables 1.2 and 1.5. Testing commenced at 0345 on March 17, 1985 with the initial power increase above the power levels maintained for low power physics testing.

The turbine-generator was synchronized to the grid at 1813 on March 18, 1985, with the reactor at approximately 10% power. Twenty percent power operation was reached at approximately 0750 on April 12, 1985; this marked the first major test plateau. Testing at 20% power was completed at 1908 on April 18, 1985, when the initial increase to 50% reactor power commenced.

The test results of the power ascension tests performed through 20% power are further discussed in detail in Section 6.0.

1.2.6 Power Ascension Testing From 20% Through 50% Power

Power ascension testing through 50% power was performed in accordance with test procedure SIT-TP-700, "Power Ascension Test Controlling Document", and other test procedures of the SIT-TP-700 series, as shown in Tables 1.2 and 1.5. Testing commenced with an increase in reactor power from the 20% power test plateau at 1908 on April 18, 1985. Minor test plateaus were established at 30% and 40% power and maintained for 9.25 and 9 hours respectively. Fifty percent power was achieved at 2337 on April 19, 1985. Testing at 50% power was completed at 1120 on May 6, 1985.

The test results of the power ascension tests performed from 20% through 50% power are further discussed in detail in Section 6.0.

1.2.7 Power Ascension Testing From 50% Through 80% Power

Power ascension testing through 80% power was performed in accordance with test procedure SIT-TP-700, "Power Ascension Test Controlling Document", and other test procedures of the SIT-TP-700 series, as shown in Tables 1.2 and 1.5. Testing commenced with an increase in reactor power from the 50% power test plateau at 1120 on May 6, 1985. Minor test plateaus were established at 60% and 70% power and maintained for 10.5 and 9 hours respectively. Eighty percent power was achieved at 1845 on May 7, 1985. Testing at 80% power was completed at 0800 on June 26, 1985.

The test results of the power ascension tests performed from 50% through 80% power are further discussed in detail in Section 6.0.

1.2.8 Power Ascension Testing From 80% Through 100% Power

Power ascension testing through 100% power was performed in accordance with test procedure SIT-TP-700, "Power Ascension Test Controlling Document", and other procedures of the SIT-TP-700 series, as shown in Tables 1.2 and 1.5. Prior to commencing the power increase to 100% power, the 80% Total Loss of Flow test, followed by the Loss of Offsite Power test at 20% power were performed. The initial power escalation from 80% to 100% power commenced at 0800 on June 26, 1985 following completion of "post 80% power plateau testing" and a return to criticality and 80% power. Minor test plateaus were established at 90% and 95% power and maintained for approximately 8.2 and 4.9 hours respectively. One hundred percent power was achieved at 1844 on July 1, 1985. Testing at 100% power was completed at 1730 on July 12, 1985.

The test results of the power ascension tests performed from 80% through 100% power are further discussed in detail in Section 6.0.

SECTION 2.0

INITIAL FUEL LOADING

2.1 Preparations

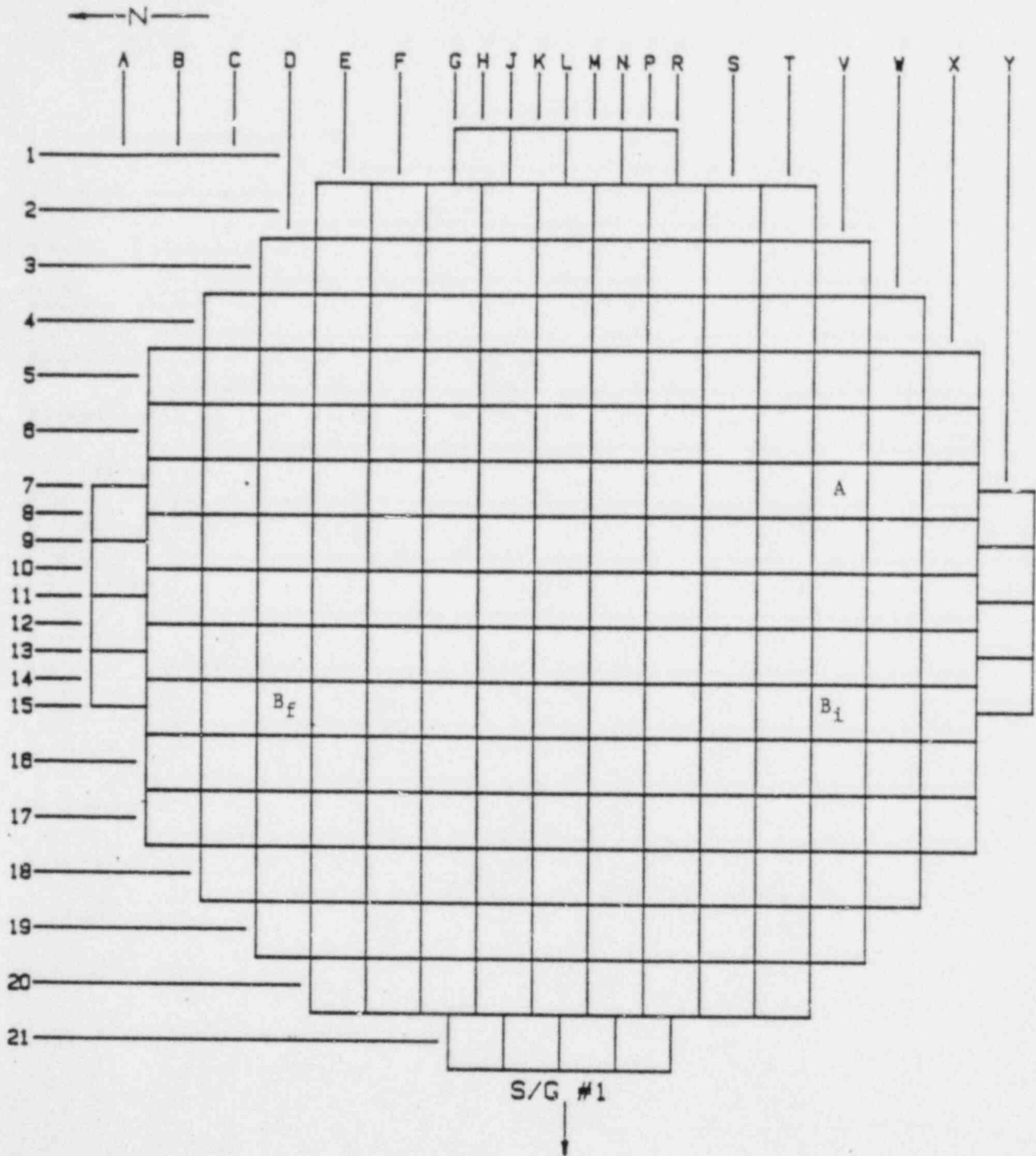
Initial preparations for fuel load commenced in the first quarter of 1983 with the receipt on site of the 217 fuel assemblies destined to make up the WSES-3 initial core. As the capacity of the new fuel storage racks is insufficient to accommodate an entire core, the fuel was stored dry in the spent fuel storage racks in a checker-board arrangement. Following their receipt, the 5-fingered CEA's were loaded into the fuel assemblies designated to host them during the first cycle (the 4-fingered CEA's, which straddle the fuel assemblies, were placed into the upper guide structure (UGS) when this was ready to receive them). Each core component was inspected during the process of removal from its shipping container and placement in storage. The selected storage location also helped minimize the amount of handling/transferring required for each core component.

Prior to commencing fuel load, the containment refueling pool deep end, the transfer canal, and the transfer pit in the fuel storage building were filled with borated water, at a concentration slightly in excess of 2000 ppm, to a level of approximately one foot above the top of the transfer canal. This was accomplished utilizing the fuel pool purification system return line, thereby eliminating the need to overflow the reactor vessel. The chance of leakage around the seal ring, and a clean-up of the upper cavity floor to permit unrestricted access to the reactor vessel flange by fueling observers were avoided in this manner. Filling of the refueling pool, as described, assured containment integrity as required by the Station Technical Specifications, and provided lubrication for the fuel transfer equipment.

The reactor vessel was filled to approximately one foot above the top of the RCS hot legs with borated water, also at a concentration slightly above 2000 ppm. The shutdown cooling system was subsequently maintained in operation as required by the Station Technical Specifications.

Two temporary incore neutron detectors and associated electronics provided by Combustion Engineering were set up and calibrated. The detectors were placed in detector housings and set in place at core locations V-7 and V-15 as channels "A" and "B", respectively (Figure 2.1.1). The electronics were set up as a neutron counting station (Figure 2.1.2) at the plant southeast corner of the refueling pool on the +46 foot level of containment, from where the reactor vessel and fuel loading operations could be closely observed. A strip chart recorder was connected to one of the channels to provide a continuous visual display of the neutron count rate in addition to the audible count rate provided in containment by the other temporary channel, and one of the permanent plant start-up channels. The two permanent plant start-up channels had neutron counting equipment connected to them that was set up within the control room, such that a total of four detectors would provide information on the neutron multiplication throughout the core load. One of the start-up channels also provided an audible count rate in the control room, as required by the Station Technical Specifications. Following satisfactory set-up and checkout of both temporary and permanent plant start-up neutron detectors, a background count rate was determined for each detector without fuel or start-up neutron sources in containment.

The response check of the neutron detectors required by the Station Technical Specifications was performed using the first fuel assembly (B077) to be loaded with a start-up neutron source in one of its CEA guide tubes. The fuel assembly was lowered into the reactor vessel adjacent to the permanent start-up and the temporary neutron detectors, remaining grappled to the fuel handling machine at all times. A neutron count rate significantly above the previously

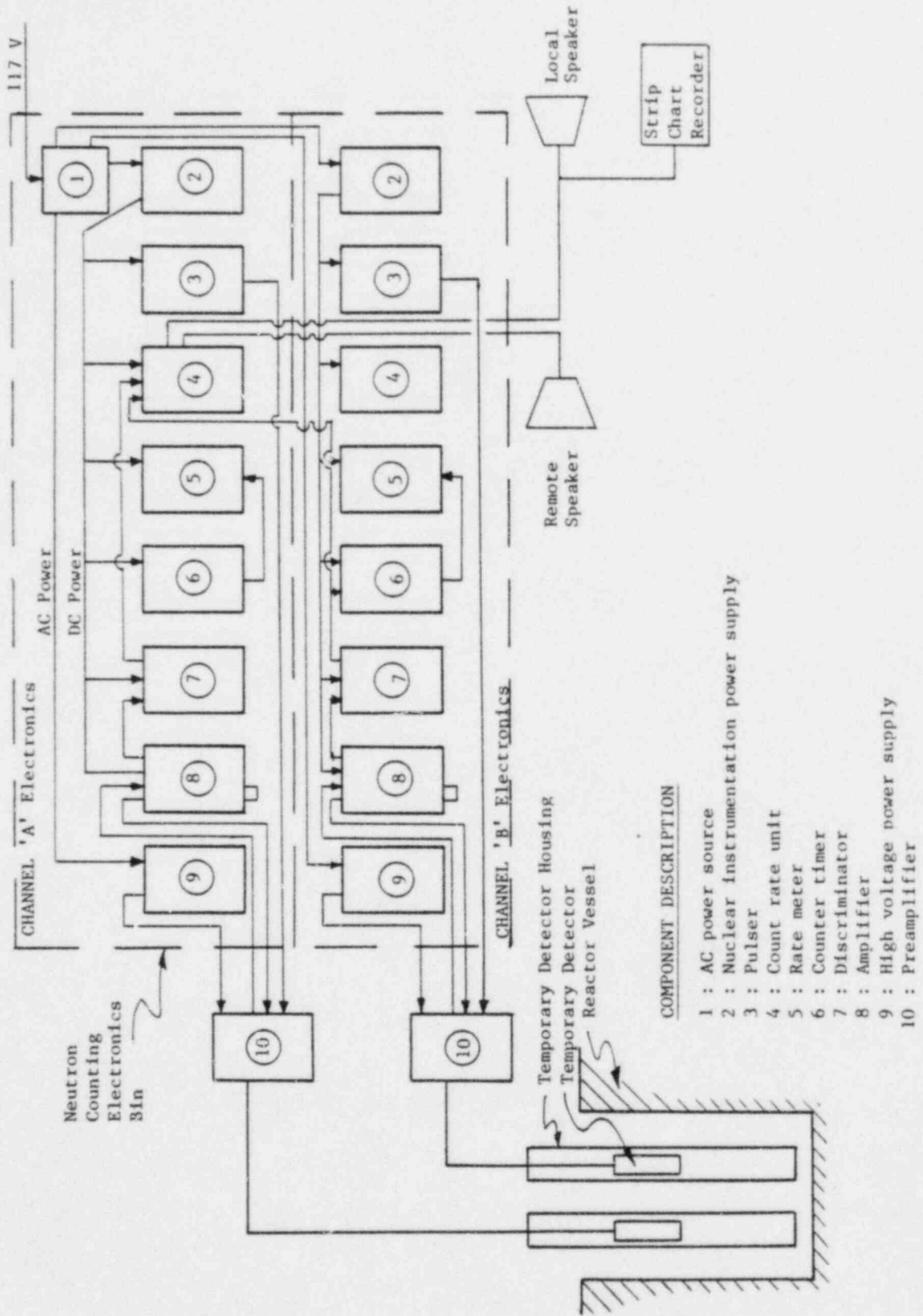


NOTES:

- A = Location of temporary neutron detector channel A
- B_i = Location of temporary neutron detector channel B before loading of second neutron source
- B_f = Location of temporary neutron detector channel B after loading of second neutron source

LOCATION OF TEMPORARY FUEL LOADING NEUTRON DETECTORS 'A' AND 'B'

FIGURE 2.1.1



SCHEMATICS OF TEMPORARY NEUTRON COUNTING STATION SETUP

FIGURE 2.1.2

measured background countrate indicated a response to neutrons and verified operability of all four detectors. Upon completion of the response check fuel assembly B077 was placed in core location X-11.

2.2 Reactivity Monitoring

The neutron multiplication of the core was closely monitored at all times during core load by means of an inverse multiplication versus number of fuel assemblies loaded ("1/M") plot for each of the four neutron detection/counting channels. After the first fuel assembly (B077) containing start-up neutron source "B" was inserted into the reactor vessel, at core location X-11, a base countrate, C_0 , was determined by averaging at least five individual counts over a 100 second period. All subsequent countrates, C_i , determined by averaging at least three individual counts over a 100 second period, were divided into this base countrate; the resultant C_0/C_i values were plotted against the number of fuel assemblies loaded for the four channels being monitored, providing the 1/M plots. A new base countrate was redetermined for the temporary detectors when these were moved. The new base countrate was normalized to the old one to assure continuity of the 1/M plots. Countrates were corrected for background if the background contributed greater than 5% of the countrate.

Following the insertion of every fuel assembly into the core, a neutron count was taken on each of the four detectors. These counts were translated into inverse multiplication (1/M) numbers, and plotted against the number of assemblies loaded into the core to assure nuclear safety.

For approximately the first fifteen and the last five fuel assemblies to be inserted into the core, the $1/M$ value was determined prior to the refueling machine ungrappling from the fuel assembly. This was done because of the core coupling changes, that dramatically increase the neutron count rate during the first fifteen assemblies to be loaded into the core, and as a precaution while loading the last five.

While loading the 16th through 212th assemblies a strip chart trace of the count rate off a temporary neutron detector channel was used to determine visually any variations in subcritical neutron multiplication. Based on the trend of this trace, it was possible to permit the refueling machine to ungrapple from the fuel assembly placed into the core prior to the $1/M$ value having been determined. This method of monitoring the neutron multiplication provided additional safety and shortened the fuel loading operation by at least 12 hours.

Throughout the core loading, the neutron multiplication behavior was as expected. Table 2.2.1 lists the count rates for all four neutron detector channels for the first 20, and selected subsequent assemblies inserted into the core.

TABLE 2.2.1

DETECTOR COUNT RATES (CPS)
(Uncorrected for Background)

NO. ASSYS. IN CORE	TEMPORARY DET. A	TEMPORARY DET. B	STARTUP DET. 1	STARTUP DET. 2
BACKGROUND	0.0067	0.005	0.08	0.08
1	1.40	5.25	1.10	0.01
2	1.45	5.39	1.18	0.07
3	1.59	5.54	2.08	0.05
4	1.62	7.83	2.12	0.09
5	1.57	14.35	2.14	0.10
6	2.26	17.29	2.31	0.08
7(1)	3.27	17.37	2.34	0.10
8	5.24	17.91	2.32	0.08
9	5.71	17.80	2.55	0.10
10	6.84	18.09	2.44	0.08
11	18.80	18.28	2.70	0.10
12	22.24	18.36	2.64	0.08
13	22.60	18.35	2.71	0.07
14	22.58	24.29	2.71	0.08
15	22.52	37.72	2.80	0.11
16	22.93	48.07	2.65	0.05
17	23.47	55.48	2.92	0.27
18(2)	122.52	253.61	3.08	0.06
19	122.62	261.52	3.13	0.09
20	122.00	272.54	3.03	0.07
131	143.57	283.50	3.05	0.07
132(3)	142.25	282.72	2.99	1.25
133(4)	98.07	64.55	3.31	1.16
215	97.37	104.41	3.06	3.07
216(5)	97.90	--	3.09	3.14
217(6)	--	--	3.05	3.29

NOTES:

- (1) Temporary detector cables relocated; new base countrate determined
- (2) Temporary detector cables relocated; new base countrate determined
- (3) Startup neutron source "A" placed into core
- (4) Temporary detector "B" moved to core location D-15; new base countrate determined for both detectors
- (5) Temporary detector "B" removed from core before placement of this assembly
- (6) Temporary detector "A" removed from core before placement of this assembly

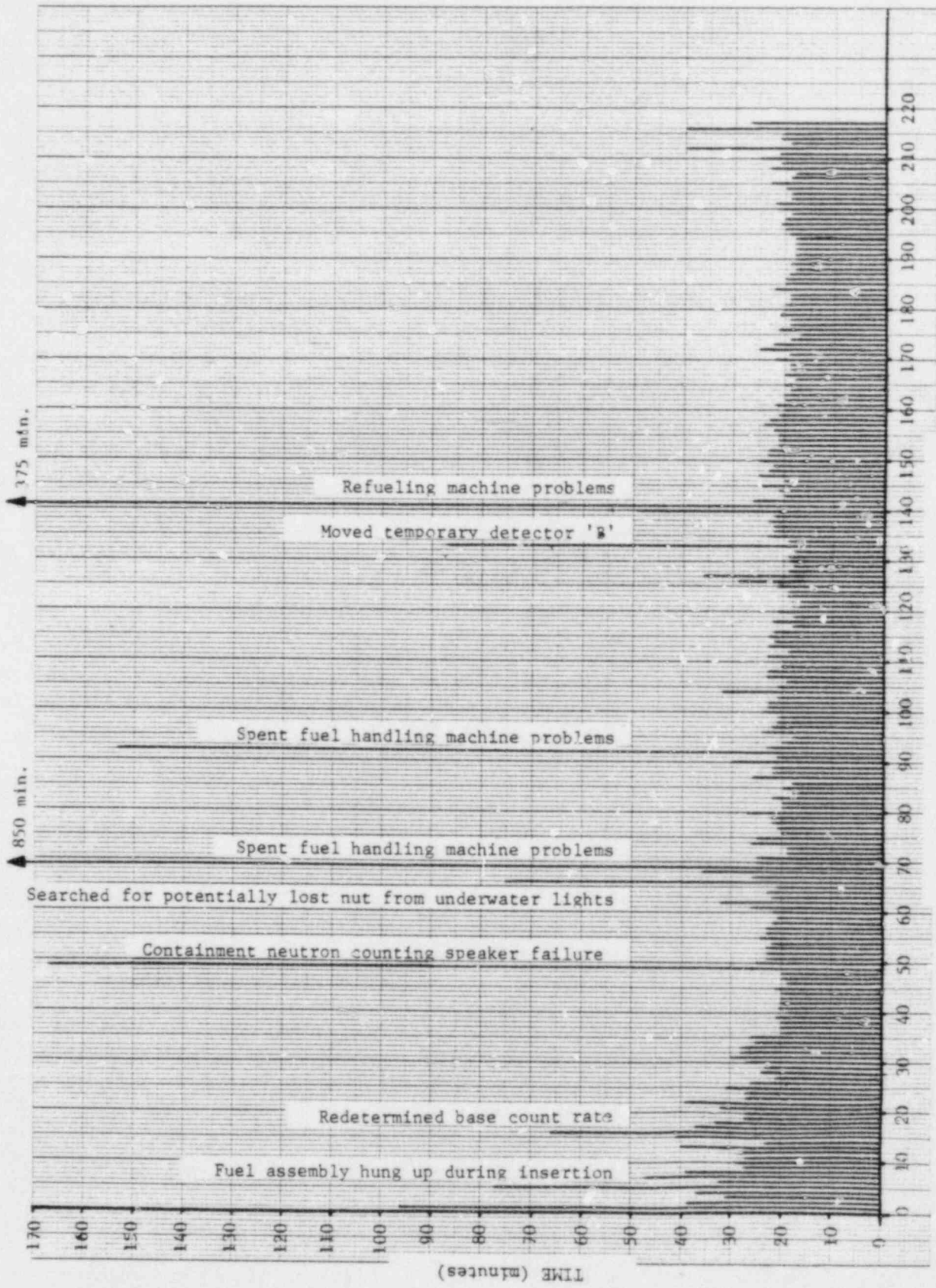
2.3 The Fuel Loading Sequence

The fuel loading sequence started at core location X-11 (reactor south side) where fuel assembly B077 containing neutron startup source "B" was placed as a free-standing assembly. Subsequent assemblies were loaded around the first assembly and, as loading progressed, around the temporary neutron detectors located at core locations V-7 and V-15, until a closely coupled slab nine assemblies wide had been formed. This slab was continued to the reactor north side, with loading alternating between an east and west direction. Core location D-15 was left vacant to accommodate temporary neutron detector "B" following insertion of the fuel assembly (B031; the 132nd assembly to be loaded) containing the second start-up neutron source, "A". Core location Y-15, vacated by the relocation of temporary neutron detector "B", was filled after the slab had been completed on the reactor north side. After the slab was complete, the east side of the core was loaded, followed by the west side, with loading occurring alternately in a north and south direction. After the east and west sides of the core had been loaded, temporary neutron detector "B" was removed from the core and the hole filled by fuel assembly B011. Finally temporary neutron detector "A" was removed from the core and the last assembly (B055) placed in its location. A two-part core loading verification verifying a) correct fuel and component location and orientation, and b) proper alignment of the fuel assemblies was then performed. This completed the core loading. Figure 2.3.1 depicts the loading sequence.

2.4 Fuel Movement

Fuel loading was executed by plant operations personnel. It was supported by Reactor Engineering Department and Combustion Engineering personnel. Fuel was loaded around the clock by three shifts per day. All personnel involved in activities involving the spent fuel handling machine, transfer systems or refueling machine were required to wear paper shoe covers, paper coveralls, cotton glove liners and head covers to maintain cleanliness requirements. Those individuals who functioned as fueling observers in the refueling pool upper level (vessel flange), were required to wear a full complement of anti-contamination clothing, (i.e., shoe covers, cloth coveralls, cloth hood and cotton glove liners under rubber gloves). Access to refueling pool was governed by a Radiation Work Permit (RWP). All personnel exiting the refueling pool area were monitored for contaminations by Health Physics.

Fuel loading officially began at 2140 on December 18, 1984, when the the spent fuel tool was latched (grappled) to fuel assembly B077 containing Startup Source "B", in spent fuel rack GG-12. This assembly was utilized to perform the neutron response check as required by the Station Technical Specifications on the two startup detectors and the two temporary detectors. The assembly was ungrappled from the refueling machine in core location X-11 at 2331 where it remained free standing until the second and third assemblies were placed in location Y-10 and Y-12 (Figure 2.3.1). Fuel loading then continued as described in section 2.3. Throughout the fuel load the reactor water level was maintained between the top of the hot legs and the vessel flange. No major fuel-related problems or delays occurred. However, several equipment problems resulted in delays to fuel loading; these are discussed in detail in section 2.6. Figure 2.4.1 shows the time elapsed between individual fuel assemblies placed in the core.



NUMBER OF FUEL ASSEMBLIES IN CORE

ELAPSED TIME BETWEEN FUEL ASSEMBLIES PLACED IN CORE

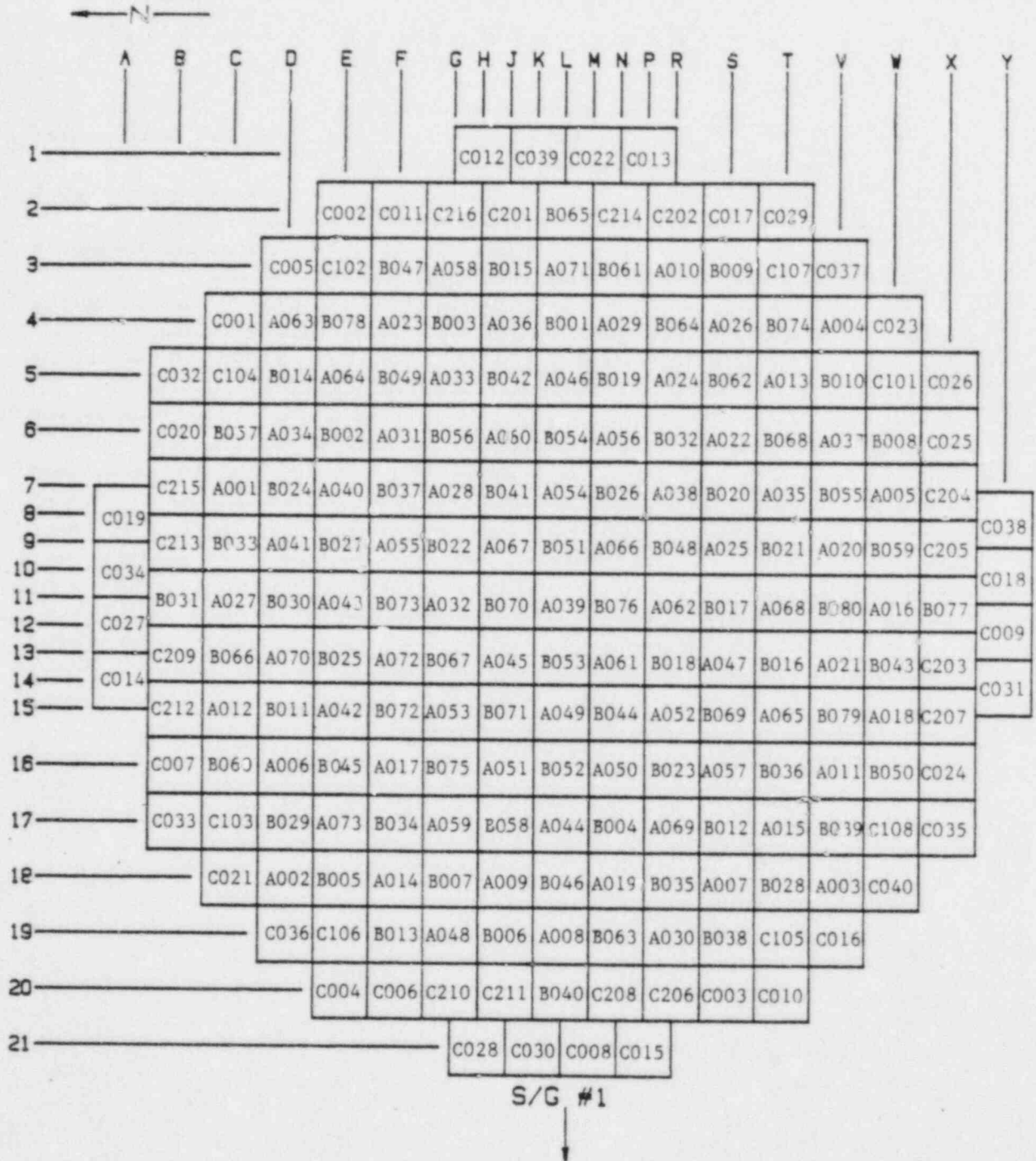
The refueling machine ungrappled from the last fuel assembly to be loaded into the core at 1500 on December 23, 1984. This completed the fuel movement portion of the initial fuel loading of WSES-3. A fuel placement and positioning verification followed.

2.5 Fuel Load Verification

The fuel load verification that followed the completion of fuel movement utilized the refueling machine fuel hoist TV system, and consisted of:

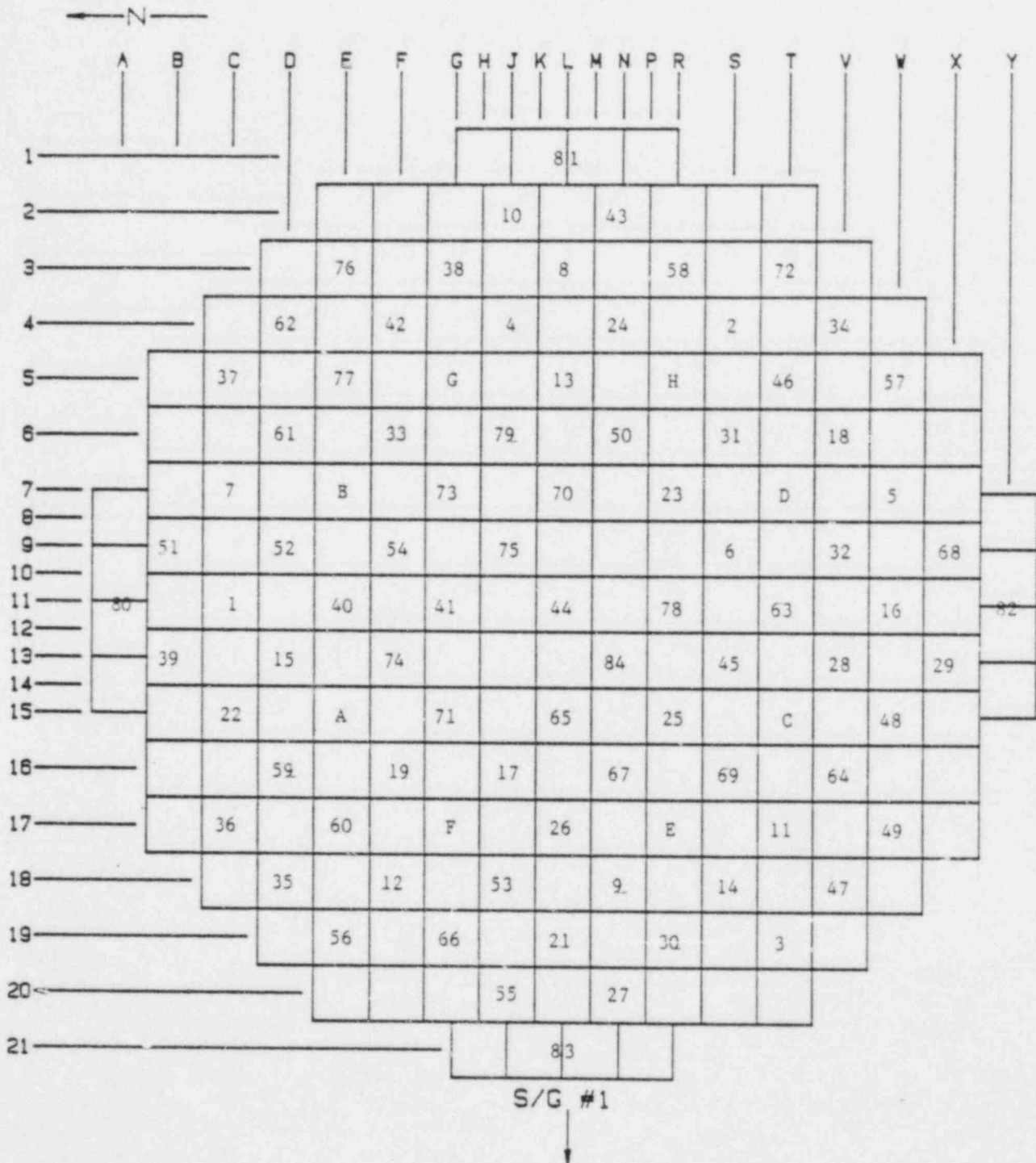
- a) Verifying all fuel assemblies, CEA's and start-up neutron sources were loaded into their pre-assigned core location and were oriented correctly. To do this the core was scanned twice: once to verify all fuel assemblies in their correct location with their serial numbers oriented to the southeast (SE), and to verify the CEA's and neutron sources in their correct host fuel assemblies; the second scan verified CEA serial numbers and double-checked their core locations. These verifications were recorded on video tape. With the exception of the 4-fingered CEA's which were loaded as an integral part of the UGS, all fuel assemblies and core components were verified correctly loaded. This verification required 11.3 hours. Figures 2.5.1, 2.5.2 and 2.5.3 show the as-loaded core.

- b) Verifying the position of the fuel assemblies to assure alignment with the fuel alignment plate of the UGS. The position of fuel assemblies with respect to the centerline of selected rows (6, 16, C, F, L, S, and W) in the core was measured, using the refueling machine fuel hoist TV camera. The data showed the fuel to have been loaded acceptably to allow the UGS to be installed into the reactor vessel. This verification required 11.5 hours.



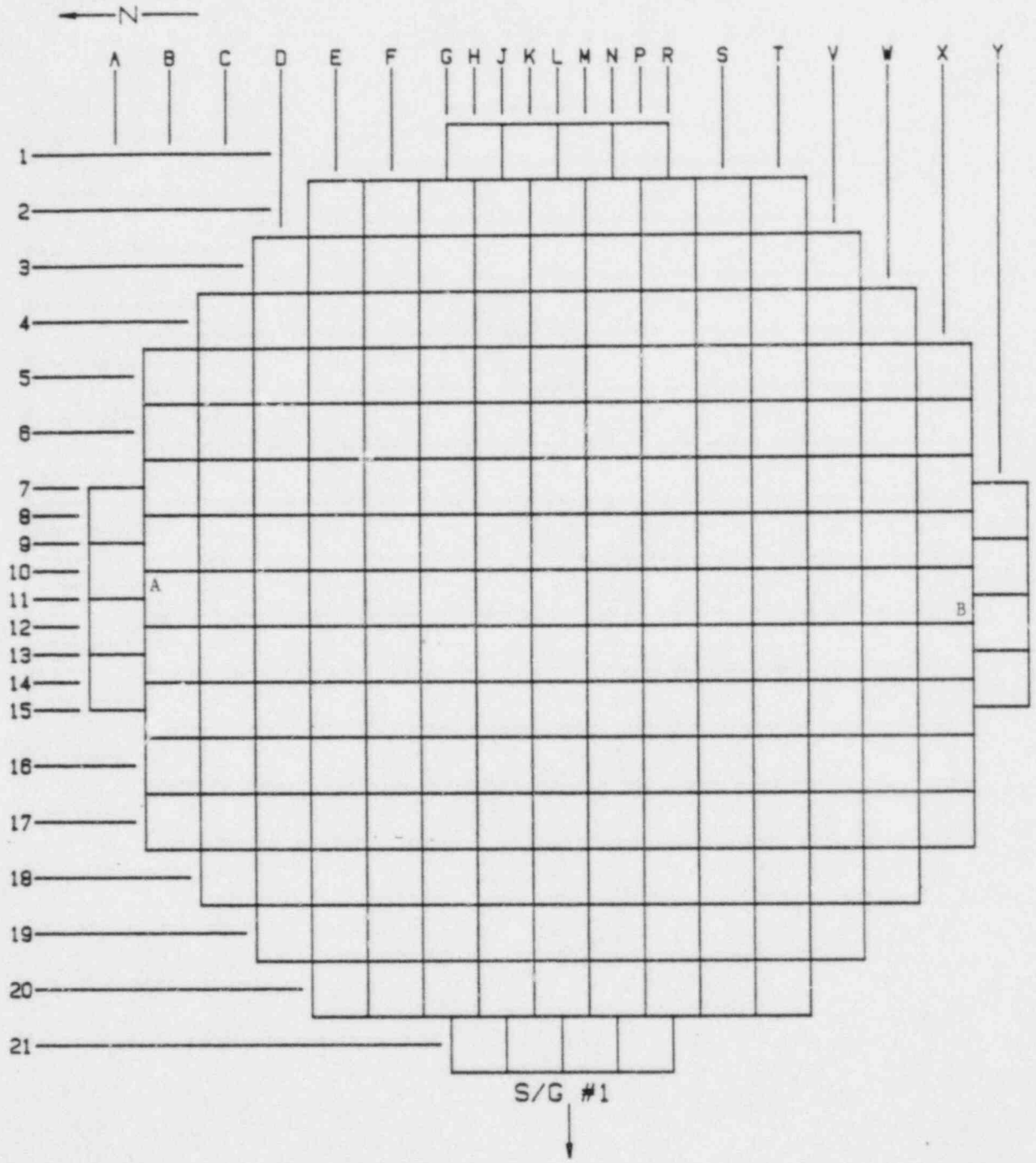
WSES-3 CYCLE 1 CORE MAP (FUEL)

FIGURE 2.5.1



WSES-3 CYCLE 1 CORE MAP (CEAs)

FIGURE 2.5.2



A = Neutron source 'A' in northeast guide tube of fuel assembly B031
 B = Neutron source 'B' in southwest guide tube of fuel assembly B077

WSES-3 CYCLE 1 CORE MAP (NEUTRON SOURCES)

FIGURE 2.5.3

2.6 Delays, Problems and Resolutions

2.6.1 Refueling machine fuel hoist underloads were experienced during fuel assembly insertion into the core at various times. In particular, fuel assembly B043 required repositioning of the refueling machine, and 29 minutes were required to finally seat the assembly in the core. Fuel assembly A016 required 14 minutes of effort and C207 took 48 minutes. Other fuel assemblies generated underloads, however none required appreciable time to correct.

Total Time Lost: ~1 hour 31 min.

2.6.2 Relocation of the handling/tie off ropes and detector cabling on the two incore detector assemblies consumed approximately 40 minutes time, in addition to the "normal" relocation and/or removal.

Total Time Lost: ~ 40 min.

2.6.3 The containment audible count rate speaker for the temporary counting station failed, resulting in a suspension of core alterations. In addition to the time required to replace the speaker - 1 hour and 41 min. - it was determined that the spent fuel handling machine operability checks would have to be reperformed, resulting in an additional delay of 3 hours 15 min.

Total Time Lost: 4 hours 56 min.

2.6.4 As a result of an overheated power cord on a "T" bar underwater light assembly, the unit was removed from within the reactor vessel. Loading activities continued, utilizing the fuel hoist TV camera lights, with no delays or problem.

Later, however, it was discovered that a $\frac{1}{2}$ -inch nominal hex nut was missing from the T-light pivot brackets. A search of the core and lower plate was made with an underwater TV system. The nut was not found.

Total Time Lost: 53 min.

- 2.6.5 A rigid coupling on the spent fuel handling machine bridge drive failed. A replacement coupling was obtained off-site, machined and installed and the spent fuel machine returned to service. After less than 8 hours of operation another drive shaft coupling failed. Closer inspection disclosed that the "C" flange mount for the gear reducer/motor unit had worked loose from the gear reducer, allowing the gear reducer/motor and output shaft to become badly misaligned with respect to the two drive shafts. The decision was made to remove the complete bridge drive train for repair. In the meantime, attempts would be made to move the bridge manually (pushed/pulled by two fuel loading personnel). The bridge was propelled this way for the remainder of the fuel load, approximately 124 fuel assemblies.

Total Time Lost: 16 hours 12 min.

- 2.6.6 The 24-volt control voltage to the refueling machine control microprocessor failed when a fuse blew, while a fuel assembly was being lowered into the core, in the lower slow zone. The fuel hoist continued to operate in the "down" mode. Main power to the machine was turned off, but not before the mechanical programmer sustained damage from being overdriven.

A cam operated switch was damaged, a coupling shear pin sheared, and cams and bearings were displaced. A replacement switch was removed from the CEA hoist mechanical programmer, a new shear pin was fabricated, the bearings and cams were repositioned and adjusted, and the machine was returned to service.

Total Time Lost: 6 hours 8 min.

Total delay, during the core load, based upon the above identified problems was just over 29 hours.

SECTION 3.0

POST-CORE HOT FUNCTIONAL TESTING

3.1 INSTRUMENTATION TESTING/CALIBRATION

3.1.1 Intercomparison of PPS, CPC, and PMC Inputs (SIT-TP-501)

PURPOSE:

The purpose of this test was to demonstrate that the inputs and appropriate outputs of the Plant Protection System (PPS), the Core Protection Calculators (CPC's), and the Plant Monitoring Computer (PMC) were in satisfactory agreement with one another. Permanent plant instruments (meters and recorders) were also intercompared.

This test satisfied the commitments of FSAR section 14.12.12.3.4.

METHOD:

Plant conditions were stabilized at each of the three test plateaus -- 120°F, 345°F, and 545°F -- during the heatup following initial fuel load. Data from each of the four sources (PPS, CPCs, PMC and meters) were simultaneously gathered for each of the following parameters:

1. RCS cold leg temperature
2. RCS hot leg temperature
3. RCP differential pressure
4. RCP speed
5. RCS pressure
6. Pressurizer level
7. Steam generator level
8. Steam generator pressure
9. Steam generator primary side differential pressure
10. Reactor vessel differential pressure

11. Containment pressure
12. Refueling water storage pool level

Based upon the data gathered for each parameter, a target value was calculated as the average of the readings from the most reliable source; the order of reliability of data sources, from most reliable to least, was as follows:

1. Core Protection Calculator data
2. Plant Protection System data
3. Plant Monitoring Computer data
4. Control Board Instrumentation Data

The deviation of each recorded value from this target value was calculated and compared to the specified tolerance to determine acceptability. If the deviation exceeded the specified tolerance, recalibration of the loop was initiated and a test deficiency was generated. The deficiency was cleared only when subsequent testing revealed that the parameter deviation fell within the specified tolerance.

RESULTS:

At the 120°F plateau, four deficiencies were generated representing forty-nine parameters' failure to meet specified criteria. Of these forty-nine, twelve were attributable to the inoperability of the Qualified Safety Parameter Display System #1 (QSPDS #1) - PMC data link, and eight were attributable to the fact that the feedwater control systems were de-energized during the performance of the data collection. Evaluation of the remaining erroneous indications was performed, and recalibration was initiated where necessary; some parameters' specific tolerances did not reflect the actual loop accuracies, and were changed accordingly.

At the 345°F plateau, a total of twenty-two parameters failed to meet their specified tolerances. Fourteen of these had also been deficient at the 120°F plateau. Four new deficiencies were written to document the eight new failures. Troubleshooting and recalibration of the problem indications continued.

At the 545°F plateau, a total of fifty parameters failed to meet their specified tolerances. The fifty parameters fell into the following three categories:

1. RCS Hot and Cold Leg RTD indications (22) - The safety-related RTD's which provide hot and cold leg temperature input to the Core Protection Calculators were all offscale at the two earlier temperature plateaus. Thus, data recorded at the 545°F plateau provided the first indication of problems with these indications. Extensive troubleshooting, recalibration, and rework of these RTD's continued throughout the power ascension test program, and a detailed history of this problem is given in section 6.2.2 of this report.
2. Remote Shutdown Panel Instrumentation (2) - Two indicators located at LCP-43, the remote shutdown panel, require transfer of pressurizer pressure and level control from the control room to LCP-43. At the time the 545°F test data were recorded, operations was unable to support this transfer. Data for these two instruments, RC-ILI-0110-1 and RC-IPI-0100-1, were successfully recorded during the performance of SIT-TP-712, the equivalent of this procedure which was performed during power ascension (see section 6.2.2).

3. Miscellaneous Indications (26) - Thirteen PMC points, ten control board meters, and three PPS inputs failed to meet their specified tolerances. Troubleshooting of these parameters continued while low power physics testing was conducted and during the wait for the unit's full power operating license. All 26 parameters were successfully tested in accordance with SIT-TP-712.

Twelve deficiencies were written at the 545°F plateau to document the fifty out-of-tolerance parameters; thirteen of these fifty had failed previously at either the 120°F or 345°F plateau.

CONCLUSIONS:

Of the fifty out-of-tolerance indications remaining at the completion of the test, twenty-three were safety-related. Only four of these were not related to the CPC hot and cold leg RTD's; these four indications were resolved and retested satisfactorily prior to initial criticality.

An evaluation of the impact of the out-of-tolerance CPC RTD's was performed, and it was determined that power operation at levels up to 20% would not be restricted. Evaluation of the RTD problems continued with the performance of SIT-TP-712 (see section 6.2.2).

3.1.2 Incore Instrumentation Baseline Data (SIT-TP-507)

PURPOSE:

This test was performed to verify that the resistance of each incore detector and background detector and their associated cabling at operating conditions was equal to or greater than 1×10^7 ohms. The test also collected baseline data for core exit thermocouple temperature readings during plant heatup.

This test satisfied in part the commitments of FSAR section 14.2.12.3.3.

METHOD:

The test was performed from January 9 through February 9, 1985. With the reactor coolant system at normal hot standby operating conditions ($\geq 525^\circ\text{F}$ and 2250 ± 15 psia) the detector resistances were measured. Each detector cable was removed at the input of the amplifier card and, using a high potential ($< 50\text{V}$) resistance meter, the individual detector and background detector resistances were measured.

At various times during the heatup, both at stable temperature plateaus and during heatup transients, the core exit temperatures were recorded using the thermocouple in each detector string. Data was recorded via computer printouts.

RESULTS:

All incore detector resistance values were greater than 1×10^7 ohms. Cable connectors at the input to amplifiers E-4 and E-6 required rework before they could be measured. Baseline core exit thermocouple data was collected at various temperatures throughout the heatup.

CONCLUSIONS:

The resistance reading for each incore detector and background detector was satisfactorily verified to be greater than 1×10^7 ohms, thereby indicating negligible impact on the incore signals from current leakage. Adequate baseline data was collected for the core exit thermocouples during plant heatup for future reference. All test objectives and acceptance criteria were met.

3.1.3 Moveable Incore Instrumentation Operation Verification
(SIT-TP-512)

PURPOSE:

The purpose of this test was to:

- a) measure the movable incore detector guide tube path lengths with the reactor coolant system cold (≤ 120 °F) for paths 18 and 23 only
- b) to measure the guide tube path lengths with the reactor coolant system hot (> 525 °F) for all 56 paths using drive machines 1 and 2
- c) to operate the movable incore detector system (MICDS) from the control room using the plant monitoring computer (PMC) as the controller
- d) to demonstrate the mechanical operation of the movable incore detector system.

This test satisfied in part the requirements of FSAR Sections 14.2.12.2.58 and 14.2.12.3.3.

METHOD:

Measurements of the guide tube path lengths for cold and hot RCS conditions were performed using the manual control box (MCB) with a dummy detector cable installed in the drive machine being tested. The dummy detector cable was inserted in the selected guide tube path until the encoder reading stopped changing. The encoder reading was recorded as step #1. The dummy detector cable was then withdrawn approximately

20 inches and reinserted until the encoder reading stopped changing. This second encoder reading was recorded as step #2. If the difference between step #1 and step #2 encoder readings was greater than 0.3 inch, the withdrawal/reinsertion was repeated and a third encoder reading was recorded as step #3. The average of the two or three encoder readings was recorded. The average reading was taken as the guide tube path length.

Cold guide tube path measurements were taken for paths 18 through 23 using drive machine 1 in the normal and alternate configurations through transfer machines 1 and 2 (a total of 12 measurements). These measurements were taken to clear a deficiency from preoperational test SPO-65C-001.

Hot guide tube path measurements were taken for all paths using drive machines 1 and 2 in the normal and alternate configurations through transfer machines 1 and 2 (a total of 112 measurements). Data from the hot guide tube path measurements was incorporated into the MICDS software on the (PMC).

The MICDS was operated from the control room using the PMC MICDS software as the controller in the manual mode using drive machines 1 and 2 and in the semiautomatic mode using drive machines 1 and 2. Proper operation of the MICDS and detector positioning to within 0.3 inch of the desired position were verified. Due to the availability of only one good dummy detector cable, PMC MICDS software operation was performed using both real detector cables installed in drive machines 1 and 2.

RESULTS:

Data from the hot MICDS guide tube path measurements yielded the following results:

- 1) The encoder readings were repeatable generally to within 0.1 inch, and at worst to within 0.4 inch.
- 2) Hot path measurements were 0.1 to 0.5 inches longer than the cold path measurements taken for paths 18 through 23. This difference can be attributed to thermal expansion.
- 3) Hot path measurements were consistent with the cold path measurements taken in preoperational test SPO-65C-001. The only exception was path 6 for transfer machine B with readings which differed by about 20 inches. Based on the repeatability of the data taken during this test, the preoperational test data is deemed to be incorrect.
- 4) The difference between the normal and alternate configurations was small and can be considered to be zero.
- 5) The MICDS hardware operated satisfactorily using the manual control box.

The MICDS software operated in the manual and semiautomatic modes, as required by this test. Two problems which affect operation using the MICDS software were discovered:

- a) The Transfer Enable switch did not indicate a "Not Enable" state when the detector was inserted past the switch. This problem would affect operation in the automatic mode only.

- b) Path verification alarm messages occurred when there were no apparent failures. This problem would affect MICDS operation in all modes.

Although these two problems were not entirely resolved, operation of the MICDS in manual and semiautomatic modes was satisfactorily demonstrated.

CONCLUSION:

The MICDS operated as required by this test. All test objectives and acceptance criteria were satisfactorily met.

3.1.4 Post-Core Vibration and Loose Parts Monitoring System
(SIT-TP-513)

PURPOSE:

To establish steady state vibration and loose parts monitoring baseline data for the four reactor coolant pumps (RCPs), the two steam generators, the reactor lower vessel and reactor upper vessel under various RCP configurations. This test satisfied, in part, the commitments of FSAR Chapter 14, Section 14.2.12.3.40, Baseline Vibration and Loose Parts Monitoring.

METHOD:

Data was recorded on cassette tapes via the vibration and loose parts monitoring system's (V&LPMS) tape recorders, during stable RCP configurations established per SIT-TP-502, Postcore RCS Flow and Coastdown Measurements. Each channel of the recorded data was then analyzed using a spectrum analyzer, and plotted using an X-Y Plotter to generate the power spectral density (PSD) signatures.

RESULTS:

This test was performed on February 10 and 11, 1985 during the performance of SIT-TP-502, as discussed above. A total of thirteen cassette tapes were used to record this data. There are two sections of recorded data, each containing four different channels, for a total of eight channels of data on the first eight tapes. Several tapes were played back through the audio monitor during the test, and it was discovered that several channels have very high levels of background noise.

An evaluation of this problem by a technician produced no resolution. To circumvent this problem, the noisy channels were switched to other tape tracks and recorded on separate tapes while the problem evaluation continued. This strategy was successful, and good results were obtained.

CONCLUSION:

Baseline data was recorded for all RCP configurations specified in SIT-TP-502, and the data acquisition acceptance criterion was thus satisfied. Evaluation of the PSD's will be performed following the installation and calibration of a new spectrum analyzer.

3.2 REACTOR COOLANT SYSTEM TESTING

3.2.1 Reactor Coolant System Flow and Flow Coastdown Measurement (SIT-TP-502)

PURPOSE:

The purpose of this test was to:

- a) Determine the as-built post-core reactor coolant system (RCS) flow rate
- b) Determine the post-core flow coastdown characteristics and to verify that the flow coastdown is consistent or conservative with respect to the coastdown characteristics assumed in the safety analysis
- c) Verify the validity of the flow-related algorithms and constants in the core protection calculator (CPCs) and the core operating limits supervisory system (COLSS)
- d) Establish reference post-core differential pressures (ΔP s) within the RCS

This test satisfied the requirements of FSAR section 14.2.12.3.2

METHOD:

This test was performed at nominal hot standby conditions of 545°F and 2250 psia. The measurements were made through a sequential combination of steady state and transient flow

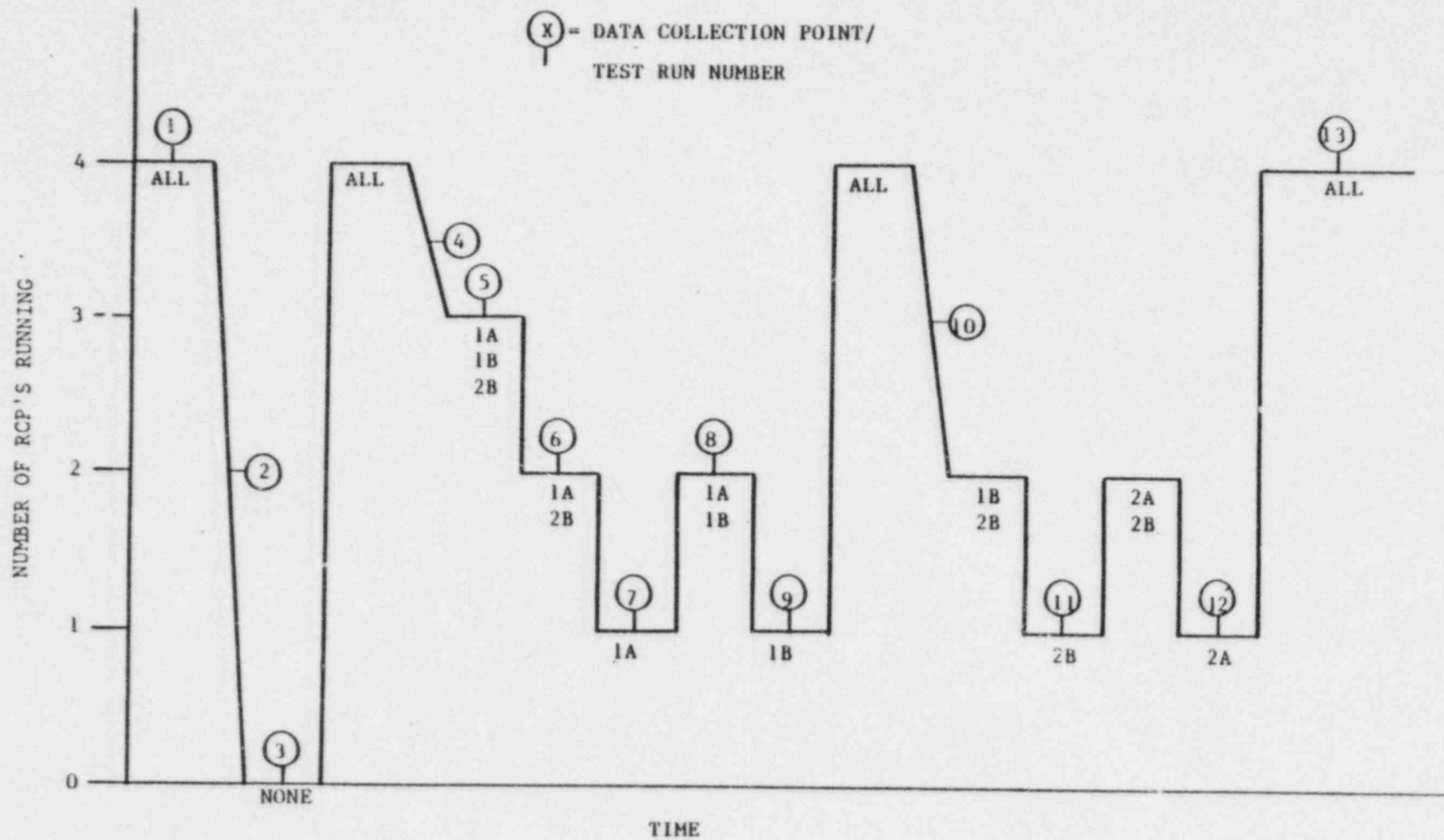
conditions as depicted in Figure 3.2.1.1. Steady state measurements were those made with a stabilized RCS flow rate provided by either 1, 2, 3, or 4 reactor coolant pumps (RCPs) running. These configurations provided data for the determination of the RCS flow rate, the verification of the CPC and COLSS constants, and the establishment of reference post-core RCS Δ Ps. Transient measurements were those made following the trip of 1, 2, or 4 RCPs, while the RCS flow was changing from one steady state configuration to another. These configurations provided data for the determination of the flow coastdown characteristics.

Within 15 days of commencing the test, all twenty RCS Δ P transmitters (8 for the RCPs, 4 for the reactor vessel (RV), and 8 for the steam generators (SG)) were calibrated to provide accurate pre-test calibration data. Following completion of test data collection the transmitters were all calibration checked to provide instrument drift data. Any drift data was subsequently figured into the flow calculations.

The four-RCP steady state RCS flow rate was determined by two different methods:

- i) using RV Δ Ps
- ii) using RCP Δ Ps

The RV Δ P method result, being the more accurate of the two, was used to meet the RCS flow rate acceptance criterion. The RCP Δ P method value was required for adjustment of COLSS flow constants, and was compared to the RV Δ P method value for information. Data collection for both methods consisted of recording RCS Δ P, RCS temperature and RCS pressure data concurrently on a high speed test data acquisition system (TDAS) at a rate of 1 sample per second. Backup data was



RCS FLOW AND FLOW COASTDOWN MEASUREMENT TEST SEQUENCE

FIGURE 3.2.1.1

recorded using the plant monitoring computer (PMC) and strip chart recorders. Averaged ΔP data was calibration corrected before the RV ΔP data was normalized to 545°F and 2250 psia, and the RCP ΔP data was normalized to a reactor coolant medium specific gravity of 0.75, such that all measured ΔP data was compatible with the respective flow vs. differential pressure curves from which the RCS flow rate was determined.

During every steady state configuration not previously established, process noise data was recorded on each of the three data collection devices for information and possible application during test data evaluation. This was accomplished by recording data at high speed (20 samples per second on the TDAS, 1 sample per second off the PMC, and at ~ 10 mm/second on the strip charts) simultaneously on all recording devices for a predetermined period of time.

Three flow coastdown measurements were performed:

- i) a 1-RCP trip flow coastdown
- ii) a 2-RCP trip flow coastdown
- iii) a 4-RCP trip flow coastdown

The 1-RCP trip flow coastdown was initiated from a 4-RCPs running steady state configuration by turning the RCP 2A switch to the "STOP" position. RCP 2A was selected based on the requirement to investigate the loss of the strongest RCP, as determined during the pre-core RCS flow measurement. This trip test collected data to verify the coastdown due to a locked rotor.

The 2-RCP trip flow coastdown was initiated from a 4-RCPs running steady state configuration by simultaneously turning the RCP 1A and 2A switches to the "STOP" position. This trip test collected data to verify the coastdown due to a loss of power from a two pump bus.

The 4-RCP trip flow coastdown was initiated from a steady state configuration by simultaneously tripping all four RCPs from a previously temporarily installed special "total-loss-of-flow" (TLOF) trip switch. This trip test collected data to verify the coastdown due to a total loss of forced reactor coolant flow.

Data collection for all three coastdowns consisted of recording RCS ΔP , RCS temperature, RCS pressure, RCP shaft speed, and RCP breaker status data concurrently on the TDAS at a rate of 20 samples per second. Backup data was recorded off the PMC and on strip charts. The TDAS was then used to calculate the flow coastdown at 50 msec intervals, using the data that it has previously collected. The calculation results provided the input for the flow coastdown curves, whose plotting was optional for the 1- and 2-RCP coastdowns, but required for the 4-RCP coastdown (Figure 3.2.1.22). The plotted curve(s) allowed evaluation of the shape of the measured curve(s) with respect to the one(s) assumed in the safety analysis to assure conservatism. An evaluation of the time (T_{90}) required by the tripped RCPs to reach 90% of rated speed (≤ 1070 rpm) was also performed as part of the verification for conservatism. For each transient test T_{90} was determined for every RCP that had been tripped. The largest T_{90} for a given transient was compared to a table of T_{90} vs. COLSS EPOL1 (Constant for power operating limit uncertainty) penalty factors specific for that transient, to determine the magnitude of the COLSS penalty factor required to be implemented into COLSS to assure conservatism for that particular flow coastdown. After all

transient testing was complete the previously determined COLSS penalty factors were compared to each other, and the largest, enveloping all others, selected as the one to be implemented into COLSS until satisfactory completion of the 80% total loss of flow test (see section 6.6.4). This approach of determining a COLSS penalty factor in place of the CPC core coolant mass flow rate calibration constant FC2 (CPC PID 061) to assure conservatism was the result of investigations made by Combustion Engineering to facilitate and expedite the post-core flow measurement based on previous performance of this test at Arkansas Nuclear One Unit 2, and San Onofre Nuclear Generation Station Units 2 and 3.

Following the satisfactory completion of the test sequence, the measured RCS flow rate was used to make the initial adjustments to the CPC and COLSS flow constants. The CPC core coolant mass flow rate calibration constant FC1 (CPC PID 060) was adjusted for each CPC channel such that the base core coolant mass flow rate constant MDBAR (CPC PID 265) for that channel reflected the calculated normalized measured flow rate value $+0.000$, -0.005 . The COLSS positive flow bias constants D15(1) through D15(4) were adjusted such that for each RCP the difference, $\Delta F(j)$ (with $j = 1-4$), between the COLSS calculated individual RCP average volumetric flow rate and the measured individual RCP volumetric flow rate normalized to the total vessel flow rate was $-396 \text{ gpm} \leq \Delta F(j) \text{ gpm} \leq +396 \text{ gpm}$, AND the difference, $\Delta F(RV)$, between the COLSS calculated average RCS flow rate and the measured RCS flow rate as a percentage of design flow was $-0.2\% \leq \Delta F(RV) \leq +0.2\%$.

RESULTS:

This test was performed twice. Its first execution was terminated following completion of the steady state and transient flow calculations prior to adjusting the CPC and COLSS constants, because data evaluation revealed a significant difference in the pre-test calibration and post-test calibration check ΔP data, making the 4-RCP steady state and 4-RCP flow coastdown test results highly questionable. The 1-RCP and 2-RCP flow coastdown portions were unaffected by this deficiency, because only T_{90} , which is independent of the ΔP transmitter calibration, was used in the determination of flow coastdown conservatism. Furthermore, the establishment of baseline post-core differential pressures within the RCS does not require repeatability to the same degree of accuracy required for the valid determination of a 4-RCP steady state RCS flow rate and validation of the 4-RCP flow coastdown curve assumed in the safety analysis, and was therefore not required to be repeated either. Thus only the 4-RCP steady state and flow coastdown portions of the test were reformed, following a recalibration of the ΔP transmitters.

The steady state RCS flow rate was satisfactorily determined during the retest. The test results are shown in Table 3.2.1.1.

TABLE 3.2.1.1

4-RCP STEADY STATE PCHFT RCS FLOW RATE MEASUREMENT TEST RESULTS

METHOD	RCS FLOW RATE		ACCEPTANCE CRITERIA [gpm]
	gpm	Normalized to 148×10^6 lbm/hr	
RV ΔP	449648.6	1.1495	$418400 \leq \text{FLOW} \leq 452800$
RCP ΔP	447458.9	1.1439	N/A

The values in Table 3.2.1.1 were calculated using only pre-test ΔP calibration data in order to expedite completion of testing and data evaluation. When post-test ΔP calibration check data became available, this was compared to pre-test data in the form of plots included in this report for documentation as Figures 3.2.1.2 through 3.2.1.21. The satisfactory repeatability eliminated the need to reperform the flow calculations to compensate for instrument drift. It should be noted that RCP ΔP transmitter PDT-110 for RCP 1A (Figure 3.2.1.2) was not used in performance of the flow calculations due to its erratic response.

The actual four-RCP trip flow coastdown was much more conservative than the flow coastdown assumed in the safety analysis. The conservatism of the shape of the measured coastdown (Figure 3.2.1.22) was, however, questionable due to the electronic noise components of the measured parameters incorporated into the flow calculations. Although the best fitted flow coastdown curve was satisfactory not all of its data points lay above the FSAR flow coastdown curve. Thus, to assure that COLSS be conservative and the plant be operated in its analyzed operating space, the value of -4.7175 determined

for EPOL1 during all coastdown testing, was increased to -7.0000. This value was implemented and retained until later power ascension test results allowed a decrease to this penalty factor to be made.

The initial adjustments to the CPC and COLSS flow constants were satisfactorily determined and implemented into the respective data bases, as required. Tables 3.2.1.2 and 3.2.1.3 list the as-left CPC and COLSS constants, respectively.

TABLE 3.2.1.2

AS-LEFT PCHFT CPC FLOW CONSTANTS

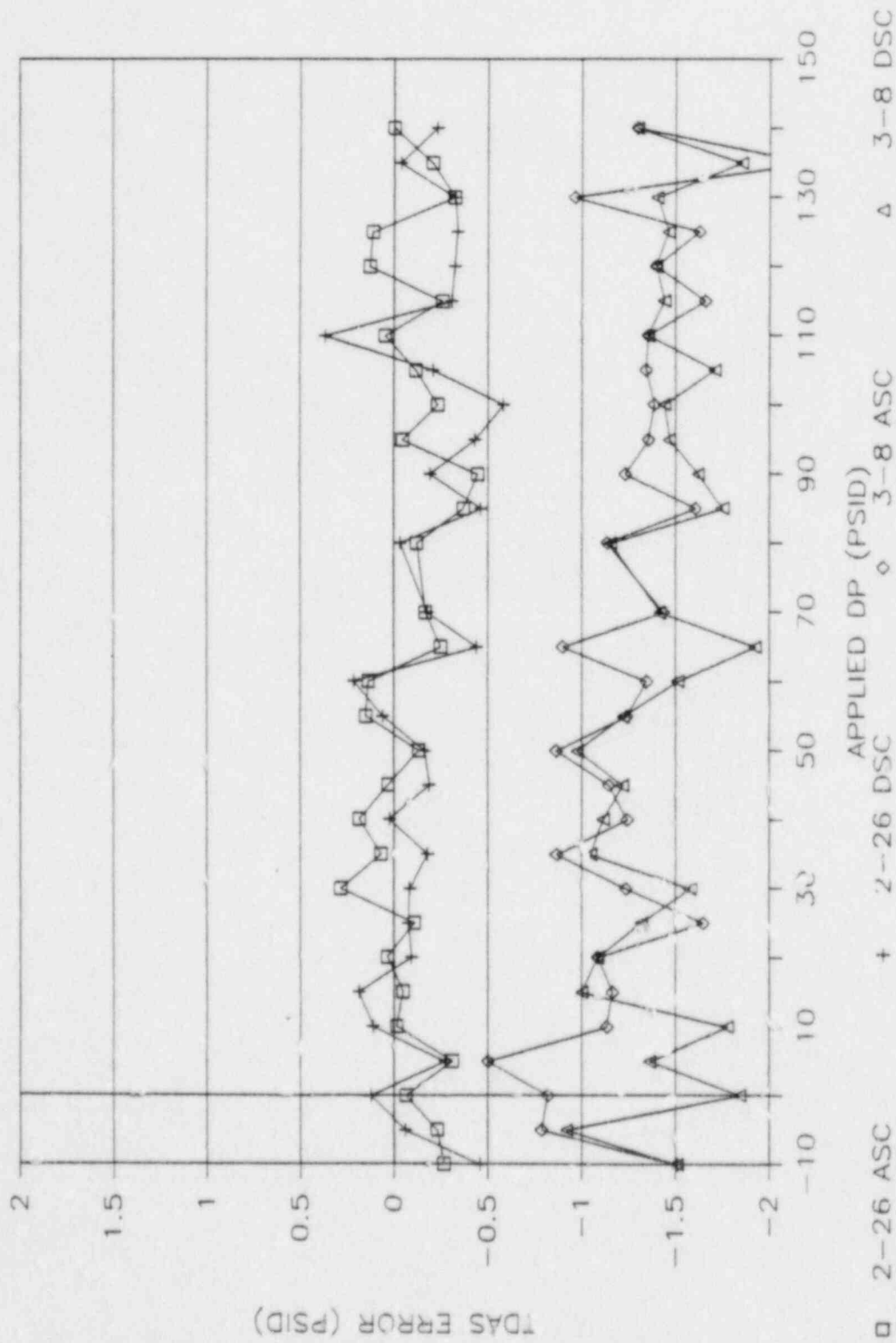
CPC CHANNEL	FLOW CONSTANT		
	FC1	FC2	MDBAR
A	1.1213	0.0	1.1488
B	1.1212	0.0	1.1482
C	1.1218	0.0	1.1490
D	1.1209	0.0	1.1489

TABLE 3.2.1.3

AS-LEFT PCHFT COLSS FLOW CONSTANTS

CONSTANT DESCRIPTION	CONSTANT VALUE
D15(1) - RCP 1A	-410.1
D15(2) - RCP 1B	-1392.4
D15(3) - RCP 2A	-109.1
D15(4) - RCP 2B	-227.9
EPOL1	-7.0000

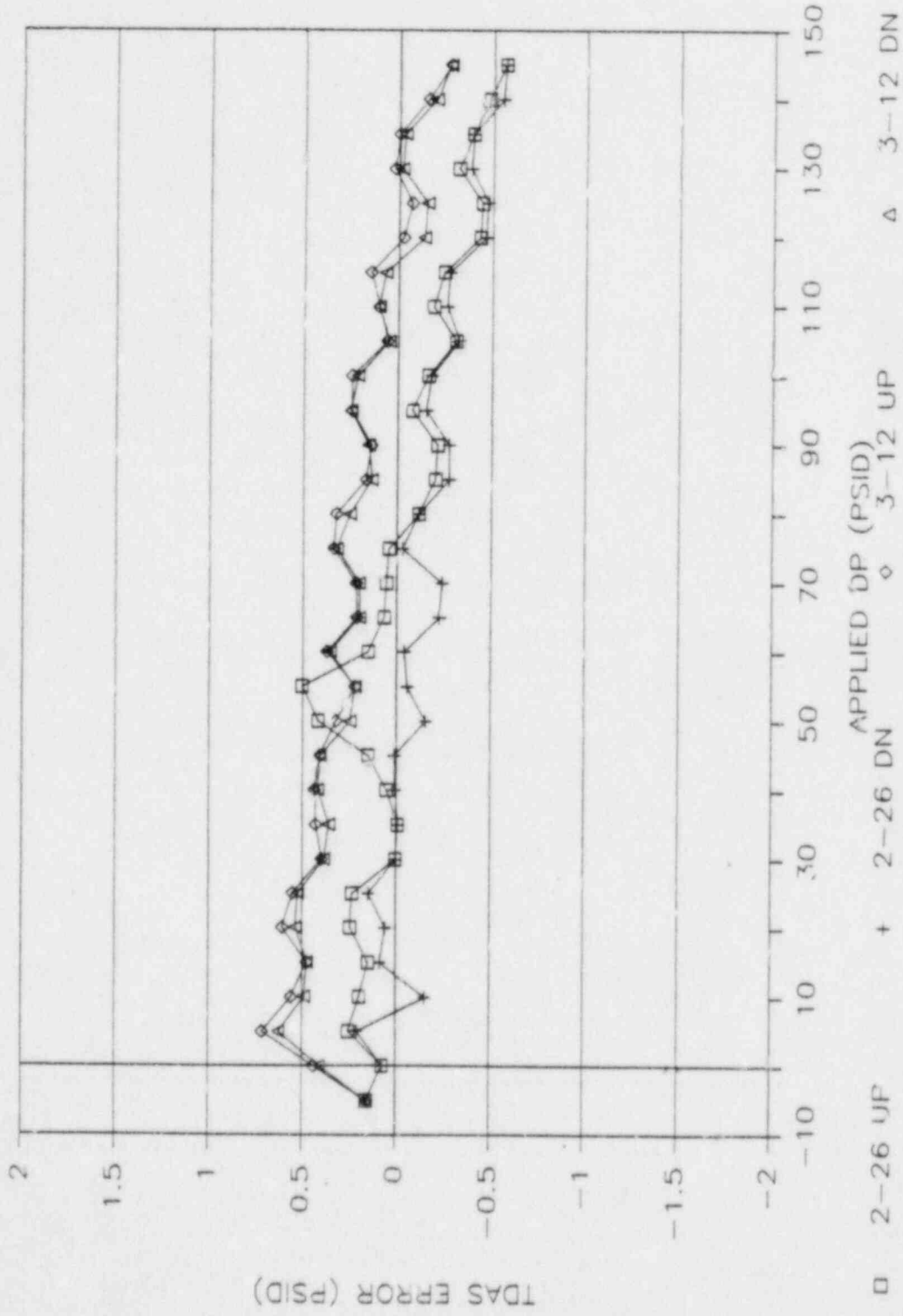
PDT-0110



RCP 1A DIFFERENTIAL PRESSURE TRANSMITTER PDT-0110 CALIBRATION CURVES

FIGURE 3.2.1.2

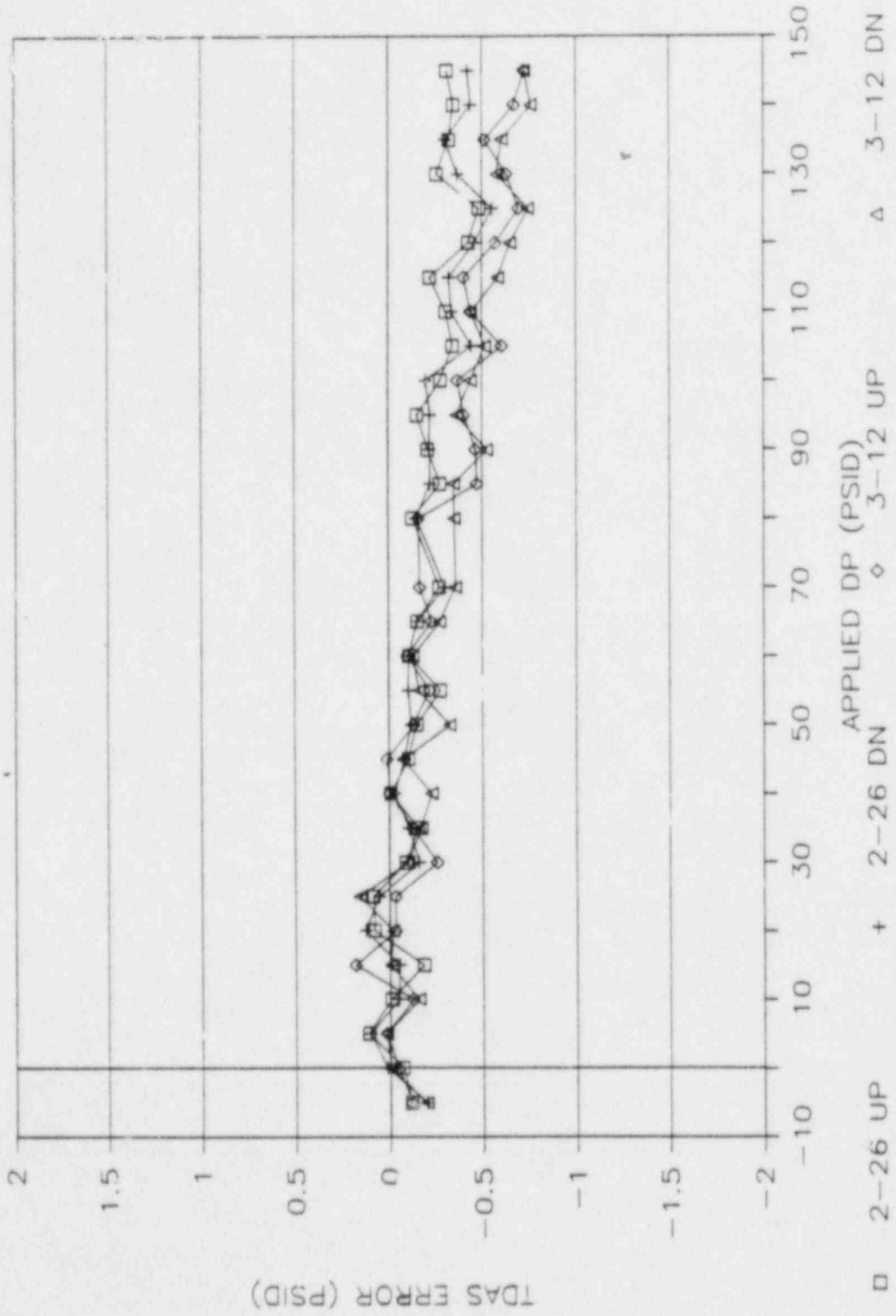
PDT-0111



RCP 1A DIFFERENTIAL PRESSURE TRANSMITTER PDT-0111 CALIBRATION CURVES

FIGURE 3-2.1.3

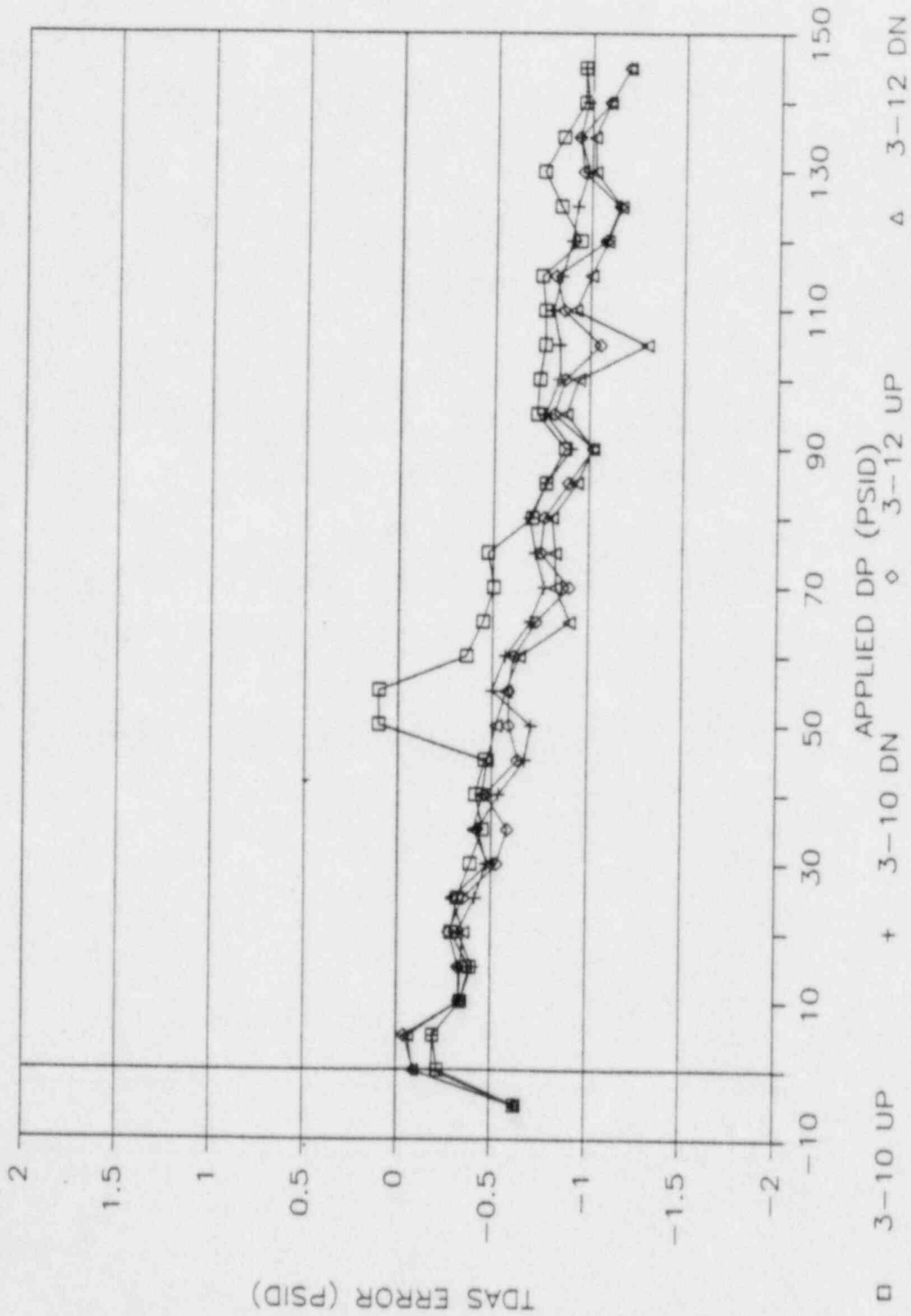
PDT--0112



RCP 1B DIFFERENTIAL PRESSURE TRANSMITTER PDT-0112 CALIBRATION CURVES

FIGURE 3.2.1.4

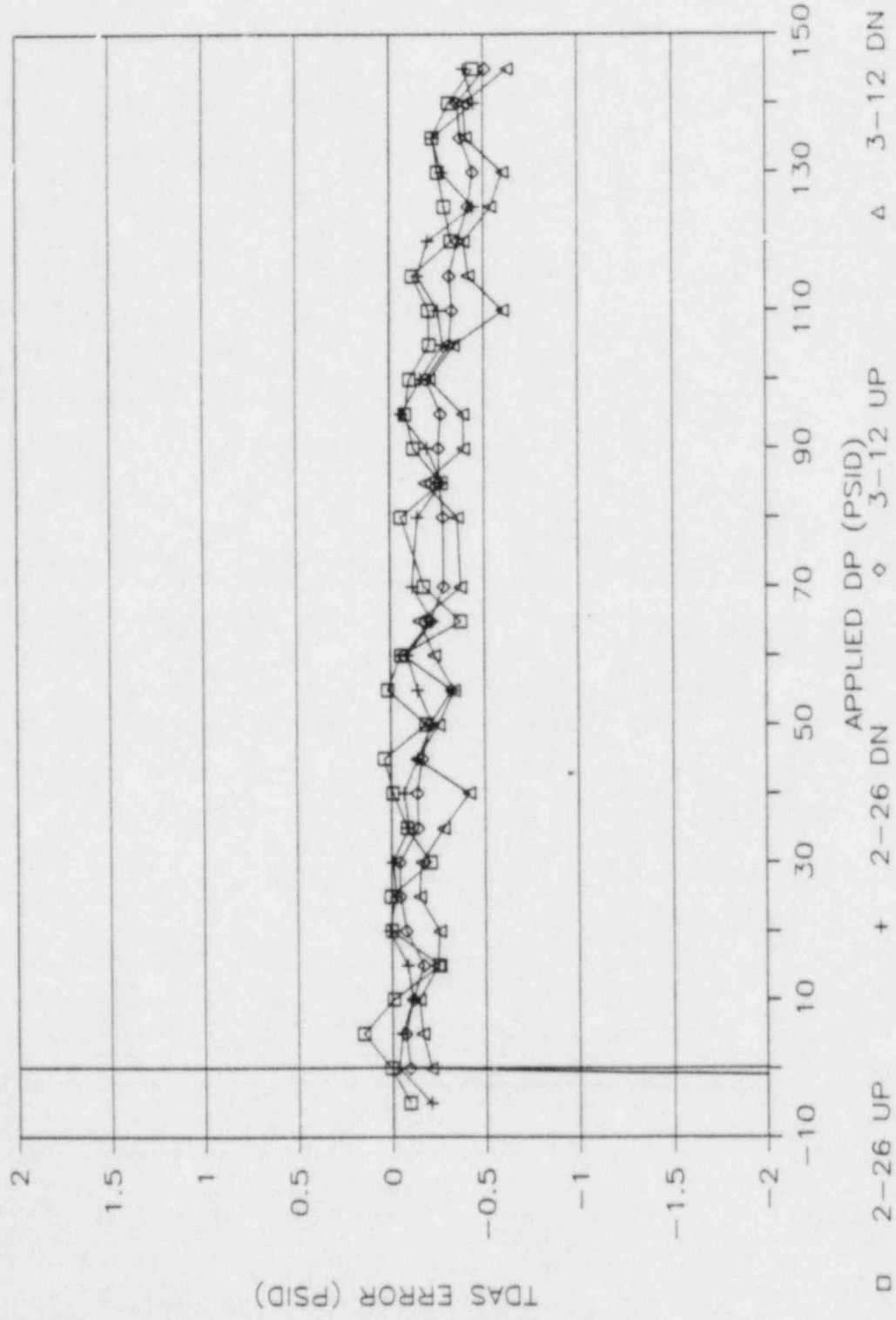
PDT-0113



RCP 1B DIFFERENTIAL PRESSURE TRANSMITTER PDT-0113 CALIBRATION CURVES

FIGURE 3.2.1.5

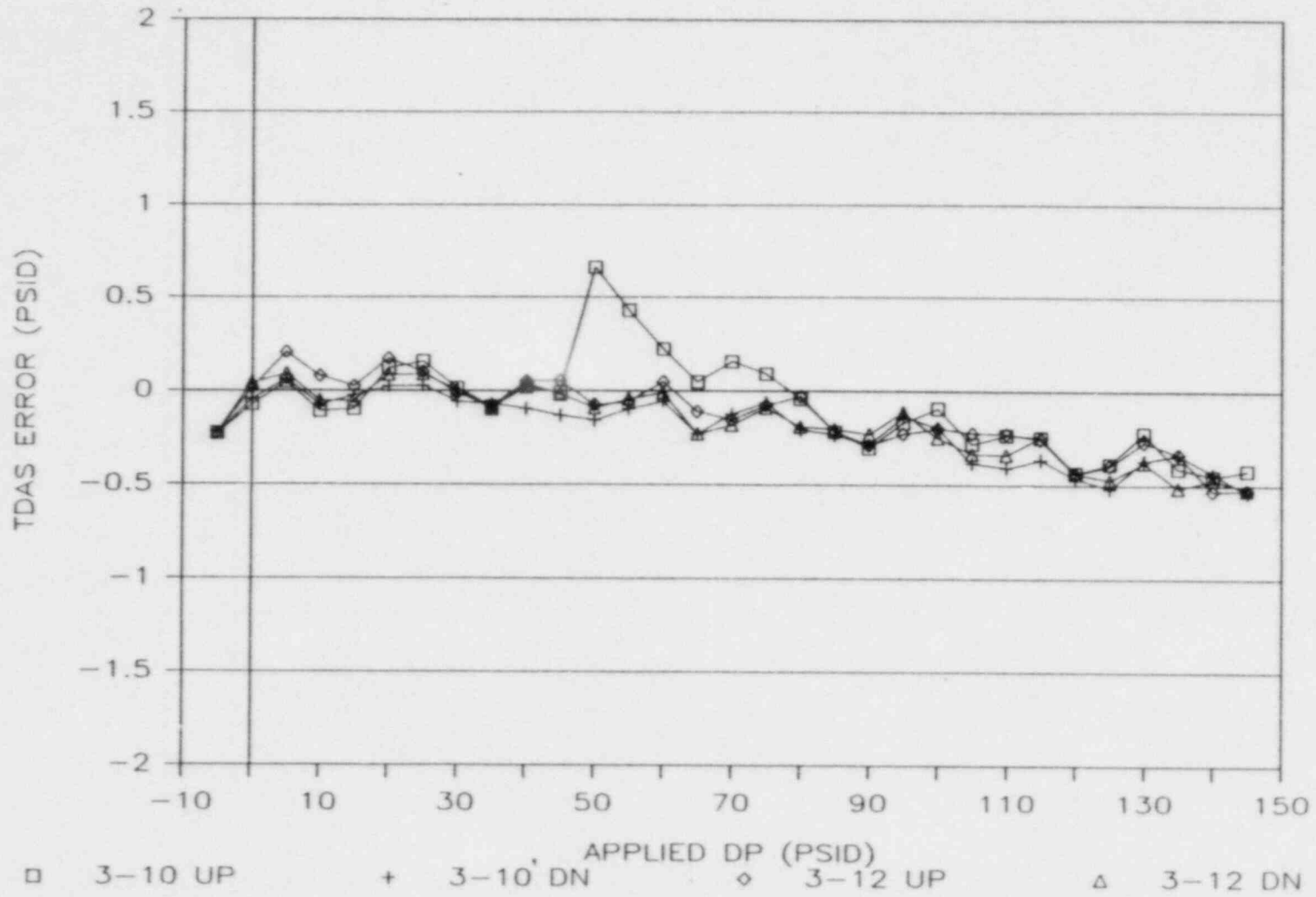
PDT-0120



RCP 2A DIFFERENTIAL PRESSURE TRANSMITTER PDT-0120 CALIBRATION CURVES

FIGURE 3.2.1.6

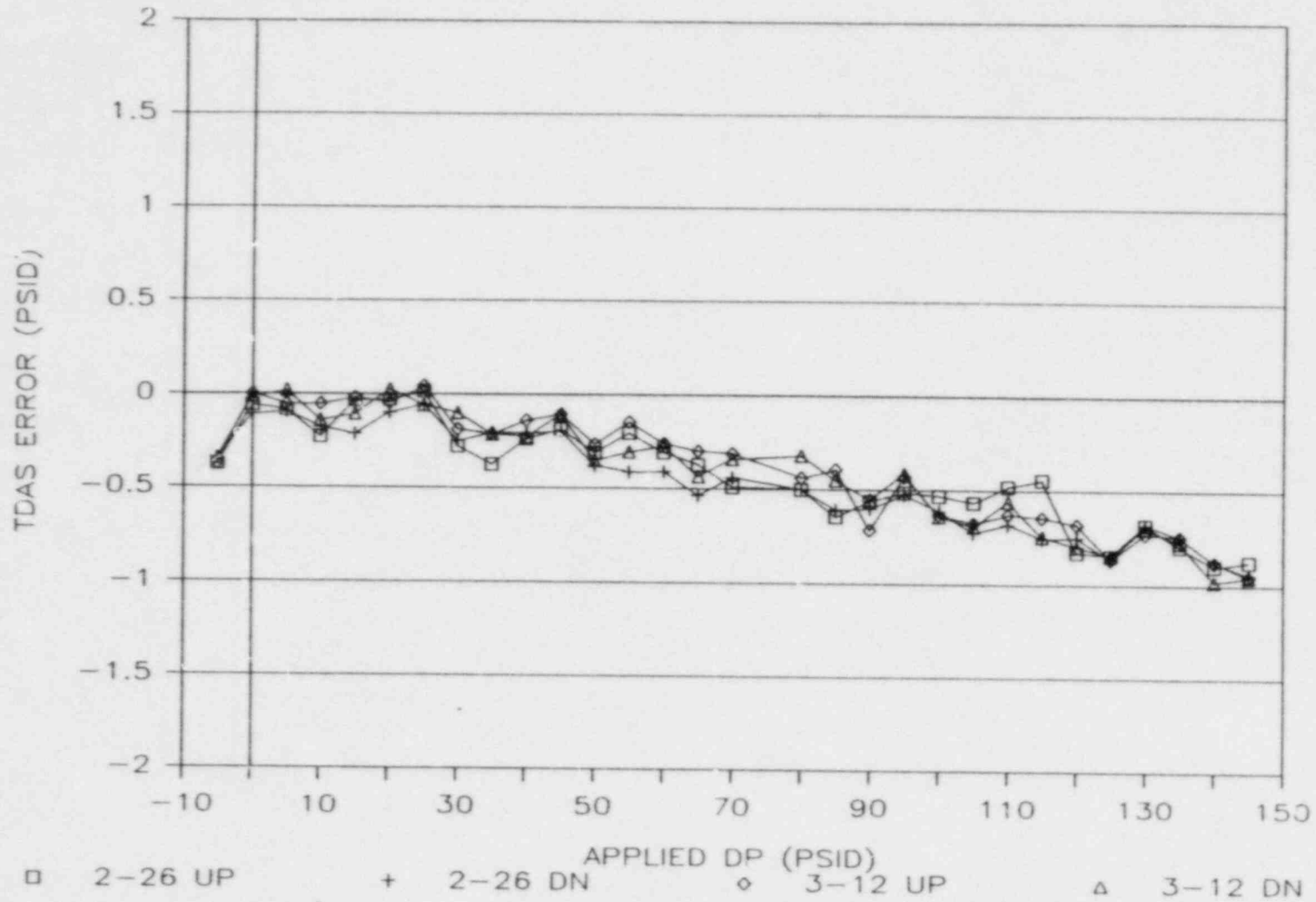
PDT-0121



RCP 2A DIFFERENTIAL PRESSURE TRANSMITTER PDT-0121 CALIBRATION CURVES

FIGURE 3.2.1.7

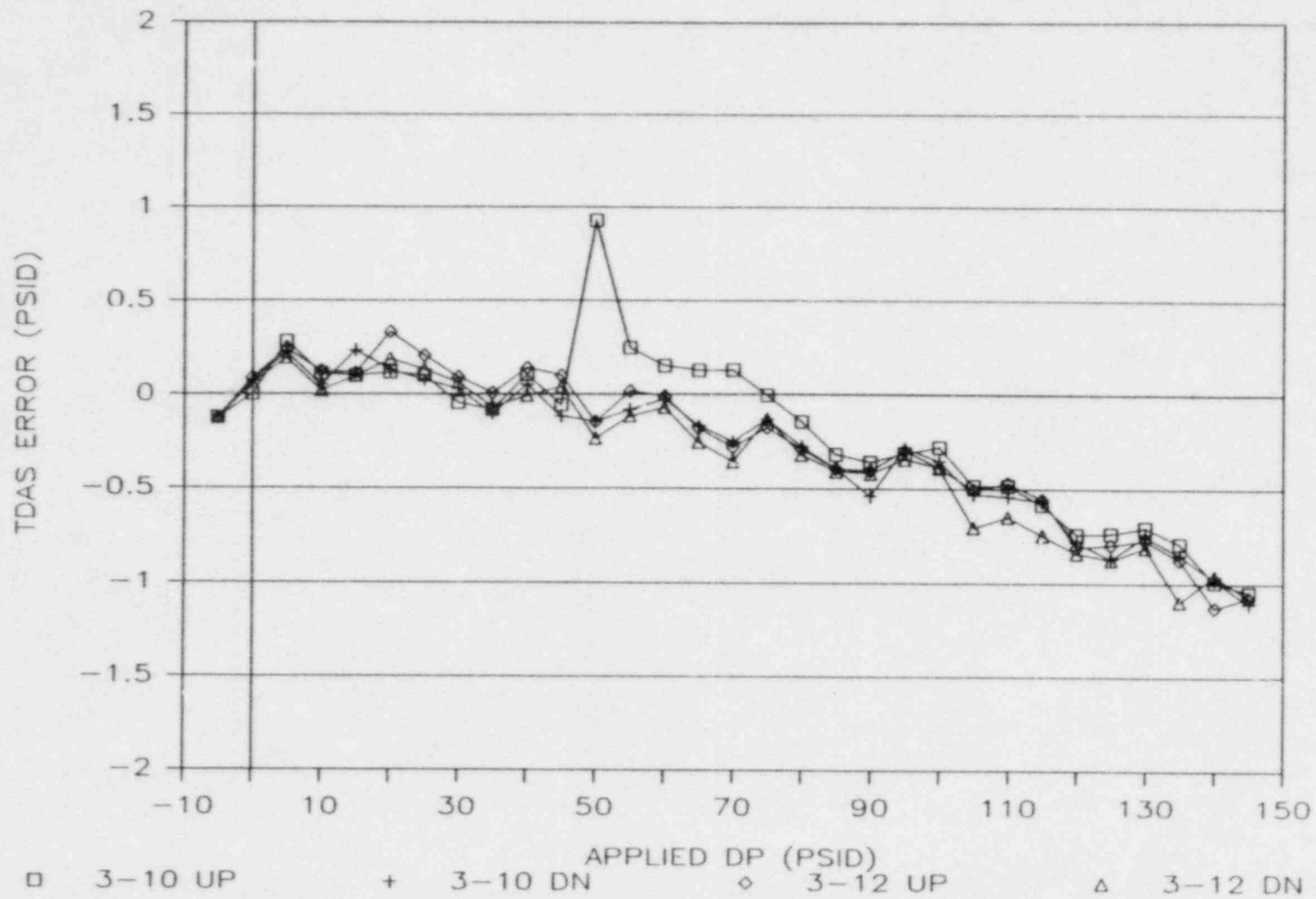
PDT-0122



RCP 2B DIFFERENTIAL PRESSURE TRANSMITTER PDT-0122 CALIBRATION CURVES

FIGURE 3.2.1.8

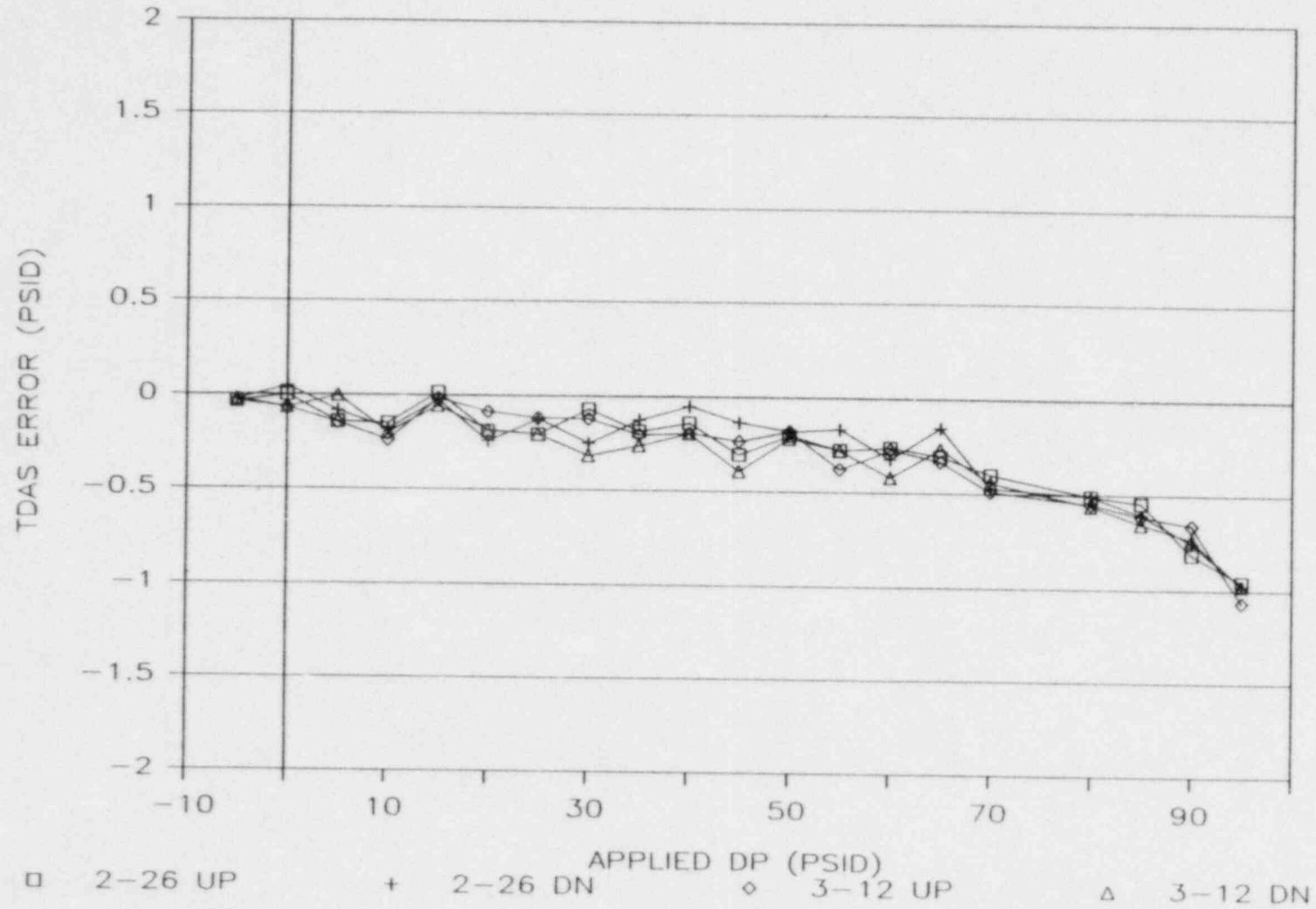
PDT-0123



RCP 2B DIFFERENTIAL PRESSURE TRANSMITTER PDT-0123 CALIBRATION CURVES

FIGURE 3.2.1.9

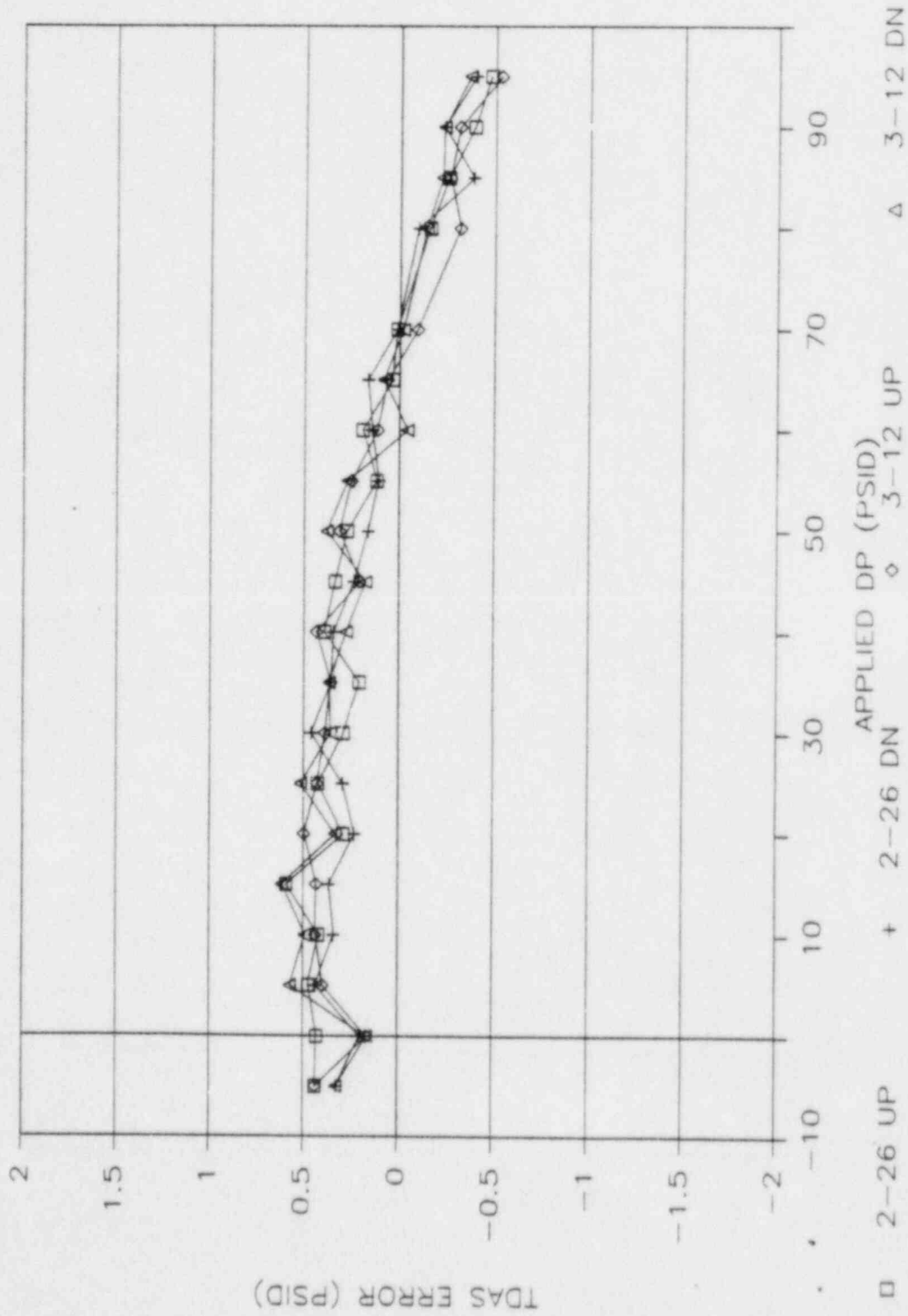
PDT-124W



REACTOR VESSEL 1A DIFFERENTIAL PRESSURE TRANSMITTER PDT-0124W CALIBRATION CURVES

FIGURE 3.2.1.10

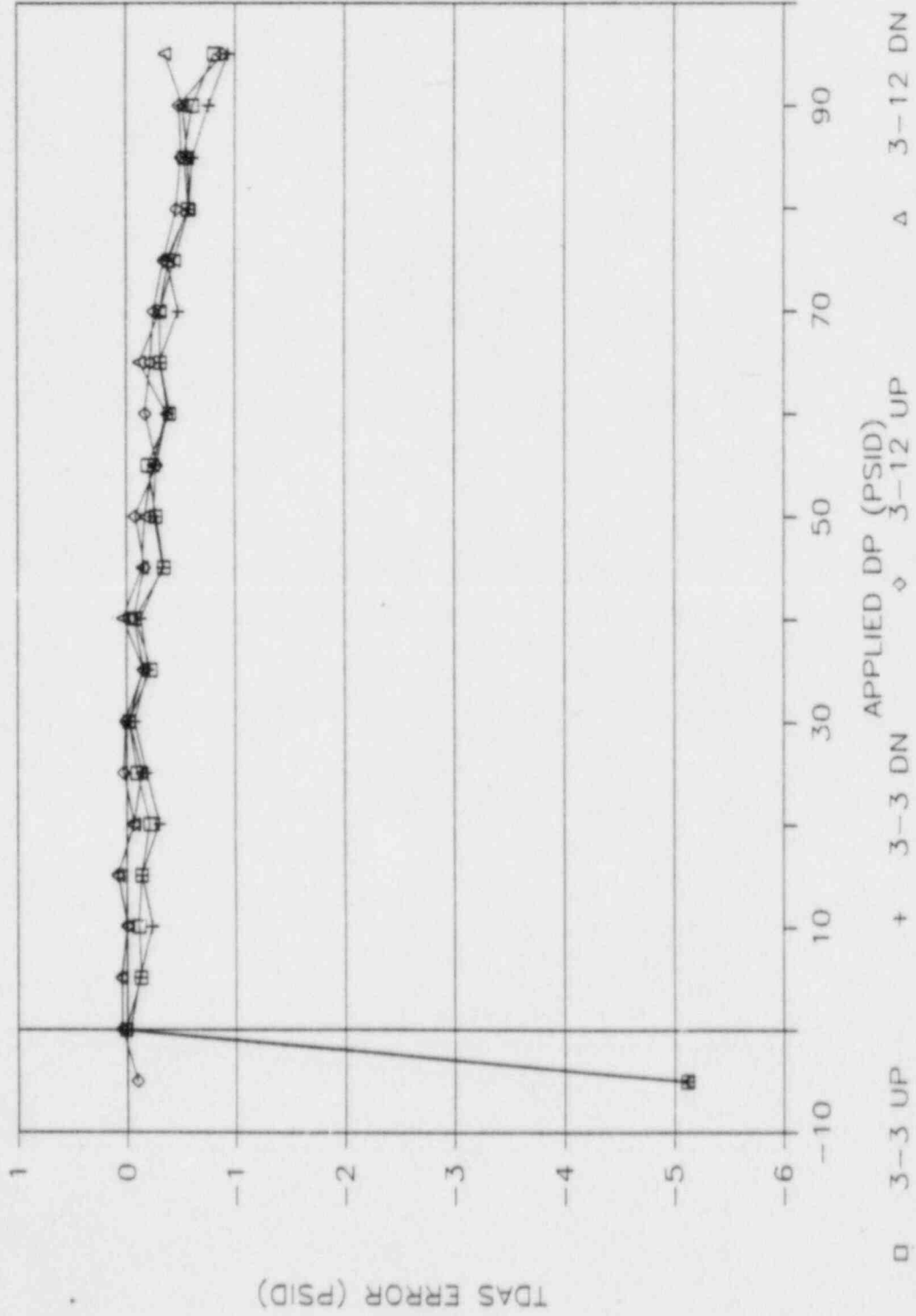
PDT-124X



REACTOR VESSEL 1B DIFFERENTIAL PRESSURE TRANSMITTER PDT-0124X CALIBRATION CURVES

FIGURE 3.2.1.11

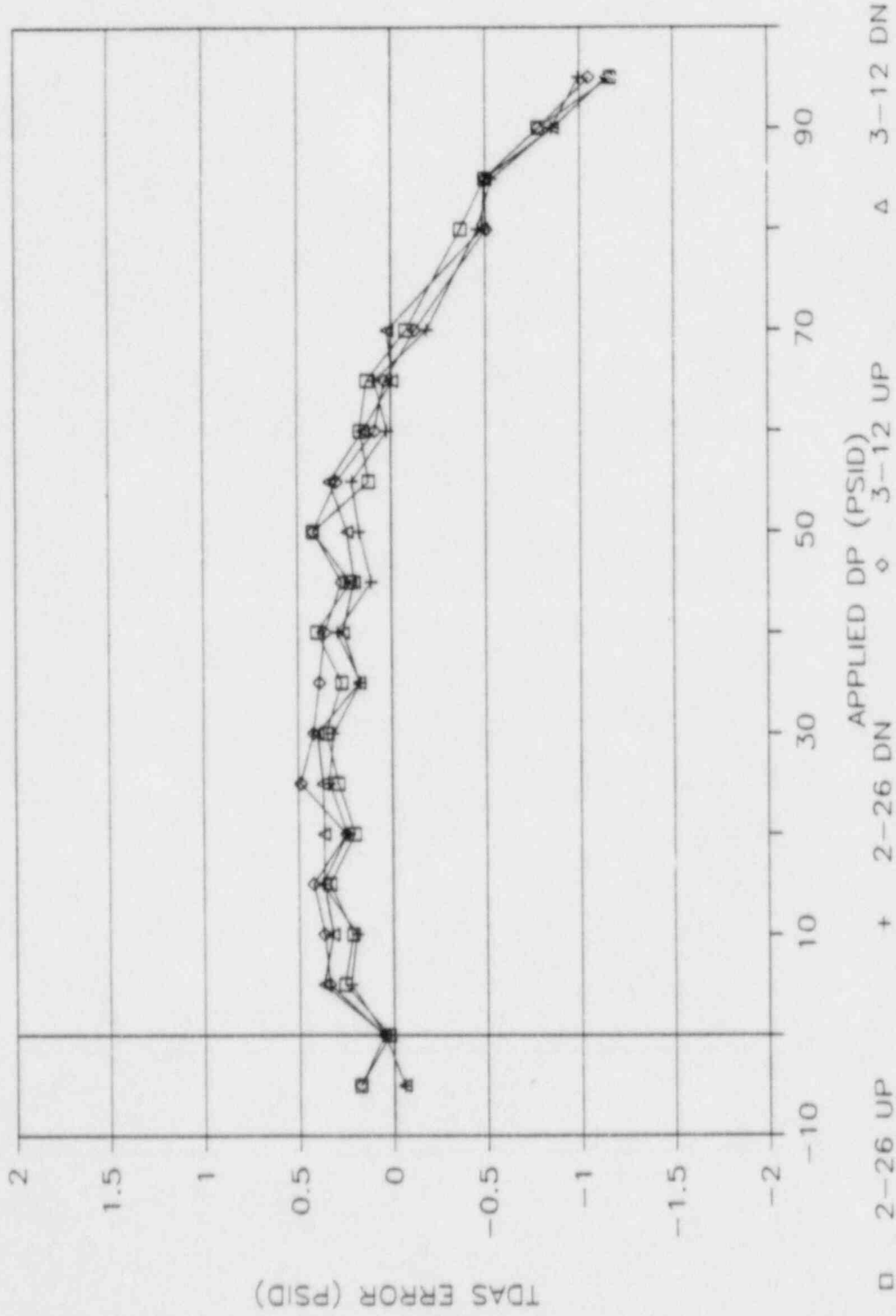
PDT-124Y



REACTOR VESSEL 2A DIFFERENTIAL PRESSURE TRANSMITTER PDT-0124Y CALIBRATION CURVES

FIGURE 3.2.1.12

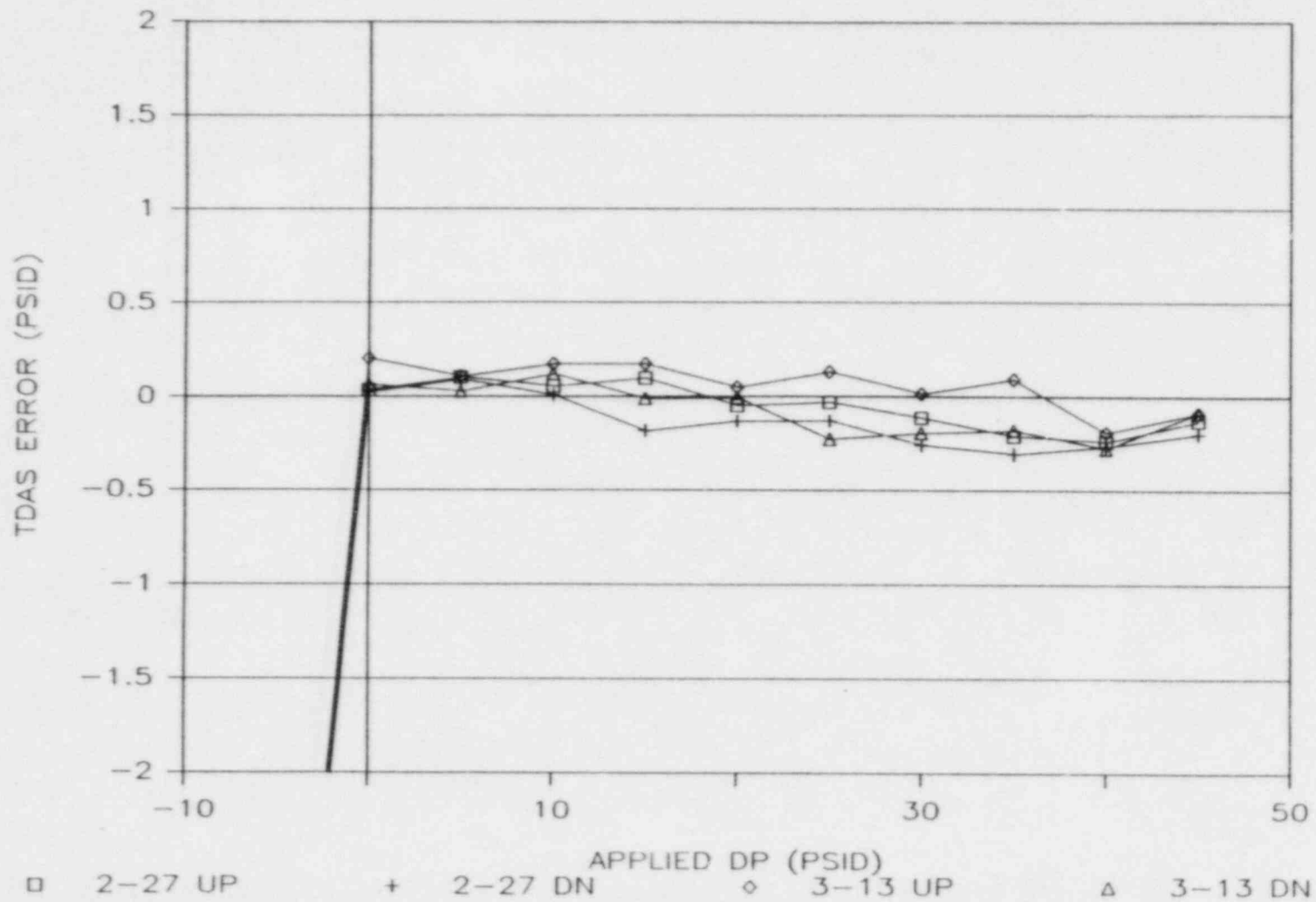
PDT-124Z



REACTOR VESSEL 2B DIFFERENTIAL PRESSURE TRANSMITTER PDT-0124Z CALIBRATION CURVES

FIGURE 3.2.1.13

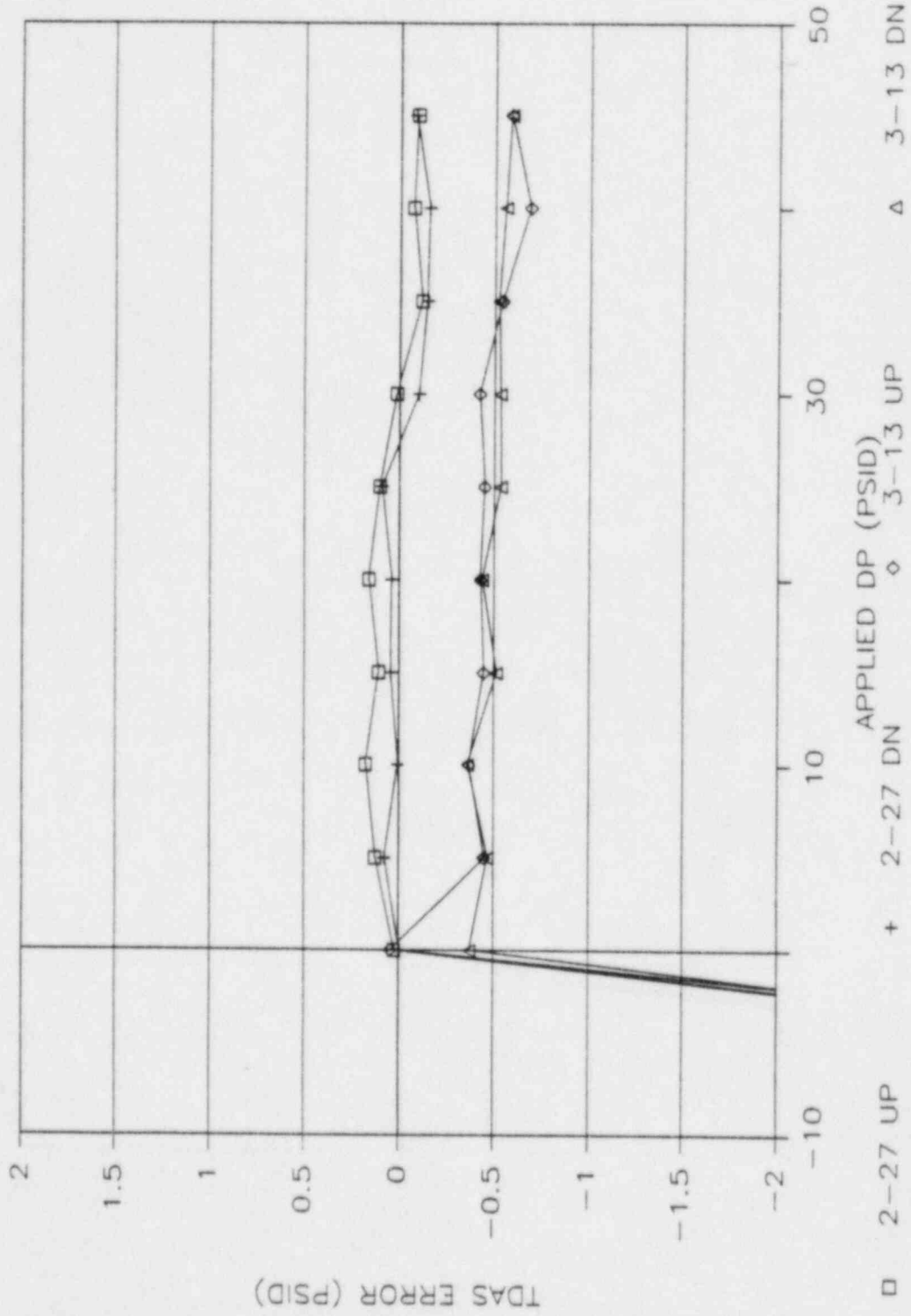
PDT-9116-SMA



STEAM GENERATOR #1 DIFFERENTIAL PRESSURE TRANSMITTER PDT-9116-SMA CALIBRATION CURVES

FIGURE 3.2.1.14

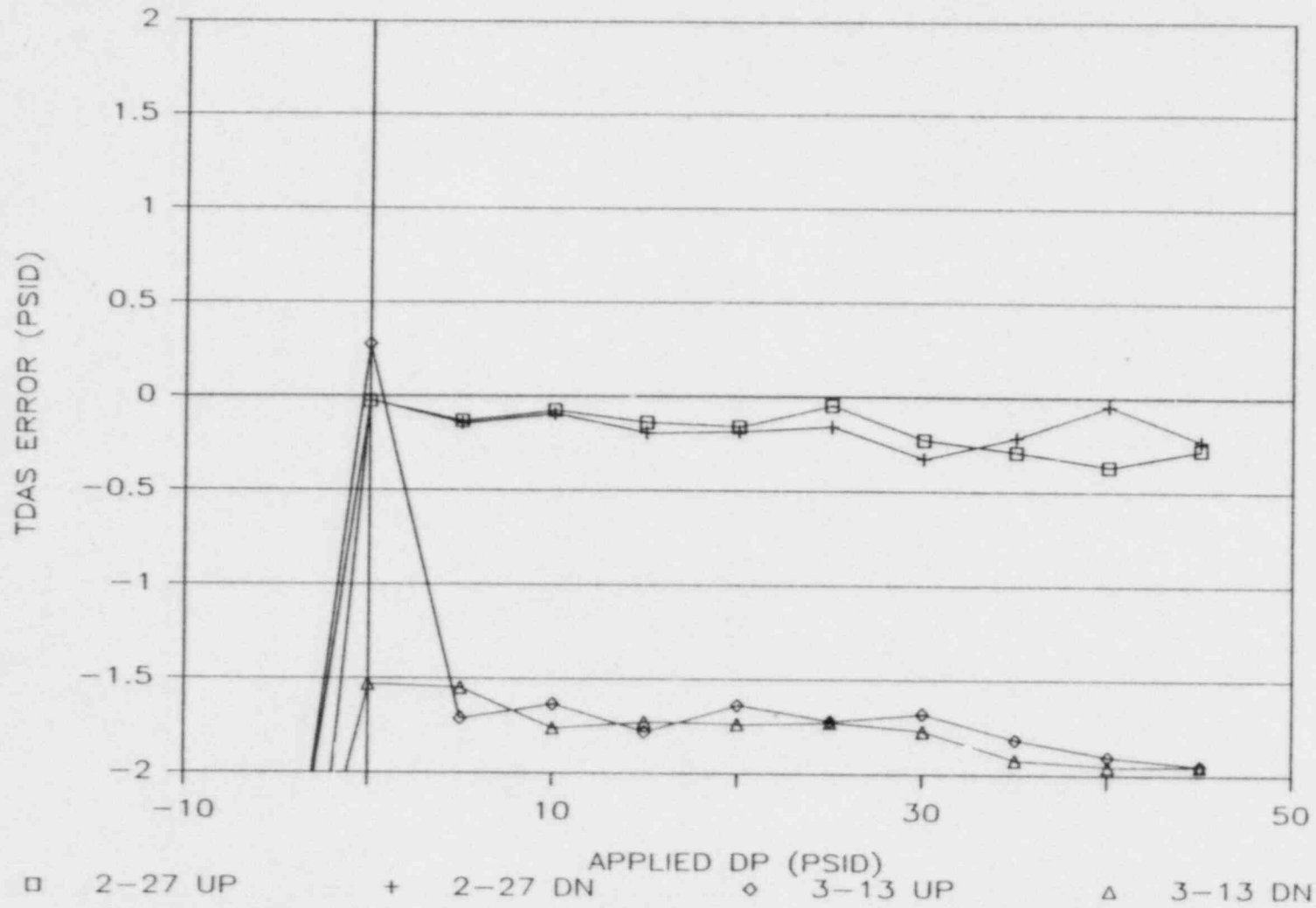
PDT-9116-SMB



STEAM GENERATOR #1 DIFFERENTIAL PRESSURE TRANSMITTER PDT-9116-SMB CALIBRATION CURVES

FIGURE 3.2.1.15

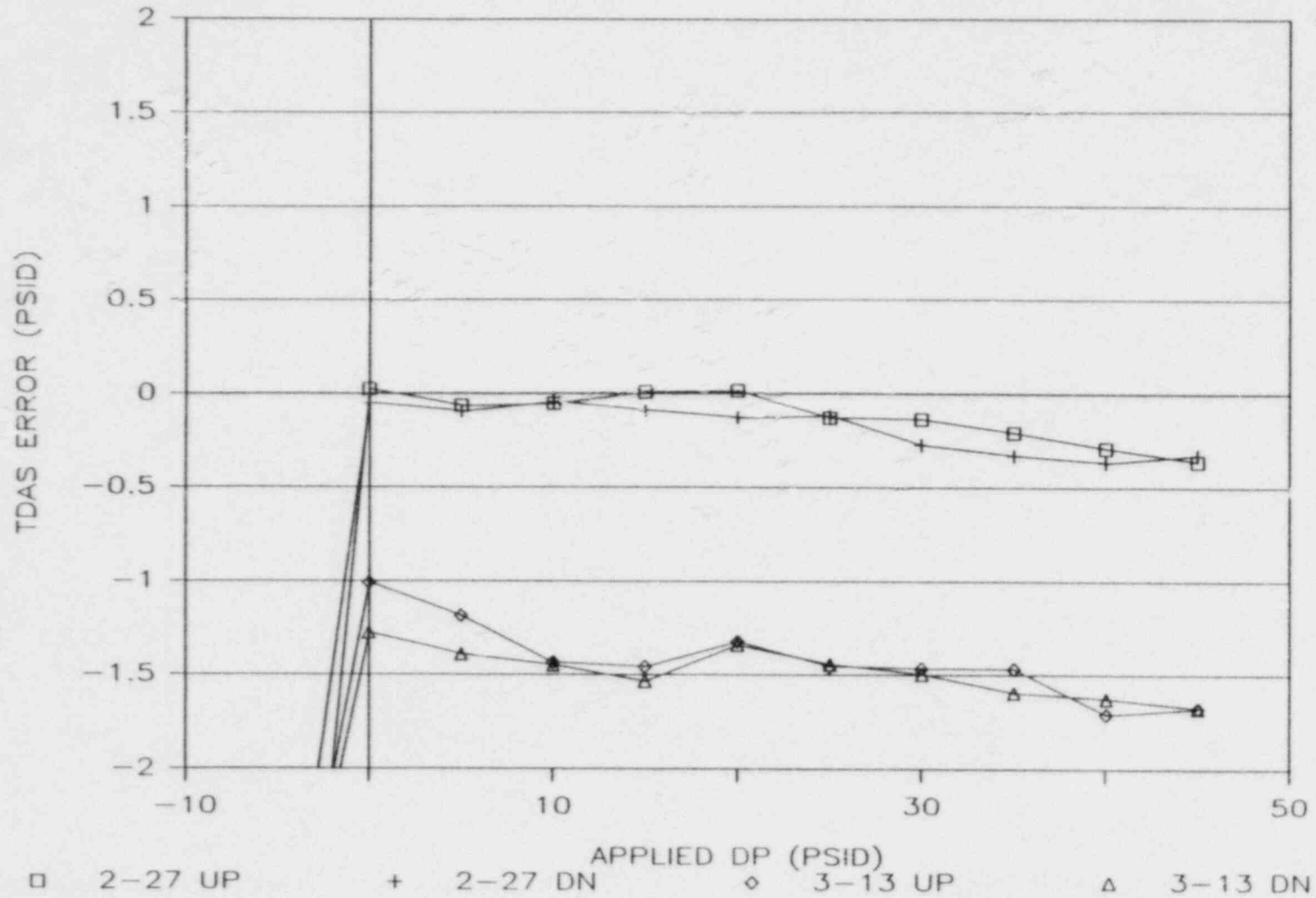
PDT-9116-SMC



STEAM GENERATOR #1 DIFFERENTIAL PRESSURE TRANSMITTER PDT-9116-SMC CALIBRATION CURVES

FIGURE 3.2.1.16

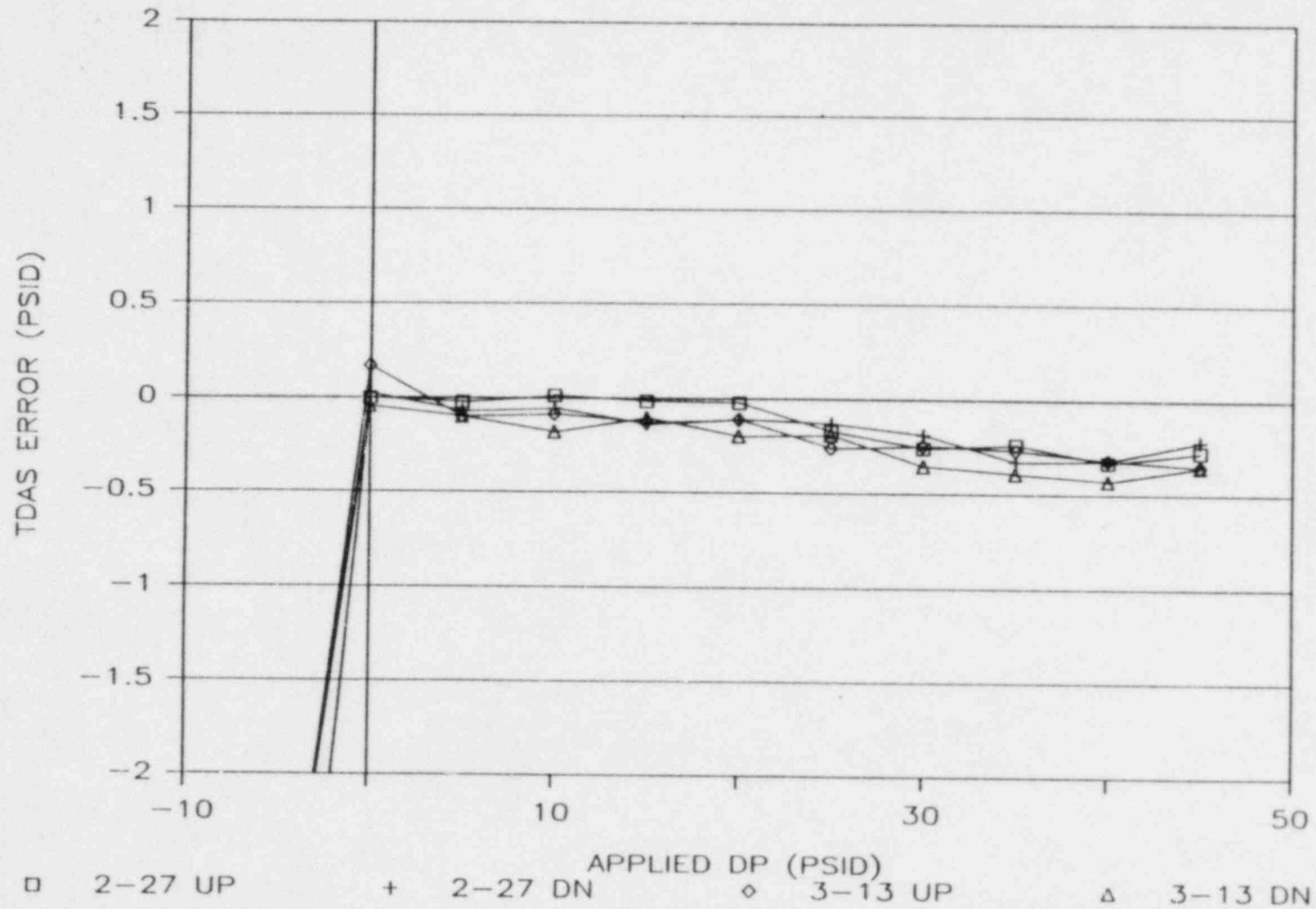
PDT-9116-SMD



STEAM GENERATOR #1 DIFFERENTIAL PRESSURE TRANSMITTER PDT-9116-SMD CALIBRATION CURVES

FIGURE 3.2.1.17

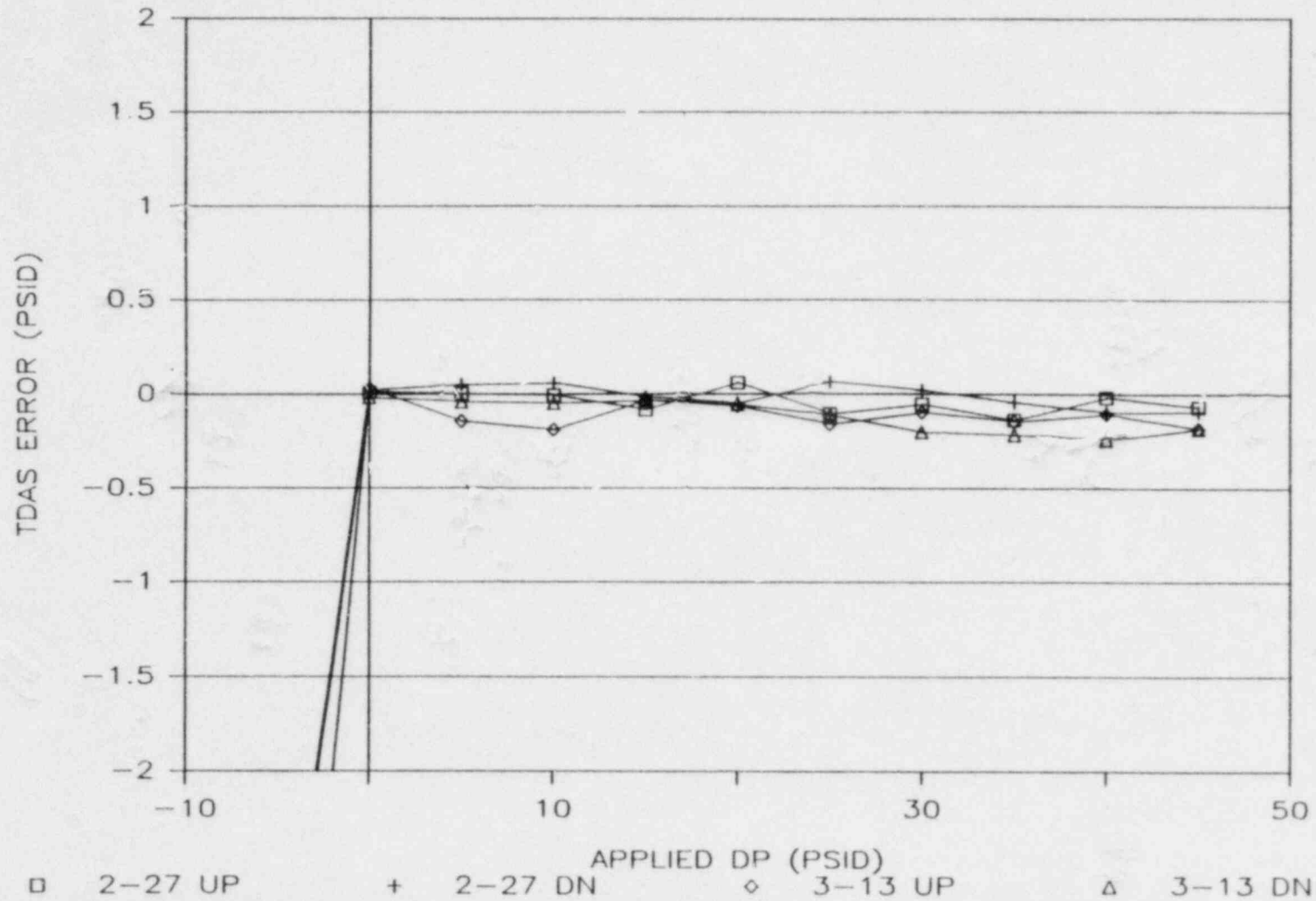
PDT-9126-SMA



STEAM GENERATOR #2 DIFFERENTIAL PRESSURE TRANSMITTER PDT-9126-SMA CALIBRATION CURVES

FIGURE 3.2.1.18

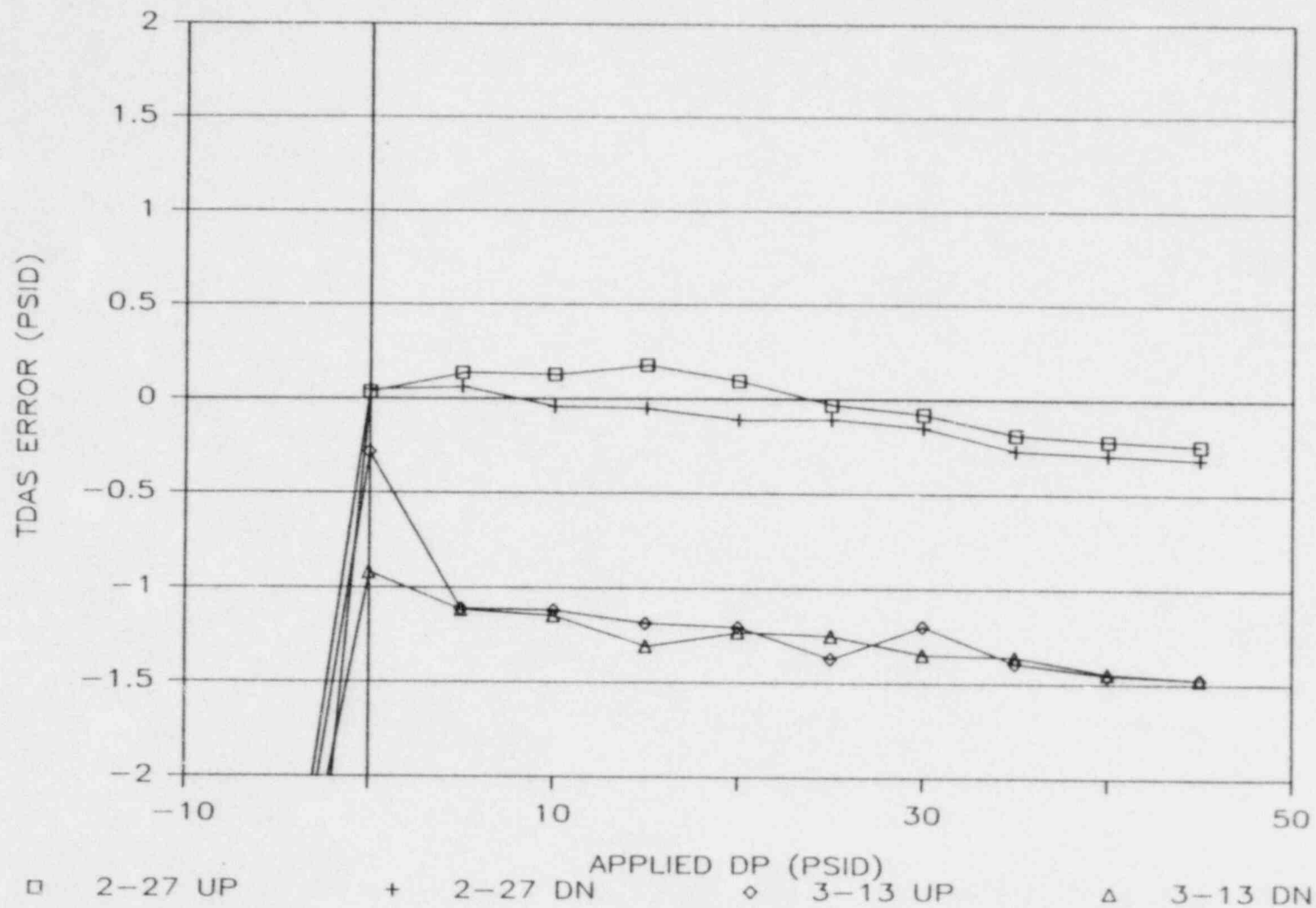
PDT--9126--SMB



STEAM GENERATOR #2 DIFFERENTIAL PRESSURE TRANSMITTER PDT-9126-SMB CALIBRATION CURVES

FIGURE 3.2.1.19

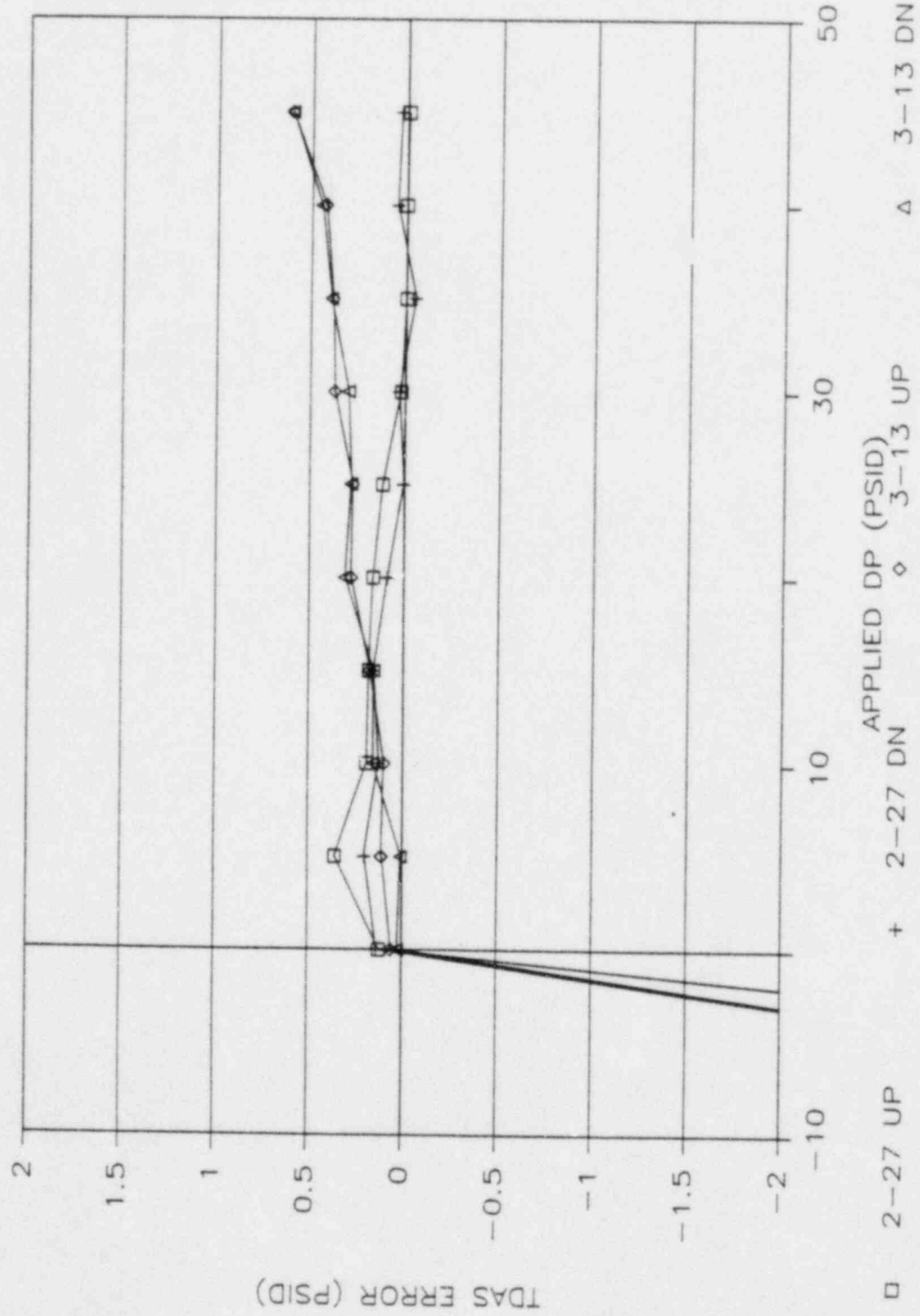
PDT-9126-SMC



STEAM GENERATOR #2 DIFFERENTIAL PRESSURE TRANSMITTER PDT-9126-SMC CALIBRATION CURVES

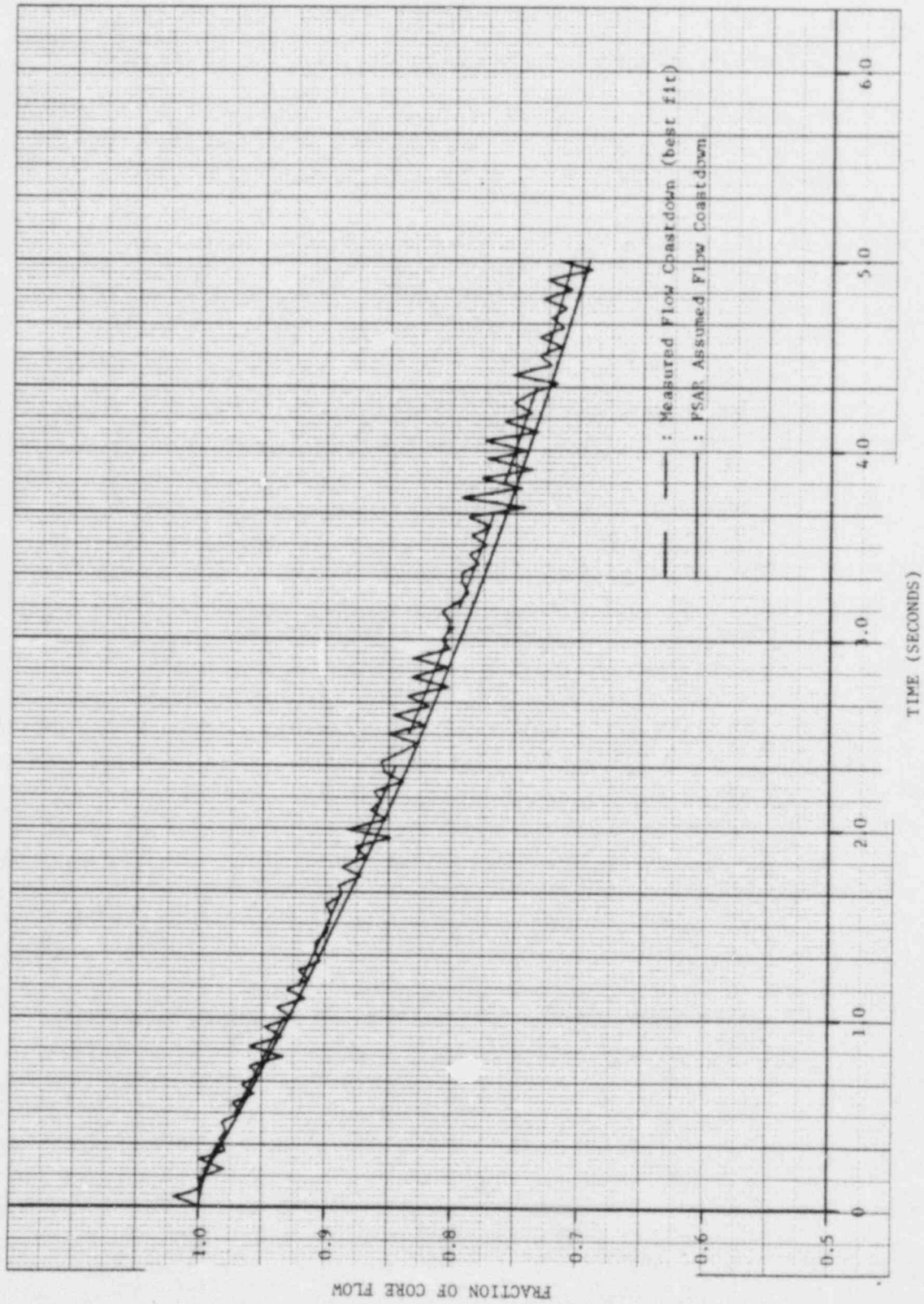
FIGURE 3.2.1.20

PDT-9126-SMD



STEAM GENERATOR #2 DIFFERENTIAL PRESSURE TRANSMITTER PDT-9126-SMD CALIBRATION CURVES

FIGURE 3.2.1.21



MEASURED FLOW COASTDOWN vs. FSAR ASSUMED FLOW COASTDOWN

FIGURE 3.2.1.22

CONCLUSION:

The post-core RCS flow rate was satisfactorily determined and found to be within the acceptance criterion. The RCS flow coastdown characteristics were also satisfactorily determined. Although conservatism of the 4-RCP coastdown was found to be questionable with respect to the flow coastdown assumed in the safety analysis, this possible non-conservatism was compensated for by increasing the COLSS penalty factor, EPOL1. The magnitude of this penalty was based on the time for the RCPs to reach 90% of rated speed during the coastdown. The CPC and COLSS flow constants were determined and satisfactorily input into their respective data bases to assure a conservative operation of the plant. The reference post-core ΔP data base was adequately established. All test objectives were achieved and all test acceptance criteria were satisfactorily met.

3.2.2 RCS Leak Rate Measurement (SIT-TP-506)

PURPOSE:

The post-core RCS leak rate measurement was performed to demonstrate that the RCS leakage at normal operating temperature and pressure is within the limits of the Technical Specifications. The test also demonstrated that the plant operations procedure gives acceptable results and provided independent calculations of leak rate in the event that unacceptable results were obtained from this leak rate procedure. Finally this test demonstrated that a known leak rate (~1 GPM) can be accurately detected using the operations procedure.

METHOD:

This test was performed twice during hot functional testing. The first run on February 5, 1985 yielded unacceptable results and was repeated satisfactorily on February 7, 1985.

With the RCS and CVCS in steady state conditions, a plant computer snapshot of plant conditions was obtained. The snapshot consisted of information on water levels, pressures and temperatures for the following components.

- Reactor Coolant System
- Pressurizer
- Reactor Drain Tank
- Volume Control Tank

- Quench Tank
- Containment Sump
- Equipment Drain Tank
- Holdup Tanks
- Safety Injection Tanks

Plant conditions were maintained steady for at least one hour after which time a second plant snapshot was obtained. Using predetermined constants relating change in volume to change in temperature or level of the associated components, the operations procedure calculated a leak rate using a change in volume during the one hour time period.

If these results were unacceptable, then an independent calculation using this test procedure, which performs a mass balance on the system using existing thermodynamic conditions, was to be performed.

The procedure was repeated after establishing a 1 GPM sample flow rate to demonstrate that the above methods can detect this leak rate.

RESULTS:

Both calculations are extremely sensitive to changing plant conditions which led to the unacceptable results during the first test run. Close review of the operation procedure generated changes which corrected and simplified some of the calculations.

The rerun of the operations procedure yielded acceptable results, as listed below in Table 3.2.2.1, so no verification using this test procedure was required.

TABLE 3.2.2.1
RCS LEAK RATE TEST RESULTS (GALLONS PER MINUTE)

SOURCE	BASELINE	WITH KNOWN LEAK SUPERIMPOSED
Identified	0.05	0.05
Unidentified	0.09	1.11
Total	0.14	1.16

CONCLUSIONS:

The Reactor Coolant System leak rate at normal operating temperature and pressure was within the limits of the Technical Specifications. The operations surveillance procedure accurately measured leakage from the reactor coolant system in the range of allowable leak rates, and a 1 gpm leak rate was detectable. All test objectives and acceptance criteria were met.

3.2.3 Postcore Reactor Coolant System Heat Loss (SIT-TP-508)

PURPOSE:

This test was performed to measure the heat loss from the entire reactor coolant system (RCS), and from only the pressurizer with spray and without spray. These measured values were then implemented into the plant monitoring computer (PMC) data base to be used in various Core Operating Limit Supervisory System (COLSS) calculations. For use in calculating the heat loss, this procedure also measured the heat input to the RCS from the reactor coolant pumps (RCPs) and the pressurizer heaters.

This test satisfied the commitment of FSAR section 14.2.12.3.6.

METHOD:

This test was performed three times during postcore hot functionals on February 6, March 3 and March 13, 1985. The measurement of heat loss was performed by means of heat balance on the RCS. Heat input to the system was from the RCPs and pressurizer heaters. RCP heat input was calculated using the measured voltage and current to each pump and an assumed efficiency. Pressurizer heat input was calculated using the measured voltage and current and the time each heater was energized. Heat loss from the CVCS was calculated using charging and letdown flows and enthalpies. Heat output from the RCS was calculated by "steaming down" the generators. This was accomplished by raising the levels above normal then securing feedwater and blowdown. Using the volume of water that "steamed down" during a one hour period,

the heat removed from the RCS was calculated. The RCS heat loss was simply the difference between the measured heat inputs and outputs.

RESULTS:

NOTE - The final test results are tabulated in Table 3.2.3.1; all other data presented in this discussion of test results is given to document the evolution of the derivation of the final test values.

The first performance of this test provided the following results:

Parameter	Results (BTU/hr)	Acceptance Criteria(BTU/hr)
- Pressurizer heat loss without spray	3.56×10^5	$< 4.30 \times 10^5$
- Pressurizer heat loss with spray	8.43×10^5	$< 5.10 \times 10^5$
- Total RCS heat loss	2.84×10^7	N/A
- RCP heat input	7.79×10^7	N/A
- Pressurizer heater input	2.42×10^5	N/A

The pressurizer heat loss without spray met the acceptance criteria. The pressurizer heat loss with spray exceeded the acceptance criteria; however, based on an evaluation by Combustion Engineering of this data considering the impact of the cooler than expected spray temperature, as measured in the pressurizer spray valve and control adjustment test per SIT-TP-505 (see section 3.2.6), the measured heat loss value was found to be acceptable.

Both the RCP heat input and pressurizer heater input were satisfactorily determined; neither had an acceptance criterion to meet.

The total RCS heat loss was almost twice that measured during pre-core hot functional testing (1.435×10^7 BTU/hr). Based on this large difference in measurement values, this portion of the test was repeated to check for repeatability of the post-core value. The second measurement of total RCS heat loss yielded a value of 2.149×10^7 BTU/hr. This value, although relatively close to the initial one, was still significantly larger than both the pre-core value, and the magnitude of the expected post-core value. A subsequent walkdown of the RCS found a large section of pressurizer surge line insulation removed. Following reinstallation of the removed insulation, the total RCS heat loss measurement was performed for a third time, and gave acceptable results of 1.58×10^7 BTU/hr.

TABLE 3.2.3.1
FINAL RCS HEAT LOSS TEST RESULTS

PARAMETER	RESULTS (BTU/hr)	ACCEPTANCE CRITERIA (BTU/hr)
Pressurizer heat loss without spray	3.56×10^5	$\leq 4.30 \times 10^5$
Pressurizer heat loss with spray	8.43×10^5	$\leq 5.10 \times 10^5$
Total RCS heat loss	1.518×10^7	N/A
RCP heat input	7.79×10^7	N/A
Pressurizer heater input	2.42×10^5	N/A

CONCLUSIONS:

The RCS heat loss and heat input parameters were satisfactorily measured and installed into the PMC data base for use in the COLSS calorimetric calculations. The heat loss and heat input values tabulated in Table 3.2.3.1 were those used throughout the initial test program by other tests utilizing heat loss/input terms. All acceptance criteria of this test were satisfied or the test results were determined acceptable.

3.2.4 RCS Expansion Measurements (SIT-TP-509)

DATES PERFORMED:

Prerequisite baseline data was taken on 1/8/85. Measurements at the 120°F plateau were made on 1/9/85. The 260°F plateau data was taken on 1/23/85, followed on 1/25/85 by the 345°F plateau measurements. Initial measurements at the 545°F plateau were performed on 2/4/85; final measurements at this plateau were taken on 2/8/85, following a required 72 hour soak. Resolution of all out-of-tolerance clearances was achieved by 3/3/85.

PURPOSE:

The purpose of this test was to demonstrate the unobstructed thermal expansion of RCS components during plant heatup, and optionally during plant cooldown. Verification that shims installed during precore hot functional testing (in accordance with SIT-TP-302) were correctly sized was a second objective of this test.

This test satisfied the requirements of FSAR section 14.2.12.3.17.

METHOD:

Baseline data was taken prior to filling and venting the RCS. Subsequently, plant conditions were stabilized at each of four RCS temperature plateaus during the heatup to hot standby conditions; the specified plateaus were at 120°F, 260°F, 345°F, and 545°F. Reactor vessel support lateral restraint gap, reactor vessel anchor bolt grillage-to-washer

gap, and steam generator sliding base x-direction gap measurements were taken at each plateau to verify unobstructed thermal expansion of these components. Following a 72 hour soak at 545°F, precise measurements of the above gaps were performed to verify not only that the clearances were sufficient, but also that they were not excessive.

RESULTS:

Throughout the heatup, all gaps were verified to be large enough so that thermal growth of RCS components was unobstructed. The specific checks performed are detailed below:

1. The reactor vessel support lateral restraint gaps were verified to be greater than 0.020 in. at each measurement point.
2. The minimum gap between each steam generator sliding base and its x-direction stop was verified to be greater than 0.080 in.
3. Each reactor vessel support anchor bolt grillage-to-washer gap was verified to be greater than 0.005 in.

Following the 72 hour soak at 545 °F, precise measurements were taken with the following results:

1. The reactor vessel support lateral restraint gaps were found to be acceptable; that is, the minimum total clearance between the support block and the shim pack mounted on the lateral restraint was measured to be greater than 0.040 in. and less than 0.100 in. for each reactor vessel cold leg support. The actual test data is presented in Figure 3.2.4.1.

2. The steam generator sliding base x-direction gaps were found to be unacceptable on both generators; that is, the measured gaps fell outside the acceptable range of 0.183 in. to 0.215 in. The shim packs were replaced to bring the gaps into tolerance. Figure 3.2.4.2 provides the measured clearances, both prior to and following rework of the shim packs.
3. The reactor vessel support anchor bolt grillage-to-washer gaps were also found to be unacceptable at 545°F; that is, the measured grillage-to-washer gaps fell outside the acceptable range of 0.005 in. to 0.015 in. Shims were fabricated and installed to bring these gaps into tolerance. The measured grillage-to-washer gaps, both prior to and following installation of the shims, are shown on Figure 3.2.4.3.

A steam generator #1 anchor bolt nut installed during precore hot functional testing was checked during this test to ensure that the nut-to-washer gap had been properly set. The measured gap at 545 °F exceeded the 0.010 in. to 0.020 in. specification. All anchor bolts on both steam generators were then checked and several were found to be out of tolerance. Those found out of tolerance were subsequently adjusted to within specifications. As-left gap data is shown in Figure 3.2.4.4.

CONCLUSION:

The RCS components were determined to be free to expand thermally during plant heatup to the normal operating temperature of 545°F.

The shim packs installed during precore hot functional testing on the reactor vessel support lateral restraints were found to be sized properly.

The clearance measured at the steam generator sliding base x-direction stops were found to be inadequate to accommodate the hot leg thermal growth anticipated from zero power to 100% power. The shim packs were removed and reworked to provide the requisite clearances.

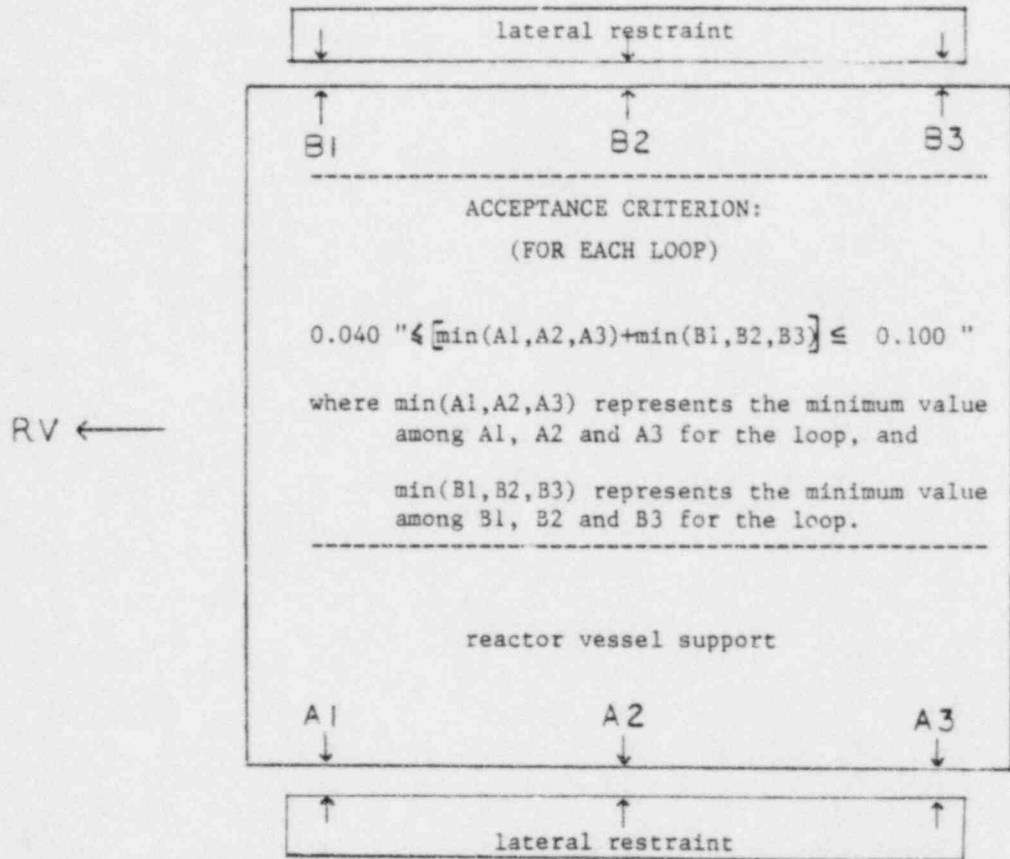
The reactor vessel support anchor bolt grillage-to-washer gaps were found to be too large to adequately restrain vertical motion of the vessel during design seismic events. Installation of shims between the grillage and the washers was accomplished to bring the gaps, with one exception, to within the allowable tolerances. The out-of-tolerance gap (.016" at the A2 gap on loop 1B) was deemed acceptable based upon a review performed by Combustion Engineering.

Steam generator anchor bolt nut-to-washer gaps were measured for all eight bolts on each steam generator. Those nuts whose gaps were found out-of-tolerance were tightened to achieve the requisite clearance.

All test objectives and acceptance criteria were satisfactorily met.

FIGURE 3.2.4.1

REACTOR VESSEL SUPPORT LATERAL RESTRAINT GAPS

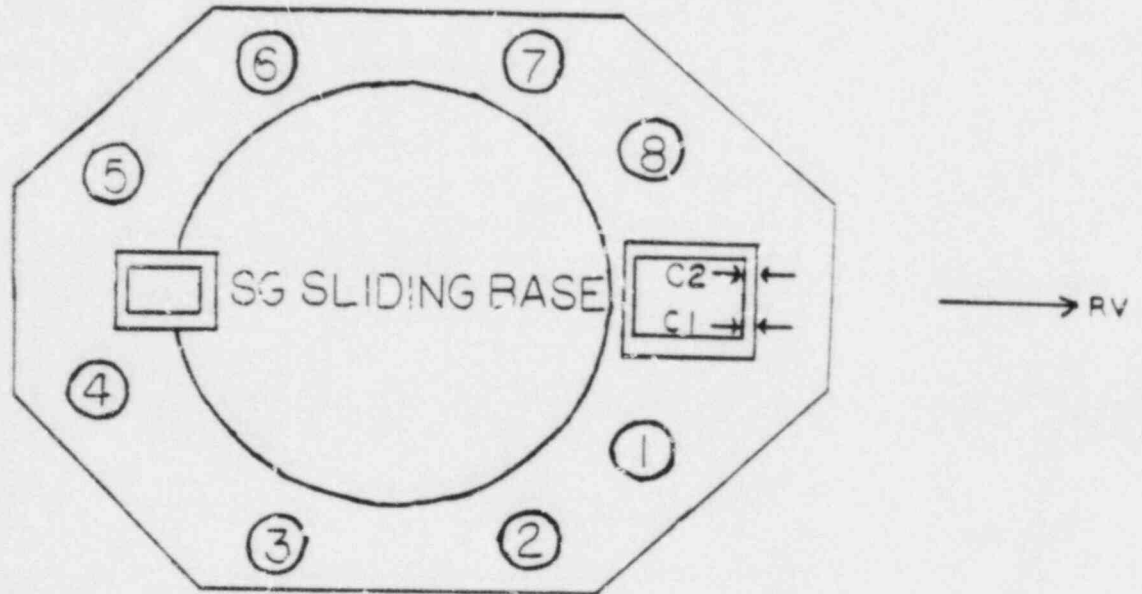


LOOP	A1 GAP	A3 GAP	A3' GAP	B1 GAP	B3 GAP	B3' GAP
1A	.022 "	.037 "	.043 "	.041 "	.055 "	.055 "
1B	.028 "	.043 "	.040 "	.042 "	.043 "	.044 "
2A	.029 "	.042 "	.057 "	.029 "	.042 "	.057 "
2B	.021 "	.043 "	.048 "	.044 "	.041 "	.046 "

(A3' and B3' Gaps are measured directly below A3 and B3 Gaps.)

FIGURE 3.2.4.2

STEAM GENERATOR SLIDING BASE X-DIRECTION GAPS



AS-FOUND

(545°)

	C1	C2
SG1	.155 "	.158 "
SG2	.125 "	.125 "

AS-LEFT

(545°)

	C1	C2
SG1	.195 "	.192 "
SG2	.209 "	.190 "

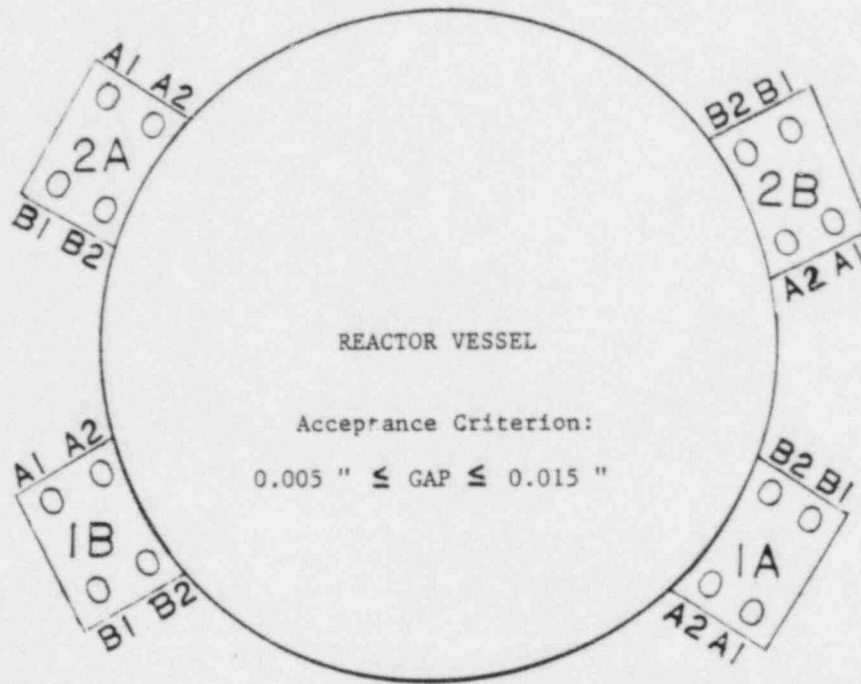
The acceptance criteria for the steam generator sliding base x-direction gaps are:

$$0.183 \text{ " } \leq C1 \leq 0.215 \text{ "}$$

$$0.183 \text{ " } \leq C2 \leq 0.215 \text{ "}$$

FIGURE 3.24.3

REACTOR VESSEL SUPPORT ANCHOR BOLT GRILLAGE-TO-WASHER GAPS



AS-FOUND

LOOP	A1 Gap	A2 Gap	B1 Gap	B2 Gap
1A	.030 "	.039 "	.040 "	.075 "
1B	.040 "	.033 "	.034 "	.033 "
2A	.016 "	.016 "	.025 "	.034 "
2B	.030 "	.030 "	.021 "	.026 "

AS-LEFT

LOOP	A1 Gap	A2 Gap	B1 Gap	B2 Gap
1A	.006 "	.015 "	.013 "	.013 "
1B	.013 "	.016 "	.007 "	.006 "
2A	.015 "	.007 "	.006 "	.013 "
2B	.005 "	.010 "	.012 "	.013 "

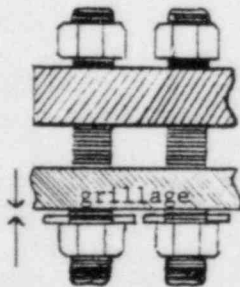
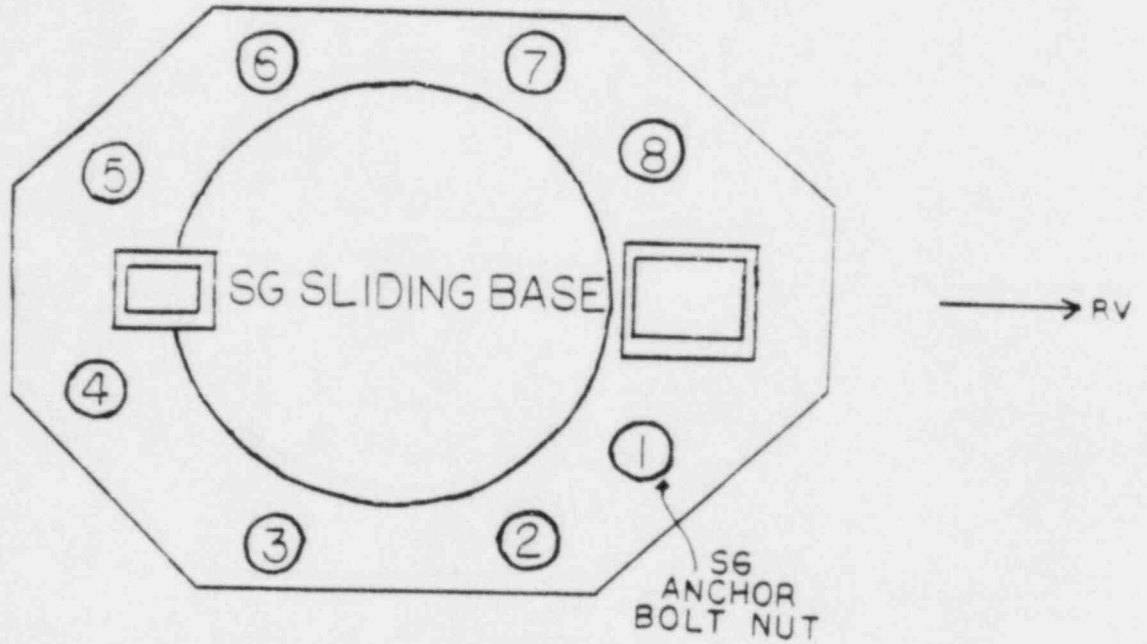


FIGURE 3.2.4.4

STEAM GENERATOR ANCHOR BOLT NUT-TO-WASHER GAPS



AS-LEFT NUT-TO-WASHER GAPS

	bolt 1	bolt 2	bolt 3	bolt 4	bolt 5	bolt 6	bolt 7	bolt 8
SG1	.020 "	.020 "	.020 "	.015 " .020 "	.012 "	.014 "	.012 "	.017 "
SG2	.020 "	.016 "	.013 "	.014 "	.015 "	.019 "	.020 "	.016 "

The acceptance criterion for each anchor bolt's nut-to-washer gap is:

$$0.010 \text{ " } \leq \text{gap} \leq .020 \text{ "}$$

3.2.5 Control Element Drive Mechanism (CEDM) and Control Element Assembly (CEA) Tests (CEDM Performance; SIT-TP-503)

PURPOSE:

The objectives of this test were to verify proper operation of the control element assemblies (CEAs), their respective control element drive mechanisms (CEDMs) and associated indications and alarms under hot shutdown and hot standby conditions. The test consisted of the following:

- A demonstration of the proper operation of the control element drive mechanisms (CEDMs) and control element assemblies (CEAs) under hot shutdown and hot standby conditions.
- A check of the CEA position indication systems and a verification that the indications by core protection calculators (CPCs) and CRT are within 3 inches.
- A verification of the proper functioning of the CEDM upper and lower electrical limits.
- A measurement of CEA withdrawal and insertion rates.
- A verification that each of the 91 individual CEAs has the proper drop time from a fully withdrawn position to its 90% insertion position at hot shutdown and hot standby conditions.
- A verification by inspection of CEA position versus time recorder trace, that the dropped CEA decelerates as it approaches the fully inserted position.

- A demonstration of the proper operation of the CEDM holding bus.
- A verification of proper operation of the CEDM Control System (CEDMCS) and its associated computer alarms and limits under hot standby conditions.

METHOD:

At hot shutdown the CEAs were withdrawn and inserted in manual individual. Careful checks were made of the CEDM position indicating systems as well as verifying proper CEDM operation by analyzing CEDM coil traces. The CEAs were again withdrawn and dropped to measure 90% and 100% insertion times. Those CEAs outside two standard deviations were dropped three more times. While at hot shutdown, the CEDM holding busses were tested by placing each subgroup on the bus and verifying it would not drop when its subgroup breaker was opened.

At hot standby, each CEA was again tested in manual individual, and 90% and 100% insertion times were recorded. Those CEAs outside two sigma were dropped three more times.

At hot standby the CEDMs were tested in manual group and manual sequential to verify functions such as Upper and Lower Group Stop, Upper and Lower Sequential Permissives, Exercise Limits, Power Dependent Insertion Limits, Minor and Major Deviation Alarms and Out of Sequence alarms by moving groups of CEAs to the proper location and verifying proper control or alarm function.

RESULTS:

CEA slipping and sticking was experienced on a few CEAs during the test. These problems were attributed to sluggish gripper action and misalignment of the CEA extension shaft and the upper gripper. These problems were accommodated with modified CEA timing and voltage adjustments.

Minor problems were experienced with the CEA processing software in the plant monitoring computer (PMC). Also, the Out of Sequence and Power Dependent Insertion Limit (PDIL) alarms were not satisfactorily verified during this test. They and all other test deficiencies were, however, reverified during subsequent CEA movements (e.g. during initial criticality, low power physics testing, etc.).

CEA drop times (to 90% inserted) and reed switch functional testing were both satisfactory for satisfying Station Technical Specifications 3/4.1.3.3 and 3/4.1.3.4 for entering mode 2. All 90% insertion times were less than 3.0 seconds (2.74 seconds maximum) at hot standby, as shown in Tables 3.2.5.1 and 3.2.5.2, and Figure 3.2.5.1. Reed switch position transmitters were always within 4.5 inches of each other (no deviations greater than 2.0 inches); also the reed switch position transmitters were within 3.0 inches of the CEA pulse counting system.

CONCLUSION:

With the satisfactory retest of all deficient test items, all acceptance criteria of this test were met, and the CEAs and CEDMs were shown to work as expected.

TABLE 3.2.5.1
 Part 1 of 3
 CEA DROP TIMES TO 90% INSERTED

CEDM #	90% Insertion Times (seconds)		100% Insertion Times (seconds)	
	320°F	545°F	320°F	545°F
1	2.42	2.63	2.73	2.93
2	2.56	2.62	2.89	2.91
3	2.52	2.51	2.88	2.80
4	2.53	2.64	2.87	2.96
5	2.21	2.59	2.51	2.88
6	2.39	2.61	2.74	2.91
7	2.12	2.55	2.42	2.84
8	2.36	2.57	2.70	2.88
9	2.20	2.63	2.51	2.93
10	2.00	2.57	2.28	2.85
11	1.73	2.63	2.1	2.93
12	2.16	2.69	2.49	3.01
13	2.65	2.63	3.05	2.94
14	2.58	2.59	2.86	2.84
15	2.59	2.61	2.91	2.91
16	2.52	2.65	2.80	2.93
17	2.42	2.58	2.71	2.88
18	2.55	2.56	2.87	2.85
19	2.45	2.66	2.84	2.97
20	2.55	2.61	2.87	2.95
21	2.59	2.67	2.95	3.01
22	2.43	2.69	2.79	3.01
23	2.68	2.64	3.04	2.90
24	2.39	2.64	2.72	2.94
25	2.30	2.67	2.60	2.95
26	2.20	2.64	2.48	2.90
27	2.40	2.59	2.74	2.92
28	2.25	2.40	2.54	2.70
29	2.37	2.40	2.65	2.68
30	2.00	2.42	2.28	2.71
31	2.35	2.38	2.65	2.67
32	2.30	2.45	2.57	2.74
33	2.32	2.38	2.61	2.67
34	2.32	2.39	2.58	2.68
35	2.40	2.42	2.69	2.71
36	2.49	2.54	2.77	2.80
37	2.65	2.67	2.99	2.97
38	2.46	2.66	2.76	2.92
39	2.40	2.60	2.71	2.91
40	2.67	2.65	2.99	2.93
41	2.69	2.65	3.03	2.93

TABLE 3.2.5.1
 (continued)
 Part 2 of 3
 CEA DROP TIMES TO 90% INSERTED

CEDM #	90% Insertion Times (seconds)		100% Insertion Times (seconds)	
	320°F	545°F	320°F	545°F
42	2.58	2.62	2.94	2.91
43	2.63	2.61	3.00	2.89
44	2.63	2.67	2.95	2.95
45	2.70	2.72	3.04	3.01
46	2.65	2.66	3.00	2.95
47	2.04	2.63	2.35	2.94
48	2.55	2.66	2.89	2.95
49	2.47	2.72	2.78	2.96
50	2.52	2.62	2.86	2.93
51	2.60	2.66	2.91	2.94
52	2.60	2.68	2.92	2.94
53	2.61	2.70	2.91	2.99
54	2.45	2.60	2.77	2.90
55	2.52	2.67	2.85	2.97
56	2.60	2.67	2.91	2.96
57	2.70	2.68	3.04	2.97
58	2.58	2.56	2.90	2.86
59	2.54	2.62	2.84	2.92
60	2.56	2.66	2.89	2.98
61	2.61	2.74	2.89	3.02
62	2.62	2.60	2.94	2.90
63	2.54	2.65	2.82	2.92
64	2.53	2.64	2.83	2.91
65	2.38	2.70	2.69	2.99
66	2.32	2.62	2.63	2.90
67	2.10	2.60	2.40	2.88
68	2.28	2.67	2.58	2.96
69	2.29	2.65	2.58	2.94
70	2.54	2.64	2.85	2.92
71	2.58	2.58	2.86	2.85
72	2.56	2.58	2.86	2.86
73	2.56	2.62	2.87	2.90
74	2.58	2.64	2.89	2.92
75	2.61	2.66	2.93	2.97
76	2.60	2.62	2.85	2.89
77	2.56	2.63	2.87	2.91
78	2.62	2.64	2.93	2.93
79	2.55	2.58	2.86	2.90
80	2.54	2.59	2.85	2.89
81	2.58	2.62	2.90	2.94
82	2.57	2.55	2.88	2.87

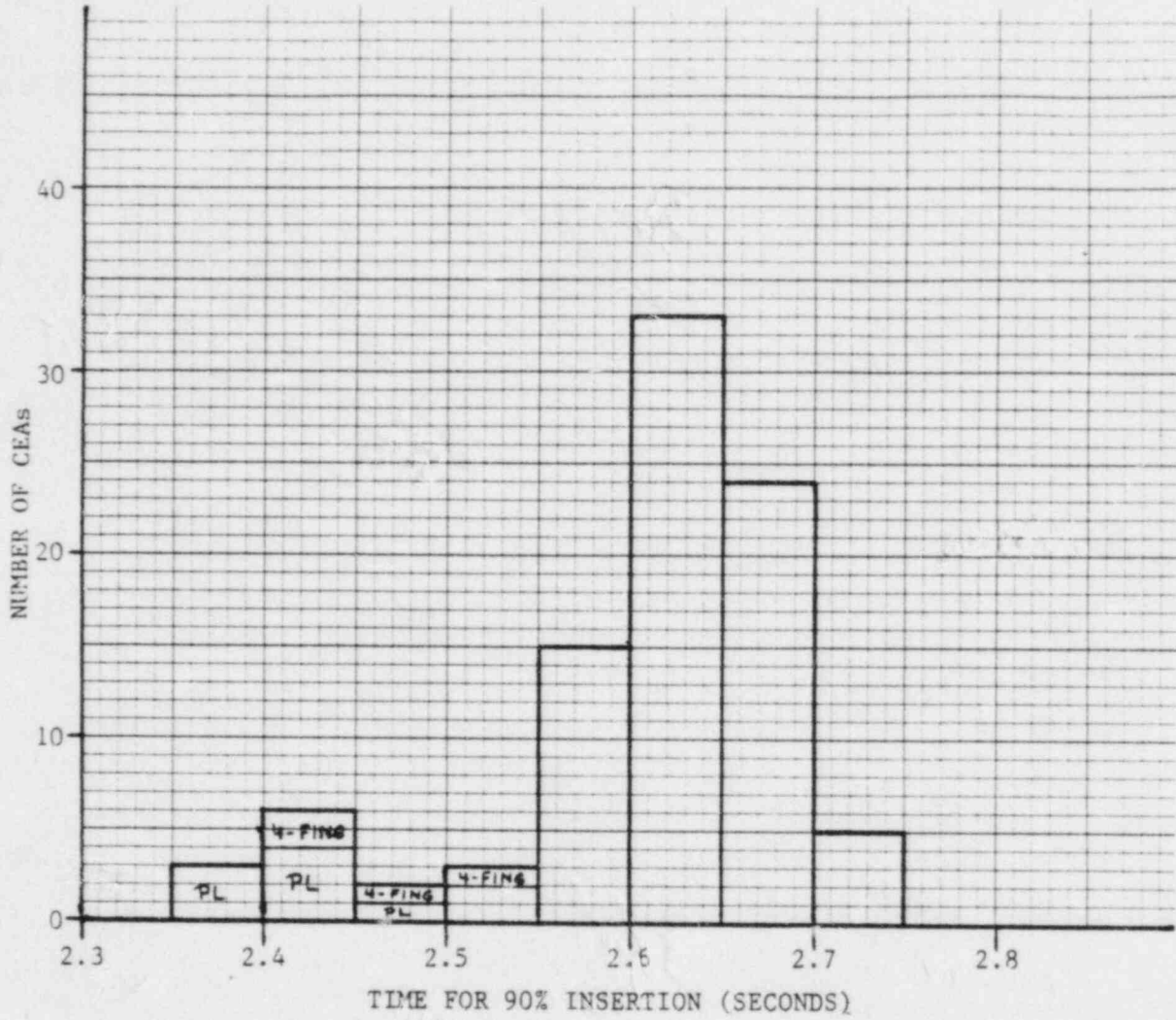
TABLE 3.2.5.1
 (continued)
 Part 3 of 3
 CEA DROP TIMES TO 90% INSERTED

CEDM #	90% Insertion Times (seconds)		100% Insertion Times (seconds)	
	320°F	545°F	320°F	545°F
83	2.55	2.61	2.85	2.89
84	2.55	2.64	2.87	2.96
85	2.60	2.67	2.92	2.98
86	2.59	2.60	2.88	2.87
87	2.55	2.59	2.87	2.87
88	2.38	2.42	2.68	2.69
89	2.38	2.46	2.67	2.73
90	2.44	2.43	2.74	2.69
91	2.44	2.50	2.73	2.74

TABLE 3.2.5.2
 AVERAGE DROP TIMES TO 90% INSERTED
 OF THREE DROPS OF CEAs OUTSIDE 2 σ

RETEST#	320°F		545°F	
	CEA #	TIME	CEA #	TIME
1	7	2.50	3	2.52
2	7	2.52	3	2.52
3	7	2.52	3	2.51
1	10	2.55	36	2.53
2	10	2.56	36	2.54
3	10	2.56	36	2.53
1	11	2.58	45	2.71
2	11	2.57	45	2.66
3	11	2.57	45	2.71
1	30	2.38	49	2.68
2	30	2.41	49	2.66
3	30	2.37	49	2.65
1	47	2.53	61	2.69
2	47	2.57	61	2.72
3	47	2.56	61	2.71
1	67	2.56	--	--
2	67	2.60	--	--
3	67	2.57	--	--

FIGURE 3.2.5.1
 HISTOGRAM OF CEA DROP TIMES TO 90% INSERTED
 AT 545°F AND 2250 PSIA



4-FING = 4 Fingered CEA
 PL = Part-Length CEA

CEA TYPE	MEAN (\bar{X})	2X STD. DEV. (2σ)
PART LENGTH (8)	2.40	0.04
FOUR FINGER (4)	2.45	0.06
FULL LENGTH (79)	2.63	0.08

3.2.6 Pressurizer Spray Valve and Control Adjustment (SIT-TP-505)

PURPOSE:

The objectives of this test were two-fold:

1. To establish the proper flow settings for the pressurizer continuous spray valves (RC-302A and RC-302B) at steady-state conditions, so as to minimize the temperature differential between the RCS cold legs and the pressurizer spray nozzle.
2. To measure the rate at which the pressurizer/reactor coolant system pressure could be reduced, utilizing pressurizer spray flowing through the pressurizer main spray valves (RC-301A and RC-301B) in parallel (required) and individually (for information only).

This test satisfied the requirements of FSAR Section 14.2.12.3.5.

METHOD:

Seven temporary thermocouples were mounted on the spray piping at various locations upstream of the pressurizer main spray valves as shown in Figure 3.2.6.1, to provide spray line temperature data. The reactor coolant system was stabilized at approximately 550°F and 2250 psia. The temperature reading of thermocouple #7 was compared to the averaged RCS cold leg temperatures. Both continuous spray valves (RC-302A and RC-302B) were adjusted fully open, to minimize the temperature differential between the pressurizer spray line and the average temperature of the RCS cold legs.

The pressurizer spray effectiveness was demonstrated by manually controlling the pressurizer main spray valves to the full open position, with all heaters off, while measuring the time required to reduce pressurizer pressure from 2250 to 2100 psia, with the RCS at hot, zero-power conditions. The acceptance criteria were based on both valves operating in parallel. However, depressurization times for each valve separately were also to be determined for information purposes. To assure that the spray valves were fully open while pressure was decreased through the test range, the initial pressure was raised to 2330 ± 10 psia. The valves were then actuated collectively and singly. The pressure/time data was recorded via computer printout.

RESULTS:

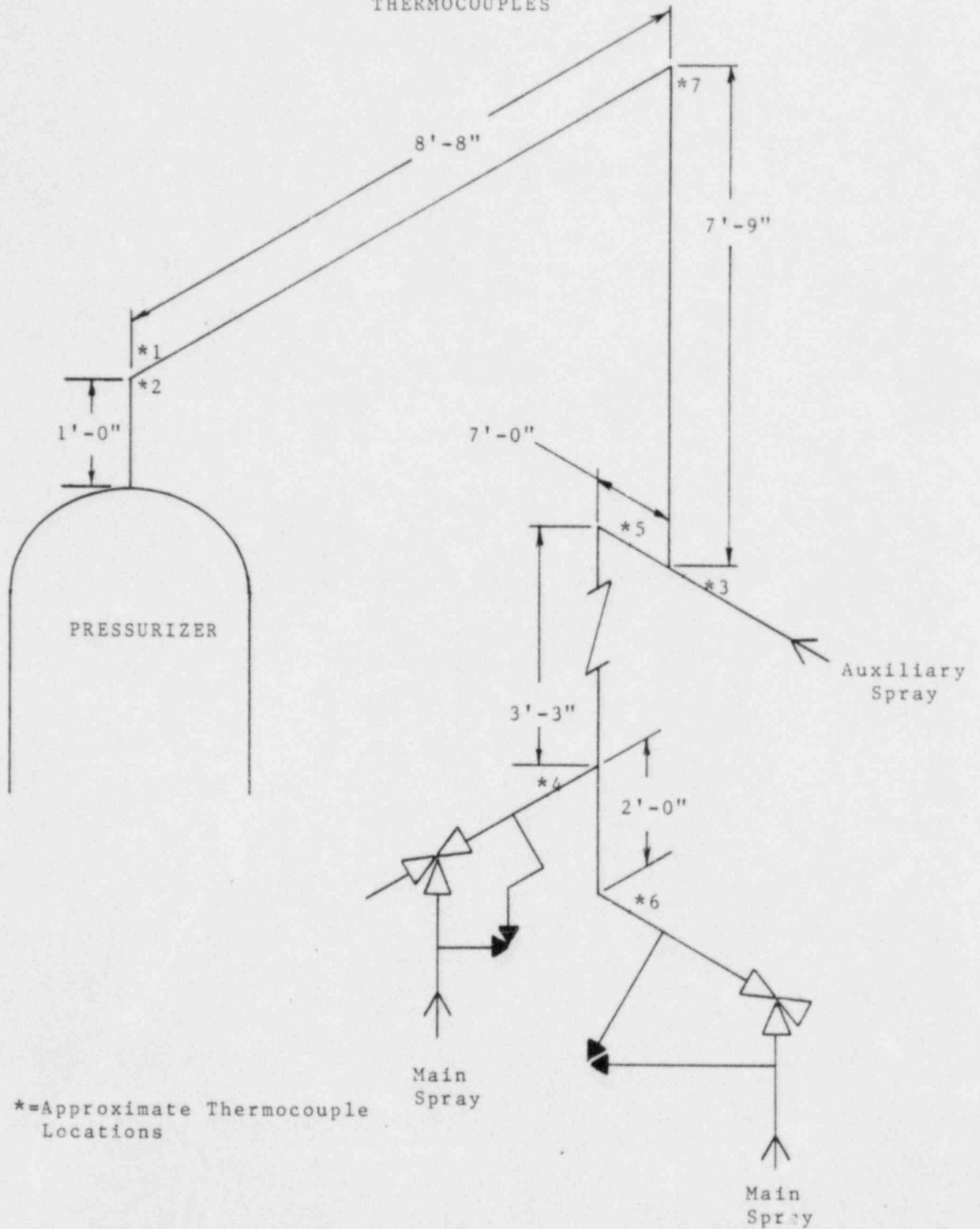
The acceptance criterion of maintaining the pressurizer spray line temperature at no more than 25° to 30° colder than the average RCS cold leg temperature, at steady-state conditions, could not be met. With the continuous spray valves fully open, the actual temperature difference was approximately 52°F . A reevaluation of the acceptance criterion by Combustion Engineering indicated that the spray nozzle portion of the system would not be adversely affected if the temperature difference was maintained at 85°F , or less. A reevaluation of the spray piping by Ebasco, utilizing the revised ΔT value of 85°F , indicated that the system would also not be adversely affected.

The pressurizer spray effectiveness was demonstrated to be well within the 93 second time limit for both valves. The actual depressurization time was 79 seconds. The individual depressurization times for valves RC-301A and RC-301B were 107 and 108.6 seconds, respectively. The pressure vs. time curves are shown on Figure 3.2.6.2.

CONCLUSION:

Following a reevaluation of the acceptance criterion for the maximum pressurizer spray line temperature differential, all objectives of this test were met and all acceptance criteria satisfied.

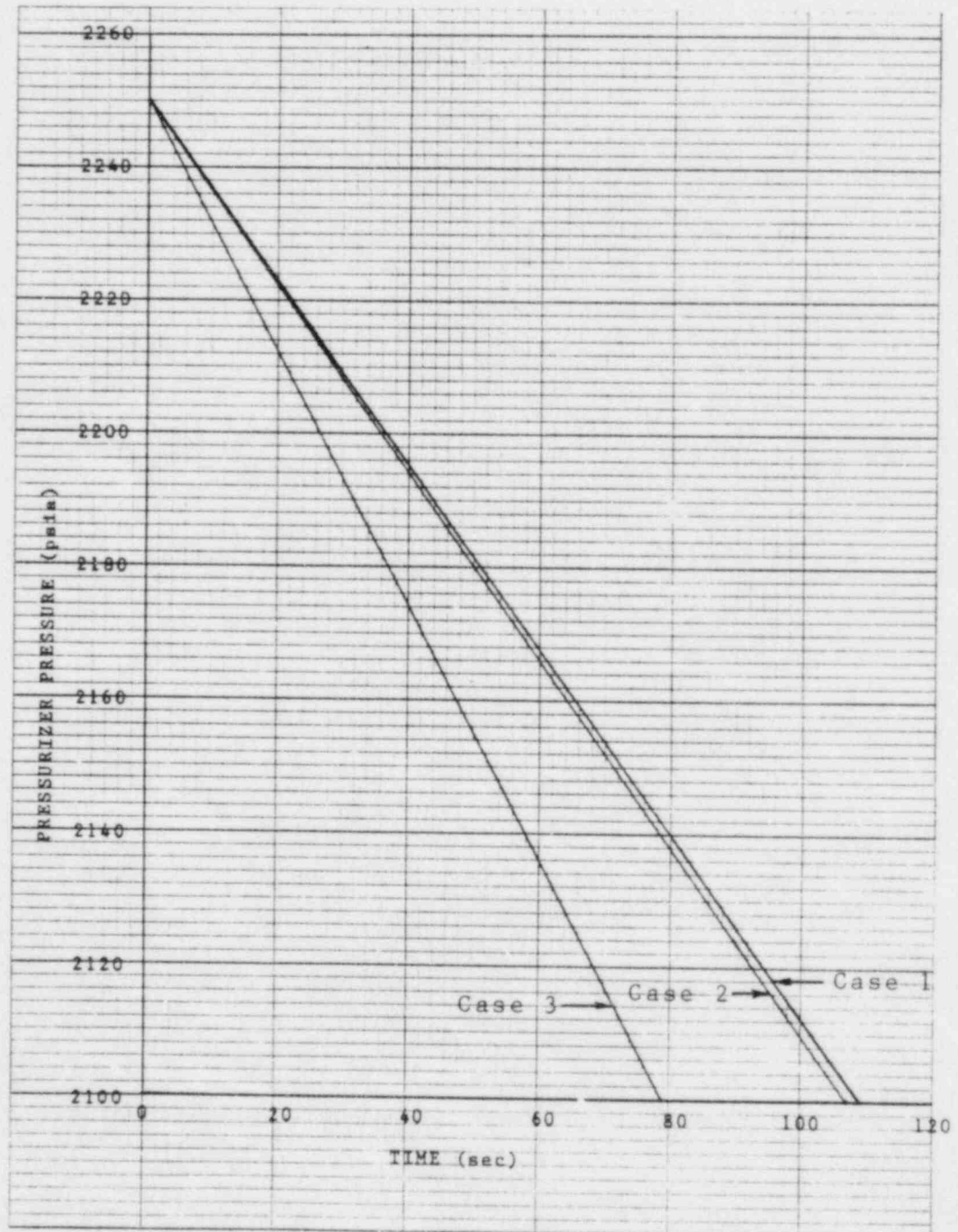
FIGURE 3.2.6.1
LOCATION OF TEMPORARY
THERMOCOUPLES



*=Approximate Thermocouple Locations

FIGURE 3.2.6.2
 PRESSURIZER/REACTOR COOLANT SYSTEM
 DEPRESSURIZATION VERSUS TIME CURVE

Case	Valve(s)	Time (sec)
1	RC-301A	109
2	RC-301B	108.6
3	RC-301A&B	79



3.3 OTHER TESTING

3.3.1 Post-Core Test Data Record (SIT-TP-511)

PURPOSE:

The purpose of this test was to provide a permanent baseline data record of plant parameter indications during the post-core hot functional test program.

METHOD:

After completion of the RCS fill and vent following the initial fuel loading, and prior to commencing system heatup and pressurization, data collection consisting of the following plant systems parameters was initiated:

- RCS temperatures and pressures
- Charging and letdown
- Pressurizer
- Steam generator
- Secondary
- Safety injection
- PPS
- RCPs and RCP motors
- Containment atmosphere
- Leak detection

Data was collected in the form of computer snapshots using the plant monitoring computer (PMC), once per hour or once per shift, depending on the system. Parameters not expected to change much over the course of a shift (i.e., containment atmosphere; leak detection; PPS; safety injection) were

recorded at the lower frequency, all others at the higher frequency. Data collection continued throughout the post-core hot functional test program (see also section 6.7.1).

RESULTS:

The required data was gathered at the specified intervals.

CONCLUSION:

A substantial data base of significant plant parameters was established for plant conditions corresponding to RCS conditions ranging from about 120°F/350 psia (Mode 5) to 545°F/2250 psia (Mode 3). This data was placed in the plant historical file for future reference. All test objectives and acceptance criteria were satisfactorily met.

3.3.2 Heated Junction Thermocouple Operation Verification
(SIT-TP-500, Attachment 8.2.6)

PURPOSE:

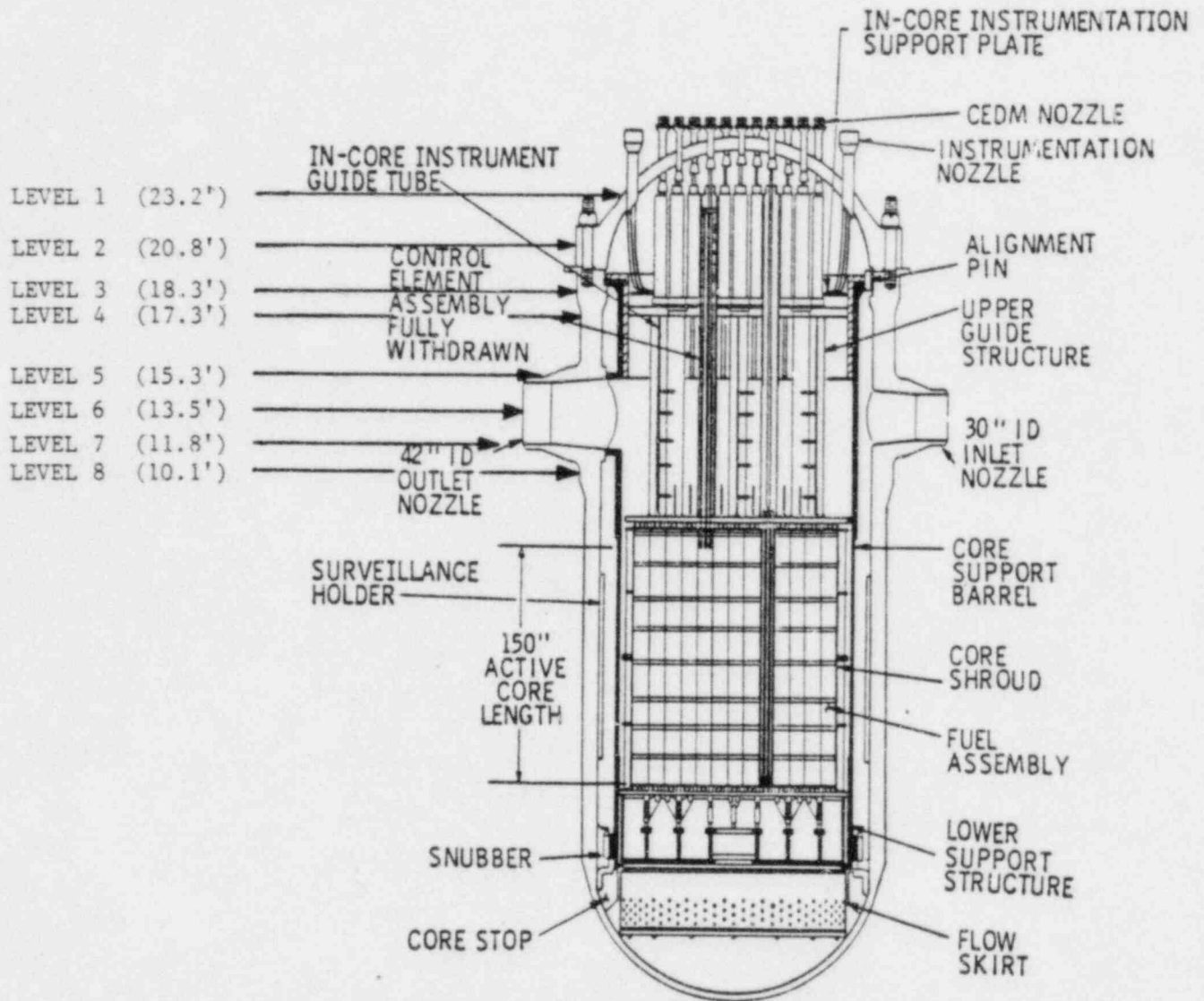
The purpose of this test was to demonstrate the sequential change of state from uncovered to covered of the heated junction thermocouples (HJTCs) during the reactor coolant system (RCS) fill and vent.

METHOD:

Reactor vessel water level was established at approximately 14 ft. (i.e., between the hot leg center-line and the top of the hot leg nozzle), as shown in Figure 3.3.2.1. During the RCS fill and vent, the reactor vessel water level indications on the qualified safety parameters display system (QSPDS) channel 1 and 2 were compared to each other and to actual levels as indicated on a temporarily installed tygon tubing level gage.

RESULTS:

At the start of the test, sensors 8, 7, and 6 were already covered due to their depth within the reactor vessel and the requirement to have the RCS water level to at least the center-line of the hot leg to permit coolant circulation by the shutdown cooling system. The remaining sensors, 5 through 1, changed state sequentially starting with sensor #5 and ending with sensor #1 as the water level within the reactor



APPROXIMATE LOCATION OF HEATED JUNCTION THERMOCOUPLE LEVELS

FIGURE 3.3.2.1

was raised. Both QSPDS channels indicated the respective sensors' change of state from uncovered to covered almost simultaneously, and the time of the sensors' change corresponded well with the level indications shown by the tygon tubing level gage.

CONCLUSION:

The heated junction thermocouples satisfactorily changed state during the RCS fill and vent, to provide an accurate indication of the coolant level within the RCS.

3.3.3 RCS and Steam Generator Parameters (SIT-TP-500, Attachment 8.2.2 - 8.2.4))

PURPOSE:

The purpose of this measurement was to provide baseline data correlating RCS temperature and pressure data with steam generator pressures during RCS heatup.

METHOD:

During the RCS heatup data was recorded off the plant monitoring computer (PMC), or control panel indications if the PMC was not operational, for the following parameters:

- Reactor coolant loop 1B cold leg temperature
- Reactor coolant loop 2A cold leg temperature
- Pressurizer temperature
- Pressurizer pressure
- Steam generator #1 pressure
- Steam generator #2 pressure

Data was recorded at the 260°F/350 psia, the 345°F/392 psia, and the 545°F/2250 psia plateau.

RESULTS:

The required data was satisfactorily collected and is shown in Table 3.3.3.1.

TABLE 3.3.3.1

RCS AND STEAM GENERATOR PARAMETERS

PARAMETER	TEST PLATEAU		
	260°F/ 350 psia	345°F/ <392 psia	545°F 2250 psia
RC Loop 1B Cold Leg Temperature, °F	261.4	341.6	543.6
RC Loop 2A Cold Leg Temperature, °F	257.7	340.9	544.4
Pressurizer Temperature, °F	430.3	428.0	652.6
Pressurizer Pressure, psia	354.0	344.4	2246.2
Steam Generator #1, Pressure, psia	37.3	120.3	978.9
Steam Generator #2, Pressure, psia	35.0	118.0	977.4

CONCLUSION:

All data required to satisfactorily establish a data base correlating RCS temperature and pressure data with steam generator pressures during RCS heatup was obtained. The measurement objectives were met.

3.3.4 Determination of Auxiliary Spray Flow Split (SIT-TP-500, Attachment 8.4.4)

PURPOSE:

The purpose of this test was to collect data for a response to an NRC question concerning the RCS depressurization capability using auxiliary spray provided by the charging pumps with a failed open loop charging valve.

METHOD:

With the RCS stable at approximately 545°F and 2250 psia, both auxiliary spray isolation valves were verified closed, while makeup was supplied to the RCS through at least one charging loop isolation valve. Care was taken to minimize heat removal from the RCS by securing blowdown and minimizing steam demand. A second charging pump was started, loop 2 charging isolation valve was verified open and loop 1 charging isolation valve was verified closed before commencing data collection.

Before initiating the transient the spray valve controller was placed in manual with 0% output and all pressurizer heaters were secured. All four reactor coolant pumps (RCPs) were then stopped, and both auxiliary spray valves were opened while the open charging isolation valve was closed. When pressurizer pressure had decreased to 2150 psia the loop 2 charging isolation valve was reopened and pressure decreased further to 2000 psia. Both auxiliary spray valves were then closed and the RCS returned to normal hot standby configuration at approximately 545°F and 2250 psia.

RESULTS:

The failure during the test of a clamp-on sonic flow meter attached to the auxiliary spray line to measure its flow rate caused this data to have been lost. Additionally, evaluation of charging flow data collected per the plant monitoring computer (PMC) showed that the output of the two charging pumps run during the test dropped from approximately 88 gpm just prior to the test to approximately 44 gpm for most of the test only to return to about 88 gpm.

With the above exceptions the test progressed smoothly and sufficient data was collected to allow an evaluation of the depressurization capability using auxiliary spray flow provided by the two charging pumps with a failed open loop charging valve to be made.

CONCLUSION:

The data collection sufficed to permit a response to the subject NRC question to be made. This response was transmitted to the NRC via LP&L letter W3P85-2115, dated June 13, 1985, from K. Cook to G. Knighton.

3.3.5 Post Core Thermal Expansion Testing (SPO-99P-003)

PURPOSE:

The purpose of this test was to verify that piping and component expansions are free, unrestrained and within tolerance (during plant heat-up and normal operation) as predicted by analysis. This test satisfied the commitments of FSAR Chapter 3, Section 3.9.2.1, Preoperational Vibration, Thermal Expansion and Dynamic Testing on Piping, and FSAR Chapter 14, Sect. 14.2.12.3.17, Piping Thermal Growth, Vibration and Shock (see also section 3.2.4).

METHOD:

The systems selected for testing were identified by engineering as a result of re-analysis, and to clear test deficiencies from testing performed during pre-core hot functional testing.

Rigid restraints or building steel were utilized as reference points to measure movements at various locations by establishing a bench mark on the restraint and/or pipe. Spring hangers and snubbers were also used to measure pipe movements independently of the built-in scale provided. Carpenter squares, plumb bobs and steel rulers were used for measurement. Piping temperatures were measured using hand held digital pyrometers and thermocouples probes.

Prior to the beginning of hot functional testing, systems involved in thermal expansion monitoring were walked down to ensure that piping and piping components were free to expand in an unrestrained direction.

Insulation was temporarily removed at measuring points to allow clearance observation/measurement, and pipe temperature measurement.

Problems encountered during testing, which caused inappropriate pipe movements, were resolved by engineering and corrective action was implemented before proceeding.

RESULTS:

All thermal movements measured during testing were acceptable based on the following criteria:

- 1) Thermal movements were within the acceptable range of 20% or $\frac{1}{2}$ " (whichever was greater) of the calculated movement.
- 2) Because of heat losses, actual piping temperatures were slightly less than maximum operating temperatures. Measured movements were declared acceptable based on interpolation between actual and maximum operating temperature values.

All piping systems monitored for thermal movements fell within acceptable limits. The following significant events occurred during testing, and corrections were made as necessary:

- 1) The main steam line to the emergency feedwater pump turbine and the blowdown from steam generator to blowdown tank experienced fluid transients during testing. Damaged restraints and piping were replaced per design.

- 2) Main steam line (SMS 40-15) restraints were modified per SMP-306 to bring thermal movements within acceptable range.
- 3) Sealant material in some of the sleeves were replaced or removed to allow pipe movements as required.
- 4) Clearances provided between piping and restraints at several locations were inadequate to allow for thermal growth. These deficiencies were corrected prior to further heat-up.
- 5) Steam generator space sampling system thermal movements were out of tolerance due to the excessive weight of pipe support components. This deficiency was cleared by redesigning pipe supports.

CONCLUSION:

This thermal expansion testing of piping systems performed in accordance with procedure SPO-99P-003, satisfactorily demonstrated that piping and component expansions were free, unrestrained and acceptable during plant heat-up and normal operation.

SECTION 4.0

INITIAL CRITICALITY

The initial criticality of the WSES-3 reactor occurred on March 4, 1985 at 2148, CST. The criticality was controlled by procedure SIT-TP-600, Initial Criticality, and was attained in a safe, orderly manner by first pulling the CEAs to a predetermined configuration (in a predetermined sequence) and then diluting the RCS Boron concentration until criticality was achieved. Concurrent with the CEA withdrawal and boron dilution, inverse count rate ratios (also called inverse multiplication ratios, or 1/M's) were calculated and used to estimate when criticality would occur. The basis for using 1/M's was that count rates increase to large values as criticality is approached. If a base count rate taken when the reactor is subcritical is divided by the count rate measured as the reactor approaches criticality, the ratio will approach zero. Extrapolation to zero provides an estimate of criticality.

4.1 CEA Withdrawal

The CEA withdrawal portion of the approach to criticality commenced on March 4, 1985 at 0328. The reactor was in mode 3 with the RCS temperature and pressure at about 545°F and 2250 psia. All CEAs were fully inserted and the RCS boron concentration was approximately 1780 ppm. VCT, pressurizer and letdown line boron samples were within 10 ppm of the RCS sample value.

Hourly boron sampling was initiated and a plant monitoring computer (PMC) collect log was started on a five-minute trend. The CEAs were pulled in a controlled sequence that was chosen such that each step in the sequence resulted in about a 0.5-1.0% $\Delta\rho$ reactivity addition. The shutdown and part-length CEA groups were withdrawn in the Manual Group (MG) mode while regulating groups 1-6 were withdrawn in the Manual Sequential (MS) mode. The CEA withdrawal sequence took thirteen steps and resulted in all CEAs being fully withdrawn, except CEA group 6, which was left at 75 inches withdrawn to provide reactivity control when criticality was achieved. At the completion of each step of the sequence a CEAC snapshot was taken, which was used as a CEA position record.

Prior to the initiation of the CEA withdrawal and following each of the steps in the withdrawal sequence, 1/M's were calculated and used to estimate criticality. Before the first CEAs were withdrawn the base countrate consisting of the average of five one-hundred second counts was determined for the two startup neutron detectors. Subsequent countrates used for the 1/M's were determined from the average of three one-hundred second counts. The 1/M's for the CEA withdrawal portion are summarized in Table 4.1 and presented in Figure 4.1. Using a figure similar to Figure 4.1, estimates of criticality were made. In no case was criticality estimated to occur for the next immediate CEA pull, which was as expected.

Problems encountered during this phase of the approach were minimal and easily fixed. CEAs 49, 37, 81 and 46 slipped during CEA pulls, and CEAs 34, 72 and 23 did not initially move when required.

During the CEA withdrawal, a deficiency from post-core hot functional test procedure SIT-TP-503, CEDM Performance (see section 3.2.5) concerning the Out-of-Sequence (OOS) alarm and interlock was successfully cleared. The last CEA withdrawal step was completed at 0832. The OOS testing was completed at about 1114.

4.2 RCS Dilution

The RCS dilution portion of the approach to criticality began on March 4, 1985 at 1124. The RCS was at 545°F, 2250 psia and 1780 ppm boron. Three charging pumps were running and dilution was via the VCT. The PMU charging rate to the VCT was 130 gpm. The RCS boron sampling frequency was changed to once every 30 minutes. At 1136 charging pump A/B was secured due to back pressure regulator valve oscillations. At 1440, the charging pump was returned to service. At 1628, the dilution was halted to allow boron mixing in the RCS (boron samples were as follows: RCS-1090 ppm, Pzr-1255 ppm, and VCT-55 ppm). At 1730 countrates greater than $\frac{1}{2}$ cps above background

were verified for both startup channels (39.30 and 38.35 cps, respectively, for startup 1 and startup 2). At 1900, the RCS boron was sufficiently mixed (boron samples were as follows: RCS-990 ppm, Pzr-1010 ppm, and VCT-990 ppm) to allow for the dilution to resume. Direct dilution was then employed by manually manipulating PMU-140. At this time the boron sampling frequency was increased to every 15 minutes. Criticality was declared at 2148. The critical configuration was as follows: 545°F, 2260 psia, 820 ppm boron and CEA group 6 at 75 inches withdrawn. In diluting from 1780 to 990 ppm boron 37,590 gallons of PMU were required. In diluting from 990 to 820 ppm boron 13,550 gallons of PMU were required. At 2220, CEA group 6 was withdrawn to 81.5 inches withdrawn and power was stabilized at 5.0×10^{-5} % power, in anticipation of Low Power Physics Tests.

Coincident with the RCS dilution phase was the calculation of 1/M's. The calculations were performed every 30 minutes through 1900 and every 15 minutes thereafter until criticality was attained. A new base count rate for each startup channel was determined prior to commencing the RCS dilution from the average of five one-hundred second counts. Subsequent countrates used for the 1/M's were determined from one 120-second count. A summary of the 1/M's is found in Table 4.1 and Figure 4.1. Estimations of criticality using the 1/M's were as expected. Boron concentrations for the entire approach to criticality are shown on Figure 4.2. Figure 4.3 shows inverse multiplication versus boron concentration.

During the dilution portion of this approach, log power channel data was also recorded in order to verify overlap between the startup channels and log power channels. The overlap verification showed that the log power channels behave reliably before the startup channels reach their upper limit. The startup detectors are highly sensitive detectors designed to monitor low power ($<10^{-6}$ % power) conditions, while the log power detectors are much less sensitive,

large, or logarithmic range detectors. Overlap was verified as shown in Table 4.2 and Figure 4.4. Startup channels 1 and 2 automatically deenergized at 2218 and 2225, with log power at $1.0 \times 10^{-6}\%$ power.

TABLE 4.1
Part 1 of 2
1/M SUMMARY FOR THE APPROACH TO INITIAL CRITICALITY

TIME	CEA GP/POSITION	BORON CONCENTRATION	INVERSE MULTIPLICATION	
			STARTUP 1	STARTUP 2
0328	ARI		1.00	1.00
0330		1800		
0337	A/25		1.00	1.02
0346	A/40		1.02	1.00
0427	A/60		.95	.98
0430		1800		
0446	A/150		.80	.79
0505	B/30		.79	.80
0513	B/50		.81	.82
0530		1800		
0547	B/150		.84	.80
0609	P/150		.81	.82
0629	1/90		.82	.80
0630		1800		
0641	2/105		.68	.69
0657	3/105		.70	.70
0723	5/30		.68	.68
0730		1800		
0830		1800		
0832	6/75		.69	.68
0945		1790		
1045		1790		
1114	6/75		.67/1.00*	.68/1.00*
1124§	6/75	1780	1.01	1.01
1154	6/75	1770	.98	.99
1230	6/75	1710	.95	.97
1300	6/75	1660	.87	.85
1330	6/75	1560	.82	.81
1400	6/75	1440	.74	.73
1430	6/75	1380	.69	.67
1500	6/75	1230	.64	.62
1530	6/75	1210	.56	.58
1600	6/75	1150	.50	.52
1630	6/75	1090	.44	.45
1700	6/75	1030	.43	.42
1730	6/75	980	.42	.44
1800	6/75	990	.41	.43
1815	6/75	990	.42	.43
1830	6/75	990	.43	.45
1845	6/75	990	.44	.44
1900	6/75	990	.43	.44
1915	6/75	980	.41	.42

§ RCS Dilution commences

* 1/M's renormalized to pre-dilution base countrate

TABLE 4.1
 (continued)
 Part 2 of 2
 1/M SUMMARY FOR THE APPROACH TO INITIAL CRITICALITY

TIME	CAA GP/POSITION	BORON CONCENTRATION	INVERSE MULTIPLICATION	
			STARTUP 1	STARTUP 2
1930	6/75	970	.40	.39
1945	6/75	960	.39	.38
2000	6/75	940	.37	.36
2015	6/75	920	.34	.33
2030	6/75	900	.31	.31
2045	6/75	880	.28	.28
2100	6/75	860	.23	.24
2115	6/75	840	.17	.18
2130	6/75	820	.12	.12
2145	6/75	820	.03	.03

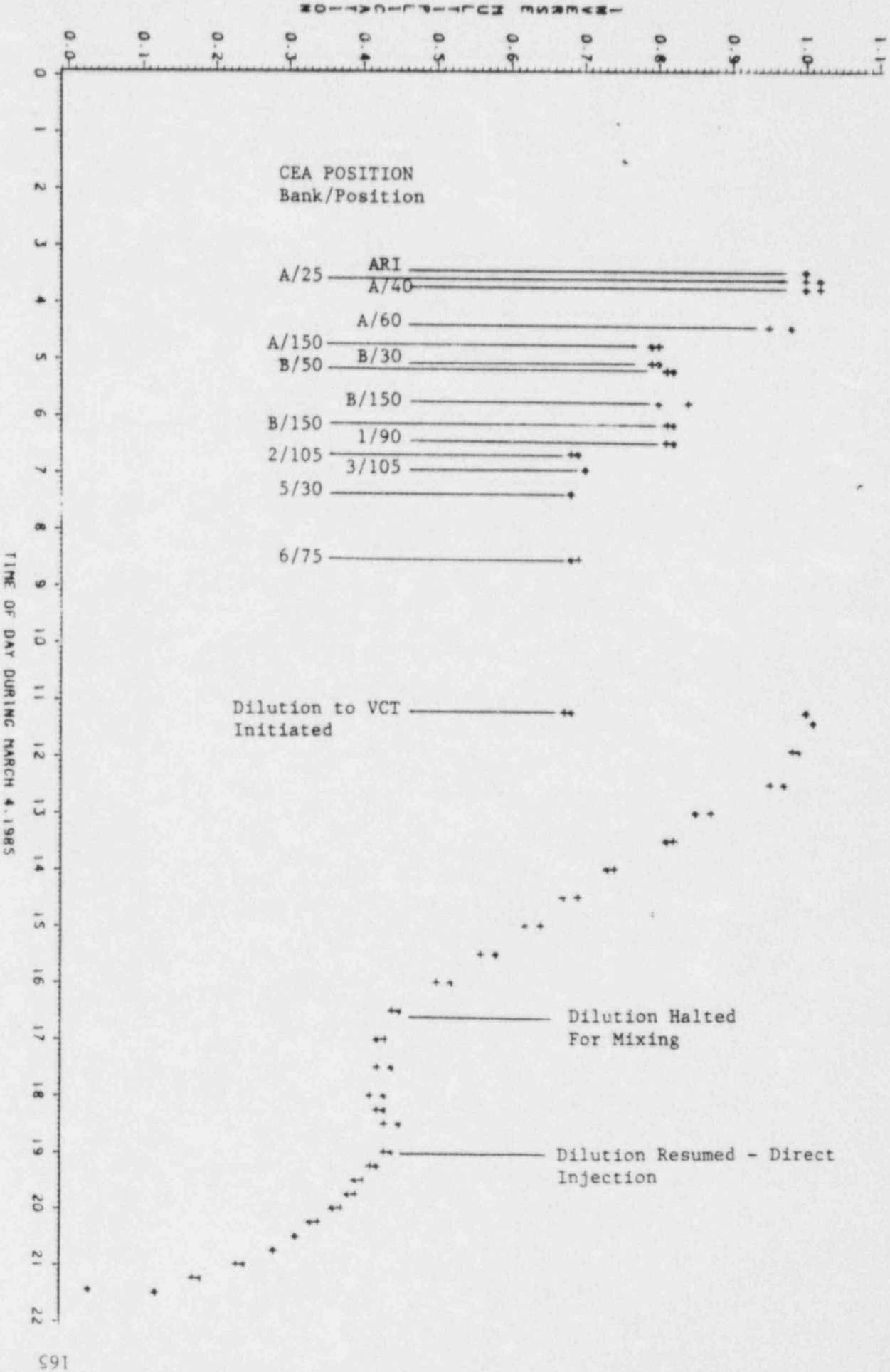
TABLE 4.2
 VERIFICATION OF STARTUP AND LOG POWER CHANNEL OVERLAP

TIME	STARTUP 1 (counts)	STARTUP 2 (counts)	LOG POWER CHANNELS			
			1	2	3	4
(% Power)						
1124	1986	2015	3.0×10^{-8}	3.0×10^{-8}	3.0×10^{-8}	7.0×10^{-8}
1154	2035	2051	3.0×10^{-8}	3.0×10^{-8}	3.0×10^{-8}	6.0×10^{-8}
1230	2095	2102	3.0×10^{-8}	3.0×10^{-8}	4.0×10^{-8}	5.0×10^{-8}
1300	2293	2396	3.0×10^{-8}	3.0×10^{-8}	4.0×10^{-8}	5.0×10^{-8}
1330	2443	2516	3.0×10^{-8}	3.0×10^{-8}	4.0×10^{-8}	6.0×10^{-8}
1400	2700	2765	3.0×10^{-8}	3.0×10^{-8}	4.0×10^{-8}	5.0×10^{-8}
1430	2908	3029	3.0×10^{-8}	3.0×10^{-8}	4.0×10^{-8}	6.0×10^{-8}
1500	3128	3258	3.0×10^{-8}	3.0×10^{-8}	3.0×10^{-8}	5.0×10^{-8}
1530	3552	3473	3.0×10^{-8}	3.0×10^{-8}	3.0×10^{-8}	5.0×10^{-8}
1600	3968	3915	3.0×10^{-8}	3.0×10^{-8}	3.0×10^{-8}	5.0×10^{-8}
1630	4491	4498	3.0×10^{-8}	3.0×10^{-8}	3.0×10^{-8}	5.0×10^{-8}
1700	4685	4852	3.0×10^{-8}	3.0×10^{-8}	3.0×10^{-8}	3.0×10^{-8}
1730	4716	4662	3.0×10^{-8}	3.0×10^{-8}	3.0×10^{-8}	3.0×10^{-8}
1800	4852	4684	3.0×10^{-8}	3.0×10^{-8}	3.0×10^{-8}	4.0×10^{-8}
1815	4723	4768	3.0×10^{-8}	3.0×10^{-8}	3.0×10^{-8}	3.0×10^{-8}
1830	4610	4559	3.0×10^{-8}	3.0×10^{-8}	3.0×10^{-8}	3.0×10^{-8}
1845	4570	4659	3.0×10^{-8}	3.0×10^{-8}	3.0×10^{-8}	4.0×10^{-8}
1900	4669	4650	3.0×10^{-8}	3.0×10^{-8}	3.0×10^{-8}	3.0×10^{-8}
1915	4855	4815	3.0×10^{-8}	3.0×10^{-8}	3.0×10^{-8}	3.0×10^{-8}
1930	5016	5191	3.0×10^{-8}	3.0×10^{-8}	3.0×10^{-8}	3.0×10^{-8}
1945	5161	5408	3.0×10^{-8}	3.0×10^{-8}	3.0×10^{-8}	4.0×10^{-8}
2000	5393	5640	3.0×10^{-8}	3.0×10^{-8}	3.0×10^{-8}	4.0×10^{-8}
2015	5883	6105	3.0×10^{-8}	3.0×10^{-8}	3.0×10^{-8}	4.0×10^{-8}
2030	6484	6632	3.0×10^{-8}	3.0×10^{-8}	4.0×10^{-8}	5.0×10^{-8}
2045	7226	7148	4.0×10^{-8}	3.0×10^{-8}	4.0×10^{-8}	5.0×10^{-8}
2100	8521	8536	4.0×10^{-8}	4.0×10^{-8}	4.0×10^{-8}	6.0×10^{-8}
2115	11606	11451	4.0×10^{-8}	4.0×10^{-8}	5.0×10^{-8}	7.0×10^{-8}
2130	16982	16485	4.0×10^{-8}	4.0×10^{-8}	7.0×10^{-8}	9.0×10^{-8}
2145	65351	62327	1.0×10^{-7}	1.0×10^{-7}	2.0×10^{-7}	2.0×10^{-7}
2150	240000	180000	3.0×10^{-7}	3.0×10^{-7}	7.0×10^{-7}	6.0×10^{-7}

W3 INITIAL CRITICALITY - INVERSE MULTIPLICATION

FIGURE 4.1

STARTUP CHANNEL 1 - - -
STARTUP CHANNEL 2 - - -



TIME OF DAY DURING MARCH 4, 1985

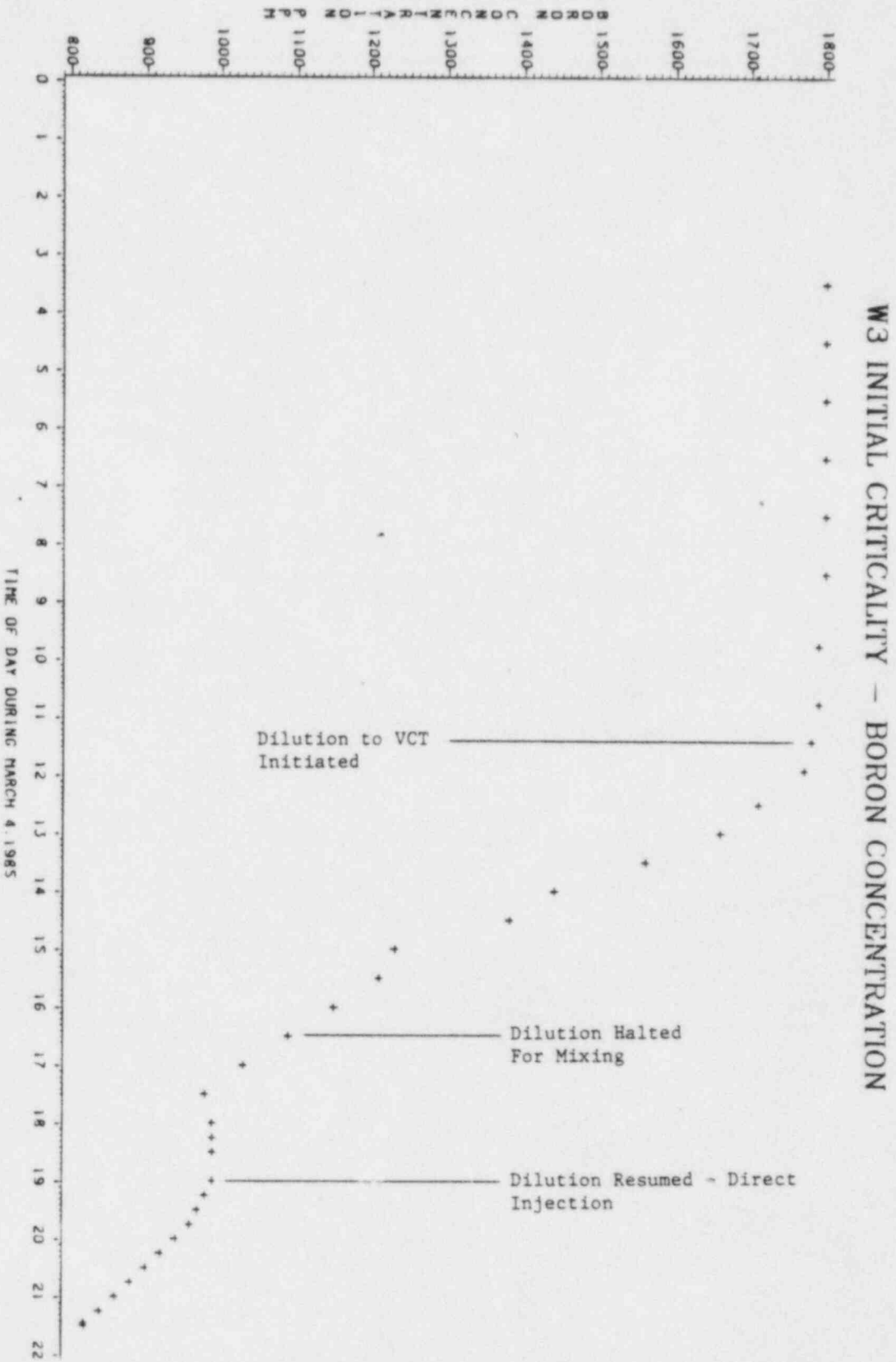


FIGURE 4.3

W3 INITIAL CRITICALITY - 1/M VERSUS BORON

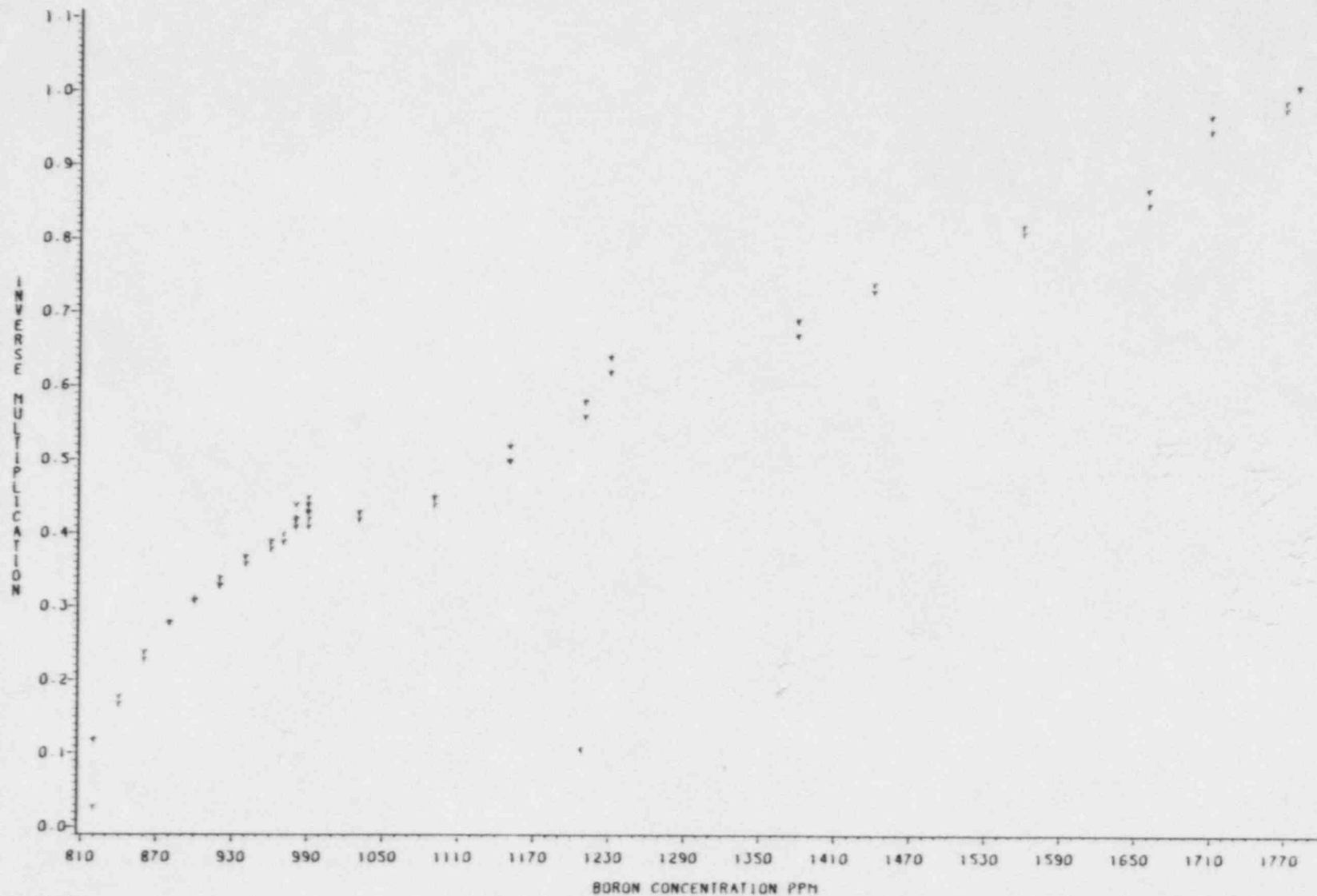
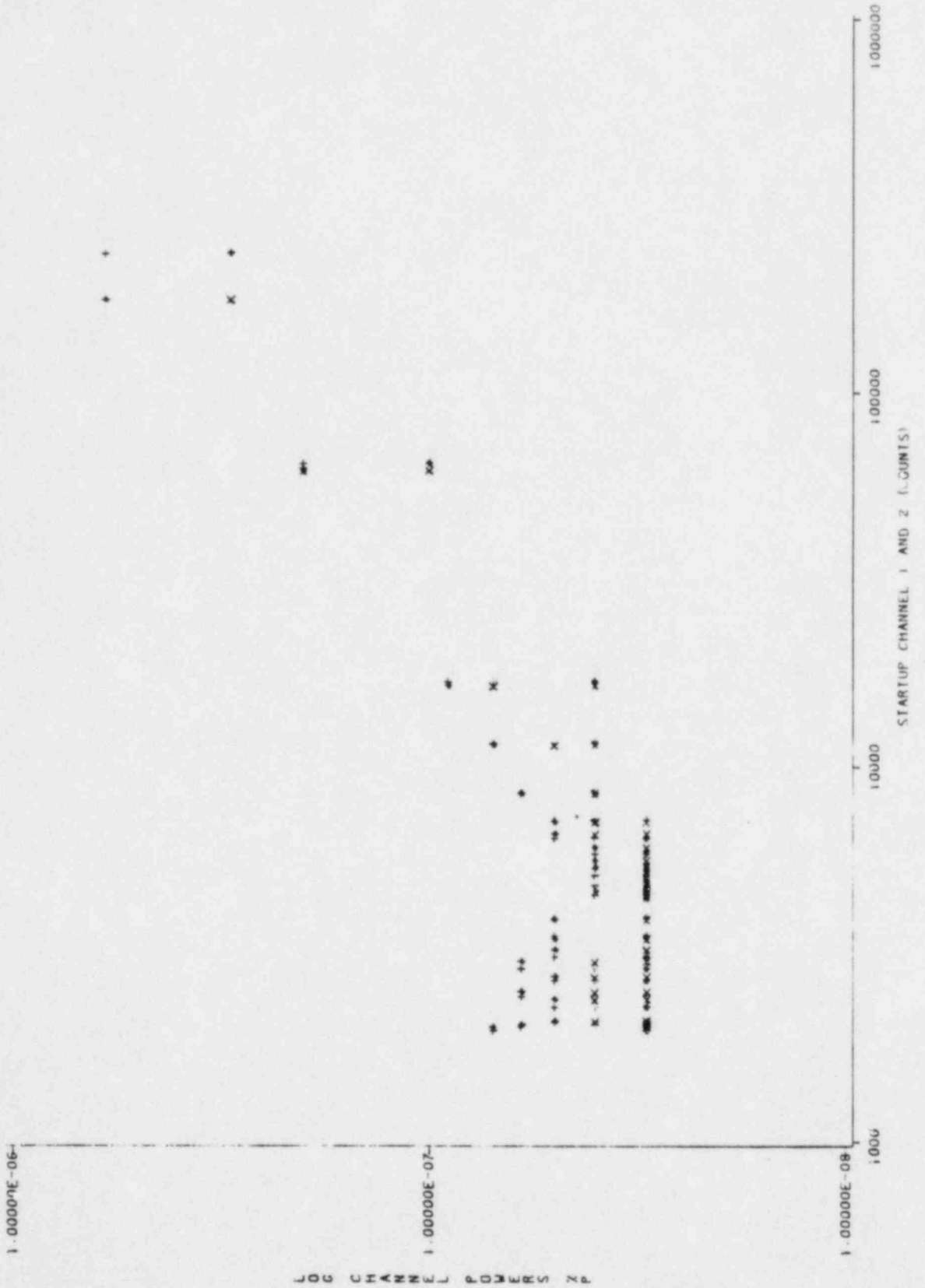


FIGURE 4.4

W3 INITIAL CRITICALITY - OVERLAP VERIFICATION



SECTION 5.0

LOW POWER PHYSICS TESTING

The Low Power Physics Test (LPPT) program at Waterford 3 SES was conducted between March 4 and March 10, 1985, to verify the physics parameters pertinent to the Waterford 3 SES reactor by comparing measured results to predicted values. Specifically, the following physics parameters were determined and verified:

- 1) CEA Symmetry Checks,
- 2) Shutdown CEA and Regulating CEA Worth Measurements,
- 3) Isothermal Temperature Coefficient Measurements,
- 4) Critical Boron Concentration Measurements
- 5) Boron Worth Measurements.

The measurement of these parameters is discussed in more detail in following sections. The results of the LPPT measurements are summarized in Table 5.0.1.

The LPPT satisfied the commitments of the following FSAR Chapter 14 sections:

- 1) 14.2.7.13.3, Psuedo-Ejected CEA,
- 2) 14.2.12.3.10, Isothermal Temperature Coefficient,
- 3) 14.2.12.3.11, Critical Boron Concentration,
- 4) 14.2.12.3.12, Shutdown and Regulating CEA Group Worth,
- 5) 14.2.12.3.13, Inverse Boron Worth
- 6) 14.2.12.3.14, CEA Symmetry.

It should be noted that the psuedo-ejected CEA test was not performed as this test was only to be performed if the remainder of the low power physics tests demonstrated that the Waterford 3 SES core was significantly different from the San Onofre Nuclear Generating Station, Unit #2 (SONGS 2) core. Since the Waterford 3 SES core was demonstrated not to be significantly different from the SONGS-2 core, this test was not performed.

The only major problem encountered during the LPPT were related to slipping/dropping CEAs and failures of the plant monitoring computer (PMC). Most of the CEA problems were only minor slips and/or drops which were quickly recoverable. However, on March 6, 1985 at 1348, problems were encountered with CEA #38 when it dropped from approximately 75" withdrawn. The problems with CEA #38 were not resolved until 0230 on March 7, 1985, creating a delay in the LPPT of almost 13 hours. The PMC failures encountered during the LPPT occurred primarily during the CEA symmetry check portion of the LPPT. Most of the PMC failures were easily resolved by rebooting the computer. The PMC failures usually were not major problems, simply a hindrance to continued testing, generally creating only minor delays.

All Low Power Physics Test objectives and acceptance criteria were satisfied.

5.1 CEA Symmetry Checks

The CEA symmetry check was performed to verify the proper, symmetric loading of CEAs within symmetric CEA groups, the proper coupling of each CEA to its extension shaft, and to verify that no core loading or fuel fabrication errors had occurred.

Each CEA should have approximately the same reactivity worth as its symmetric counterparts. This was verified by trading the withdrawal of a CEA with the insertion of a symmetric CEA and measuring the reactivity worth difference between the fully inserted CEA and the fully withdrawn CEA.

The CEAs were divided into 16 symmetric groups. The smallest symmetric group contained two CEAs, while the largest groups were made up of eight CEAs. The first CEA inserted from each symmetric group was the reference CEA. At the completion of the measurement of a symmetric group, the reference CEA was again fully inserted. Reinserting the reference CEA was performed in order to collect data required to correct individual worth measurements for any drift which occurred during the measurements of the symmetric group.

The center CEA, which has no symmetric counterpart, was inserted to produce a negative deflection in the reactivity computer output trace in order to verify that the CEA was coupled to its extension shaft.

All 16 symmetric groups were successfully tested for symmetric CEA worth. All CEAs within a symmetric CEA group were demonstrated to be within ± 1.5 cents of the symmetric CEA group average deviation, as shown in Figure 5.1.1. All CEAs were shown to be properly coupled to their extension shaft, and no evidence was found which would indicate the presence of either a core loading or fuel fabrication error. All CEA symmetry check acceptance criteria were satisfied.

5.2 Shutdown CEA and Regulating CEA Worth Measurements

To measure the group worth of the various CEA groups, regulating groups 6 through 1, shutdown group B and the part length CEA group were diluted into the core in the manual group (MG) mode and the magnitude of the reactivity change was measured from the reactivity traces produced by the reactivity computer.

The nonoverlap group worths are tabulated in Table 5.0.1. The resulting CEA group worth curves are shown in Figures 5.2.1 through 5.2.4. All CEA group worth acceptance criteria were satisfied.

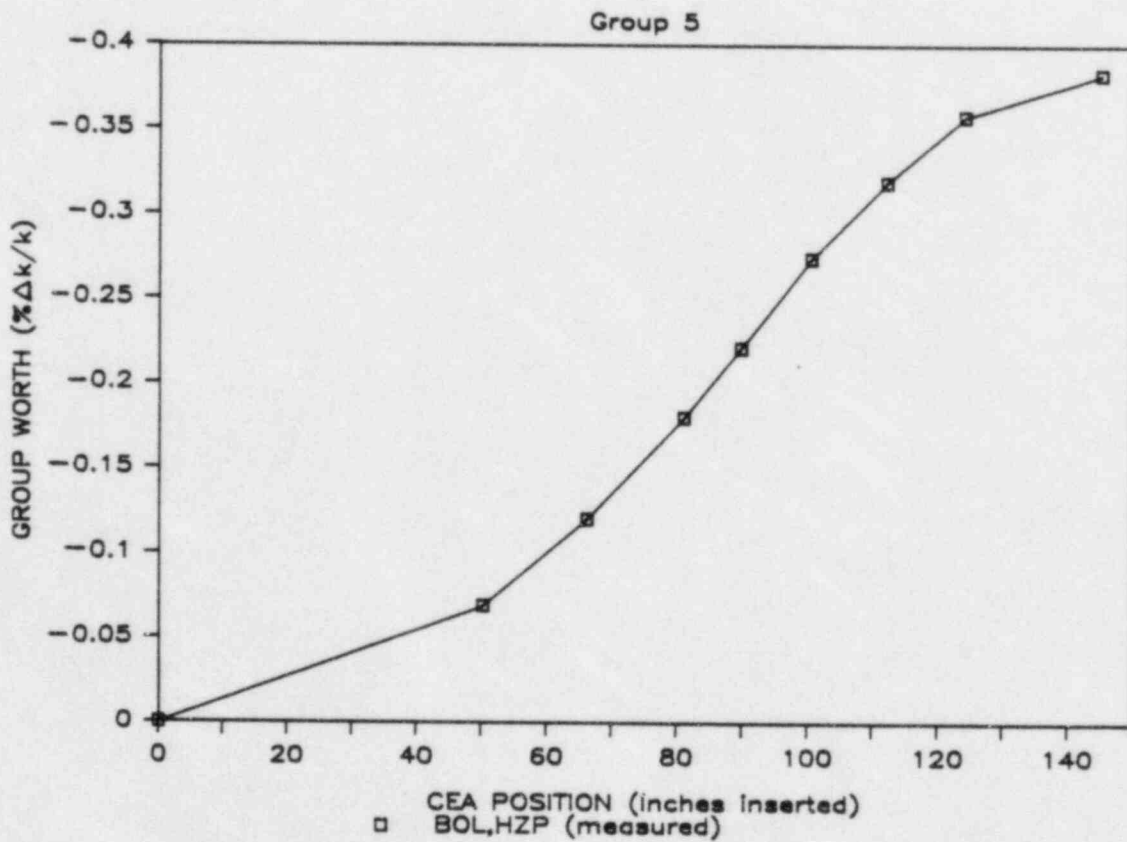
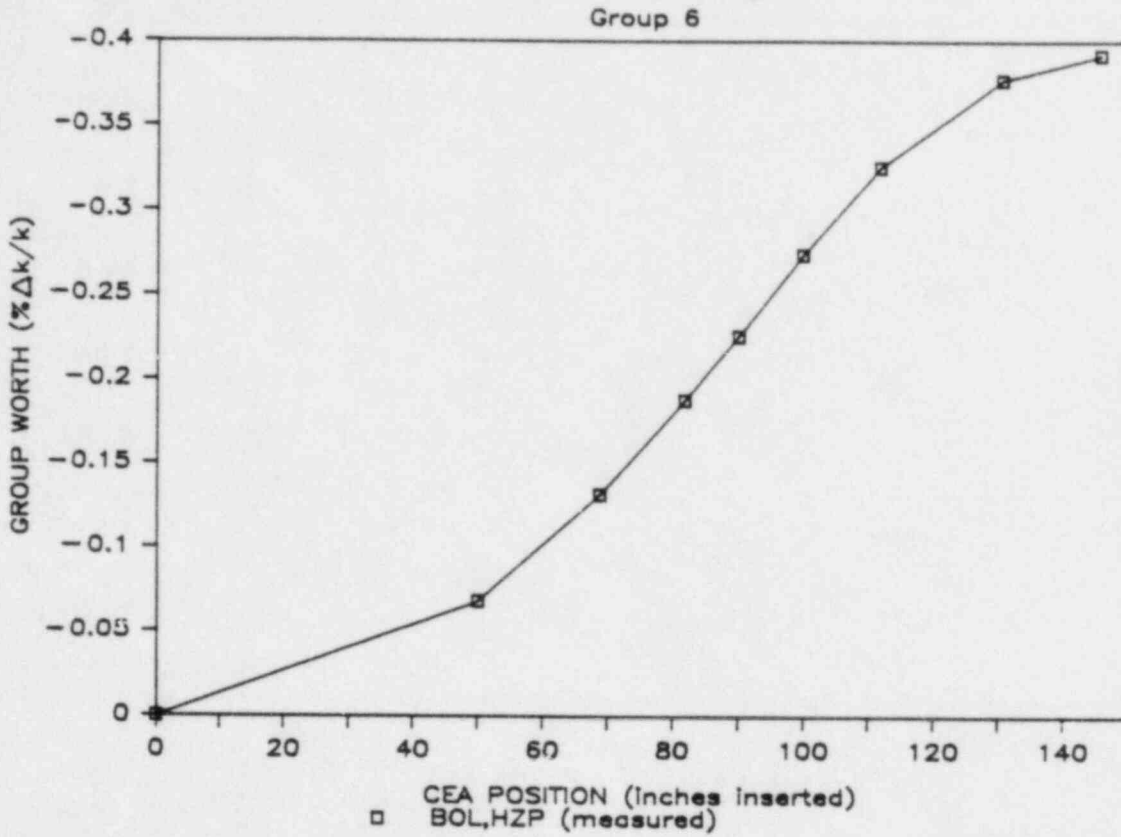
The total inserted worth (nonoverlap) of CEA groups 6 through 1, group P and group B was calculated from the measured data as 11.252% $\Delta k/k$. The predicted total worth was 11.327% $\Delta k/k$. The measured total worth differed from the predicted total worth by only -0.66%, well within the $\pm 10\%$ acceptance criteria.

The shutdown margin at the zero power insertion limit (ZPIL) was calculated to be 9.398% $\Delta k/k$, verifying that the CEA Insertion Limit was acceptable since $\geq 5.15\%$ $\Delta k/k$ margin was available.

5.3 Isothermal Temperature Coefficient Measurements

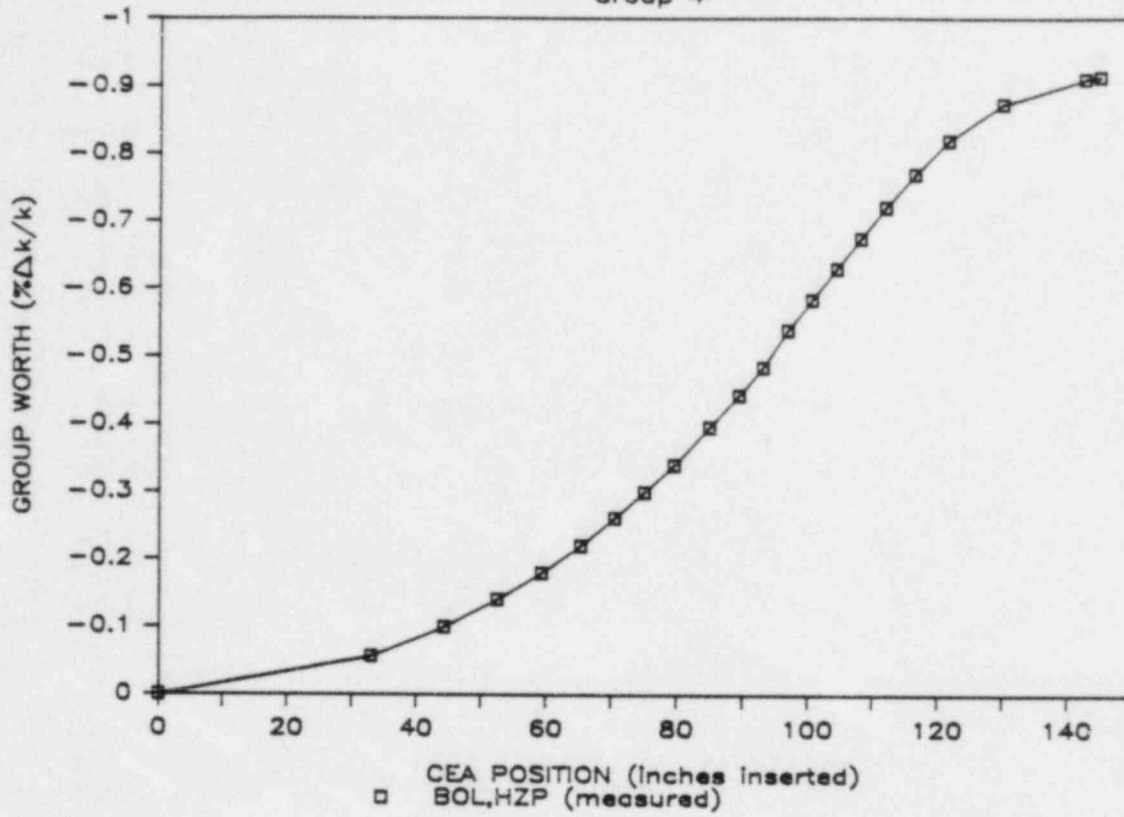
The isothermal temperature coefficients (ITCs) were measured by slowly raising and then lowering RCS temperature approximately five to ten degrees F while maintaining constant boron concentration and CEA position. The resulting reactivity changes were calculated by the reactivity computer and recorded on an x-y plotter as a function of RCS temperature. The slope of the line produced on the x-y plotter was the ITC. The ITC was measured for the following CEA configurations:

INTEGRAL CEA WORTH, NO OVERLAP

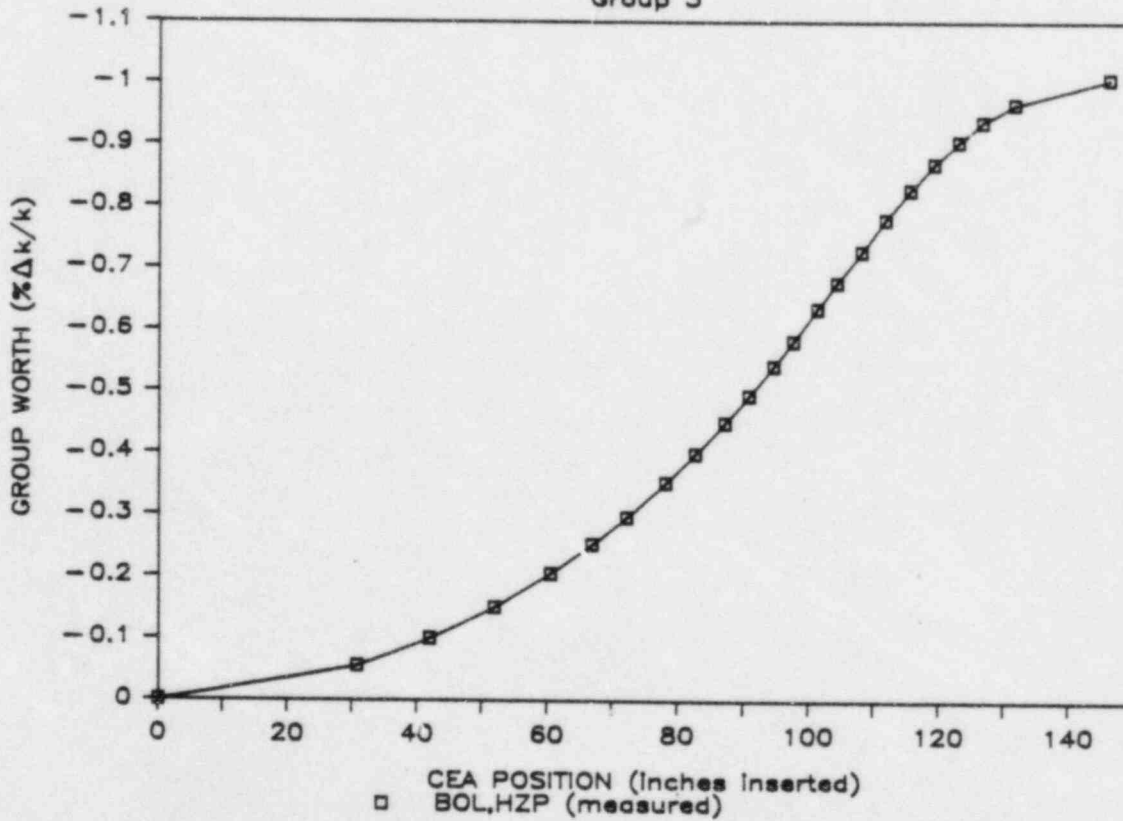


INTEGRAL CEA WORTH, NO OVERLAP

Group 4

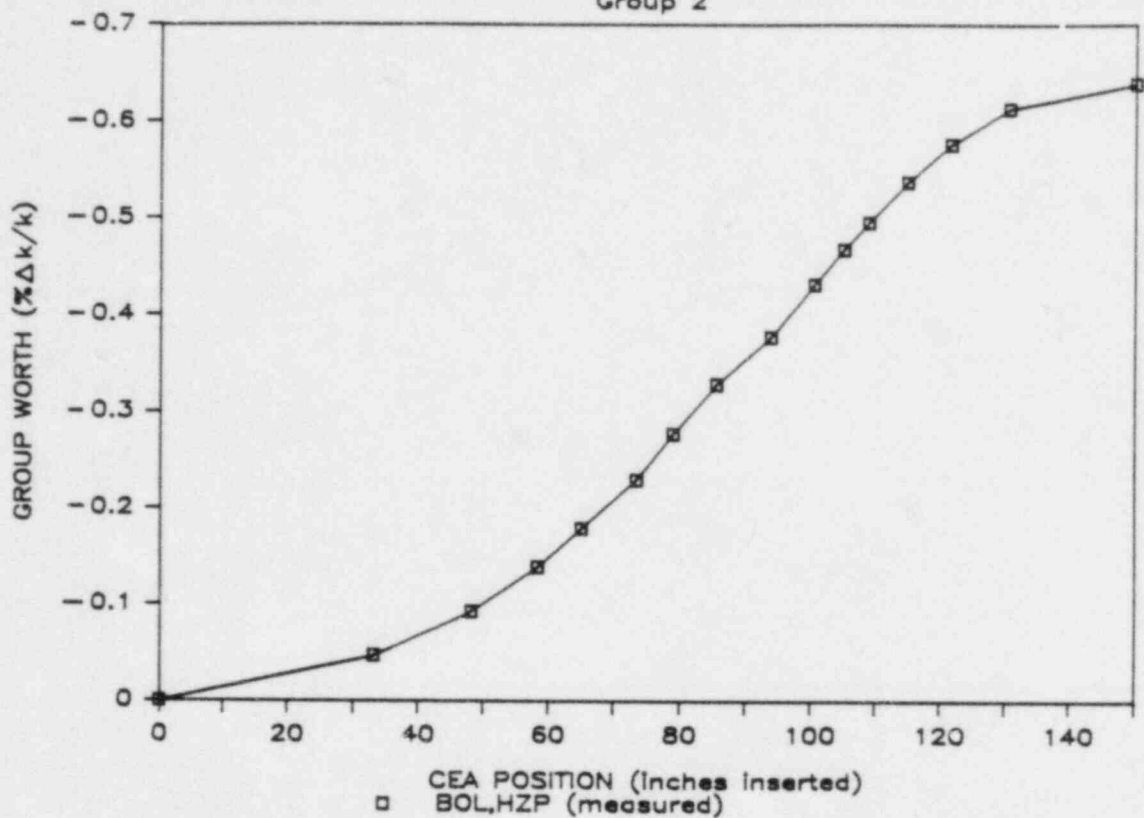


Group 3



INTEGRAL CEA WORTH, NO OVERLAP

Group 2



Group 1

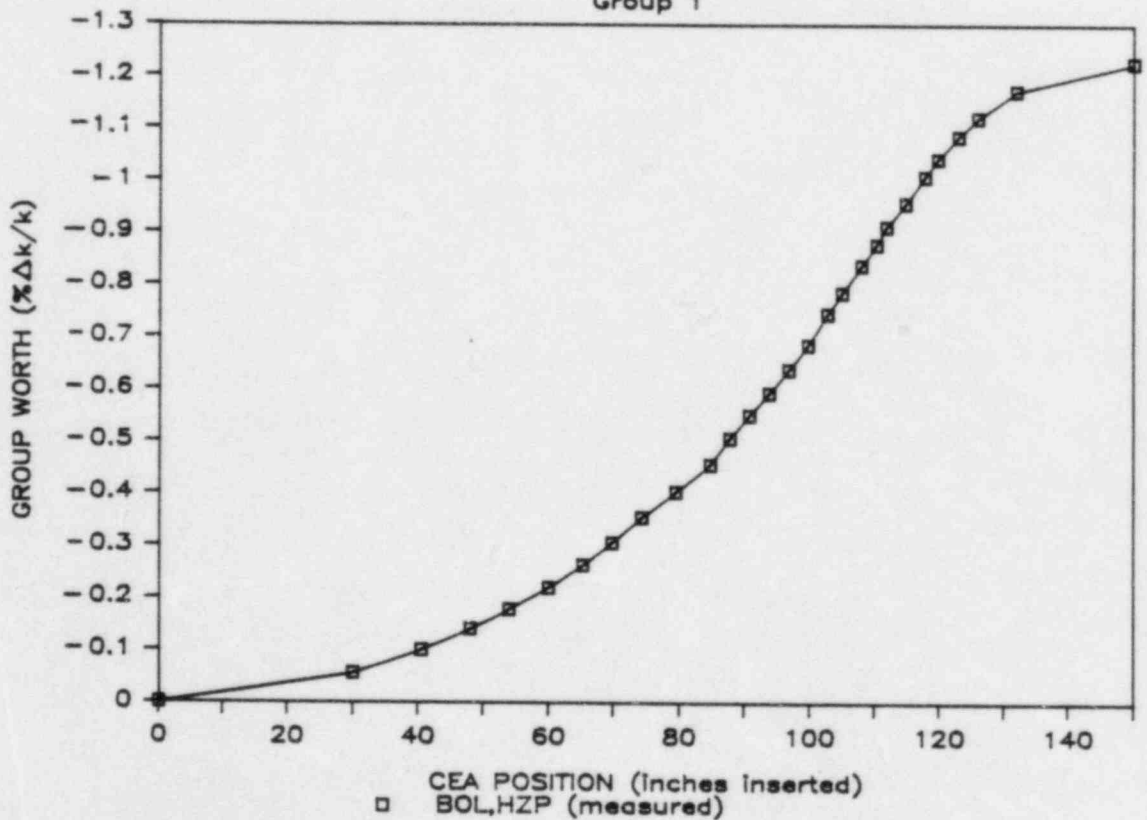
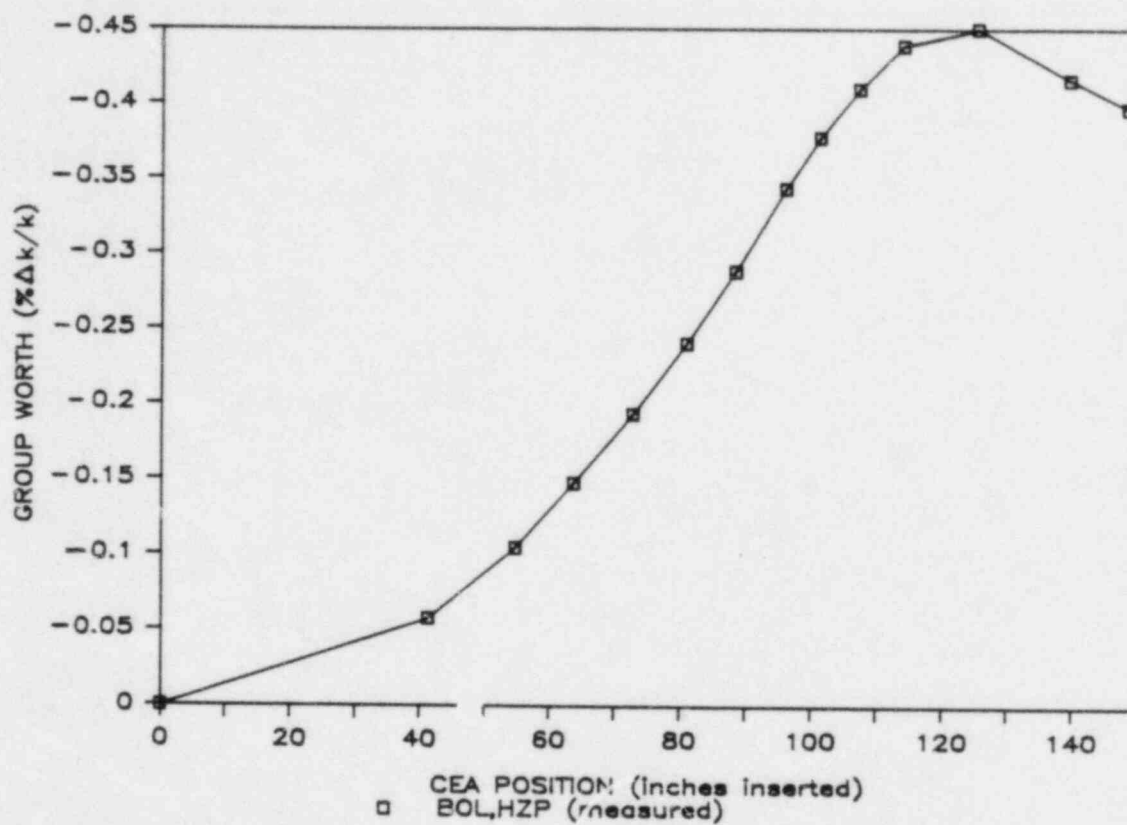


Figure 5.2.4
INTEGRAL CEA WORTH (GROUP P)



- 1) CEA Group 6 \geq 135 inches withdrawn (essentially all rods out (EARO))
- 2) CEA Groups 6 through 3 at the lower electrical limit (LEL)
- 3) CEA Groups 6 through 1 at the LEL

The ITC is the sum of the fuel temperature coefficient (FTC) and the moderator temperature coefficient (MTC). The FTC is a negative constant (supplied by the reactor vendor), while the MTC may be slightly positive at high boron concentrations and large and negative for low concentrations. The MTC was calculated by subtracting the FTC from the measured ITC.

The results of the ITC/MTC tests are summarized in Table 5.0.1. All ITC/MTC acceptance criteria were satisfied.

5.4 Critical Boron Concentration Measurements

The critical boron concentrations (CBCs) were measured by stabilizing the plant in the desired configuration and maintaining temperature, pressure and CEA position as constant as possible. Once the RCS conditions were stable, RCS boron samples were collected and analyzed to determine the actual CBC. During the LPPT, it was not always practical to establish the CEAs at exactly the required position; rather the CEAs were positioned near the desired point and then briefly withdrawn or inserted to the required position and the residual reactivity worth measured. The measured residual reactivity worth was then converted to an equivalent boron concentration and added to or subtracted from the measured CBC.

Critical boron concentrations were measured in the same configurations as, and just previous to, the ITC/MTC measurements. The CBC test results are summarized in Table 5.0.1. All critical boron concentration acceptance criteria were satisfied.

5.5 Boron Worth Measurements

The inverse boron worth (IBW) was calculated using CBCs and CEA group worths measured previously. The IBW was calculated by dividing the difference in CBCs by the difference in CEA group worths between two CEA positions. Inverse boron worths were calculated for the following configurations:

- 1) CEA Groups 6 through 3 fully inserted, and
- 2) CEA Groups 6 through 1 fully inserted.

The results of the IBW calculations are summarized in Table 5.0.1. All inverse boron worth acceptance criteria were satisfied.

TABLE 5.0.1
WATERFORD 3 SES LPPT RESULTS

PARAMETER	UNITS	MEASURED VALUE	ACCEPTANCE CRITERIA
5.1 CEA SYMMETRY CHECKS	¢	1.07¢ (max) (see Figure 5.1.1)	within $\pm 1.5¢$ of group average
5.2 CEA GROUP WORTHS			
Group 6	% $\Delta k/k$	0.392	0.409 ± 0.05
Group 5	% $\Delta k/k$	0.383	0.390 ± 0.05
Group 4	% $\Delta k/k$	0.913	0.913 ± 0.09
Group 3	% $\Delta k/k$	1.008	1.020 ± 0.10
Group 2	% $\Delta k/k$	0.640	0.662 ± 0.07
Group 1	% $\Delta k/k$	1.230	1.214 ± 0.12
Group B	% $\Delta k/k$	3.008	3.076 ± 0.31
Group P	% $\Delta k/k$	0.397	0.369 ± 0.05
Total Inserted Worth	% $\Delta k/k$	11.252	11.327 ± 1.13
Shutdown Margin at t.e ZPIL	% $\Delta k/k$	9.398	≥ 5.15
5.3 ITC MEASUREMENTS			
ITC @ EARO	$\Delta k/k/^\circ F$	-0.391×10^{-4}	$-0.393 \times 10^{-4} \pm 0.3 \times 10^{-4}$
MTC @ EARO	$\Delta k/k/^\circ F$	-0.235×10^{-4}	$-0.237 \times 10^{-4} \pm 0.3 \times 10^{-4}$
ITC w/6-3 @ LEL	$\Delta k/k/^\circ F$	-1.025×10^{-4}	$-1.302 \times 10^{-4} \pm 0.3 \times 10^{-4}$
MTC w/6-3 @ LEL	$\Delta k/k/^\circ F$	-0.870×10^{-4}	$-1.142 \times 10^{-4} \pm 0.3 \times 10^{-4}$
ITC w/6-1 @ LEL	$\Delta k/k/^\circ F$	-1.530×10^{-4}	$-1.810 \times 10^{-4} \pm 0.3 \times 10^{-4}$
MTC w/6-1 @ LEL	$\Delta k/k/^\circ F$	-1.370×10^{-4}	$-1.650 \times 10^{-4} \pm 0.3 \times 10^{-4}$
5.4 CBC MEASUREMENTS			
CBC @ EARO	ppm	829.10	832 ± 50
CBC w/6-3 @ LEL	ppm	619.52	629 ± 50
CBC w/6-1 @ LEL	ppm	506.80	499 ± 50
5.5 INVERSE BOPON WORTH MEASUREMENTS			
IBW w/6-3 @ LEL	ppm/% $\Delta k/k$	-77.7	-74.3 ± 10
IBW w/6-1 @ LEL	ppm/% $\Delta k/k$	-60.0	-69.7 ± 10

SECTION 6.0

POWER ASCENSION TESTING

6.1 POWER LEVEL DETERMINATION

6.1.1 Reactor Coolant System Delta-T Power Determination (SIT-TP-704)

PURPOSE:

The purpose of this test was to determine the thermal output of the reactor at power levels up to approximately 20% by means of a primary system calorimetric. The power level calculated in this test was then used as the standard for calibrating the core protection calculators and the excore nuclear instrumentation (see section 6.2.1).

METHOD:

RCS hot leg and cold leg temperatures were recorded and averaged. (The hot leg temperatures were corrected for temperature bias, previously determined during hot zero power plant conditions.) From these temperatures the enthalpy rise across the core (Δh) was determined. The core thermal power (Q) was then calculated by multiplying Δh by the core mass flow rate (M). The core thermal power (Q), when divided by the rated thermal power (RTP) of the core (3390 MWth), and multiplied by 100%, yielded the percent of rated thermal power at which the reactor was operating.

Thus:

$$Q(\text{MWth}) = M(\text{lb}_m/\text{hr}) \Delta h(\text{BTU}/\text{lb}_m) / 3412141. (\text{BTU}/\text{MWth-hr})$$

and

$$\% \text{ RTP} = Q(\text{MWth}) \times 100(\%) / 3390(\text{MWth})$$

RESULTS:

The reactor coolant system delta-T power determination was performed ten times during the power ascension test program. There were no significant difficulties encountered in the performance of this test.

The results are summarized in Table 6.1.1.1 below.

TABLE 6.1.1.1

RCS DELTA-T POWER DETERMINATION TEST RESULTS

Date	RCS Mass Flow Rate ($10^6 \text{lb}_m/\text{hr}$)	Δh (BTU/lb_m)	Reactor Power (%)
3/17/85	169.71	3.04	4.46
3/17/85	169.86	2.86	4.20
3/19/85	169.42	8.57	12.55
3/20/85	168.69	14.58	21.26
4/12/85	170.16	11.92	17.54
4/13/85	169.92	14.18	20.83
4/14/85	169.86	14.32	21.02
4/14/85	170.05	14.48	21.29
4/18/85	170.08	13.73	20.19
4/18/85	170.04	14.24	20.93

CONCLUSION:

Reactor power was satisfactorily determined, thereby providing a reliable standard for calibration of the core protection calculators and excore nuclear instrumentation. All test objectives were met and acceptance criteria satisfied.

6.1.2 NSSS Calorimetric (SIT-TP-709)

PURPOSE:

The NSSS calorimetric power measurement provided an accurate determination of reactor power based on a secondary plant energy balance. This power measurement was used to meet the following objectives:

1. Verify that the secondary calorimetric based core power calculated by the Core Operating Limits Supervisory System (COLSS) is an accurate determination of core power.
2. Calibrate the reactor coolant system delta-T power determined by COLSS to achieve satisfactory agreement with the secondary calorimetric power.
3. Verify the secondary heat balance calculations performed in one of the nuclear engineering procedures.
4. Verify the secondary heat balance calculations performed by an off-line applications computer program.

METHOD:

Stable initial conditions for reactor power, reactor coolant system temperatures, pressure, feedwater temperature and steam generator levels were established. Data was then collected at 30 second intervals for one hour and averaged. The average values of the various parameters were used to calculate reactor power from the following equation:

%Reactor Power =

$$\frac{[\sum_{i=1}^2 (M_{f_i} - M_{bd_i})(h_{s_i} - h_{f_i}) + M_{bd_i}(h_{bd_i} - h_{f_i})] + M_{ch}(h_{ld} - h_{ch}) + Q_{loss} - Q_{rcp} - Q_{pZR}}{3390 \text{ MWt}} \times K \times 100\%$$

Where: M_{f_i} = Mass flow of feedwater supplied to steam generator i

M_{bd_i} = Mass flow of blowdown from steam generator i

h_{s_i} = Enthalpy of steam from steam generator i (corrected for 99.8% quality)

h_{f_i} = Enthalpy of feedwater supplied to steam generator i

h_{bd_i} = Enthalpy of blowdown from steam generator i

M_{ch} = Mass flow of charging to the reactor coolant system

h_{ld} = Enthalpy of letdown from the reactor coolant system

h_{ch} = Enthalpy of charging to reactor coolant system

Q_{loss} = RCS Heat Loss

Q_{rcp} = Heat input from reactor coolant pumps

Q_{pZR} = Heat input from pressurizer

K = Conversion factor from BTU/hr to MW = $1/(3.412 \times 10^6)$

100% = Conversion factor from fraction of full power to % of full power

3390 MWt = Rated full core power level

NOTE: All steam and water properties (i.e. enthalpy, specific volume) were obtained from 1967 ASME Steam Tables.

For both equilibrium and non-equilibrium xenon conditions the hand calculated calorimetric power was compared to the average COLSS calculated secondary calorimetric power (BSCAL). At equilibrium xenon conditions, these values were to agree within $\pm 0.2\%$ of rated thermal power ($\pm 0.5\%$ at 20% power); at non-equilibrium xenon conditions, they were to agree within $\pm 2.0\%$ at all test plateaus. If necessary the test data and COLSS constants were evaluated and this procedure repeated until the desired agreement was obtained.

For both equilibrium and non-equilibrium xenon conditions the hand calculated calorimetric power was compared to the average core delta-T power (BDELTA). At equilibrium xenon conditions these values were to agree within $\pm 0.2\%$ of rated thermal power ($\pm 0.5\%$ at 20% power); at non-equilibrium xenon conditions, they were to agree within $\pm 2.0\%$ at all test plateaus. If this agreement was not achieved, a new delta-T power gain, E19, was calculated from the following relationship:

$$E19 = \frac{\text{Average BSCAL}}{(\text{Average Static Delta-T Power} - E20)}$$

where E20 is the delta-T power bias term.

After setting the delta-T power gain into the plant computer, a new set of data were taken at 30-second intervals for 5 minutes. The average value of BDELTA was then compared with the hand calculated calorimetric power or an average value of BSCAL and the difference verified as acceptable.

When the plant was at equilibrium xenon, NE-5-201, Heat Balance Calculation, and NE-72-03, POWER Program were executed using the average data collected for this procedure. The power levels calculated by means of these two procedures were compared to the calorimetric power calculated for this test. If these power levels agreed within $\pm 0.5\%$ ($\pm 1.0\%$ at 20% power) of the calorimetric power, then NE-5-201 and NE-72-03 were considered acceptable.

RESULTS:

The NSSS calorimetric procedure was performed thirteen times between April 13 and July 3, 1985. No significant problems were encountered in performing this procedure. Results of each test are summarized in Table 6.1.2.1.

CONCLUSION:

The power levels calculated from NE-5-201 and NE-72-03 were in good agreement with the hand calculated calorimetric power, thereby verifying acceptability of the methodology and accuracy of both procedures.

The COLSS delta-T power (BDELTA) and COLSS calorimetric power (BSCAL) were within the required tolerance of the hand calculated power, although on several occasions it was necessary to adjust the delta-T power gain and show acceptability of the BDELTA value by comparison to BSCAL. All acceptance criteria for non-equilibrium and equilibrium xenon were satisfactorily met.

TABLE 6.1.2.1
NSSS CALORIMETRIC RESULTS (1)

Date	Calorimetric Power ⁽²⁾	BSCAL ⁽²⁾	BDELT ⁽²⁾ (before)	BDELT ⁽²⁾ (after)	BSCAL ⁽²⁾ (after)	NE-5-201 Power ⁽²⁾	Power Program ⁽²⁾	Equilibrium (Yes/No)
4/13	18.73	18.73	21.04	18.77	-	-	-	NO
4/14	19.20	19.35	21.34	19.44	19.48	19.31	19.30	YES
4/18	29.97	29.99	27.27	30.39	-	-	-	NO
4/19	41.14	41.00	41.08	41.08 ⁽³⁾	-	-	-	NO
4/20	49.97	49.97	50.08	50.08 ⁽³⁾	-	-	-	NO
4/21	50.57	50.63	50.12	50.11	50.11	50.34	50.30	YES
5/6	59.22	59.22	59.63	59.63 ⁽³⁾	-	-	-	NO
5/7	70.21	70.25	70.73	70.73 ⁽³⁾	-	-	-	NO
5/8	79.72	79.70	81.06	81.06 ⁽³⁾	-	-	-	NO
5/9	80.64	80.65	82.31	79.44	79.40	80.63	80.60	YES
7/1	94.11	94.16	94.67	94.67 ⁽³⁾	-	-	-	NO
7/2	98.63	99.07	100.80	101.58	100.67	-	-	NO
7/3	99.29	99.32	98.69	99.56	99.44	99.15	99.30	YES

(NOTES to table on next page)

Notes to Table 6.1.2.1

- (1) Criteria used to determine the acceptability of a parameter were as follows:

Non-Equilibrium Xenon

a. $-2.0\% \leq (\text{Calorimetric Power}) - (\text{BSCAL}) \leq 2.0\%$ and
(before)

b. $-2.0\% \leq (\text{Calorimetric Power}) - (\text{BDELT}) \leq 2.0\%$ or
(before)

$$-2.0\% \leq (\text{BSCAL}) - (\text{BDELT}) \leq 2.0\%$$

(after) (after)

Equilibrium Xenon

a. $-0.2\% \leq (\text{Calorimetric Power}) - (\text{BSCAL}) \leq 0.2\%$ ($\pm 0.5\%$ at 20% power) and
(before)

b. $-0.2\% \leq (\text{Calorimetric Power}) - (\text{BDELT}) \leq 0.2\%$ ($\pm 0.5\%$ at 20% power) or
(before)

$$-0.2\% \leq (\text{BSCAL}) - (\text{BDELT}) \leq 0.2\%$$
 ($\pm 0.5\%$ at 20% power)
(after) (after)

c. $-0.5\% \leq (\text{Calorimetric Power}) - (\text{NE-5-201 Power}) \leq 0.5\%$

d. $-0.5\% \leq (\text{Calorimetric Power}) - (\text{POWER Program}) \leq 0.5\%$

- (2) All power values reported in units of % RATED THERMAL POWER

- (3) Calibration not required

6.2 INSTRUMENTATION TESTING/CALIBRATION

6.2.1 Nuclear and Thermal Power Calibration (SIT-TP-705)

PURPOSE:

The objective of the nuclear and thermal power calibration test was to calibrate excore linear power, CPC thermal power and CPC nuclear power to a standard measurement of core power. FSAR Chapter 14, Section 14.2.12.3.27, Steady-State Core Performance, was partially satisfied by performance of this test.

METHOD:

Initial conditions were established with the reactor at steady-state conditions. A standard measurement of core power was then determined by one of the following methods:

- A. Up to approximately 20% rated thermal power, reactor power was calculated from a primary system calorimetric measurement (i.e., RCS delta-T power measurement; see section 6.1.1).
- B. Above 20% rated thermal power, reactor power was obtained from a secondary energy balance calculation performed by the Core Operating Limit Supervisory System.

Utilizing the standard power, a new voltage output from the excore linear amplifier was determined. The amplifier gain of one channel was adjusted to obtain the new voltage. After performing the adjustment for one channel and verifying acceptable agreement between excore linear power and standard power, the remaining three channels were adjusted to agree with the first.

Calibration of CPC nuclear power (PHICAL) and thermal power (BDT) was accomplished by changing the respective values of the addressable calibration constants. These constants were computed from the following:

$$\text{New Constant} = \text{Old Constant} \times \frac{\text{Standard Power}}{\text{Indicated Power}}$$

After installing the new constants in the CPCs, both the thermal and nuclear power indications for all channels were verified to be in agreement with the current value of standard power.

RESULTS:

The nuclear and thermal power calibration procedure was performed thirty-four times between March 17 and July 10, 1985. In all but three cases, the PPS excore linear power and CPC powers were calibrated within the required tolerance. In two of these cases, a reactor trip occurred before the calibration procedure could be completed. Subsequent performance of the procedure ensured that the parameters of interest were calibrated within specification.

During the performance of this procedure at a nominal 5% power on March 17, 1985, both CPC addressable calibration constants were required to be adjusted for all four CPC channels. However, the new nuclear power calibration constants for channels B, C and D and the new thermal power calibration constant for channel A were found to exceed the maximum values allowed by Technical Specifications. Consequently, the maximum allowable values were installed in place of the calculated values. This resulted in acceptable calibration of channels B and D. Channels A and C remained out-of-tolerance. Similarly, the channel C and D excore linear power indications remained out-of-tolerance after adjusting the amplifier gain potentiometers to maximum. Two days later, on March 19, 1985 these discrepancies were cleared by reperformance of the test at approximately 15% power. All PPS and CPC power indications were then calibrated to the required tolerance.

Table 6.2.1.1 summarizes the date and power level at which each procedure was performed.

TABLE 6.2.1.1
NUCLEAR AND THERMAL POWER CALIBRATION

DATE PERFORMED	STANDARD POWER (%)	DATE PERFORMED	STANDARD POWER (%)
3/17/85	4.20	5/6/85	59.57
3/19/85	12.71	5/7/85	71.50
3/20/85	21.26	5/8/85	79.13
4/12/85	17.54	5/9/85	79.55
4/14/85	19.35	5/19/85	24.14
4/14/85	21.29	5/20/85	61.77
4/18/85	20.20	5/27/85	80.37
4/18/85	19.98	6/25/85	79.42
4/19/85	29.76	6/26/85	89.85
4/19/85	41.50	7/1/85	93.79
4/20/85	49.31	7/1/85	98.44
4/21/85	50.94	7/2/85	100.00
4/23/85	50.23	7/3/85	99.98
5/2/85	50.69	7/5/85	60.18
5/4/85	19.50	7/7/85	88.97
5/6/85	50.09	7/9/85	99.30
5/6/85	49.88	7/10/85	99.35

CONCLUSIONS:

With the above noted exceptions, the PPS and CPC power indications were successfully calibrated to the standard indication of reactor power. For the cases in which the calibration was out of tolerance or not completed, associated deficiencies were cleared and the procedure was reperformed successfully.

6.2.2 Process Variable Intercomparison (SIT-TP-712)

PURPOSE:

The purpose of this test was to demonstrate that the inputs and appropriate outputs of the Plant Protection System (PPS), the Core Protection Calculators (CPCs), and the Plant Monitoring Computer (PMC) were in satisfactory agreement with one another. Permanent plant instrumentation (meters and recorders) were also included in the intercomparison.

This test satisfied the commitments of FSAR section 14.2.12.3.30.

METHOD:

Plant conditions were stabilized at each of the four test plateaus -- 20%, 50%, 80%, and 100% power -- during the initial power ascension following core load. Data from each of the four sources (PPS, CPCs, PMC, and permanent plant instrumentation) were simultaneously gathered for each of the following parameters:

1. RCS cold leg temperature
2. RCS hot leg temperature
3. RCP differential pressure
4. RCP speed
5. RCS pressure

6. Pressurizer level
7. Steam generator level
8. Steam generator pressure
9. Steam generator primary side differential pressure
10. Reactor vessel differential pressure
11. Containment pressure
12. Refueling water storage pool (RWSP) level

Based upon the data gathered for each parameter, a target value was calculated as the average of the readings from the most reliable source; the order of reliability of data sources, from most reliable to least, was as follows:

1. Core Protection Calculator data
2. Plant Protection System data
3. Plant Monitoring Computer data
4. Control Board Instrumentation data

The deviation of each recorded value from this target value was calculated and compared to the specified tolerance to determine acceptability. If the deviation exceeded the specified tolerance and a test deficiency was generated, recalibration of the loop was initiated. The deficiency was cleared only when subsequent testing revealed that the parameter deviation fell within the specified tolerance.

RESULTS:

At the 20% power plateau, thirty-two deficiencies were generated; seventeen of these were written against RCS hot and cold leg temperature indications. Four RCP speed sensors were out-of-tolerance as well as one RWGP level indication. Of the remaining seven out-of-specification indications, six were PMC or control board-related.

At the 50% power plateau, eight additional deficiencies were generated; seven of these were RCS RTD-related. Of the fifteen deficiencies written at 20% power that were not related to RCS RTDs, all but two had been reworked to meet the specified tolerances. Thus, the total number of outstanding deficiencies following completion of 50% power testing was twenty-eight; twenty-four of these were RCS temperature indications.

At the 80% power plateau, ten new deficiencies were generated; seven of these were RCS temperature indications. All deficiencies outstanding from the 50% plateau which were not related to RCS RTDs had been reworked and found acceptable at 80%. Thus, the total number of outstanding deficiencies following completion of the 80% power testing was thirty-four; thirty-one of these were RCS temperature indications.

At the 100% power plateau, eleven additional deficiencies were written; seven of these were RCS temperature indications. One of the three non-RTD-related deficiencies from 80% had been successfully reworked, leaving a total of six non-RTD-related deficiencies. Thirty-eight deficiencies relating to RCS temperature indication remained outstanding.

Two of the deficiencies not related to RCS temperature were reworked and satisfactorily retested; the other four deficiencies have also been reworked, but have not yet been retested. Three of the four deficiencies were written against PMC parameters, while the fourth was written against a control board instrument; no PPS or CPC parameters, with the exception of the RTDs, were out-of-tolerance at the completion of 100% power testing.

Discussion of RCS RTD Problems

Problems with the RCS RTDs were first noted during the performance of SIT-TP-501, Pre-critical Intercomparison of PPS, CPC, and PMC Inputs (see also section 3.1.1). An evaluation of the magnitude of the RTD errors found that operation at the 20% power plateau would not represent an unsafe condition. Analysis and troubleshooting of the RTD problems continued.

Troubleshooting of the problem revealed the following:

1. The RTDs which provide hot and cold leg temperature indication to CPC channels A and B were significantly more in error than those providing indication to channels C and D. The former RTDs were manufactured by Weed, while the latter RTDs were manufactured by Rosemount. Initially, all four CPC channels were driven by Rosemount detectors, but the requirement for dual-channel RTDs to accommodate the Qualified Safety Parameter Display System (QSPDS) led to the installation of the Weed RTDs.

2. The primary components of the Weed RTD error were identified as inaccuracies in the RTD curve used to relate resistance to degrees Fahrenheit, normal calibration inaccuracies, and a thermocouple effect which was discovered at the RTD junction; this thermocouple effect involved a potential difference induced across the RTD leads which biased the input to the temperature transmitters.
3. Corrosion at the various terminations between the RTD and the process analog control (PAC) cabinets and noise induced within the PAC cabinets due to inadequate shielding also contributed to the errors, but to a lesser extent than those items detailed in (2) above.

Corrective action was initiated as follows:

1. Four Weed RTDs were replaced, two each in channels A and B.
2. All RTDs, both Rosemount and Weed, were carefully recalibrated.
3. All terminations were cleaned of corrosion and ensured tight.
4. Evaluation of the impact of the greater-than-anticipated RTD inaccuracies was performed. As additional RTD data became available, this impact was continuously reassessed. The results of the analyses, performed by Combustion Engineering, Inc., are detailed below:

- The impact of the greater RTD inaccuracies on the CPC calculations was twofold. First, the inaccuracy in measured RCS flowrate was increased; second, the accuracy of core thermal power BDT was adversely affected.
- Operation at reactor power levels of up to 50% was deemed acceptable, on the condition that the PPS high linear power trip setpoint was adjusted to 65% instead of 70% power. This ensured that sufficient margin remained in the CPC DNBR and LPD calculations to account for the increased uncertainty associated with the RCS flowrate; also, induced errors in BDT were of greatest concern only above 65% power during a CEA deviation event.
- A preliminary analysis was conducted during plant testing at 50% power to determine whether full power operation would be permissible given the magnitude of the RTD errors. The limited availability of RTD data did not provide adequate assurance that safe operation at 100% power could be achieved. However, operation at reactor power levels of up to 90% was approved, on the condition that the following penalties were applied to all four CPC channels:

BERR1 - increase by 8.3% (above original value)

BERR3 - increase by 4.2% (above original value)

PFMLTD - increase by 17.4% (above original value)

PFMLTD - increase by 17.4% (above original value)

These additional penalties were incorporated into the CPC channels prior to increasing power above 50%. Extensive RTD data collection was then initiated to support a more accurate analysis of the problem.

- Based upon the extensive RTD data collected, a more detailed analysis was performed. It was determined that the channel C and D RTDs (manufactured by Rosemount) exhibited errors within the allowable range. Also, channel A and B RTD errors were better quantified, and more appropriate penalty factors were developed to assure conservative full power operation. Operation at power levels up to 100% was approved, on the condition that the following penalties were applied to CPC channels A and B only:

BERR1 - increase by 3% (above original value)

BERR3 - increase by 4% (above original value)

PFMLTD - increase by 17.8% (above original value)

PFMLTL - increase by 17.8% (above original value)

These modified penalties were incorporated into CPC channels A and B prior to operation above 90%. The penalty factor addressable constants in channels C and D were restored to their original values.

- Continuous monitoring of the performance of the CPC RTDs was made a prerequisite of continued power operation, to ensure that the temperature errors remain within the bounds of the Combustion Engineering analysis. This monitoring will be performed by a Nuclear Engineering procedure whenever four reactor

coolant pumps are in operation. The procedure also provides for the calculation of new penalty factor addressable constants in the event the temperature errors increase beyond current values.

In summary, the problem with CPC RTDs was discovered via the performance of SIT-TP-501 and SIT-TP-712. Troubleshooting conducted by the plant Instrument and Controls Department revealed the primary causes. The most erroneous RTDs were replaced, and recalibration of the remaining RTDs was reperformed. An analysis of the measured RTD errors, performed by Combustion Engineering, found full power operation to be acceptable, contingent upon the imposition of additional uncertainty penalties on the CPC calculations of LPD and DNBR. Monitoring of CPC RTD performance will continue until the errant Weed RTDs are replaced and the measured errors determined to fall within the bounds of the original CPC specifications.

CONCLUSIONS:

With the exception of the RCS temperature problems noted above, all safety-related indications exhibited satisfactory agreement with one another. Four non-safety indications which did not meet specified tolerances have been reworked and will be retested when plant conditions permit. The impact of the out-of-tolerance temperature indications has been evaluated and appropriate actions taken to ensure conservative operation of the CPCs.

6.2.3 Linear Power Subchannel Calibration (SIT-TP-711)

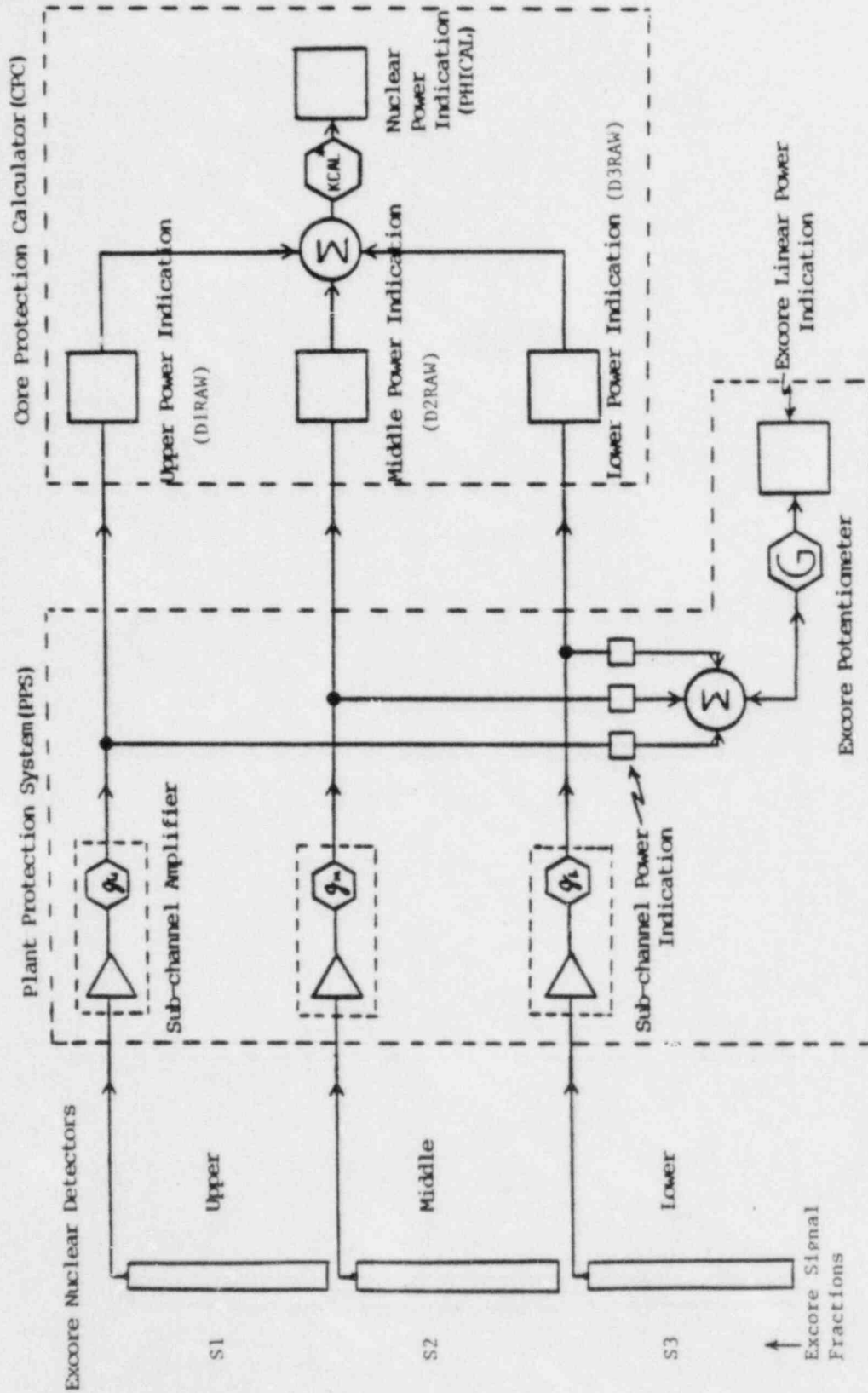
PURPOSE:

This procedure adjusted the excore linear power subchannel amplifier gains so that the fractional power distribution as measured by the excore detectors was within 0.1% of that measured by the incore detectors. After completing the adjustments, the excore 200% linear calibrate potentiometers were reset to reflect the new amplifier gains. The second part of this procedure collected baseline data on all the amplifiers to be used for routine surveillances or replacement of amplifiers.

METHOD:

Combustion Engineering's (C-E's) CECOR code uses the incore detectors to calculate normalized fractional power distributions for the upper, middle, and lower axial sections of the reactor core. By adjusting the excore amplifier gains, the excore system will read the same fractional powers as measured by the incores. Figure 6.2.3.1 illustrates the excore signal path and shows the relationship between signal fractions, excore linear power and Core Protection Calculator (CPC) power indications.

The test was completed at 20% power on April 14, 1985 and at 50% power on April 22, 1985, and was a prerequisite for measuring the Shape Annealing Matrix (see Section 6.3.6). The test was performed at equilibrium xenon conditions with ASI oscillations less than .01 ASI units in a four hour period. The stable power distributions were required so that little error was introduced during the time period from initial data collection to the completion of the first channel



*Signal modification is also performed for Rod Shadowing and Temperature Decalibration.

Figure 6.2.3.1 EXCORE SIGNAL PATHS

adjustments. With temperature, power and ASI stable, a nominal core power was determined using either the core delta-T method (at 20%) or the NSSS calorimetric method (at 50%). Using this power level and the appropriate signal fraction for upper, middle or lower core section, the output of each excore amplifier was calculated as follows:

$$D(I) \text{ RAW} = 3 \times S(I) \times \text{PWR}$$

for I = 1(upper)
 2(middle)
 3(lower)

Where S(I) = Signal fraction for each core section

PWR = % Reactor power as described above

D(I) RAW = Amplified excore detector signals sent to
 the CPCs and Excore Linear Power Indication.

Each amplifier was adjusted so that the corresponding D(I)RAW as displayed at the CPC operators module was within $\pm 0.1\%$ of the calculated value. Adjustment of the amplifiers affects the 200% calibrate setting so each of these was reset following amplifier adjustments. After the adjustments were completed for the first channel the following three channels were adjusted such that their output was within $\pm 0.1\%$ of the reading present on the first channel. This eliminated any error for power and temperature drift that occurred during the time required to adjust all four channels.

Upon completion of the excore power adjustments on all four channels, baseline amplifier data was collected to be used during routine surveillances of the Plant Protection System (PPS). At each subchannel location the appropriate detector cable was removed and a current source installed.

By inputting a known current and recording the amplifier output the amplifier (or a replacement amplifier) may be calibrated to this gain at any time in the future.

RESULTS:

Performance of this test at 20% was completed using C-E predictions for upper, middle and lower excore fractional powers. After establishing the required equilibrium conditions, adjustments were completed for all excore subchannels and their corresponding 200% linear calibrate signals. Table 6.2.3.1 shows the as-left excore subchannel signals and the resulting signal fractions.

TABLE 6.2.3.1
AS-LEFT SIGNALS AND SIGNAL FRACTIONS AT 20%

Parameter	Channel A	Channel B	Channel C	Channel D	Prediction
D1RAW	17.20	17.20	17.10	17.10	N/A
D2RAW	24.50	24.50	24.40	24.30	N/A
D3RAW	16.50	16.50	16.40	16.40	N/A
S1	.2946	.2946	.2929	.2929	.2962
S2	.4197	.4197	.4179	.4162	.4199
S3	.2826	.2826	.2810	.2810	.2839

Following completion of the 20% test plateau it was discovered that the upper and lower excore cables on channel C were reversed. After they were corrected new baseline currents were calculated for channel C upper and lower amplifiers. These amplifiers were readjusted and all subchannel signals for all four channels were reverified to be within $\pm 0.1\%$.

Upon reaching equilibrium xenon conditions at 50% power the CECOR code was executed to determine excore signal fractions. Results from CECOR case NJD-R4861GT were:

$$S1 = .2882$$

$$S2 = .4135$$

$$S3 = .2983$$

During adjustment of the first channel, reactor power changed by more than 1% but less than approximately 2%. The test was secured until initial conditions were reestablished, then completed in its entirety. Table 6.2.3.2 shows results of the excore adjustments. All 200% calibrate potentiometers were adjusted to achieve $200 \pm 1.0\%$.

TABLE 6.2.3.2
AS-LEFT-SIGNAL AND SIGNAL FRACTIONS AT 50%

Parameter	Channel A	Channel B	Channel C	Channel D	Prediction
D1RAW	42.9	42.9	42.9	42.9	N/A
D2RAW	61.8	61.8	61.8	61.8	N/A
D3RAW	44.7	44.7	44.7	44.6	N/A
S1	.2844	.2844	.2844	.2844	.2882
S2	.4097	.4097	.4097	.4097	.4135
S3	.2963	.2963	.2963	.2957	.2983

CONCLUSION:

As a prerequisite to measuring the Shape Annealing Matrix as described in section 6.3.6 of this report, each excore linear power subchannel was adjusted such that the upper, middle and lower excore powers were within $\pm 0.1\%$ of the fractional powers as measured by the incore detectors. In addition to the above adjustments the excore 200% calibrate

potentiometers were adjusted to $200.0 \pm 1.0\%$. Baseline amplifier currents were measured and transmitted to I&C for future calibration and/or replacement of the excore linear power subchannel amplifiers. All test objective and acceptance criteria were satisfactorily met.

6.2.4 Vibration and Loose Parts Monitoring System (SIT-TP-714)

PURPOSE:

To establish baseline data for all vibration, loose parts, and reactor core internals motion channels at various test plateaus and to verify that the existing loose parts alarm setpoints are acceptable for power operation. This test satisfied, in part, the commitments of FSAR Chapter 14, Section 14.2.12.3.40, Baseline Vibration and Loose Parts Monitoring.

METHOD:

Data was recorded on cassette tapes via the vibration and loose parts monitoring system (V&LPMS) tape recorders while the plant was in steady state operation.

Each channel of recorded data was then analyzed using a spectrum analyzer, and plotted using an X-Y plotter to generate power spectral density (PSD) signatures.

Data was collected at the following steady state conditions:

- 0% power (Reactor critical)
- 20% power
- 50% power
- 80% power

- Natural Circulation (following a trip from 80% power)
- 100% power

RESULTS:

All required data was successfully collected at each test plateau specified by the procedure.

At the 0%, 20%, and 50% test plateaus, high levels of background noise were initially recorded on the data tapes. These problems were resolved by either re-recording the noisy tape track on one of the good tracks, or by having a technician adjust the V&LPMS tape recorder.

During data collection for the 100% plateau, the core internals motion recorder was found to be inoperative. This problem was circumvented, without delaying the test, by substituting the vibration recorder and recording the data.

Throughout the test, the V&LPMS spectrum analyzer was unavailable. The problems with the spectrum analyzer stemmed from the fact that it was an obsolete model no longer supported by the manufacturer. The spectrum analyzer was functioning improperly and could not be repaired due to the unavailability of parts. Another problem with the spectrum analyzer was that it could not be calibrated to the manufacturer's specification. These problems will be resolved by the installation and calibration of a new spectrum analyzer.

CONCLUSION:

All data required per SIT-TP-714 was collected. However, the acceptance criterion has yet to be fully satisfied due to the continuing unavailability of a calibrated spectrum analyzer. The spectrum analyzer is required to analyze the data and produce the PSD signatures. Evaluation of the data will be performed following the installation and calibration of a new spectrum analyzer.

6.2.5 Control Systems Checkout (SIT-TP-721)

PURPOSE:

The purpose of this test was to demonstrate that:

- 1) During induced transients each individual plant control system (reactor regulating system (RRS); steam bypass control system (SBCS); and feedwater control system (FWCS)) is able to maintain/restore the appropriate plant parameters within their control bands.
- 2) During steady state operation the integrated plant control systems operate satisfactorily in automatic to maintain plant parameters stable.

If during any of the above individual or integrated system checks plant parameters were not maintained within or restored to specific operating bands, new setpoints were to be determined for the affected control system(s), and the check repeated to verify proper system operation.

This test satisfied in part the commitments of FSAR section 14.2.12.3.31 (see also section 6.6.2).

METHOD:

The individual control system checkouts had to be performed prior to performance of the integrated control systems test, but were not required to be completed in any specific sequence. Testing was performed as follows:

1. Individual Control Systems Checkout

1a. RRS Checkout:

Stable plant conditions were established with the SBCS, FWCS, pressurizer pressure control system (PPCS) and pressurizer level control system (PLCS) in automatic, and the control element drive mechanism control system (CEDMCS) in manual sequential (MS) mode. To test the automatic CEA insertion function, T_{avg} was then raised approximately 4.5°F above T_{ref} by dilution, after which the CEDMCS was placed in the auto sequential (AS) mode to insert the CEA as necessary to reduce the $T_{avg} - T_{ref}$ mismatch. During the insertion, the control system was tested for its ability to determine the magnitude of the mismatch and insert CEAs at high speed first, then change to low speed after magnitude of mismatch was reduced. The RRS was verified to have restored and stabilized T_{avg} to within $\pm 2^{\circ}\text{F}$ of T_{ref} before the CEDMCS was returned to MS. To test the automatic CEA withdrawal function, T_{avg} was reduced $2.5-3.5^{\circ}\text{F}$ below T_{ref} by dilution. When the CEDMCS was then placed in the AS mode, the control system was verified to withdraw the CEAs in low speed, (the high speed withdrawal function has been disconnected to avoid violation of the fuel preconditioning guidelines) to restore and stabilize T_{avg} to within $\pm 2^{\circ}\text{F}$ of T_{ref} .

When conditions had been restabilized, the CEDMCS was returned to MS. This test was performed at 50% and 100% power, for both RRS #1 and RRS #2.

1b. SBCS Checkout:

Stable plant conditions were established with the SBCS, FWCS, PLCS, PPCS and the digital-electro-hydraulic (DEH) system in automatic, and the CEDMCS in MS. To test the SBCS, the DEH was used to decrease the turbine load at less than 0.5% per minute. The resultant steam pressure increase was compensated for by a SBCS signal for steam bypass valve MS-319A to open. Simultaneously the SBCS was verified to limit the secondary pressure increase to less than 10 psia above the master controller setpoint. The turbine load decrease was terminated when MS-319A was approximately 50% open. The SBCS valve closing characteristic was then tested by increasing the turbine load to its initial value, to fully close MS-319A again and return secondary pressures to their original values.

This test was performed at 50% power only.

1c. FWCS Checkout:

Stable plant conditions were established with the SBCS, FWCS, PLCS and PPCS in automatic, and the CEDMCS in MS. With steam generator levels initially at normal operating levels, the level setpoint was then varied to verify that the steam generator levels follow the setpoint change. The setpoint was first changed to 10% per minute from 68% to 58%. After the level stabilized, the setpoint was ramped back to 68% at the same rate. This setpoint change was subsequently repeated at a rate of 1% per second to change the setpoint from 68% to 58% and back to 68%. Proper control system setpoints were verified by the ability of the FWCS to maintain steam generator levels within 1% of the level setpoints.

This test was performed for both FWCSs at the 50% and 80% plateaus.

2. Automatic Steady State Monitoring

Steady plant conditions were established with the SBCS, FWCS, PLCS, PPCS and DEH in automatic, and the CEDMCS in MS. At the start of the test, the CEDMCS was switched from MS to AS. No spurious CEA motion was observed and all relevant plant parameters were verified to remain stable.

This test was performed at the 50% and 80% plateaus.

RESULTS:

RRS Testing:

The RRSs were tested satisfactorily at both the 50% and 100% power plateaus. No setpoint adjustments were required for either RRS #1 or RRS #2 at either test plateau.

During the initial checkout of RRS #2 (the first system to be tested) at 50% power, difficulty was experienced in performing the automatic CEA withdrawal function. This was traced to the sequential permissive points locked into the "NOT ALLOWED" mode, thereby preventing auto sequential CEA operation. This hardware problem in the mux cabinet was resolved, and all RRS testing was completed without further problems.

Data collection showed that when the Tavg - Tref mismatch initiating CEA motion is small ($\sim 2.5^{\circ}\text{F}$), the RRS generated CEA movement signal oscillates; i.e., the signal is sent for a few seconds, then shut off for a few seconds. This cyclic process continues until the CEDMCS is taken out of the automatic mode. It should be noted, that only the insertion/withdrawal demand signals and not the actual CEA positions oscillate, such that no excessive equipment wear or damage will result.

SBCS Testing:

The SBCS was tested satisfactorily at the 80% power plateau. No setpoint adjustments were required.

Steam bypass valve MS-319A opened when the lower of two steam header pressures exceeded the master controller setpoint, and closed again when the steam pressure fell below the setpoint. Pressurizer pressure was held stable throughout the test by the PPCS. Upon completion of the test, final steam header pressures were within ± 10 psia of the initial steam header pressures which was well within the acceptance criterion of ± 15 psia.

FWCS Testing:

The FWCSs were tested satisfactorily at both the 50% and 80% power plateaus. No setpoint adjustments were required for either FWCS #1 or FWCS #2 at either test plateau.

In all cases the steam generator levels settled within the required $\pm 1\%$ of the new setpoint. Also, while one steam generator's level was being changed, the second steam generator remained unaffected.

Automatic Steady State Monitoring (Integrated Systems Testing):

This test was satisfactorily performed at both the 50% and 80% power plateaus. No unexpected characteristics were observed, and the behavior of the integrated control systems was as expected. No setpoint changes were required.

CONCLUSION:

The reactor regulating system, the steam bypass control system and the feedwater control system were shown to function as required, both as individual systems and as an integrated control system during both steady state and transient plant conditions. All installed setpoints were adequate to satisfactorily control the plant and did not require any changes. All test objectives and acceptance criteria were met.

6.2.6 Incore Detector Signal Verification (SIT-TP-735)

PURPOSE:

The purpose of this test was to verify proper operation and signal processing of the incore detector signals to assure accurate power distribution calculations. The following tests were performed to accomplish this:

- 1) Verifying that the incore amplifier zero and full scale output are within tolerance.
- 2) Measuring incore cable leakage resistance to identify potential signal problems.
- 3) Verifying that the plant monitoring computer (PMC) properly processes the incore amplifier outputs.
- 4) Verifying that the background signal contribution is less than 5% of the corresponding level 3 detector signal.

This test satisfied the commitments of FSAR section 14.2.12.3.3.

METHOD:

Figure 6.2.6.1 illustrates the layout of the incore detector system. The amplifier checks and cable leakage resistance measurements were performed at each stable power plateau (20%, 50%, 80%, and 100%) using the fixed incore detector

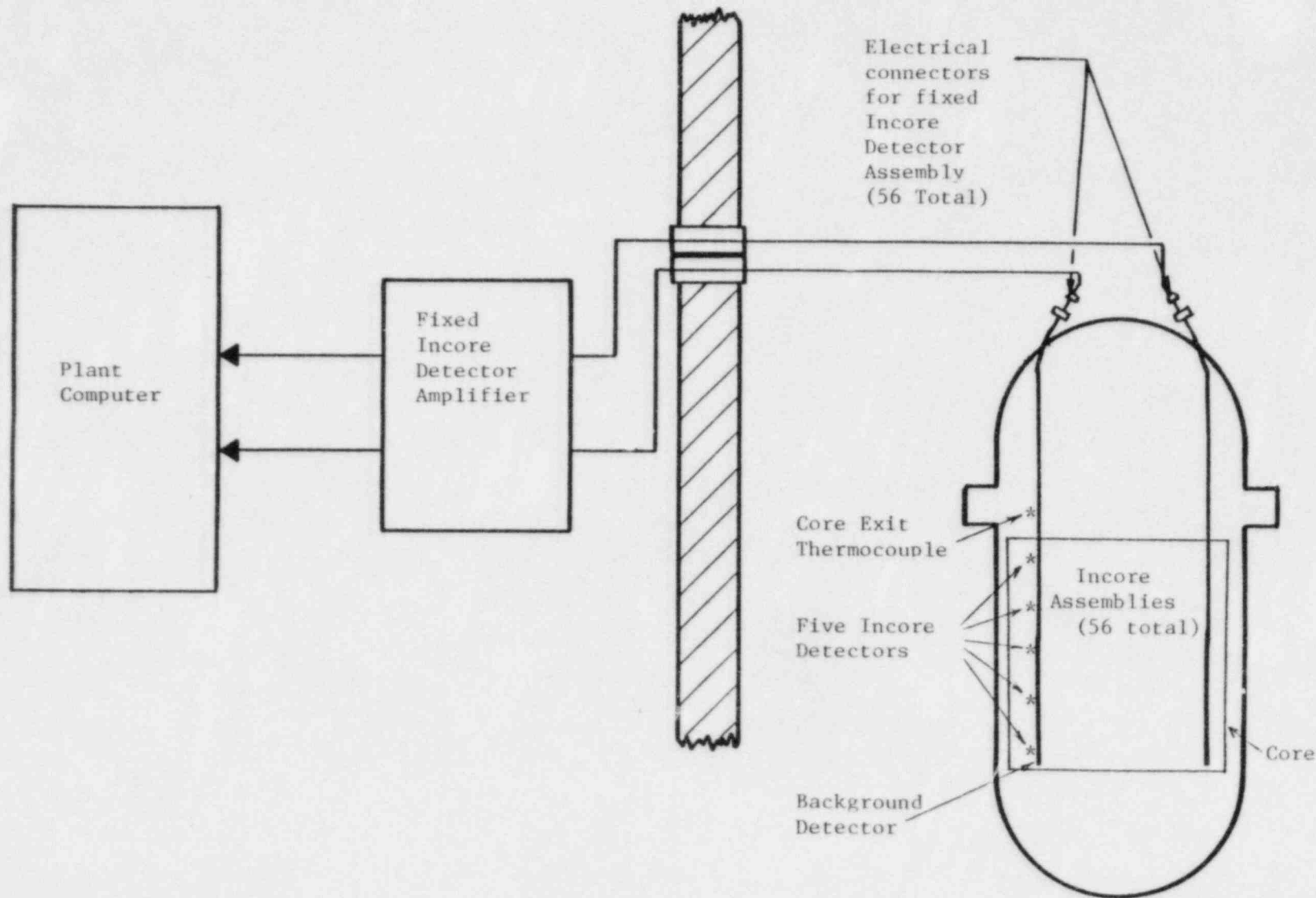


FIGURE 6.2.6.1 INCORE DETECTOR SYSTEM LAYOUT

(FICD) test feature of the incore amplifier system. With reactor power stable, COLSS in the "unscheduled" operating mode, and the incore amplifier system selected to "TEST", each of the four test pushbuttons was depressed, one at a time, which performed the following functional test:

- 1) Pushbutton one (TS-1) input a zero signal into each of the 14 amplifier cards for that channel (A, B, C or D). The amplifier output was sampled by the plant computer and verified to be 0.0 ± 0.025 VDC.
- 2) Pushbutton two (TS-2) input a full scale reference signal into each amplifier card for that channel. Amplifier output was sampled by the plant computer and verified to be $10.0 \pm .135$ VDC.
- 3) Pushbutton three (TS-3) switched into the circuit a known resistance (R_t), then sampled the output signal (V_3) using the live detector input as shown in Figure 6.2.6.2.
- 4) Pushbutton four (TS-4) removed the test resistance that was applied by TS-3 then sampled the detector output (V_4).

The cable leakage (R_l) was then calculated using the following equation:

$$R_l = \frac{R_t}{\frac{V_4}{V_3} - 1}$$

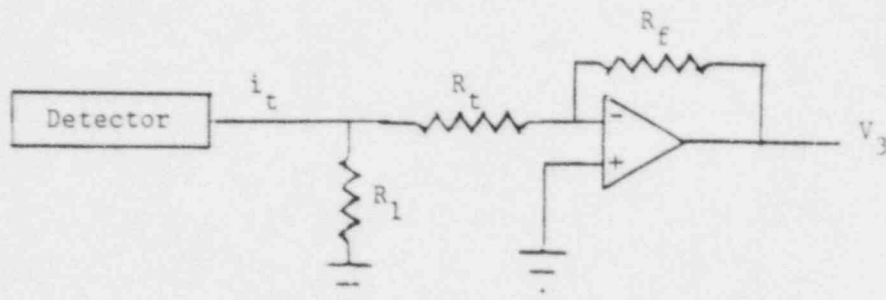
The resultant cable leakage for each detector was compared to the acceptance criterion of $\geq 10^5$ ohms.

The second portion of this test was performed only at the 20% and 100% test plateaus and verified proper signal processing

FIGURE 6.2.6.2

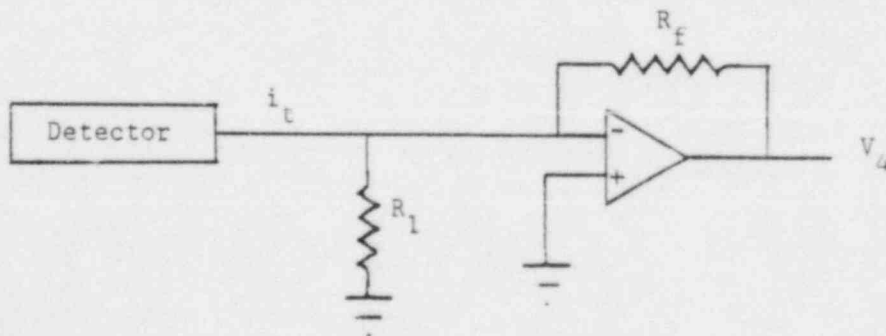
INCORE DETECTOR TEST CIRCUITS (TS-3 and TS-4)

- 1) Test Switch 3 (TS-3) switches a known resistance R_t into the detector signal loop then samples the output voltage (V_3).



- where:
- $R_f = 1 \times 10^6$ ohms
 - $R_1 =$ the leakage resistance to be measured
 - $V_3 =$ the Output Voltage
 - $i_t =$ Detector output current
 - $R_t = 5 \times 10^5$ ohms

- 2) Test Switch 4 (TS-4) switches the signal loop back to its normal configuration then samples the output voltage (V_4).



- 3) Leakage Resistance is calculated using:

$$R_1 = \frac{R_t}{\frac{V_4}{V_3} - 1}$$

of the incore detectors by the plant computer. At each amplifier card there are test points which output the incore signal in mVDC. Each detector output was measured simultaneously by reading the output as displayed on the plant computer. The acceptance criterion was that the amplifier output was within ± 14.5 mVDC of the computer reading. Correct background signals were demonstrated by verifying that each signal was less than 5% of the corresponding level 3 detector signal in that string.

Any detector that failed any of the four acceptance criteria was removed from scan by the computer so as not to adversely affect power distribution calculations.

RESULTS:

Two detectors continuously failed signal comparisons and leakage tests. Troubleshooting indicated that these detectors had failed. They have been identified and are to be replaced during a refueling outage. Four of the 280 incore detectors showed minor problems in signal stability and were therefore removed from scan until the problems can be corrected. With the exception of these six detectors the entire incore detector system operated satisfactorily.

CONCLUSIONS:

The incore detector system operated within its design limits to accurately provide inputs to the plant computer for power distribution calculations.

With the six detectors removed from scan by the plant computer the requirements of Technical Specifications 3/4.3.3.2 remain satisfied namely:

- 1) At least 75% of all incore locations are operable; and
- 2) A minimum of two quadrant symmetric incore detector locations per core quadrant are operable.

All test objectives were satisfactorily met.

6.3 CPC/ COLSS TESTING

6.3.1 COLSS Power/Flow Verification Data Record (SIT-TP-739)

PURPOSE:

This test was performed to collect data at 0% power for use in adjusting the Core Operating Limits Supervisory System (COLSS) delta-T power algorithm for zero-power conditions. The test was also used to verify that the correct values of COLSS constants affecting power and flow were inserted at 0%. Additionally, the test collected data at each 10% power plateau between 20% and 100% to be used in determining the proper constants for the COLSS calibrated turbine power calculation.

METHOD:

The zero offset term, E20, of the core delta-T power calculation was determined by setting it equal to the COLSS core static delta-T power, BSTAT, at 0% power.

The second part of this test was to calibrate the COLSS turbine power calculation. This was done by taking data every 10% power, from 20% through 100%. After the data was collected, a third order least squares fit of COLSS turbine first stage pressure (TFSP) versus COLSS secondary calorimetric power (BSCAL) was calculated to determine the coefficients G1 through G4 of the following polynomial:

$$Y = G1 + G2(X) + G3(X)^2 + G4(X)^3$$

where:

$$Y = \text{BSCAL}$$

$$X = \text{TFSP}$$

These coefficients were then used as constants in the COLSS turbine power algorithm (calibrated turbine power BTFSP) to determine power as a function of turbine first stage pressure. The resulting turbine power calculation was then compared to the secondary calorimetric power for accuracy.

RESULTS:

The zero bias term, E20 was determined by determining the value of BSTAT at 0% power. This value was found to be -0.58%.

The coefficients for the turbine power algorithm were computed upon completing data collection at 100% power; the resulting polynomial was:

$$\begin{aligned} \text{Turbine Power} = & -1.668 + 0.2501(X) - 0.2042 \times 10^{-3}(X)^2 \\ & + 0.1297 \times 10^{-6}(X)^3 \end{aligned}$$

Where:

X = Turbine First Stage Pressure (TFSP).

Table 6.3.1.1 shows the results from the different power levels and compares the calculated turbine power with the secondary calorimetric power (BSCAL); the latter is considered the most accurate power determination at steady state

operation. The calibrated turbine power function was plotted as a function of turbine first stage pressure along with the secondary calorimetric data points (measured data) in Figure 6.3.1.1.

Initially, the determined polynomial did not fit the data within the tolerances specified in the acceptance criteria. A review of the data resulted in eliminating the 30% and 40% data points from the least squares determination. The resulting least squares fit produced acceptable results for all data points, including the 30% and 40% data points, which had been excluded from the fit.

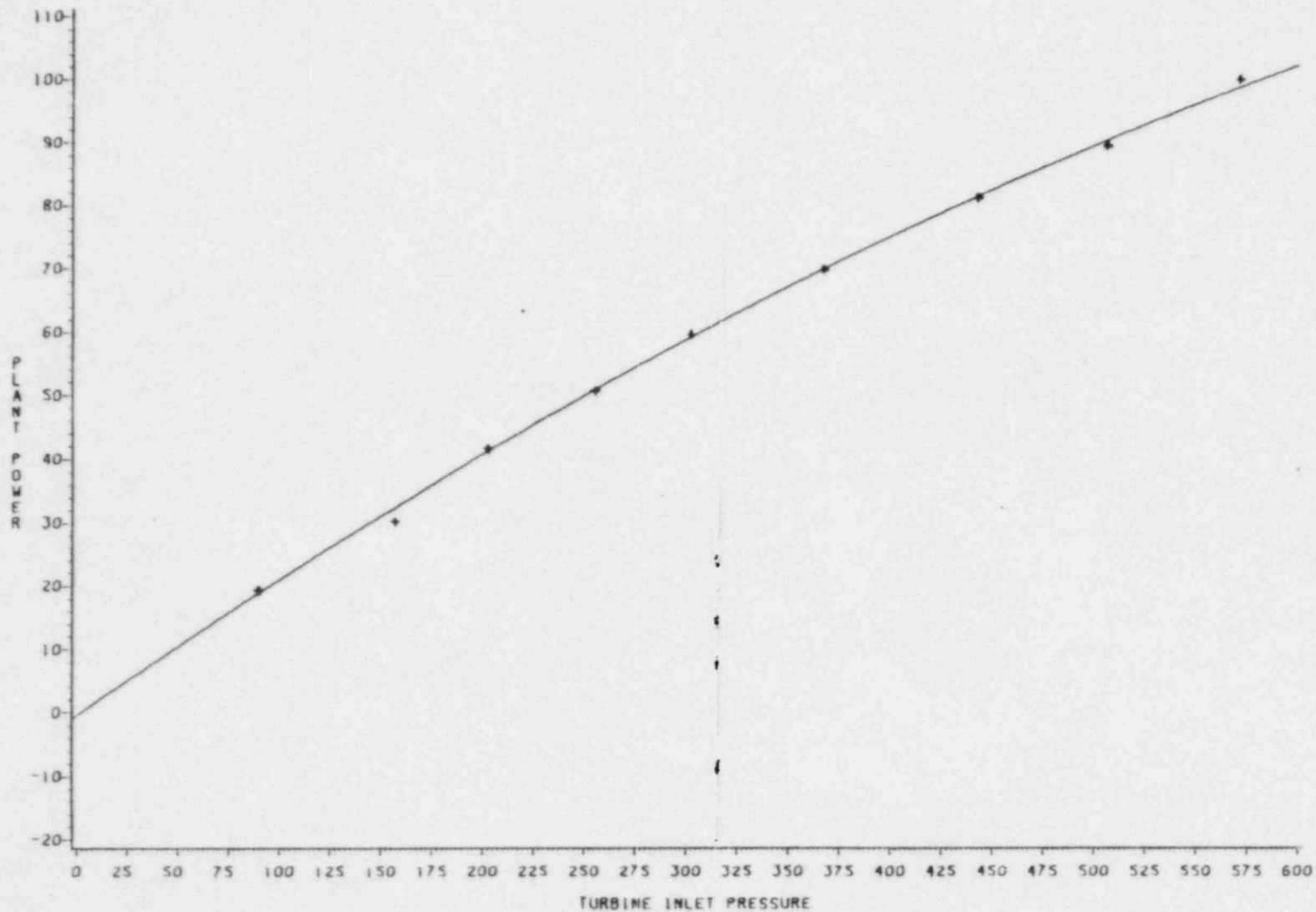
TABLE 6.3.1.1
CALIBRATED TURBINE FIRST STAGE PRESSURE (BTFSPL)
AND
SECONDARY CALORIMETRIC POWER (BSCAL)
FOR ALL DATA PLATEAUS

POWER PLATEAU % FULL POWER	TURBINE FIRST STAGE PRESSURE (TFSP)	COLSS SECONDARY CALORIMETRIC RESULTS ± ACCEPTANCE CRITERIA (BSCAL)	COLSS CALIBRATED TURBINE POWER (BTFSPL)
20	89.98 psia	19.34% ±3%	19.27%
30	157.51 psia	30.27% ±3%	33.16%
40	203.7 psia	41.72% ±2%	41.89%
50	256.31 psia	50.65% ±2%	51.20%
60	303.47 psia	59.41% ±2%	59.04%
70	368.55 psia	69.53% ±2%	69.25%
80	444.5 psia	80.75% ±1%	80.53%
90	508.67 psia	89.09% ±1%	89.77%
100	573.83 psia	99.39% ±1%	99.10%

FIGURE 6.3.1.1

CALIBRATED TURBINE POWER

+ = MEASURED DATA
— = THIRD ORDER FIT OF DATA



CONCLUSION:

All test objectives and acceptance criteria were met. Values for E20, the zero power bias term, and G1 through G4, calibrated turbine power polynomial coefficients, were properly entered into COLSS.

6.3.2 Adjustment of COLSS Secondary Pressure Loss Terms (SIT-TP-741)

PURPOSE:

The purpose of this test was to tune the COLSS algorithms which calculate steam generator pressure and feedwater pressure. These algorithms were developed under the assumption that steam generator and feedwater pressure indication would not be available within the plant computer system. The algorithms model the pressure drop between the feedwater inlet to the steam generator and the main steam header as a function of the steam flow from the steam generator; the pressure drop between the steam generator steam dome and steam header is similarly modelled. COLSS then uses live steam header pressure and steam flow data to calculate the feedwater and steam generator pressures for use in the calculation of secondary calorimetric power.

This test collected live data for both the dependent (feedwater and steam generator pressures) and the independent (steam header pressure and steam flow) parameters used in the algorithms modelling the secondary pressure losses. This data was then used to determine the constants to be implemented into the COLSS algorithms.

METHOD:

It was desired to obtain the data required for determination of the COLSS secondary pressure loss constants over the entire range of reactor power. Thus, the following values were recorded via a computer collect log at each of the major test plateaus (20%, 50%, 80% and 100%), once thermal equilibrium had been achieved:

Secondary Pressure Loss Data Set (each steam generator)

- steam generator steam flow venturi
 differential pressure : SFLOW
 - steam header pressure : PSEC
 - steam generator pressure (COLSS calculated) : PSG
 - feedwater pressure (COLSS calculated) : FWP
 - steam generator pressure (live data) : SGPRESS
 - feedwater pressure (live data) : FWPRESS

Temporary pressure gauges were installed on the feedwater train, as close as practicable to the inlet of the steam generators, as no permanent plant transmitters exist there. These gauges were used to yield the feedwater pressure (live data) listed above. Permanent plant instruments transmit steam generator pressure (live data) to the plant computer.

Average values for the above parameters are calculated, and then used to calculate the measured pressure losses from the feedwater inlet to the steam header and from the steam generator to the steam header:

$$DPFW = FWPRESS - PSEC$$

$$DPSG = SGPRESS - PSEC$$

These values were then paired with SFLOW for all plateaus for which the data was available. A linear least squares fit was performed for each set of values, and the determined slopes and intercepts constituted the COLSS secondary pressure loss algorithm constants.

These constants were then entered into the Plant Computer in place of the previously entered constants. The secondary pressure loss data set outlined on the previous page was then collected again via a computer collect log. The values were averaged, and the COLSS calculated values of feedwater pressure and steam generator pressure were then compared to the measured values. Satisfactory agreement was achieved when the difference between calculated and measured feedwater pressures was less than 50 psia, and the difference between calculated and measured steam generator pressure was less than 15 psia. These criteria were chosen to ensure that the error introduced into the secondary calorimetric power by inaccuracies in calculated pressures was limited to approximately 0.01%. The acceptance criteria are detailed below:

$$\text{FWP} - \text{FWPRESS} \leq 50 \text{ psia}$$

$$\text{PSG} - \text{SGPRESS} \leq 15 \text{ psia}$$

Data collection and associated calculations were repeated, if necessary, at a given power plateau until these criteria were satisfied.

RESULTS:

The acceptance criteria were satisfied at each plateau, without the need for additional iterations. New COLSS constants were entered following the performance of this procedure at each plateau, and COLSS calculated pressures agreed well with the corresponding measured values.

Data was taken at the 0% power plateau, but this data was not included in the calculation of COLSS constants except at the 20% plateau. The reason this data was excluded is twofold:

first, the steam flow transmitters are highly inaccurate at the low end of their range, and second, the main feedwater system was not in operation at the time the 0% data were collected, yielding suspect pressure drop values.

The test results from each plateau are summarized below. The tables reflect measured and calculated values following adjustment at the given power level.

TABLE 6.3.2.1
ADJUSTMENT OF COLSS SECONDARY PRESSURE LOSS TERMS
20% POWER TEST RESULTS

	measured	calculated	error
SG1 feedwater pressure	960.7 psia	960.54 psia	-0.16 psia
SG2 feedwater pressure	963.2 psia	962.75 psia	-0.45 psia
SG1 steam pressure	957.18 psia	957.32 psia	+0.14 psia
SG2 steam pressure	957.73 psia	958.06 psia	+0.33 psia

TABLE 6.3.2.2
ADJUSTMENT OF COLSS SECONDARY PRESSURE LOSS TERMS
50% POWER TEST RESULTS

	measured	calculated	error
SG1 feedwater pressure	936.3 psia	936.68 psia	+0.38 psia
SG2 feedwater pressure	942.70 psia	941.53 psia	-1.17 psia
SG1 steam pressure	933.90 psia	933.86 psia	-0.04 psia
SG2 steam pressure	934.40 psia	934.41 psia	+0.01 psia

TABLE 6.3.2.3
ADJUSTMENT OF COLSS SECONDARY PRESSURE LOSS TERMS
80% POWER TEST RESULTS

	measured	calculated	error
SG1 feedwater pressure	931.7 psia	930.00 psia	-1.70 psia
SG2 feedwater pressure	930.2 psia	934.50 psia	+4.30 psia
SG1 steam pressure	912.5 psia	912.60 psia	+0.10 psia
SG2 steam pressure	912.8 psia	913.20 psia	+0.40 psia

TABLE 6.3.2.4
 ADJUSTMENT OF COLSS SECONDARY PRESSURE LOSS TERMS
100% POWER TEST RESULTS

	measured	calculated	error
SG1 feedwater pressure	926.7 psia	929.10 psia	+2.40 psia
SG2 feedwater pressure	930.7 psia	932.60 psia	+1.90 psia
SG1 steam pressure	903.1 psia	903.20 psia	+0.10 psia
SG2 steam pressure	901.4 psia	902.10 psia	+0.70 psia

The final COLSS constants installed in the PMC are tabulated in table 6.3.2.5. These constants were determined based upon a linear least squares fit of data from all four test plateaus, as depicted in Figures 6.3.2.1 through 6.3.2.4. However, these values were not implemented into COLSS until after acquisition of the 100% data. Table 6.3.2.6 utilizes data taken at each plateau to simulate the COLSS calculation of feedwater pressure and steam pressure, had the above constant values been installed. Comparison of these simulated values to the comparable measured values provides assurance that the as-left COLSS constants are adequate over all power ranges. The COLSS equations for calculating steam and feedwater pressures are given below Table 6.3.2.6 for information.

TABLE 6.3.2.5
 ADJUSTMENT OF COLS; SECONDARY PRESSURE LOSS TERMS
 INSTALLED COLSS CONSTANT VALUES

constant	PMC PID	definition	value
F01	K24224	SG1 feedwater-steam header pressure drop bias term	13.8 psia
F02	K24225	SG1 feedwater-steam header pressure drop gain term	0.06%6 psia/"H ₂ O
F04	K24226	SG1 generator-steam header pressure drop bias term	12.5 psia
F05	K24227	SG1 generator-steam header pressure drop gain term	0.0195 psia/"H ₂ O
F09	K24231	SG2 feedwater-steam header pressure drop bias term	21.4 psia
F10	K24232	SG2 feedwater-steam header pressure drop gain term	0.0689 psia/"H ₂ O
F12	K24233	SG2 generator-steam header pressure drop bias term	17.9 psia
F13	K24234	SG2 generator-steam header pressure drop gain term	0.0209 psia/"H ₂ O

TABLE 6.3.2.6

VERIFICATION OF INSTALLED COLSS CONSTANTS' ADEQUACY

POWER PLATEAU	PARAMETER	COLSS INPUTS		COLSS- CALCULATED ⁽¹⁾	MEASURED	ERROR	ACCEPTABLE? ⁽²⁾
		SFLOW	PSEC				
20%	SG1 FW pressure	9.1 "H2O	960.63 psia	975.01 psia	976.10 psia	-1.09 psia	YES
	SG2 FW pressure	12.7 "H2O	956.39 psia	978.67 psia	978.00 psia	+0.67 psia	YES
	SG1 STM pressure	9.1 "H2O	960.63 psia	973.31 psia	972.80 psia	+0.51 psia	YES
	SG2 STM pressure	12.7 "H2O	956.39 psia	974.56 psia	973.48 psia	+1.08 psia	YES
50%	SG1 FW pressure	106.7 "H2O	929.93 psia	950.52 psia	947.96 psia	+2.62 psia	YES
	SG2 FW pressure	106.0 "H2O	924.62 psia	953.32 psia	952.80 psia	+0.52 psia	YES
	SG1 STM pressure	106.7 "H2O	929.93 psia	944.51 psia	945.13 psia	-0.62 psia	YES
	SG2 STM pressure	106.0 "H2O	924.62 psia	944.74 psia	945.65 psia	-0.91 psia	YES
80%	SG1 FW pressure	322.3 "H2O	893.34 psia	927.64 psia	930.20 psia	-2.56 psia	YES
	SG2 FW pressure	324.6 "H2O	887.19 psia	930.95 psia	933.70 psia	-2.75 psia	YES
	SG1 STM pressure	322.3 "H2O	893.34 psia	912.12 psia	912.25 psia	-0.13 psia	YES
	SG2 STM pressure	324.6 "H2O	887.19 psia	911.87 psia	912.45 psia	-0.58 psia	YES
100%	SG1 FW pressure	548.6 "H2O	880.00 psia	928.69 psia	927.70 psia	+0.99 psia	YES
	SG2 FW pressure	553.5 "H2O	872.60 psia	932.14 psia	930.70 psia	+1.44 psia	YES
	SG1 STM pressure	548.6 "H2O	880.00 psia	903.20 psia	903.10 psia	+0.10 psia	YES
	SG2 STM pressure	553.5 "H2O	872.60 psia	902.07 psia	901.50 psia	+0.57 psia	YES

NOTES: (1) The equations used by COLSS to calculate pressures (simulated above) are as follows:

$$\text{SG1 FW pressure: } \text{FWP1} = \text{PSEC1} + [\text{F01} + \text{F02} * \text{SFLOW1}] ; \text{ SG2 FW pressure: } \text{FWP2} = \text{PSEC2} + [\text{F09} + \text{F10} * \text{SFLOW2}]$$

$$\text{SG1 STM pressure: } \text{PSG1} = \text{PSEC1} + [\text{F04} + \text{F05} * \text{SFLOW1}] ; \text{ SG2 STM pressure: } \text{PSG2} = \text{PSEC2} + [\text{F12} + \text{F13} * \text{SFLOW2}]$$

(2) Acceptability of calculated pressures is determined as follows:

$$\text{SG FW pressures: } \text{ERROR} \leq 50 \text{ psia}$$

$$\text{SG STM pressures: } \text{ERROR} \leq 15 \text{ psia}$$

FIGURE 6.3.2.1: SGI FEEDWATER TO STEAM HEADER PRESSURE LOSS VERSUS STEAM FLOW

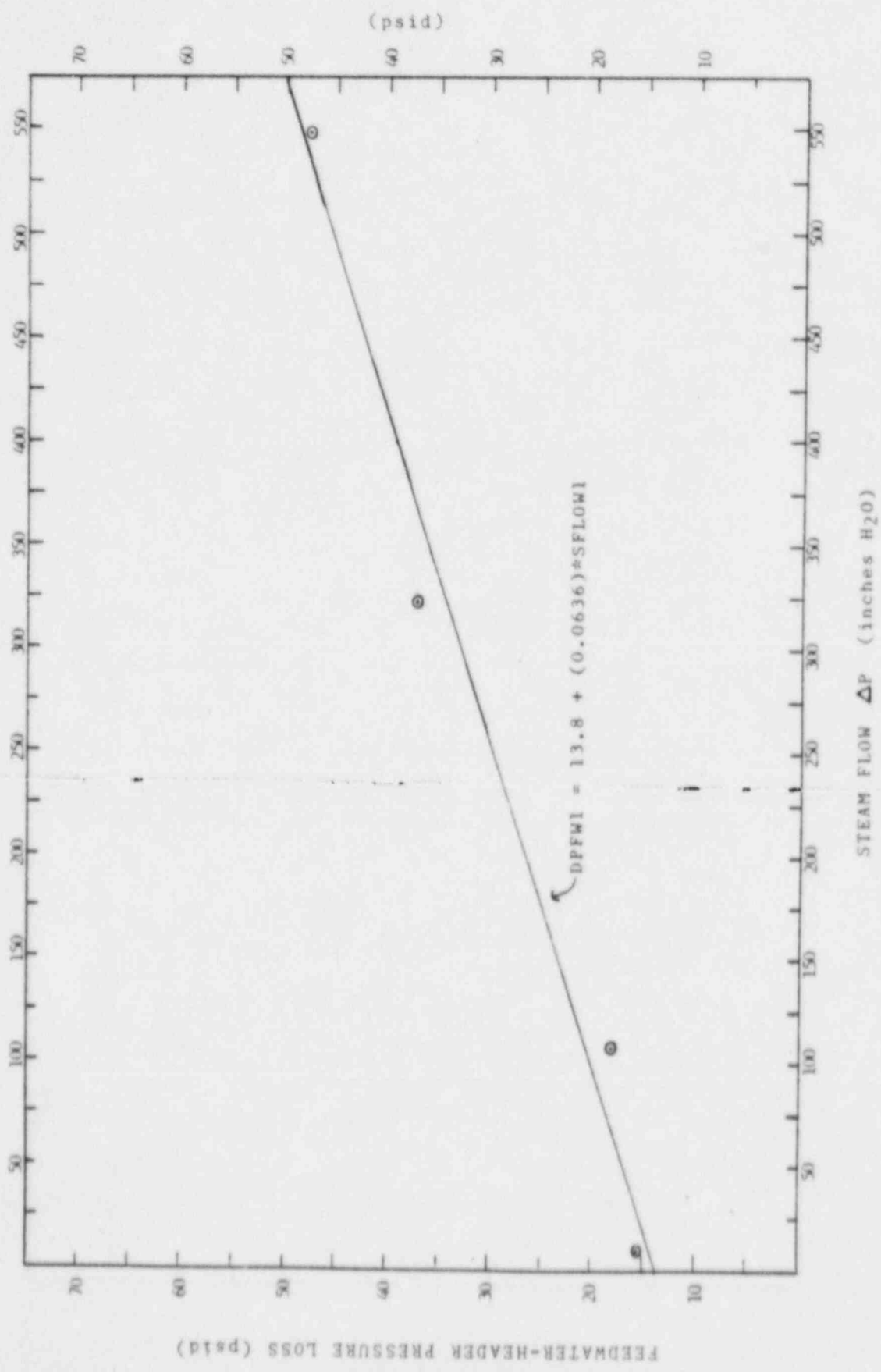


FIGURE 6.3.2.2: SG2 FEEDWATER TO STEAM HEADER PRESSURE LOSS VERSUS STEAM FLOW

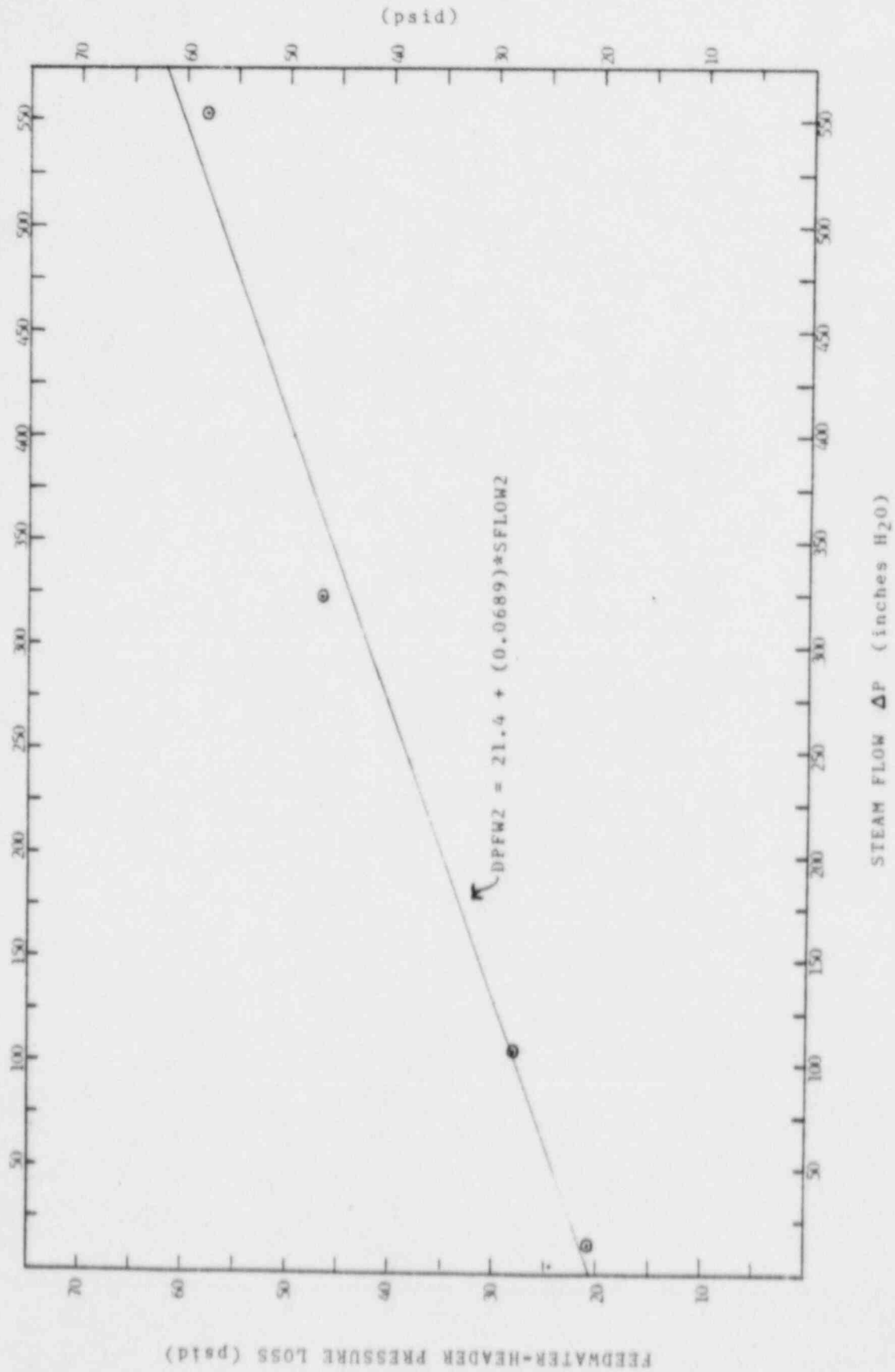


FIGURE 6.3.2.3: SG1 GENERATOR TO STEAM HEADER PRESSURE LOSS VERSUS STEAM FLOW

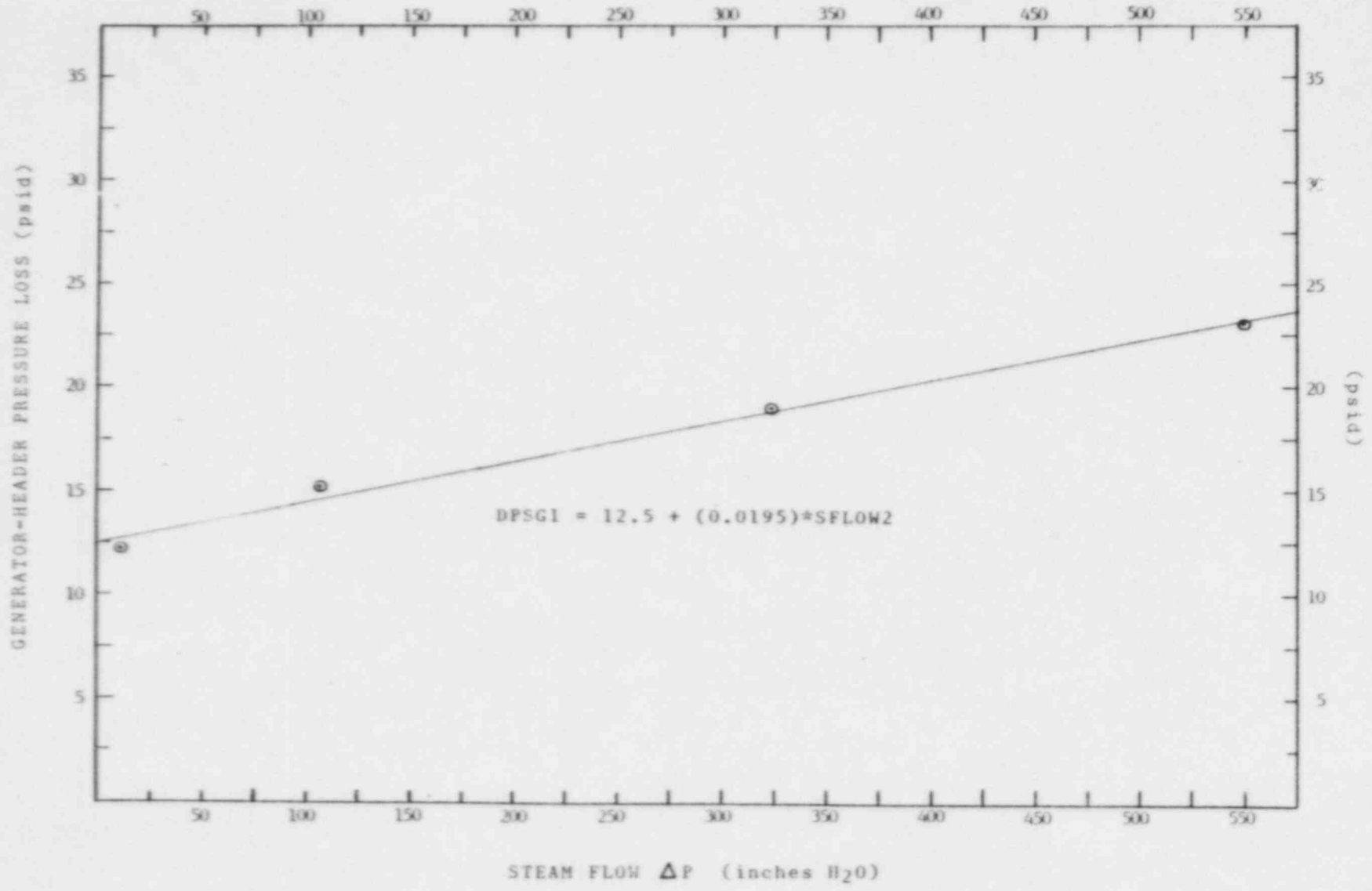
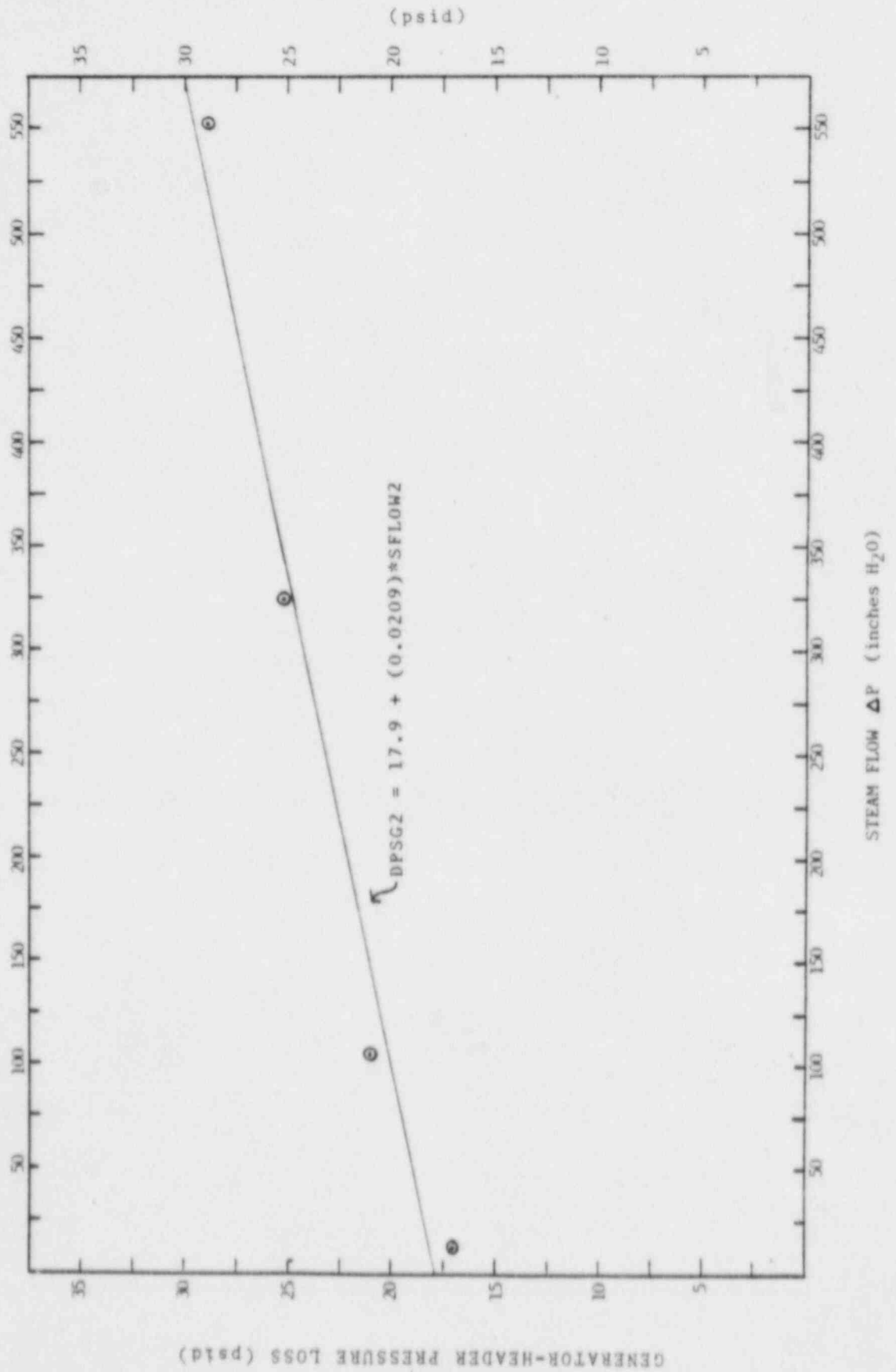


FIGURE 6.3.2.4: SG2 GENERATOR TO STEAM HEADER PRESSURE LOSS VERSUS STEAM FLOW



CONCLUSION:

At each major power plateau, new COLSS secondary pressure loss constants were determined and implemented into plant computer. COLSS calculated pressures were then compared to measured values, and found to be well within the specified tolerances. The constants determined at the 100% power plateau have been verified adequate over the entire power range in which COLSS secondary calorimetric power is utilized. All test objectives and acceptance criteria were satisfactorily met.

6.3.3 CPC/COLSS VERIFICATION (SIT-TP-717)

PURPOSE:

The CPC/COLSS Verification test was performed to verify the Core Protection Calculator (CPC) and Core Operating Limit Supervisory System (COLSS) calculations of departure from nucleate boiling ratio (DNBR) and local power density (LPD). The test also collected input recordings used to evaluate the effects of process noise on the CPC system.

This test satisfied the commitments of FSAR section 14.2.12.3.2.7.

METHOD:

This test was performed at all test plateaus including hot zero power (HZP, 20%, 50%, 80% and 100%). The CPC DNBR and LPD calculations were verified using CEDIPS, a CE-Windsor FORTRAN simulation of the CPC software. Input to CEDIPS consists of the maximum and minimum values (observed over a period of up to 30 seconds) of the following:

- 1) RCP Speed
- 2) Cold leg temperature
- 3) Hot leg temperature
- 4) Pressurizer pressure
- 5) Upper excore signal

6) Middle excore signal

7) Lower excore signal

Control element assembly (CEA) positions and CPC addressable constants are also input to CEDIPS.

Acceptance of the DNBR and LPD calculations was verified if the actual range of CPC output was within the range of predicted output as calculated by CEDIPS. COLSS DNBR and LPD acceptability was provided by CE-Windsor based upon an evaluation of information provided in the COLSS detailed report. This report is a snapshot of all COLSS inputs and outputs and all current values for addressable constants.

The process noise evaluation was performed by first determining the noisiest CPC channel based on the largest variance in calculated DNBR. All DNBR and LPD inputs to this channel were then recorded on FM tape. Recordings were analyzed to determine the nature of the noise and its effect on DNBR and LPD.

RESULTS:

All data collection by this test was completed with no problems. The large variation in RTD temperature indications affected the CEDIPS predictions of DNBR. The affected DNBR calculations generated minimum values well below what was expected and sometimes below the low DNBR trip setpoint. Comparison of actual values to this large range of predictions was not valid. Consequently, additional CEDIPS runs were performed using minimum and maximums for each cold leg

temperature rather than the minimum and maximum of the combined temperatures. This comparison provided a more realistic and more conservative acceptance limit.

Table 6.3.3.1 shows all the CEDIPS predictions and the appropriate CPC outputs. All of the LPD and DNBR outputs were within the limits generated by CEDIPS predictions. The COLSS LPD and DNBR evaluations were acceptable based on evaluations by CE-Windsor.

The twelve input and two output signals for a selected CPC channel were analyzed to determine if signal noise characteristics interfered with correct CPC system response. Methods employed in the analysis included playback of recorded signals into an oscilloscope and a spectrum analyzer. Signal noise characteristics were identified and classified in an effort to evaluate their affect on the DNBR and LPD calculations.

The analysis culminated in acceptable results. Random noise on the RCP digital speed signals was far below the existing discriminator thresholds and thus had in impact on speed measurement. The minimal changes in calculated DNBR and LPD demonstrated that CPCS operation was not affected by process noise on the analog input signals.

TABLE 6.3.3.1
(continued)
Part 2 of 2
CPC/CEDIPS COMPARISONS

50% Power

Parameter	Channel A		Channel B		Channel C		Channel D	
	CEDIPS	CPC	CEDIPS	CPC	CEDIPS	CPC	CEDIPS	CPC
LPD _{MAX}	8.7498	8.1856	9.1440	8.1319	8.3336	8.0670	8.8442	8.1397
LPD _{MIN}	8.0153	8.1357	8.0137	8.0867	7.9796	8.0450	7.9628	8.1068
DNB _{MAX}	4.3135	4.0820	4.3206	4.1389	4.3249	4.1494	4.3257	4.0878
DNB _{MIN}	3.6514	4.0201	3.5368	4.0581	3.8981	4.0897	3.5079	4.0297

80% Power

Parameter	Channel A		Channel B		Channel C		Channel D	
	CEDIPS	CPC	CEDIPS	CPC	CEDIPS	CPC	CEDIPS	CPC
LPD _{MAX}	13.2890	12.169	12.9419	12.500	12.3766	12.042	12.8640	12.302
LPD _{MIN}	11.8729	12.046	12.2154	12.366	11.8485	11.959	12.0193	12.166
DNB _{MAX}	2.2729	2.1611	2.2222	2.1310	2.2625	2.1700	2.2422	2.1306
DNB _{MIN}	1.6609	2.1160	1.8853	2.0093	1.9732	2.1370	1.8458	2.0934

100% Power

Parameter	Channel A		Channel B		Channel C		Channel D	
	CEDIPS	CPC	CEDIPS	CPC	CEDIPS	CPC	CEDIPS	CPC
LPD _{MAX}	15.3578	14.653	15.8058	15.157	14.7301	14.212	15.3143	14.318
LPD _{MIN}	14.3238	14.582	14.8399	15.006	13.9741	14.126	14.0428	14.282
DNB _{MAX}	1.7388	1.6420	1.6883	1.6181	1.8368	1.7686	1.8318	1.7360
DNB _{MIN}	0.1365	1.5879	1.3629	1.5888	1.5226	1.7553	1.431	1.7033

Rerun of Channels A and D at 100% Power Using Minimums
and Maximums for TC1 or TC2

Parameter	Channel A		Channel D	
	CEDIPS	CPC	CEDIPS	CPC
LPD _{MAX}	15.358	14.653	15.314	14.318
LPD _{MIN}	14.324	14.582	14.043	14.282
DNB _{MAX}	1.7389	1.6420	1.8318	1.7360
DNB _{MIN}	1.4398	1.5879	1.4548	1.7033

CONCLUSIONS:

LPD and DNBR calculations within the Core Protection Calculators (CPCs) and the Core Operating Limit Supervisory System (COLSS) generated results that were within the range of acceptable values. CPC input noise has a negligible affect on LPD and DNBR calculations. All test objectives and acceptance criteria were satisfactorily met.

6.3.4 Radial Peaking Factor and CEA Shadowing Factor Verification
(SIT-TP-725)

PURPOSE:

The objective of the planar radial peaking factor/CEA shadowing factor test was to obtain a direct measurement of these parameters for various CEA insertion configurations. Based upon these measurements, additional assurance of correct core loading was obtained. The core operating limits supervisory system (COLSS) and the core protection calculators (CPCs) were also calibrated such that they accounted for the measured values of these parameters.

This test was referenced in section 14.2.12.3.28 of the FSAR.

METHOD:

Initial conditions were established with the reactor at approximately 50% power, all CEAs withdrawn and equilibrium xenon. After collecting a baseline set of data, dilution of the reactor coolant system commenced. As the RCS boron concentration decreased, CEA group 6 was inserted to the lower electrical limit (LEL) to compensate for the positive reactivity addition. The dilution was terminated such that CEA group 6 was within 10 inches of its LEL or CEA group 5 was within 10 inches of its upper electrical limit (UEL) and steady-state power and temperature were re-established. Upon stabilizing reactor conditions, a data set consisting of incore detector readings, RCS power, RCS temperatures, CEA positions and various other plant parameters was collected. This process was then repeated to obtain data for the following CEA insertion configurations:

- Group 6 @ LEL and Group 5 @ LEL
- Group 6 @ LEL, Group 5 @ LEL and Group P @ 37.5" withdrawn

Note that by inserting part-length group P to 37.5" withdrawn the poison section of the PLCEAs was centered at the core mid-plane.

After data had been collected for the group 6/5/P insertion configuration, boration of the RCS was initiated. CEA group 5 was withdrawn to compensate for the negative reactivity addition while maintaining reactor power and temperatures constant. The boration was terminated such that group 5 was within 10 inches of its UEL or group 6 was within 10 inches of its LEL and steady-state reactor conditions were established. A data set was collected and the above process repeated to obtain data for the following configurations:

- Group P @ 37.5" withdrawn
- Group P @ UEL and Group 6 @ 120" withdrawn

Analysis of the test data required the determination of planar radial peaking factors and CEA shadowing factors. The CE incore analysis code CECOR was employed to determine the peaking factors (refer to section 6.4.1 for a summary description of CECOR and the associated execution procedure). CEA shadowing factors were determined from plant power and excore detector signal response obtained from the CPCs and COLSS. A detailed description of the analysis is presented below:

CPC Planar Radial Peaking Factors (F_{xy})

The planar radial peaking factor, F_{xy} , is the maximum value for the core of the ratio of the 1-pin peak power to the average pin power in a plane. This peaking factor is presented in CECOR as a function of core height in the following form:

$$F_{xy}^t = F_{xy} (1 + T_q)$$

Where T_q is the vector average azimuthal power tilt. Thus, F_{xy} was determined for the CEA configuration of interest by selecting the maximum value of F_{xy}^t and dividing by the quantity $(1 + T_q)$. Axial nodes within 22.5 inches of the top and bottom of the core and within 15 inches of a CEA tip were not considered in determining the value of F_{xy} . This was due to inaccuracies introduced into the measurement methodology by large neutron flux gradients experienced in the vicinity of a geometric or poison boundary.

Utilizing the measured value of F_{xy} from CECOR and the core burnup at the time of the measurement, a correction multiplier was calculated. This factor was determined from the following relationship for each CEA configuration:

$$ARM_i = \frac{F_{xy}^i \text{ (measured)}}{\{F_{xy}^i \text{ (installed)} [K_1^i + K_2^i \cdot B^i]\}}$$

Where:

i = index dependent upon the CEA configuration

ARM_i = CPC planar radial peaking factor multiplier

F_{xy}^i (measured) = measured value of the planar radial peaking factor determined from CECOR

F_{xy}^i (installed) = an element in an array of planar radial peaking factors installed in the CPCs

K_1^i, K_2^i = precalculated constants

B^i = core burnup (MWD/MTU) incurred at the time the measurement for group i was made.

For those cases where ARM_i was less than 1.0, no change was made in the corresponding CPC constant. For those cases where ARM_i was greater than 1.0, the value was input to the corresponding CPC constant.

COLSS Planar Radial Peaking Factors

A COLSS peaking factor adjustment was determined from the following equation and installed in the plant computer:

$$PF3 = \max(PF3^i) = \max \left\{ \frac{1.01 \cdot F_{xy}^i \text{ (measured)}}{[F_{xy}^i \text{ (installed)} (C_1^i + C_2^i \cdot B^i)]} \right\}$$

Where:

PF3 = interim correction factor applied to all COLSS installed planar radial peaking factors

C_1^i, C_2^i = precalculated constants

All other variables retain the same meaning as described in the CPC description.

Prior to completion of testing at the 50% plateau, appropriate peaking factors for each CEA configuration were installed in COLSS and the radial peaking factor correction was returned to 1.0.

CEA Shadowing Factors (Fx)

The CEA shadowing factors, Fx, were calculated for the CPCs as follows:

$$F_x = \frac{\sum_{i=1}^3 D_i^x \text{ (with CEAs inserted)}}{\sum_{i=1}^3 D_i^x \text{ (ARO)}} \times \frac{\text{Power (ARO)}}{\text{Power (with CEAs inserted)}}$$

for full-length CEAs and

$$F_x = \frac{D_2^x \text{ (with CEAs inserted)}}{D_2^x \text{ (ARO)}} \times \frac{\text{Power (ARO)}}{\text{Power (with CEAs inserted)}}$$

for part-length CEAs. In these equations,

x = CPC channel A, B, C or D

D_1^x = Upper excore detector indicated power (D1RAW)

D_2^x = Middle excore detector indicated power (D2RAW)

D_3^x = Lower excore detector indicated power (D3RAW)

Power = Reactor power from COLSS.

After calculating the CEA shadowing factors, correction multipliers (ASM2 through ASM6) were determined by dividing the measured F_x by the installed F_x for each CEA configuration. These multipliers were then entered into each of the four CPC channels.

RESULTS:

The radial peaking factor and CEA shadowing factor measurements were performed on April 24 and April 25, 1985 without difficulty. The final results of the test are given in Tables 6.3.4.1, 6.3.4.2 and 6.3.4.3.

CONCLUSION:

All objectives of this test were satisfied. Planar radial peaking factors and CEA shadowing factors were determined. Where necessary, correction multipliers were calculated and entered into the CPCs or COLSS.

TABLE 6.3.4.1
CPC PLANAR RADIAL PEAKING FACTORS

CEA GROUP POSITION	BURNUP MWD/MT	CECOR F_{xy}	ACCEPTANCE CRITERIA	CPC CORRECTION FACTOR
ARO	192	1.3820	≤ 1.4063	1.0000
6/LEL	190	1.4718	≤ 1.4398	1.0222
6/LEL,5/LEL	190	1.6120	≤ 1.5819	1.0190
6/LEL,5/LEL,P/37.5	192	1.7036	≤ 1.7089	1.0000
6/LEL,P/37.5	190	1.5529	≤ 1.5537	1.0000
P/37.5	193	1.4549	≤ 1.4640	1.0000

TABLE 6.3.4.2
COLSS PLANAR RADIAL PEAKING FACTORS

CEA GROUP POSITION	BURNUP MWD/MT	CECOR F _{xy}	ACCEPTANCE CRITERIA	CORRECTION FACTOR (PF3)
ARO	192	1.3820	≤1.4063	0.9827
6/LEL	190	1.4718	≤1.4371	1.0241
6/LEL,5/LEL	190	1.6120	≤1.5796	1.0205
6/LEL,5/LEL,P/37.5	192	1.7036	≤1.7117	0.9953
6/LEL,P/37.5	190	1.5529	≤1.5524	1.0003
P/37.5	193	1.4549	≤1.4624	0.9949

TABLE 6.3.4.3
CEA SHADOWING CORRECTION FACTORS

CEA GROUP POSITION	CPC CHANNEL A CORRECTION FACTOR	CPC CHANNEL B CORRECTION FACTOR	CPC CHANNEL C CORRECTION FACTOR	CPC CHANNEL D CORRECTION FACTOR
ARO	1.00000	1.00000	1.00000	1.00000
6/LEL	1.0043	1.0038	1.0055	1.0047
6/LEL,5/LEL	1.0466	1.0435	1.0390	1.0432
6/LEL,5/LEL,P/37.5	0.9718	0.9718	0.9618	0.9645
6/LEL,P/37.5	0.9797	0.9853	0.9799	0.9796
P/37.5	0.9788	0.9818	0.9788	0.9771

6.3.5 Temperature Decalibration Verification (SIT-TP-724)

The Core Protection Calculators (CPC's) utilize the signals from excore detectors to calculate the real time incore power distribution. Each detector contains three fission chambers positioned axially. These calculations are corrected for many effects, one of which is temperature shadowing.

Neutrons leaking from the core must travel through the water in the downcomer region to reach the excore detectors. Changes in water density due to changes in water temperature, will attenuate more or less neutrons, thereby altering the neutron flux at the detectors. Compensation for this effect is done by the CPC's using the temperature shadowing factors.

PURPOSE:

The purpose of the Temperature Decalibration Verification Test was to measure the effect of changes to the excore signals due to changes in cold leg temperature and to verify that the temperature shadowing factors installed in the CPC's are adequate. Adjustment of the temperature shadowing factors was required only if the measured effect is outside the given acceptance criteria around the installed values in the CPC's.

This test satisfied the commitments of FSAR section 14.2.12.3.28.

METHOD:

The initial conditions required stable plant conditions at equilibrium xenon at approximately 50% power. Reactor coolant system cold leg temperatures were adjusted in small increments (1 or 2°F) by boration/dilution and/or small turbine load changes. After each temperature change, plant conditions were stabilized and data was collected using the CPCs and the plant computer. This data included cold leg temperatures, raw excore detector signals and COLSS secondary calorimetric power.

The calculated power from raw detector signals (PHIRAW), which is affected by temperature shadowing, was compared to the secondary calorimetric power, which is independent of temperature shadowing effects. This ratio, designated BASE was calculated for each CPC channel and is defined as:

$$\text{BASE} = \frac{\text{PHIRAW}}{\text{BSCAL}}$$

where: PHIRAW is the sum of the raw excore detector signals for a given CPC channel and represents temperature shadowed power.

BSCAL is secondary calorimetric power from the plant computer and represents true thermal power of the core.

At each temperature (T) plateau, data was collected for each CPC channel and a new BASE was calculated.

$$\text{BASE}_T = \frac{\text{PHIRAW}_T}{\text{BSCAL}_T}$$

Initially, the procedure required power to be stable within $\pm 0.2\%$ at each temperature plateau. This proved to be difficult to accomplish and the procedure was changed to allow power to vary between each temperature increment but to be constant for a given data run without impacting the test results.

A reference condition was assigned at 553°F and the BASE values were normalized to form the Raw Temperature Shadow (RTS), where:

$$\text{RTS}_T = \frac{\text{BASE}_{553}}{\text{BASE}_T}$$

$$\text{RTS}_T = a + b (T_{\text{cold}})$$

The normalized ratio was plotted as a function of cold leg temperature and a least squares fit was applied. The resulting slope was then compared to the value of CORR1 in the CPC's.

RESULTS:

Table 6.3.5.1 shows the test results:

TABLE 6.3.5.1
SUMMARY OF TEMPERATURE DECALIBRATION VERIFICATION TEST RESULTS

CPC Channel	Predicted	Measured	Error
A	.0049	.0056	.0007
B	.0049	.0055	.0006
C	.0049	.0054	.0005
D	.0049	.0055	.0006

Figures 6.3.5.1 through 6.3.5.4 show the relationship between RTS and Tcold for the four CPC channels.

FIGURE 6.3.5.1

CPC TEMPERATURE DECALIBRATION
CPC CHANNEL A

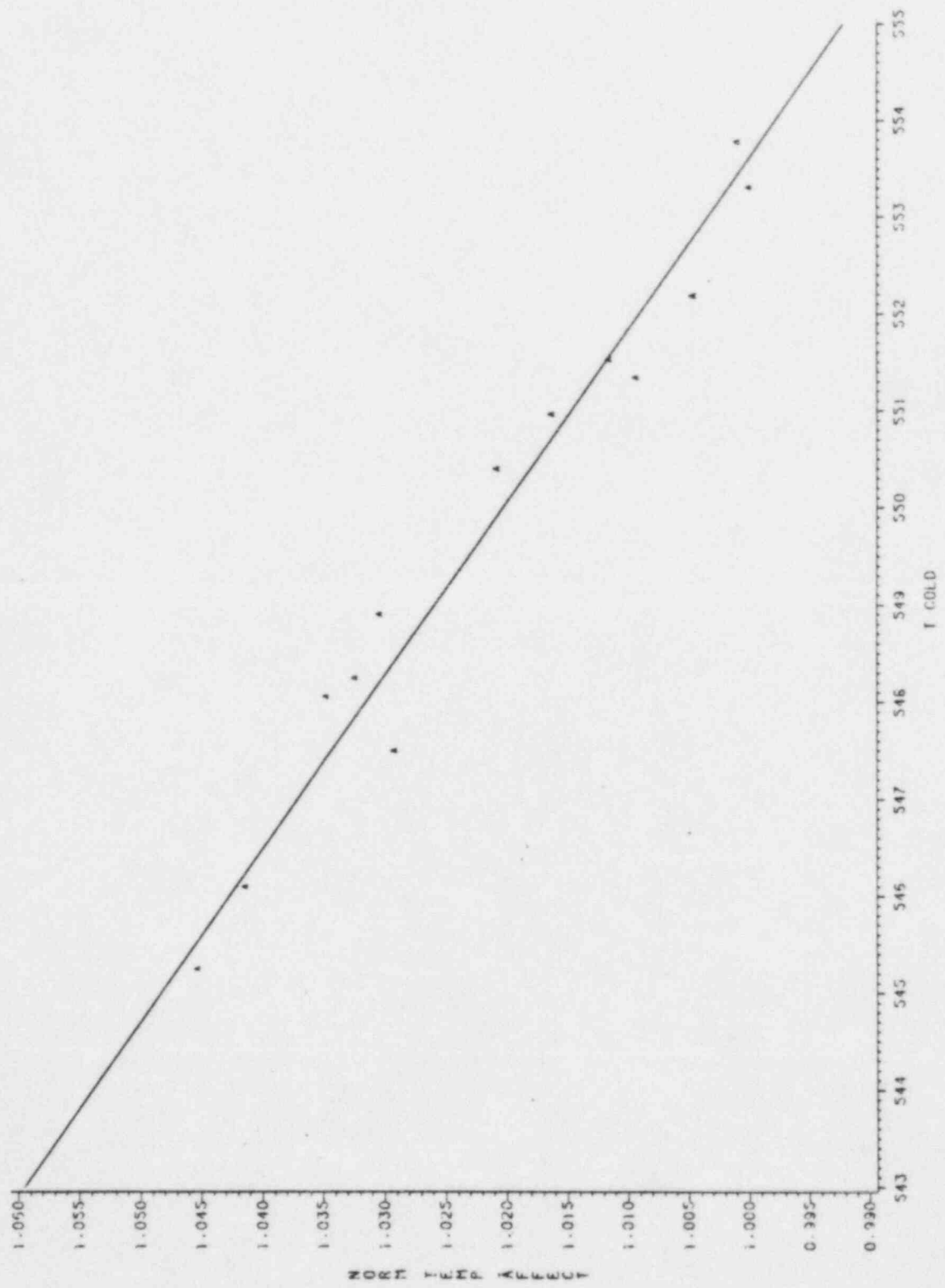


FIGURE 6.3.5.2

CPC TEMPERATURE DECALIBRATION

CPC CHANNEL B

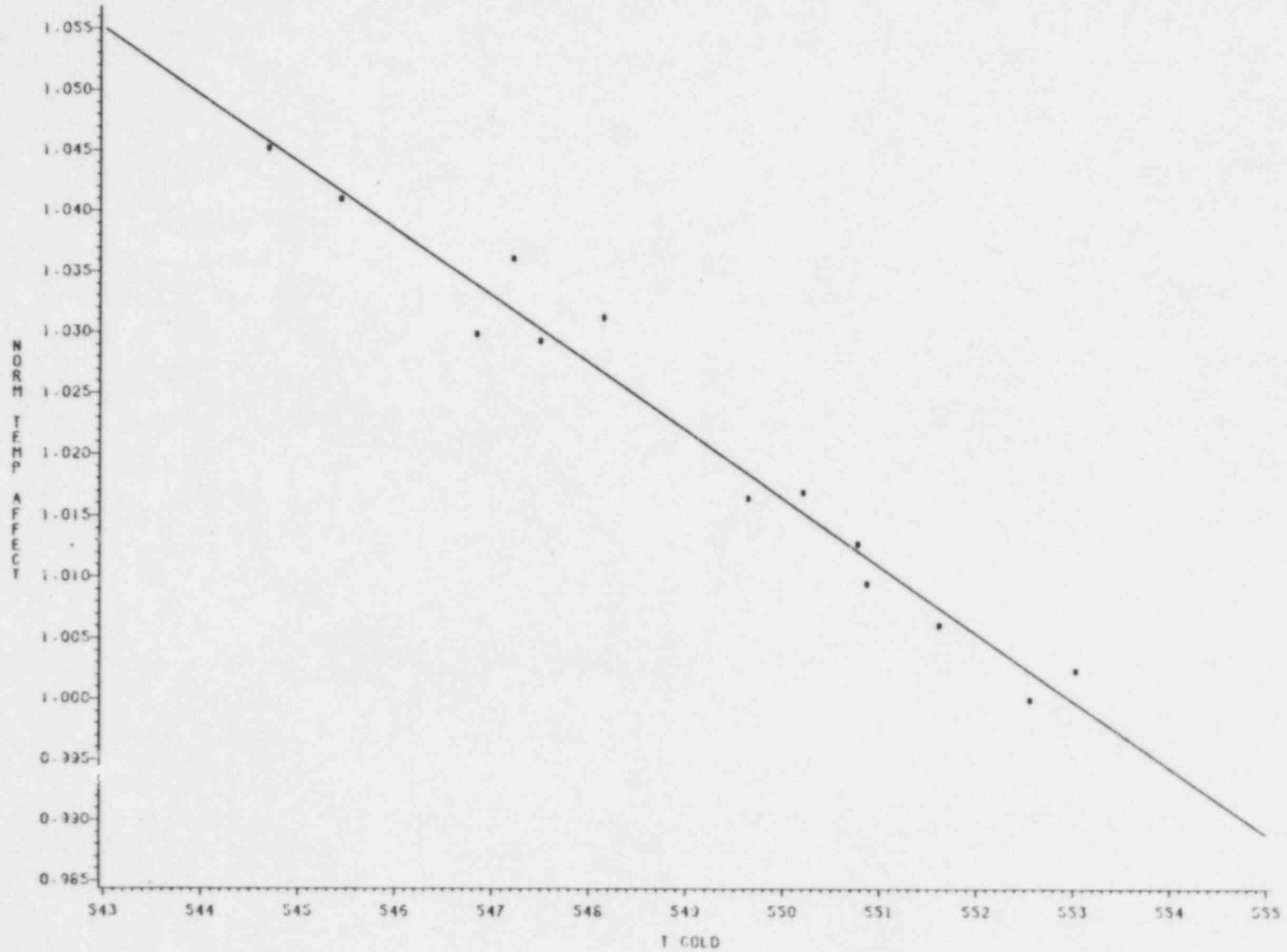


FIGURE 6.3.5.3

CPC TEMPERATURE DECALIBRATION
CPC CHANNEL C

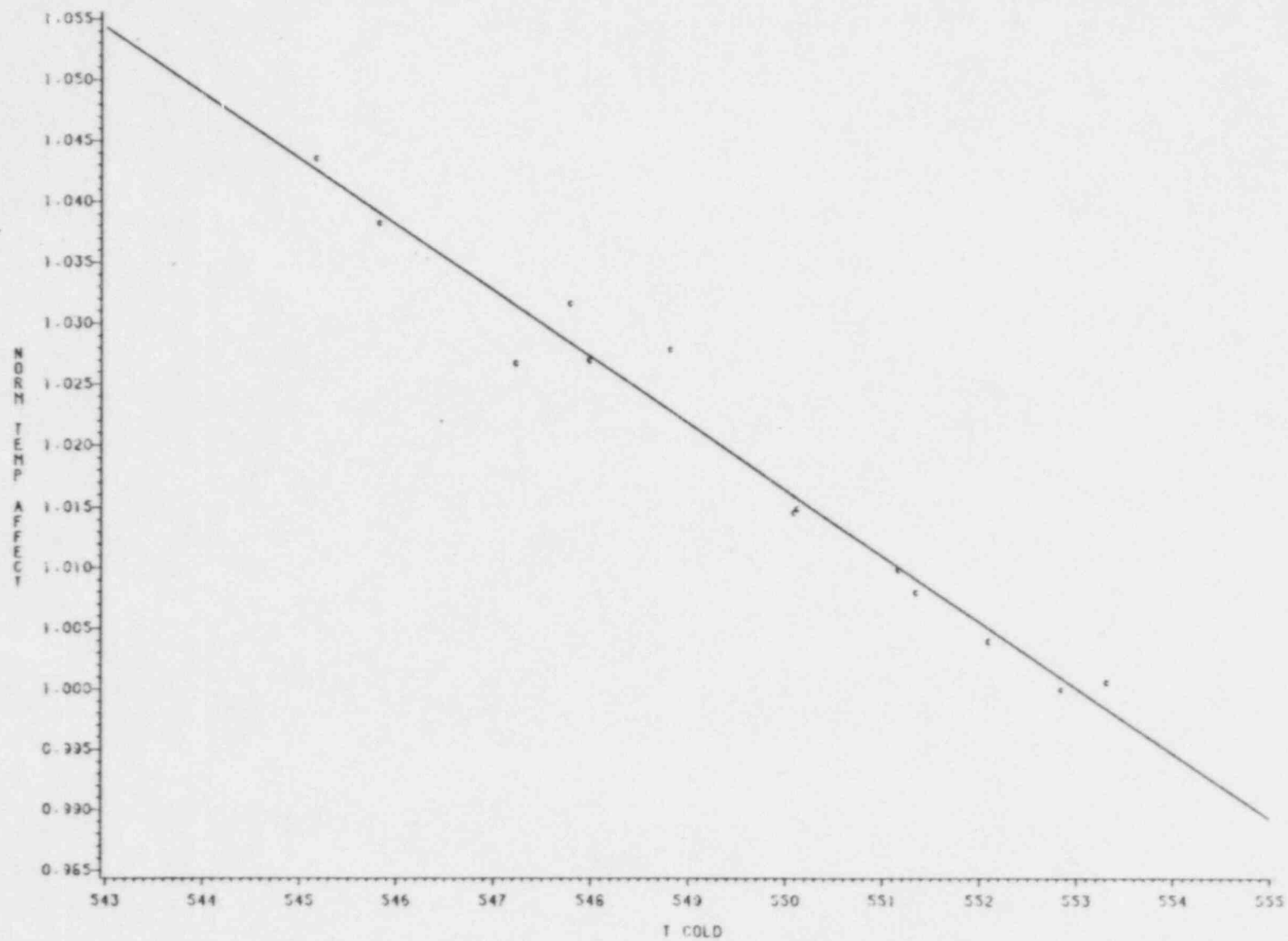
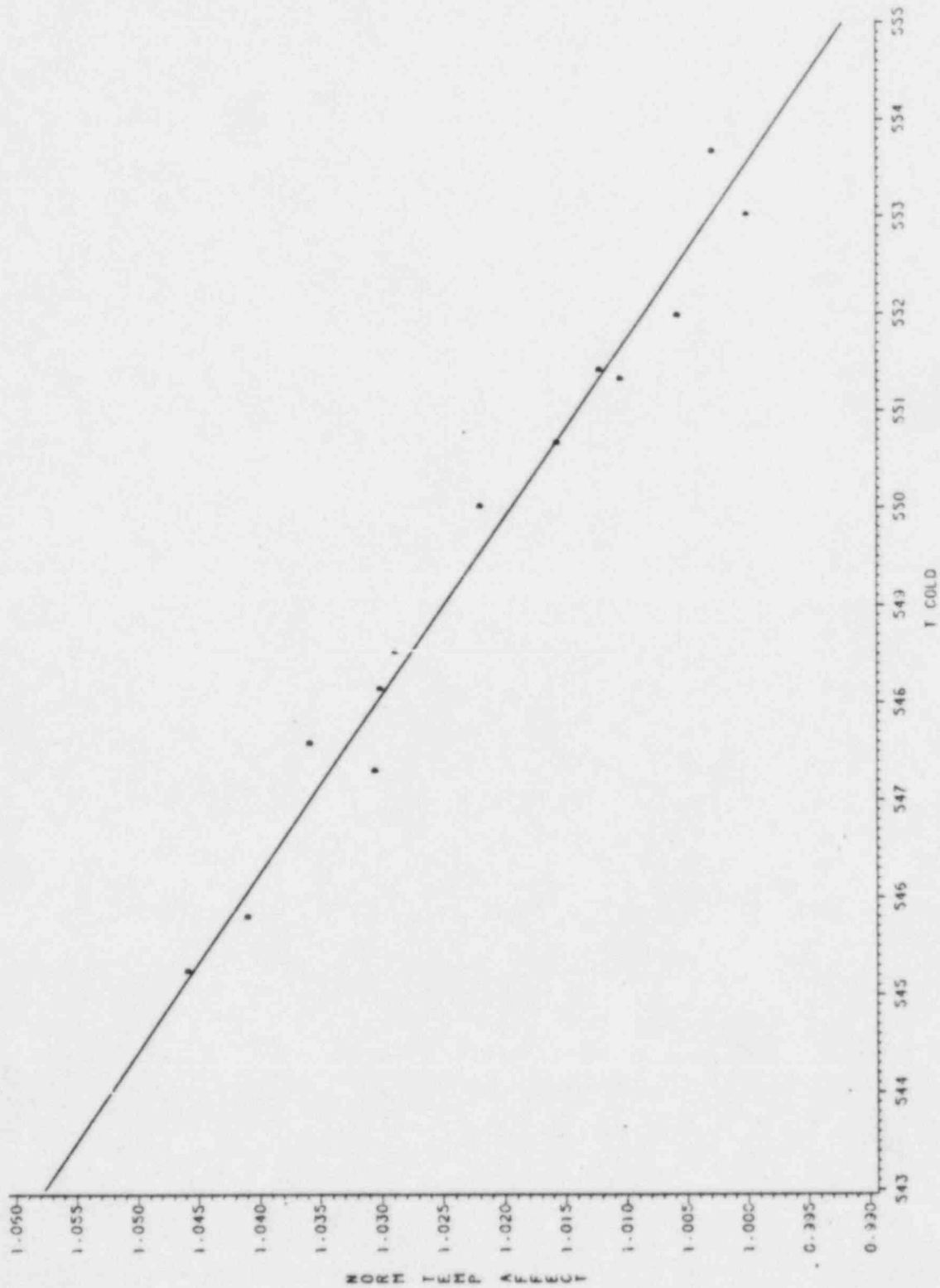


FIGURE 6.3.5.4
CPC TEMPERATURE DECALIBRATION
CPC CHANNEL D



CONCLUSION:

The measured values for temperature shadowing factors verified the adequacy of the values being used by the CPCs by meeting the specified acceptance criteria. No adjustments were necessary.

6.3.6 Shape Annealing Matrix Measurement (SIT-TP-723)

PURPOSE:

The purpose of this test was to determine the relationship between the excore detectors and the incore power distribution and to adjust, if necessary, the appropriate Core Protection Calculator (CPC) constants to ensure that the correct relationship is maintained. Specifically, the Shape Annealing Matrix (SAM) elements (i.e. SC_{ij}) and the Boundary Point Power Correlation Coefficients ($BPPCC_i$) were measured and compared to the corresponding values used by the CPCs to determine if the CPC values are appropriate.

METHOD:

An axial xenon oscillation was induced in the reactor core through CEA Group 6 motion. By comparing the measured incore power distribution to the measured excore responses, the incore/excore relationships were developed. A few details of the comparison follow:

There are four excore channels containing three axially spaced detectors per channel. There exists a one-to-one relationship between the four CPC channels and the four excore channels. Each CPC uses its respective excore channel responses to develop an incore power profile. That is, the three excore responses are used to infer three powers which approximate the upper, middle and lower one-third core powers. These three powers, with measured top and bottom boundary powers, are used to develop the axial power profile.

The relationship between the three excore responses and the three core powers is as follows:

$$P_1 = S_{11}D_1 + S_{12}D_2 + S_{13}D_3$$

$$P_2 = S_{21}D_1 + S_{22}D_2 + S_{23}D_3$$

$$P_3 = S_{31}D_1 + S_{32}D_2 + S_{33}D_3$$

where:

P_i = normalized one-third core powers (or peripheral powers, if vendor nomenclature is used) for level i ($i = 1, 2, 3$ for top, middle and bottom)

D_j = normalized excore detector response for level j

S_{ij} = constant value which relates the response of detector j to the peripheral power in core level i , i.e., the Shape Annealing Matrix (SAM)

The relationship between the top and bottom boundary powers and the core power is as follows:

$$\phi_U = \alpha_1 P_U - \alpha_3$$

$$\phi_L = \alpha_2 P_L - \alpha_4$$

where

ϕ_U = upper core boundary average power

ϕ_L = lower core boundary average power

P_U = upper one-third core fraction of average power

P_L = lower one-third core fraction of average power

By inducing a large xenon oscillation (which can be thought of as a simulation of the various power shapes which may exist through the cycle) the relationships just described may be quantified. That is, during the oscillation readings are taken at a prescribed frequency and a best set, in a least square sense, of the matrix values is determined. Consider the SAM equation for any level i :

$$\langle P_i \rangle = \sum_{j=1}^3 S_{ij} \langle D_j \rangle$$

where " $\langle \rangle$ " denotes averages over some n values of observations. In a least square sense, this equation may be rewritten as:

$$E_i^2 = \langle (P_i - \sum_{j=1}^3 S_{ij} D_j)^2 \rangle$$

where E_i^2 is the average of the square of the differences. By differentiating this equation with respect to the matrix components (the S 's) and equating that to zero, a set of equations result from which the S 's may be determined.

That is:

$$\frac{\partial E_i^2}{\partial S_{ij}} = 0$$

or

$$\frac{\partial E_i^2}{\partial S_{i1}} = 0 = 2(S_{i1} \langle D_1^2 \rangle - \langle P_i D_1 \rangle + S_{i2} \langle D_1 D_2 \rangle + S_{i3} \langle D_1 D_3 \rangle)$$

$$\frac{\partial E_i^2}{\partial S_{i2}} = 0 = 2(S_{i2} \langle D_2^2 \rangle - \langle P_i D_2 \rangle + S_{i1} \langle D_1 D_2 \rangle + S_{i3} \langle D_2 D_3 \rangle)$$

$$\frac{\partial E_i^2}{\partial S_{i3}} = 0 = 2(S_{i3} \langle D_3^2 \rangle - \langle P_i D_3 \rangle + S_{i1} \langle D_1 D_3 \rangle + S_{i2} \langle D_2 D_3 \rangle)$$

or, using matrix notation:

$$\begin{vmatrix} \langle D_1^2 \rangle & \langle D_1 D_2 \rangle & \langle D_1 D_3 \rangle \\ \langle D_1 D_2 \rangle & \langle D_2^2 \rangle & \langle D_2 D_3 \rangle \\ \langle D_1 D_3 \rangle & \langle D_2 D_3 \rangle & \langle D_3^2 \rangle \end{vmatrix} \begin{vmatrix} S_{i1} \\ S_{i2} \\ S_{i3} \end{vmatrix} = \begin{vmatrix} \langle P_i D_1 \rangle \\ \langle P_i D_2 \rangle \\ \langle P_i D_3 \rangle \end{vmatrix}$$

or finally:

$$\begin{vmatrix} S_{i1} \\ S_{i2} \\ S_{i3} \end{vmatrix} = \begin{vmatrix} \langle D_1^2 \rangle & \langle D_1 D_2 \rangle & \langle D_1 D_3 \rangle \\ \langle D_1 D_2 \rangle & \langle D_2^2 \rangle & \langle D_2 D_3 \rangle \\ \langle D_1 D_3 \rangle & \langle D_2 D_3 \rangle & \langle D_3^2 \rangle \end{vmatrix}^{-1} \begin{vmatrix} \langle P_i D_1 \rangle \\ \langle P_i D_2 \rangle \\ \langle P_i D_3 \rangle \end{vmatrix}$$

This last equation is solved for each level i ($i=1,2,3$), resulting in three 3×1 matrices. Combining the three 3×1 matrices into one 3×3 matrix results in the SAM for that channel.

Considering the boundary point equations, and following steps similar to those just noted for the SAM yields:

$$\frac{\partial}{\partial \alpha_1} = 0 = \alpha_1 \langle P_U^2 \rangle - \langle \Phi_U P_U \rangle - \alpha_2 \langle P_U \rangle$$

$$\frac{\partial}{\partial \alpha_2} = 0 = \alpha_2 + \langle \Phi_U \rangle - \alpha_1 \langle P_U \rangle$$

$$\frac{\partial}{\partial \alpha_3} = 0 = \alpha_3 \langle P_L^2 \rangle - \langle \Phi_L P_L \rangle - \alpha_4 \langle P_L \rangle$$

$$\frac{\partial}{\partial \alpha_4} = 0 = \alpha_4 + \langle \Phi_L \rangle - \alpha_3 \langle P_L \rangle$$

Using matrix notation:

$$\begin{vmatrix} \langle P_U^2 \rangle & -\langle P_U \rangle \\ -\langle P_U \rangle & 1 \end{vmatrix} \begin{vmatrix} \alpha_1 \\ \alpha_2 \end{vmatrix} = \begin{vmatrix} \langle \Phi_U P_U \rangle \\ -\langle \Phi_U \rangle \end{vmatrix}$$

$$\begin{vmatrix} \langle P_L^2 \rangle & -\langle P_L \rangle \\ -\langle P_L \rangle & 1 \end{vmatrix} \begin{vmatrix} \alpha_3 \\ \alpha_4 \end{vmatrix} = \begin{vmatrix} \langle \Phi_L P_L \rangle \\ -\langle \Phi_L \rangle \end{vmatrix}$$

or finally:

$$\begin{vmatrix} \alpha_1 \\ \alpha_2 \end{vmatrix} = \begin{vmatrix} \langle P_U^2 \rangle & -\langle P_U \rangle \\ -\langle P_U \rangle & 1 \end{vmatrix}^{-1} \begin{vmatrix} \langle \Phi_U P_U \rangle \\ -\langle \Phi_U \rangle \end{vmatrix}$$

$$\begin{vmatrix} \alpha_3 \\ \alpha_4 \end{vmatrix} = \begin{vmatrix} \langle P_L^2 \rangle & -\langle P_L \rangle \\ -\langle P_L \rangle & 1 \end{vmatrix}^{-1} \begin{vmatrix} \langle \Phi_L P_L \rangle \\ -\langle \Phi_L \rangle \end{vmatrix}$$

Calculation of the S's and α 's is straight-forward since all variables (except the S's and α 's) are known - either recorded from the CPC or calculated by the incore analysis system, CECOR.

Once a measured matrix is determined, it is compared to the design matrix. If the measured SAM elements are within $\pm 2.0\%$ of the design SAM elements, the design elements are adequate. If not, a check of the matrix test value, defined below, must be made. The same is true for the boundary points, except that the acceptance band is within $\pm 3.0\%$, and there is no test value check.

The SAM test value is defined as:

$$t = \sum_{i=1}^3 \sum_{j=1}^3 T_{ij}$$

where:

$$T_{ij} = [S_{ij}] \begin{vmatrix} S_{11} & 0 & 0 \\ 0 & S_{22} & 0 \\ 0 & 0 & S_{33} \end{vmatrix}^{-1}$$

If any of the measured SAM element are out of tolerance and $3.0 \leq t \leq 6.29$, then the measured SAM values are installed in the CPC's. If the measured values are out of tolerance and $3 > t > 6.29$, the vendor must be notified immediately.

The requirement to perform this test at 20% power was subjected to a screening test to determine acceptable closeness of the excore and incore power distributions as performed within the scope of the Core Performance Record Test (see Section 6.4.1). Meeting the criteria of the screening test allowed deletion of the SAM measurement at the 20% power test plateau.

The actual method and chronology of this test were as follows:

The screening test performed in accordance with the Core Performance Record Test (see section 6.4.1) at 20% power was acceptable and allowed the elimination of this test at the 20% power test plateau. The subsequent summary, thus, pertains only to the test as performed at 50% power.

A xenon oscillation was initiated at about 1842 on April 25, 1985, by diluting CEA group 6 to 75 inches withdrawn. At the start of the dilution, the ASI was approximately 0.016, which was 0.002 ASI units from the ESI of 0.018. During the six hour wait for peak ASI, data records and CECOR Verification Files (CVFs) were recorded at 15 minute intervals for the first two hours and at 30 minute intervals for the next four hours. During this time, RCS temperature and reactor power were held as steady as possible. When the ASI peaked (at about 0.270 ASI units), CEA group 6 was to be pulled to 150 inches withdrawn, with temperature and power held constant through boration. Problems with the chemical and volume control system (CVCS) delayed the boration/rod pull for about two hours. This delay did not, however, impact the test. Once the rods were borated out, CVFs were taken every 15 minutes while data records were taken every 15 minutes for about nine hours, then every 30 minutes for the duration of the oscillation. During the oscillation, power and temperature were held constant. Approximately 30 hours after the initiation of the oscillation data collection was terminated.

The CVFs were processed by the CECOR code. The CECOR output files were processed by two auxiliary computer codes to yield the measured SAM and boundary points. Independent vendor calculations verified the measured values. Of a possible 120 CVFs, 111 were actually used in the data reduction. Eight

CVFs were not available due to plant computer problems while one CVF was disregarded upon vendor recommendations. The omission of the nine CVFs did not meaningfully alter the measured values.

RESULTS:

Table 6.3.6.1 outlines the comparison of measured and design values. Numerous predicted values were unacceptable. However, since the test values were acceptable for all channels, all measured value were installed in the CPCs.

Figure 6.3.6.1 shows that the CPC ASI was in good agreement with the measured (CECOR) ASI. This suggests that the design SAM and boundary points were relatively good. If the test were reperformed, using the measured values in place of the design values, the ASI differences noted in the figure would be less.

Figures 6.3.6.2 through 6.3.6.17 are plots of excore response and peripheral power versus time (time 0 = time at ARO). Examination of the figure suggests that nothing unusual occurred during the test. All detector responses were consistent between and within channels. The same holds true for the peripheral powers.

CONCLUSION:

The test was performed as specified with acceptable results. All test objectives and acceptance criteria were satisfactorily met.

TABLE 6.3.6.1
COMPARISON OF MEASURED AND DESIGN SAM AND BPPCC VALUES

Parameter	CPC ID	Design Value	Measured Values				% Difference			
			CPC-A	CPC-B	CPC-C	CPC-D	CPD-A	CPC-B	CPC-C	CPC-D
SC11	81	3.7949	4.5124	4.4271	4.1756	4.1176	18.9	16.7	10.0	8.5
SC12	82	-.4654	-1.6379	-1.6021	-1.1404	-1.0944	251.9	244.2	145.0	135.2
SC13	83	-.0491	-.83432	.78717	.48385	.4265	-1799.2	-1703.2	-1085.4	-968.7
SC21	84	-1.0223	-.94375	-.97189	-.59030	-.54462	-7.7	-4.9	-42.3	-46.7
SC22	85	4.3680	4.3315	4.4616	3.7874	3.7545	-0.8	2.1	-13.3	-14.1
SC23	86	-.8740	-.97807	-1.0432	-.59277	-5.0858	11.9	19.4	-32.2	-41.8
SC31	87	-.2277	-.56860	-.45419	-.58531	-5.7301	-349.7	-349.7	-299.9	-351.7
SC32	88	-.9023	-.30642	-.14046	.35299	.33997	-134.0	-115.6	-139.1	-137.7
SC33	89	3.9234	3.1438	3.2560	3.1089	3.0820	-19.9	-17.0	-20.8	-21.5
BPPCC1	99	.01383	.01363	.01363	.01363	.01363	-1.5	-1.5	-1.5	-1.5
BPPCC2	100	.08857	.07057	.07057	.07057	.07057	-20.3	-20.3	-20.3	-20.3
BPPCC3	101	.01225	.01443	.01443	.01443	.01443	17.8	17.8	17.8	17.8
BPPCC4	102	.05150	.07672	.07672	.07672	.07672	49.0	49.0	49.0	49.0
Test Value	---	3.8577	4.3605	4.2751	4.0021	3.9569	----	----	----	----

FIGURE 6.3.6.1

W3 CYCLE 1 SHAPE ANNEALING
AXIAL SHAPE INDEX

- * = CPC A ASI
- X = CPC B ASI
- = CPC C ASI
- = CPC D ASI
- Y = CECOR ASI

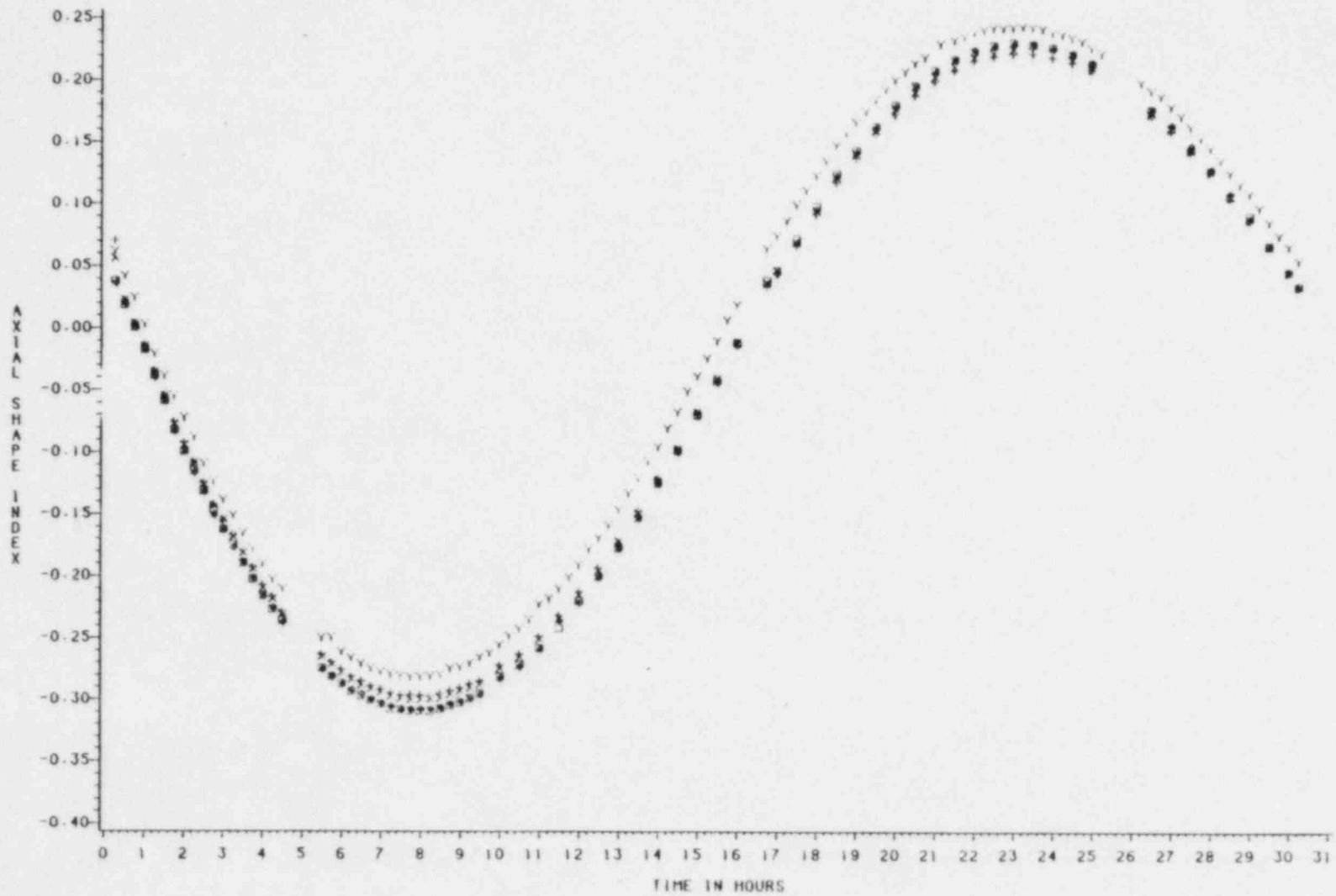


FIGURE 6.3.6.2

W3 CYCLE 1 SHAPE ANNEALING
JPPER EXCORE RESPONSES

• = CHANNEL A = GROUP 1
X = CHANNEL B = GROUP 2
* = CHANNEL C = GROUP 3
□ = CHANNEL D = GROUP 4

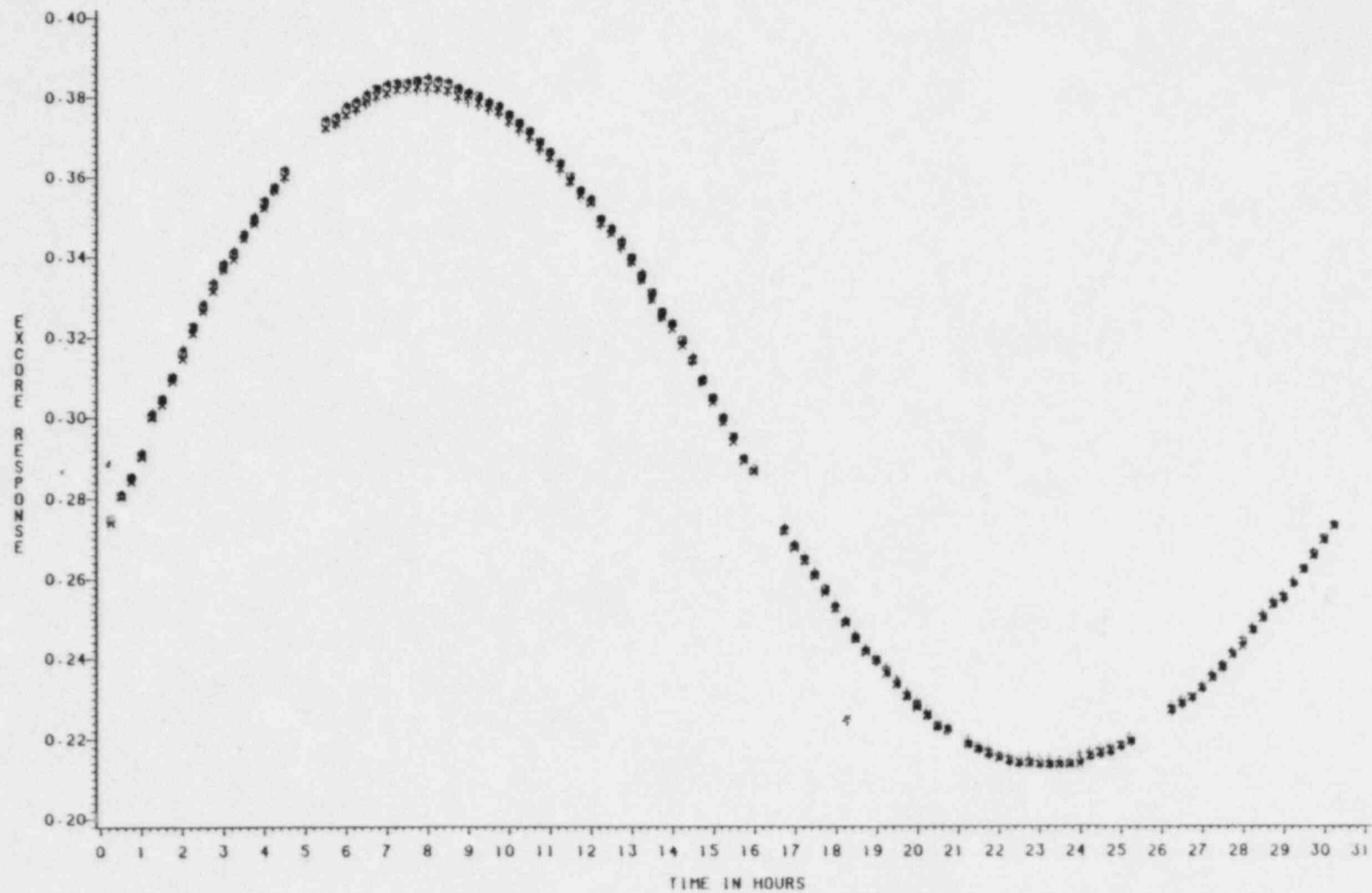


FIGURE 6.3.6.3

W3 CYCLE 1 SHAPE ANNEALING UPPER PERIPHERAL POWERS

- * = CHANNEL A = GROUP 1
- X = CHANNEL B = GROUP 2
- o = CHANNEL C = GROUP 3
- = CHANNEL D = GROUP 4

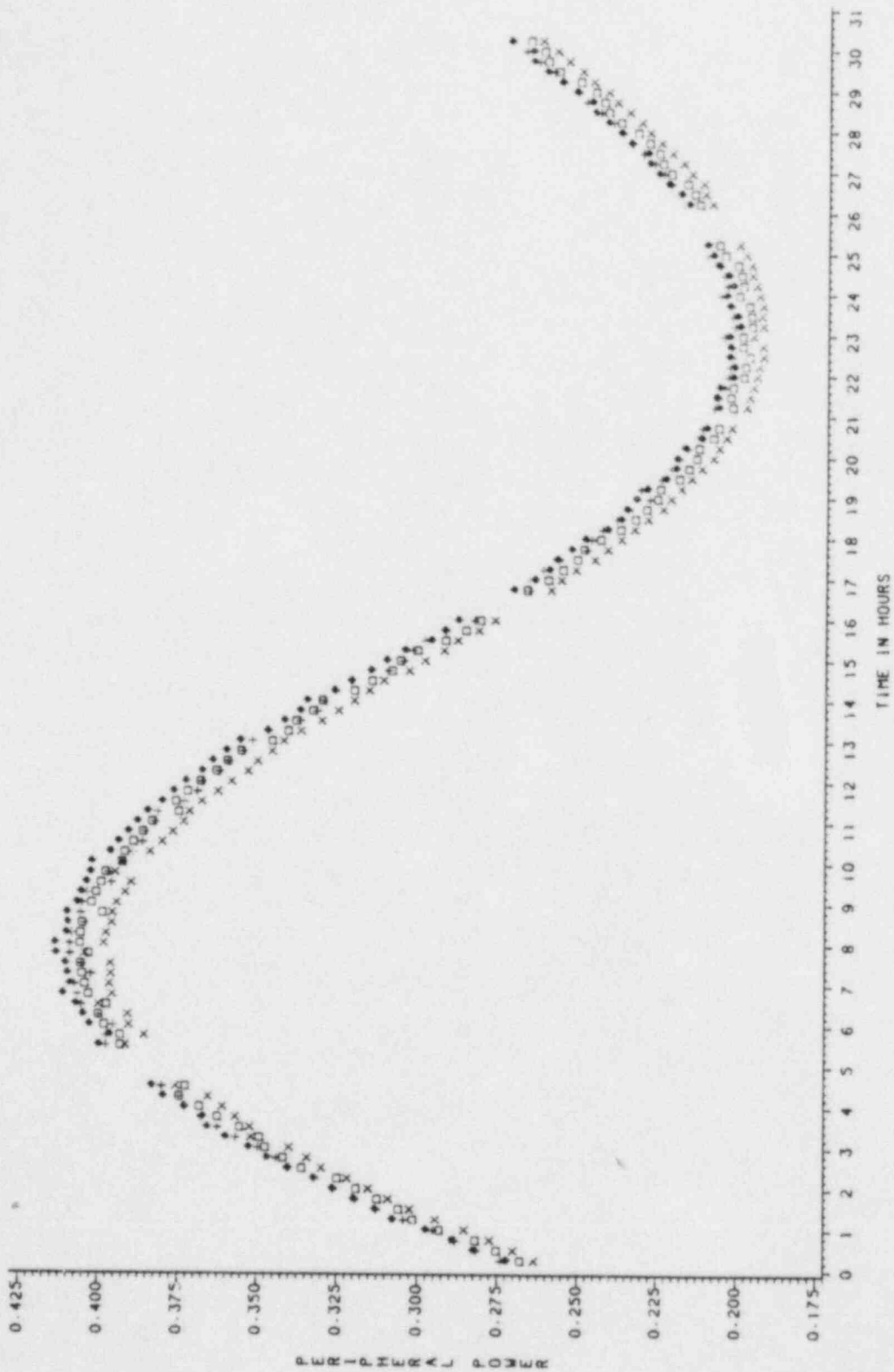


FIGURE 6.3.6.4

W3 CYCLE 1 SHAPE ANNEALING
MIDDLE EXCORE RESPONSES

- = CHANNEL A = GROUP 1
- X = CHANNEL B = GROUP 2
- = CHANNEL C = GROUP 3
- = CHANNEL D = GROUP 4

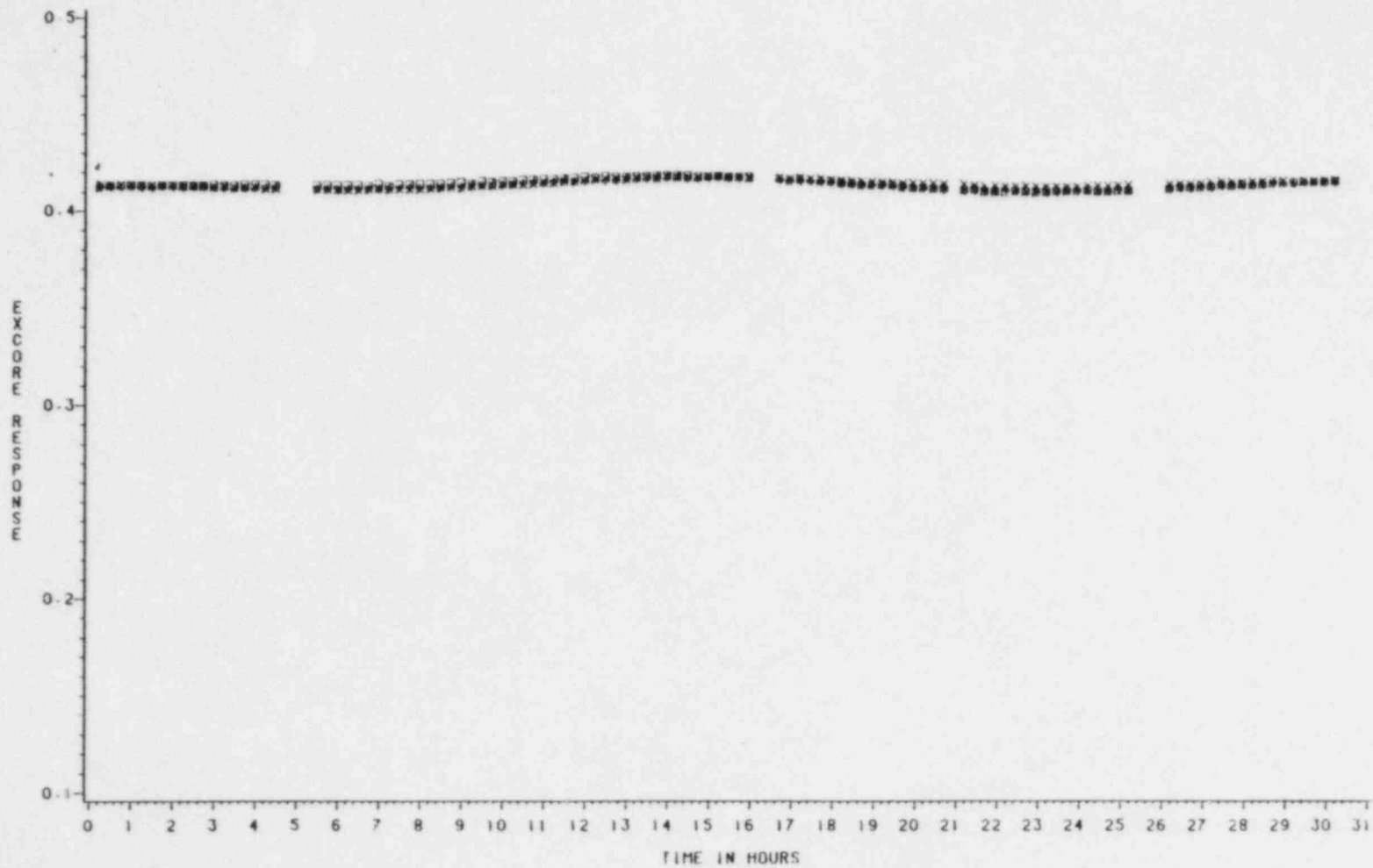


FIGURE 6.3.6.5

W3 CYCLE 1 SHAPE ANNEALING
MIDDLE EXCURE RESPONSES - EXPANDED SCALE

- = CHANNEL A = GROUP 1
- x = CHANNEL B = GROUP 2
- + = CHANNEL C = GROUP 3
- = CHANNEL D = GROUP 4

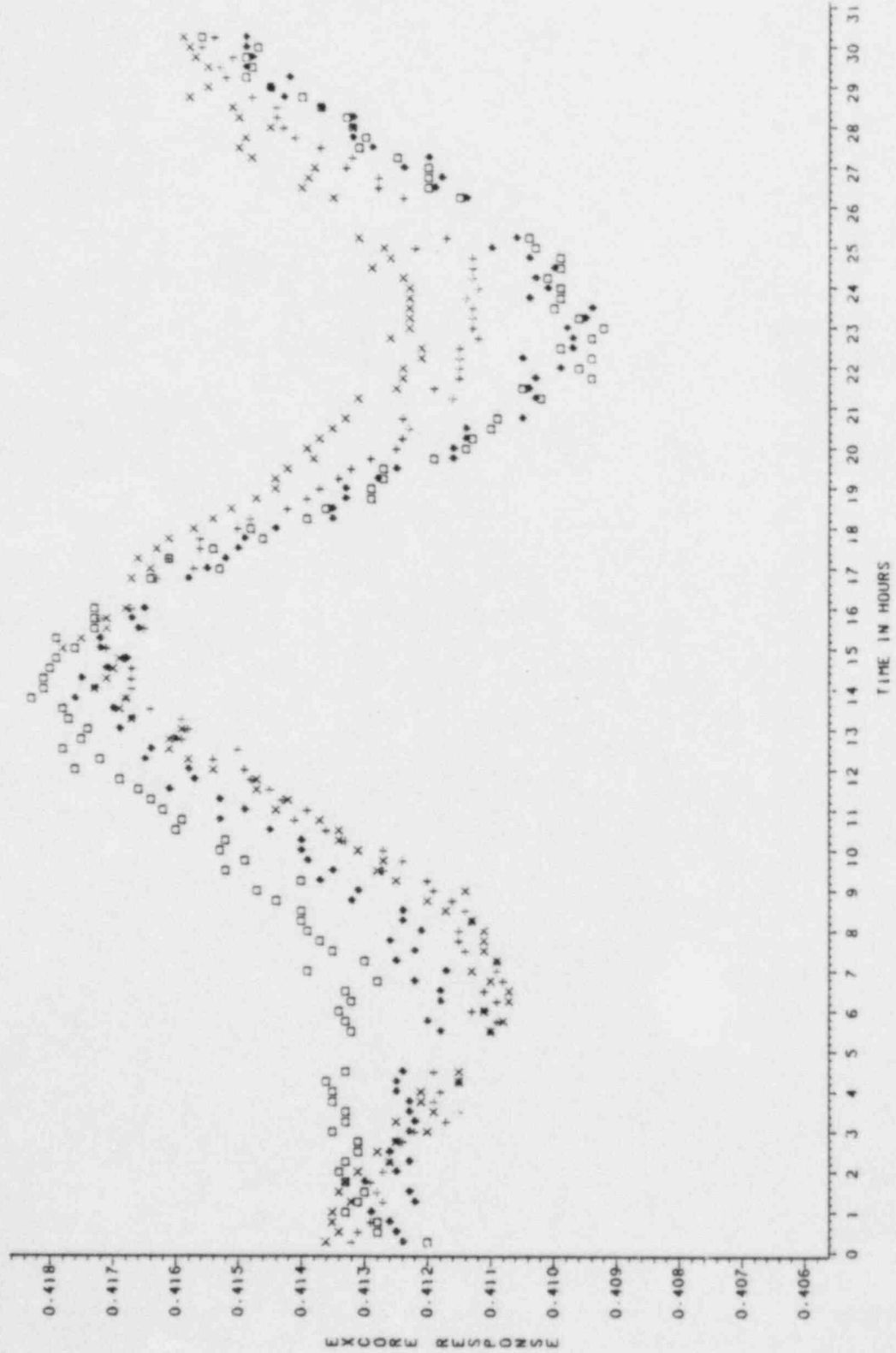


FIGURE 6.3.6.6.

W3 CYCLE 1 SHAPE ANNEALING
MIDDLE PERIPHERAL POWERS

• = CHANNEL A = GROUP 1
X = CHANNEL B = GROUP 2
* = CHANNEL C = GROUP 3
◻ = CHANNEL D = GROUP 4

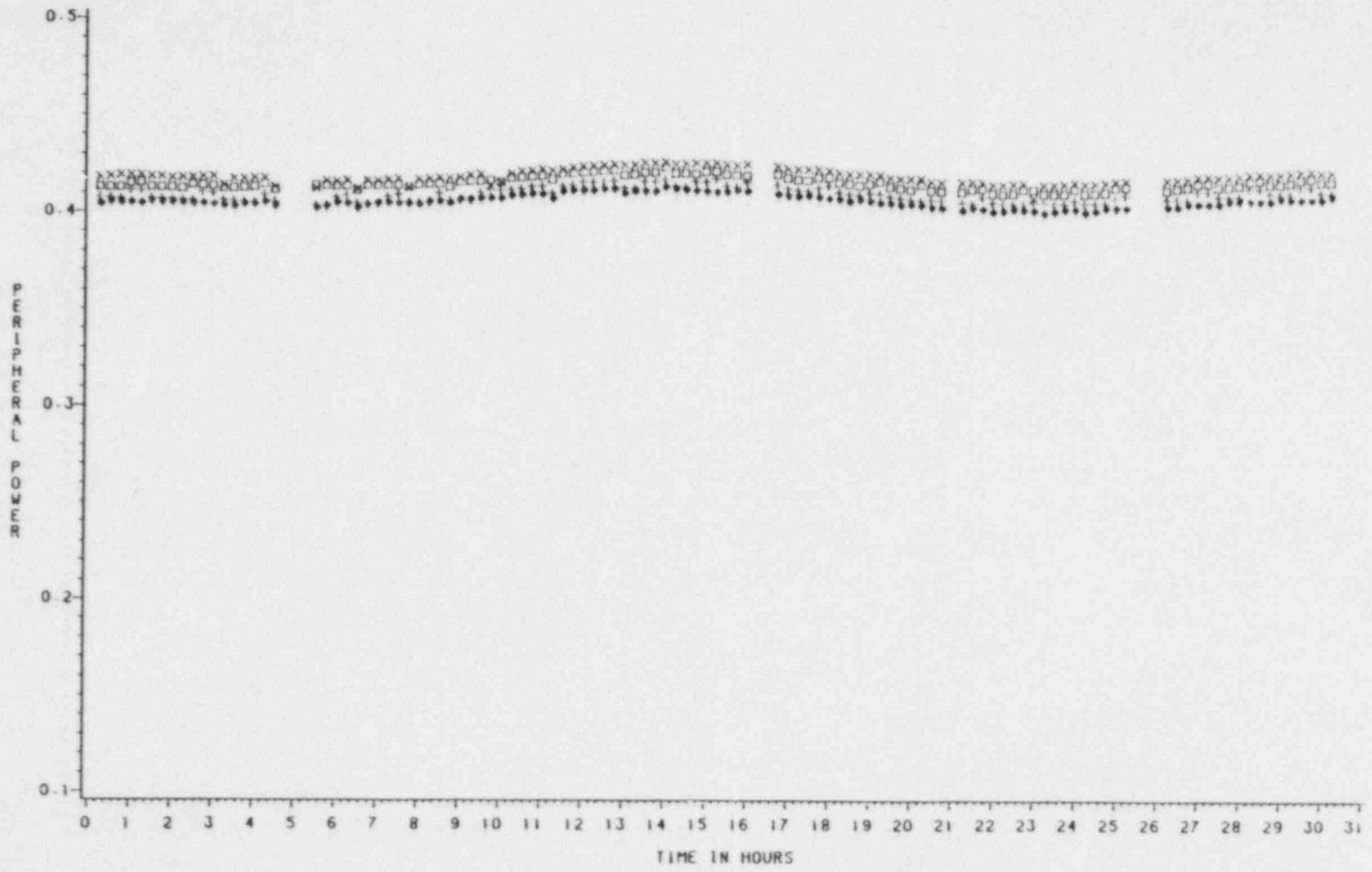


FIGURE 6.3.6.7

W3 CYCLE 1 SHAPE ANNEALING
MIDDLE PERIPHERAL POWERS - EXPANDED SCALE

- = CHANNEL A = GROUP 1
- x = CHANNEL B = GROUP 2
- + = CHANNEL C = GROUP 3
- = CHANNEL D = GROUP 4

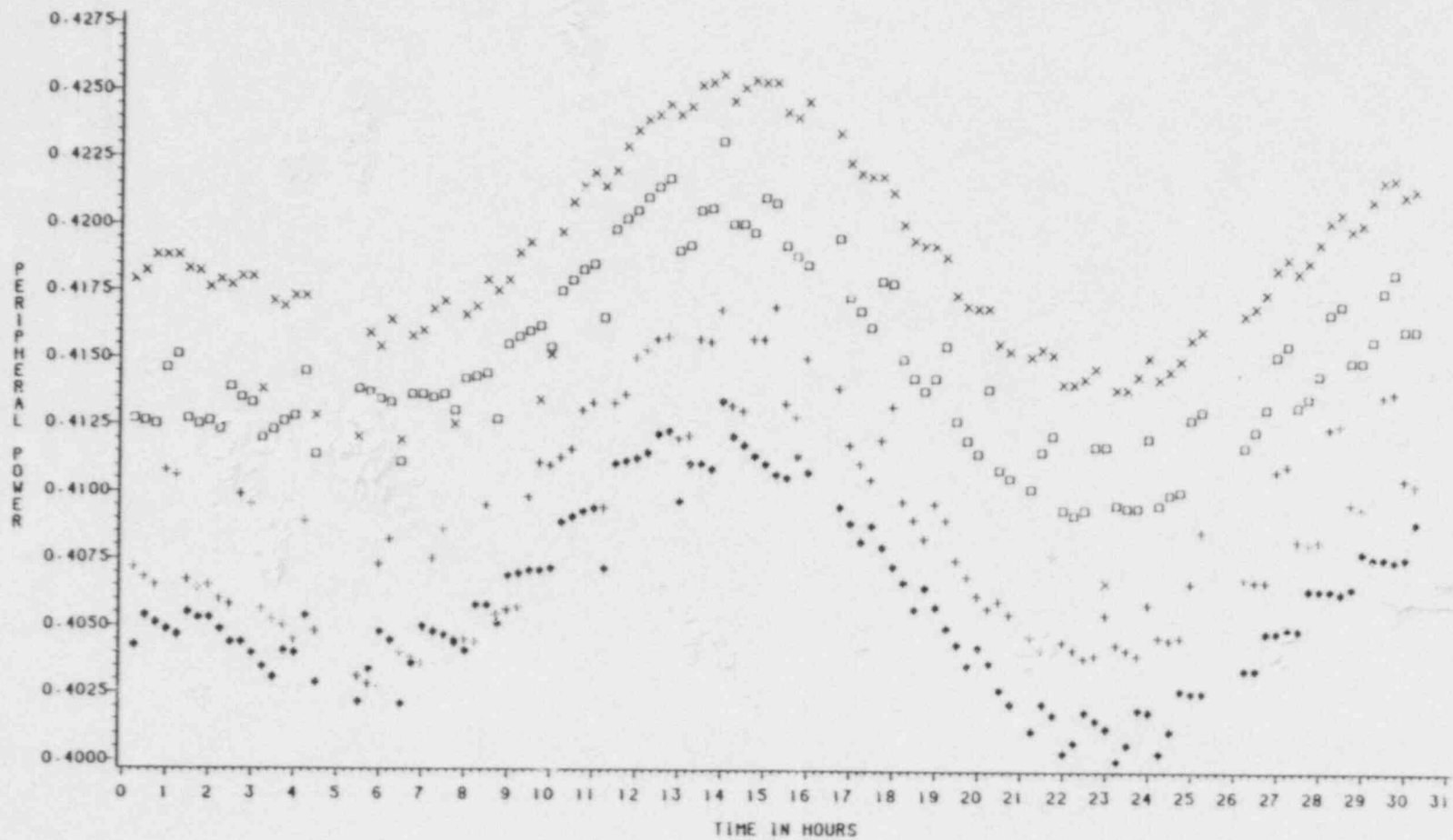


FIGURE 6.3.6.8

W3 CYCLE 1 SHAPE ANNEALING
LOWER EXCORE RESPONSES

- = CHANNEL A = GROUP 1
- X = CHANNEL B = GROUP 2
- * = CHANNEL C = GROUP 3
- = CHANNEL D = GROUP 4

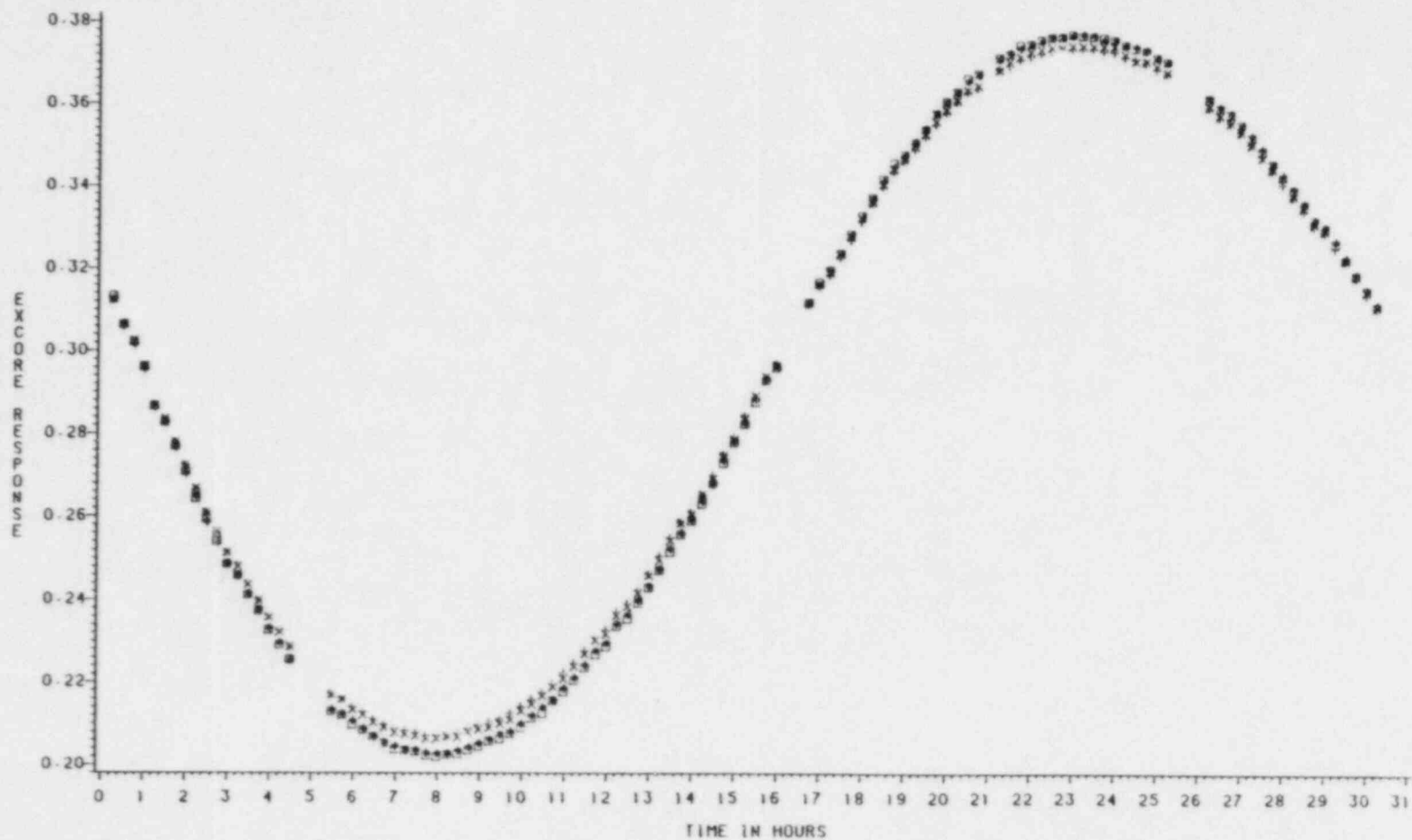


FIGURE 6.3.6.9

W3 CYCLE 1 SHAPE ANNEALING
LOWER PERIPHERAL POWERS

- = CHANNEL A = GROUP 1
- x = CHANNEL B = GROUP 2
- ◊ = CHANNEL C = GROUP 3
- ◻ = CHANNEL D = GROUP 4

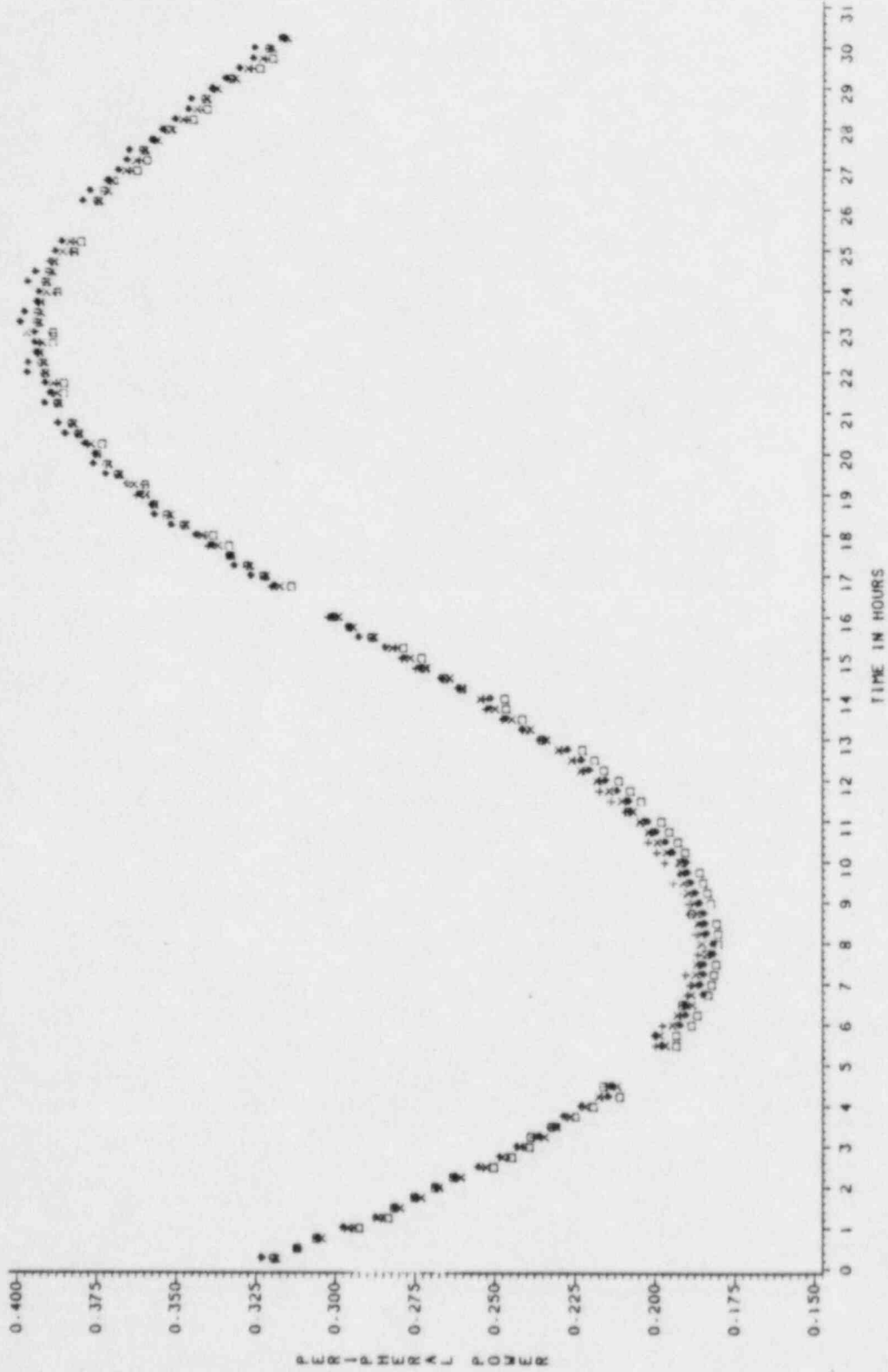


FIGURE 6.3.6.10

W3 CYCLE 1 SHAPE ANNEALING
CHANNEL A EXCORE VALUES

• = UPPER EXCORE
x = MIDDLE EXCORE
• = LOWER EXCORE

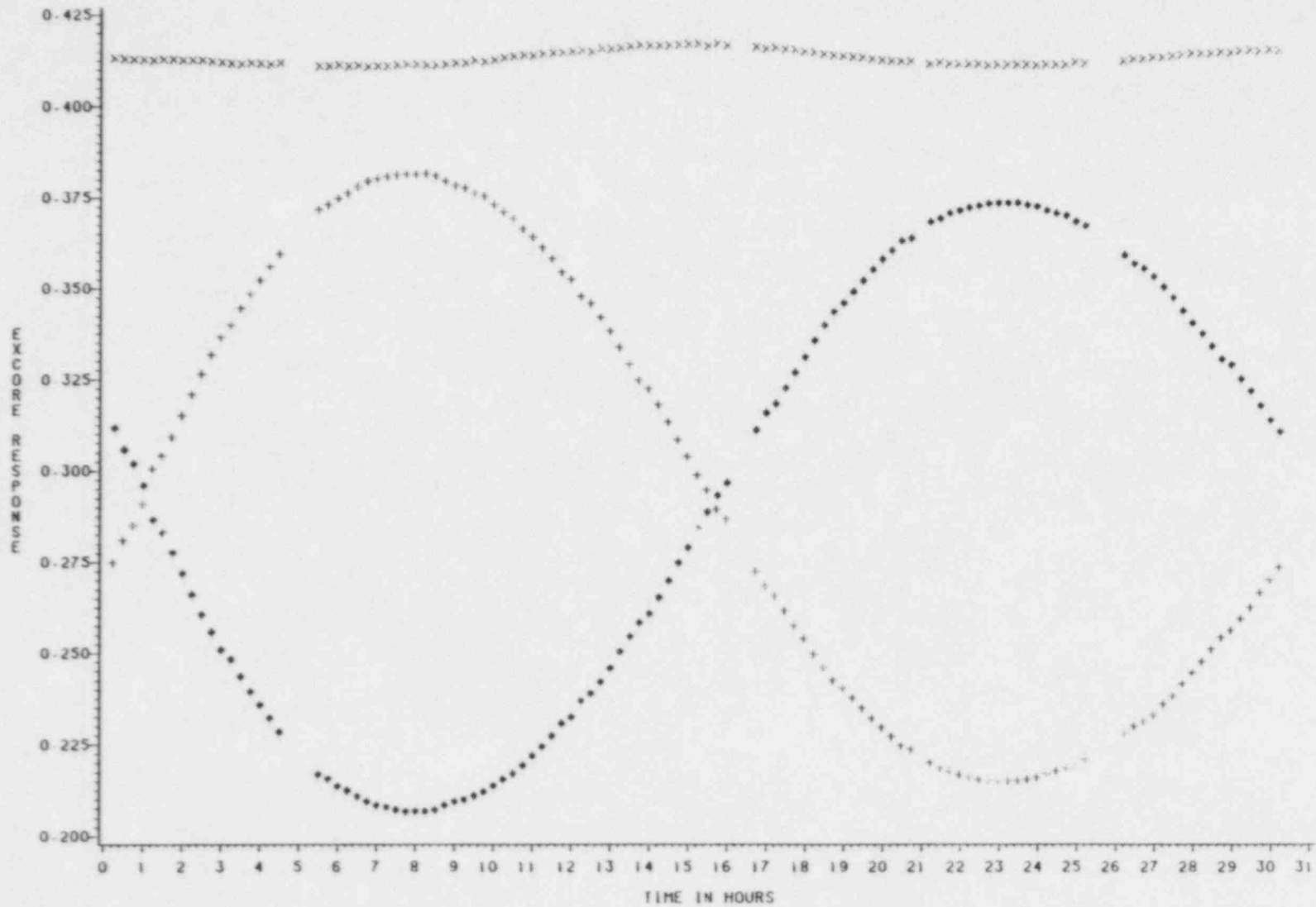


FIGURE 6.3.6.11

W3 CYCLE 1 SHAPE ANNEALING CHANNEL A PERIPHERAL POWERS

* = UPPER
X = MIDDLE
• = LOWER

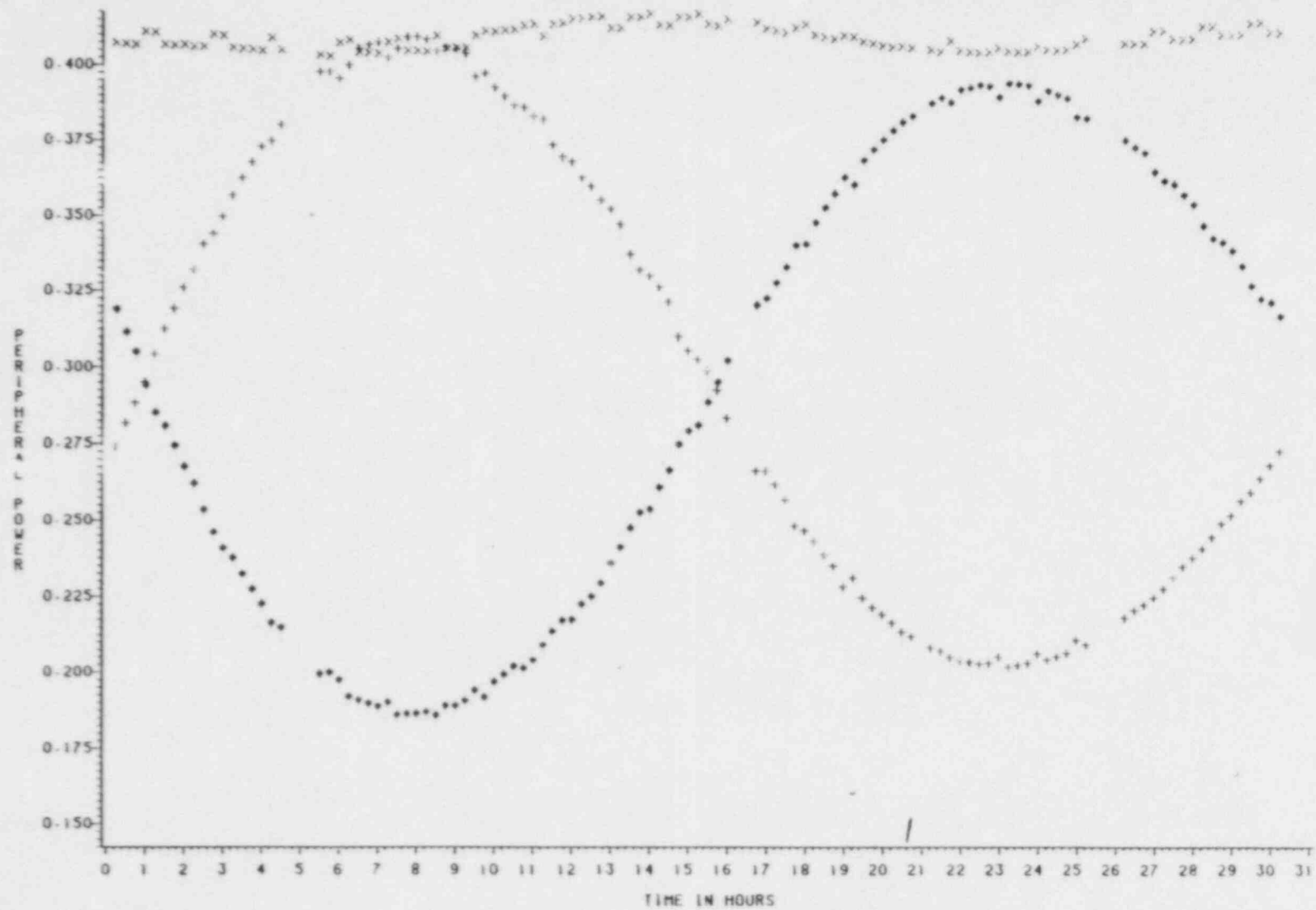


FIGURE 6.3.6.12

W3 CYCLE 1 SHAPE ANNEALING
CHANNEL B EXCORE VALUES

- = UPPER EXCORE
- X = MIDDLE EXCORE
- = LOWER EXCORE

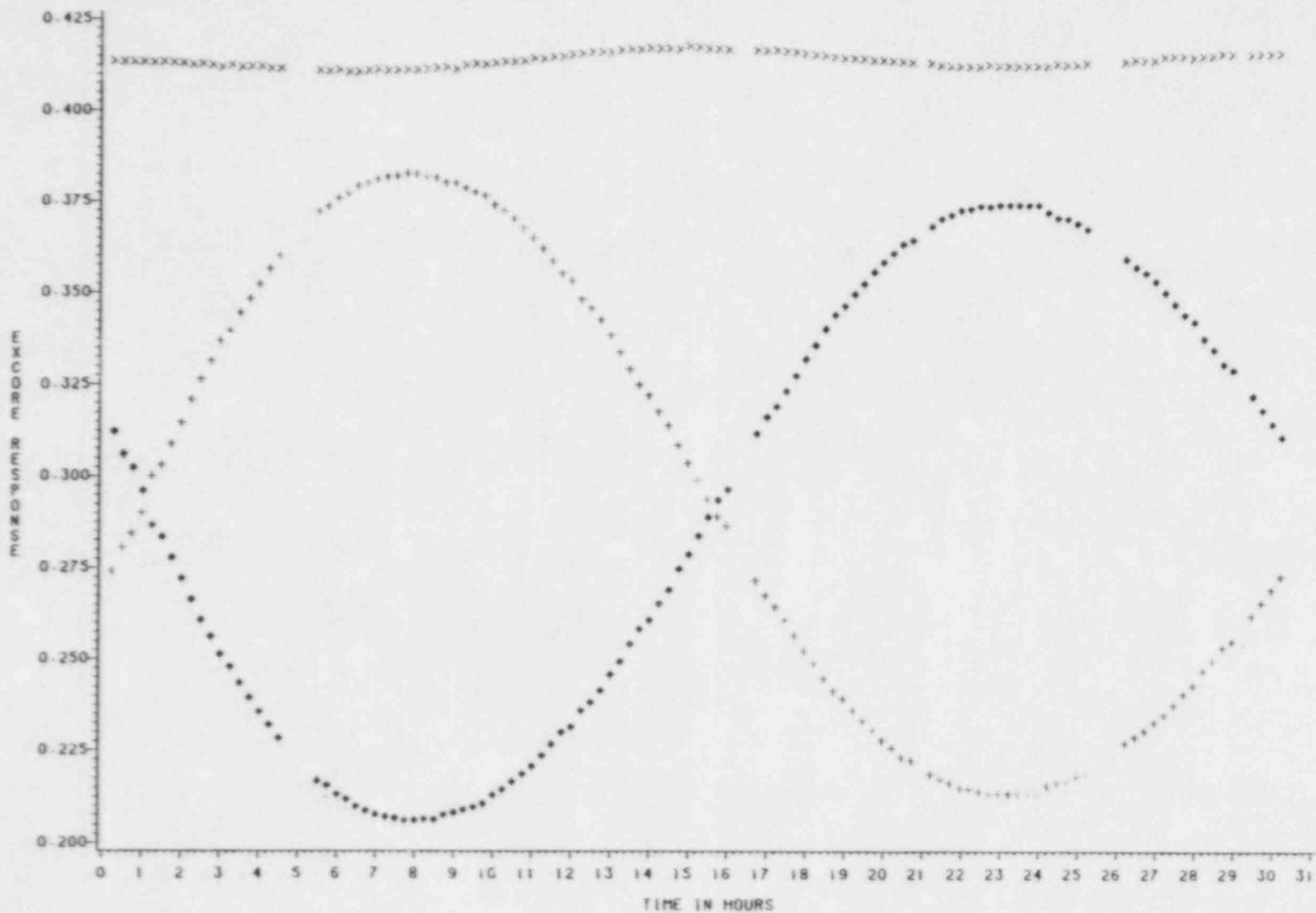


FIGURE 6.3.6.13

W3 CYCLE 1 SHAPE ANNEALING CHANNEL B PERIPHERAL POWERS

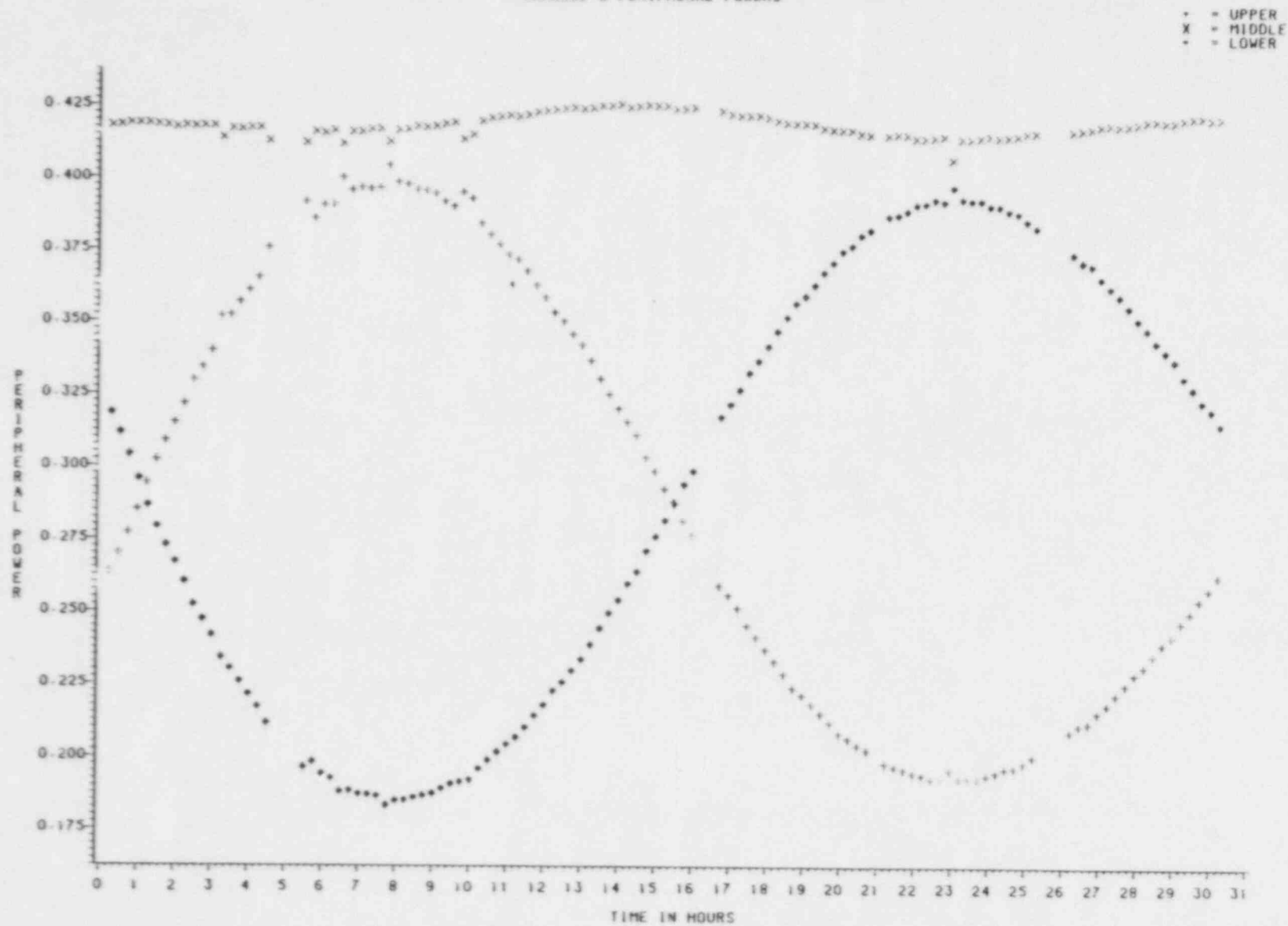


FIGURE 6.3.6.14

W3 CYCLE 1 SHAPE ANNEALING CHANNEL C EXCORE VALUES

- = UPPER EXCORE
- X = MIDDLE EXCORE
- * = LOWER EXCORE

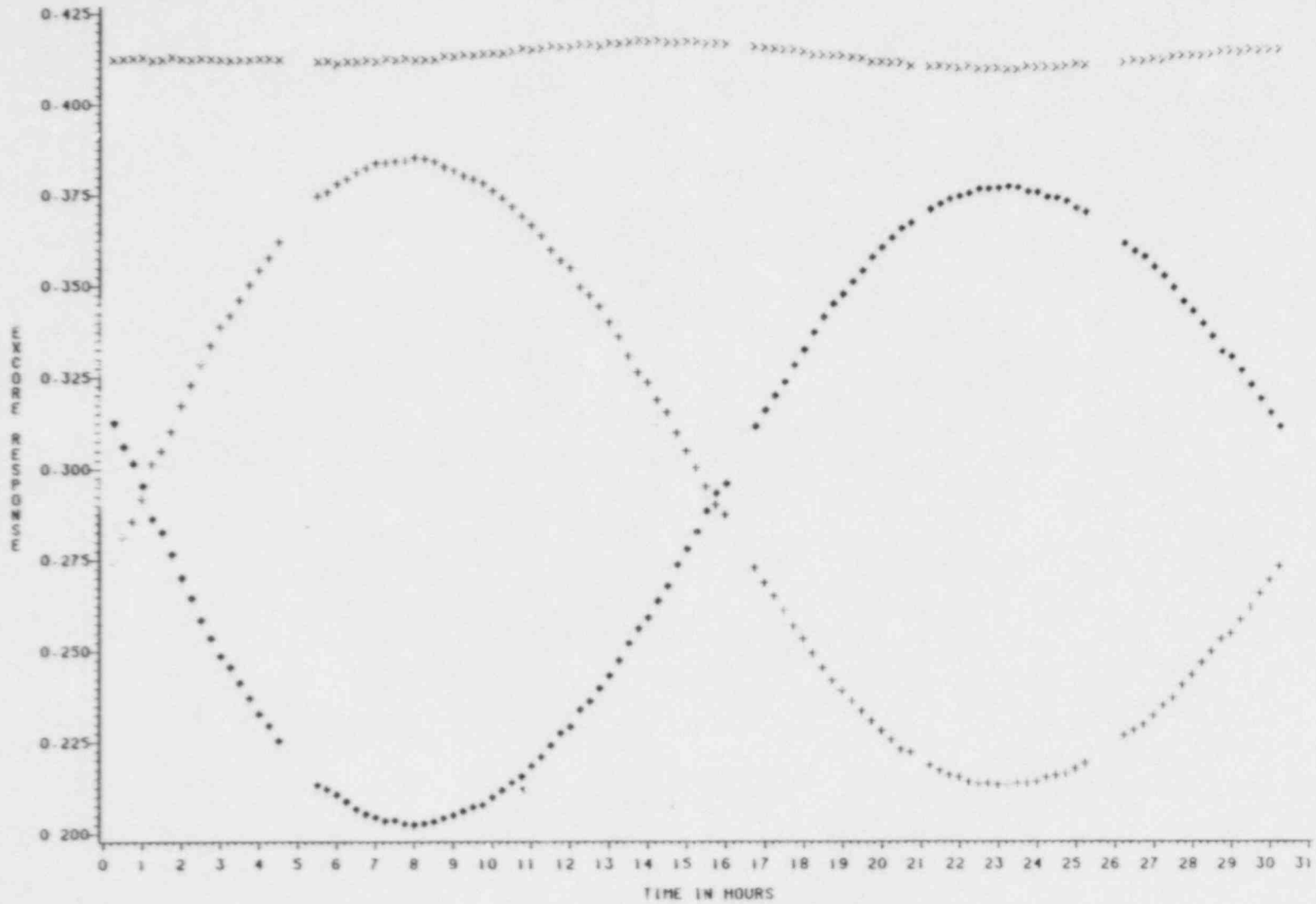


FIGURE 6.3.6.15

W3 CYCLE 1 SHAPE ANNEALING CHANNEL C PERIPHERAL POWERS

• = UPPER
X = MIDDLE
* = LOWER

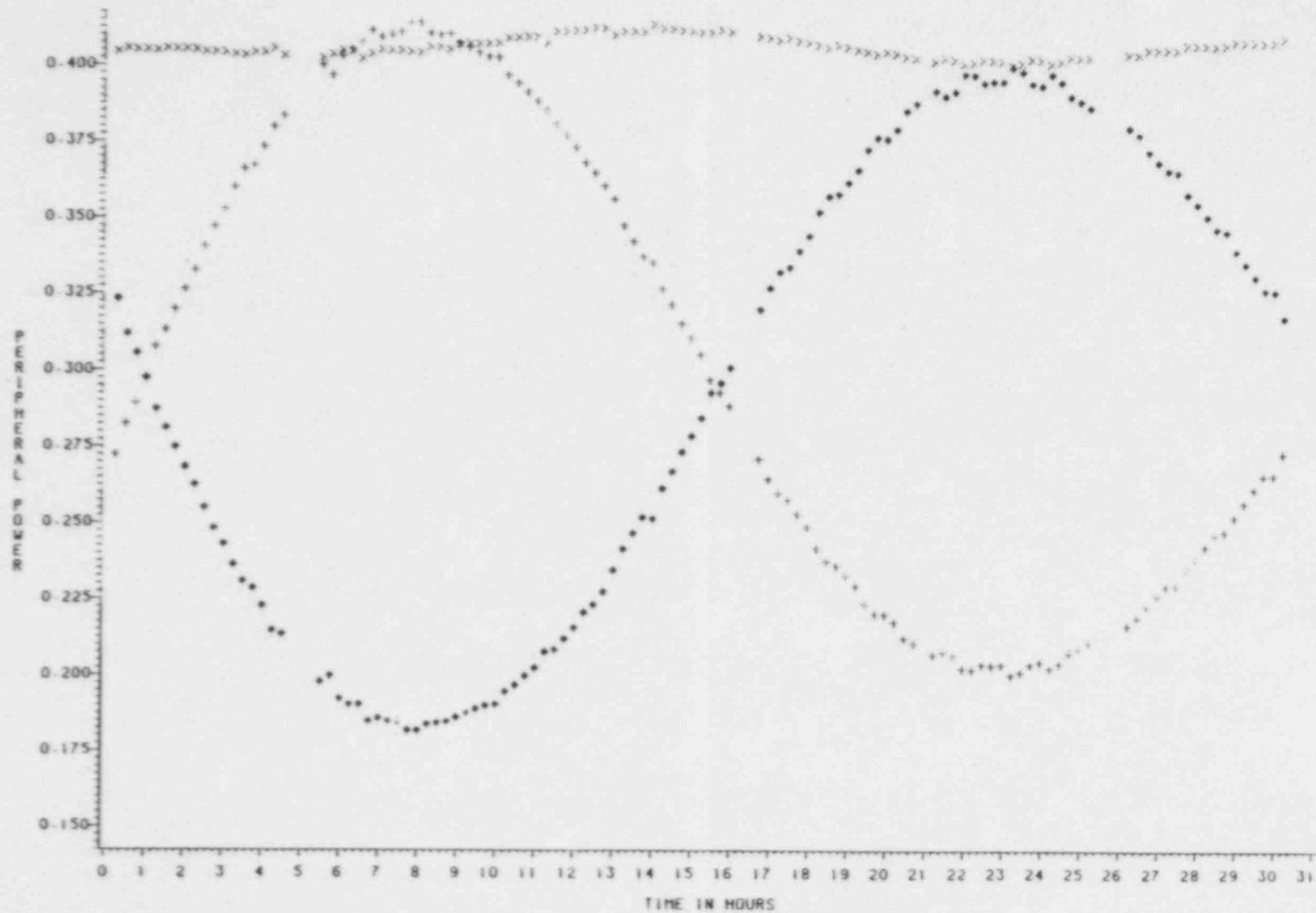


FIGURE 6.3.6.16

W3 CYCLE 1 SHAPE ANNEALING

CHANNEL D EXCORE VALUES

- * = UPPER EXCORE
- X = MIDDLE EXCORE
- = LOWER EXCORE

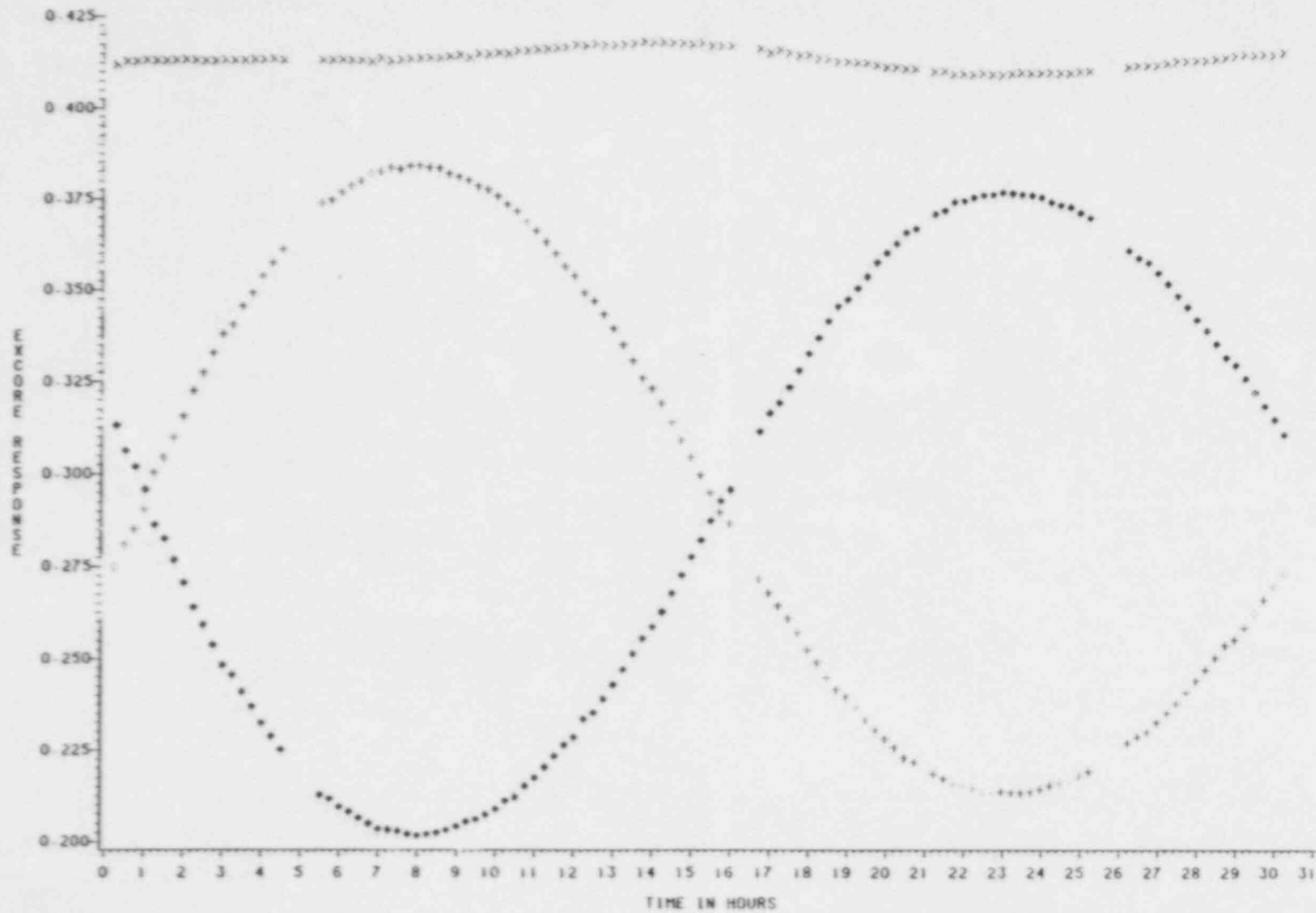
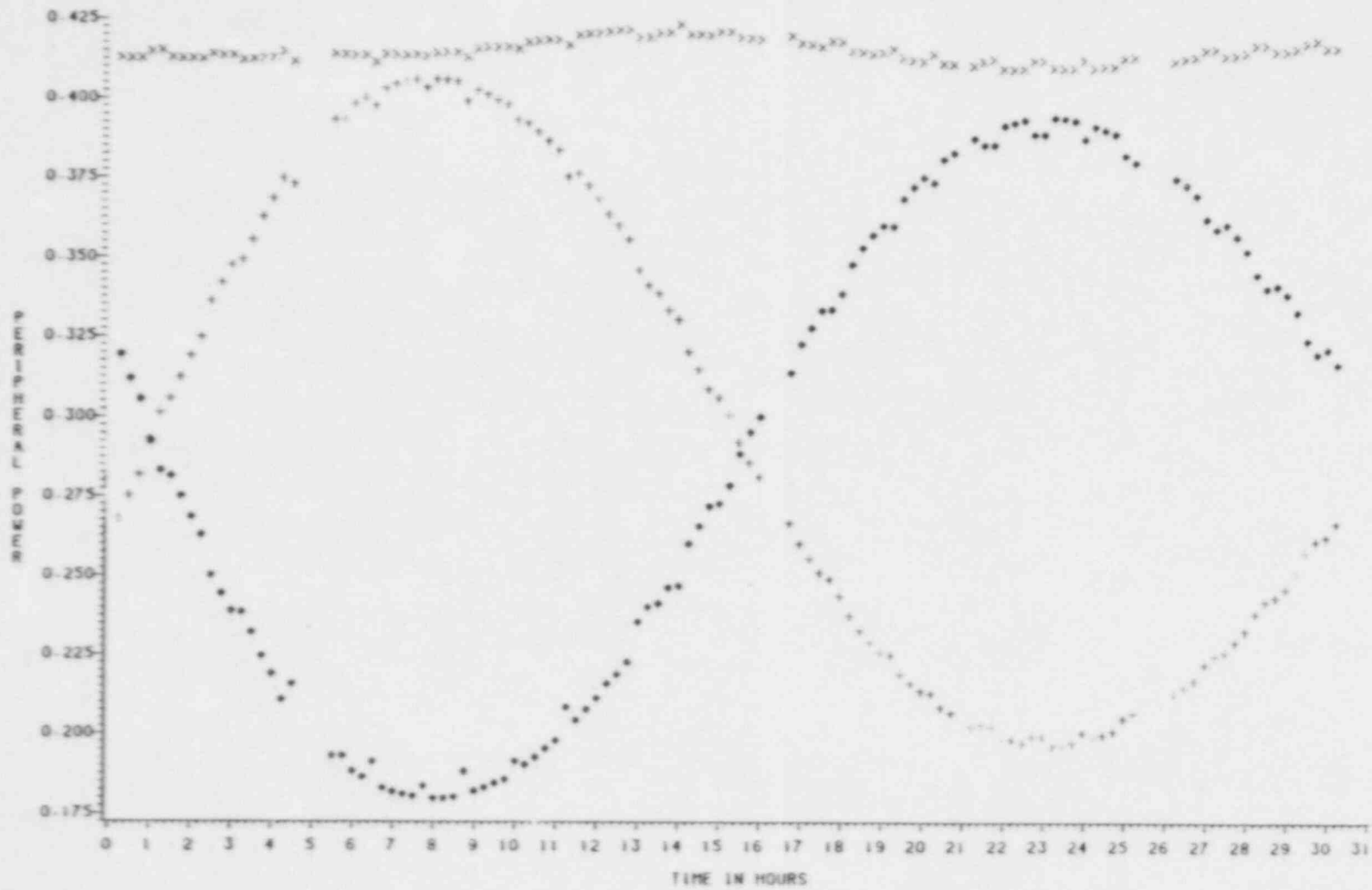


FIGURE 6.3.6.17

W3 CYCLE 1 SHAPE ANNEALING CHANNEL D PERIPHERAL POWERS

• - UPPER
X - MIDDLE
• - LOWER



6.4 PHYSICS TESTING

6.4.1 Core Performance Record (SIT-TP-716)

PURPOSE:

The objectives of the core performance tests were to:

1. Determine if the predicted CPC shape annealing matrix and boundary point power constants provided an acceptable synthesis of the core average axial power distribution until a measurement of these parameters was made at 50% rated thermal power. This screening was performed at the 20% test plateau only.
2. Verify that the core design and construction were as expected by comparing various power distribution parameters to predictions.

Performance of this test satisfied the commitment made in section 14.2.12.3.27 of FSAR chapter 14.

METHOD:

With the reactor at an all-rods-out equilibrium xenon condition, reactor power, RCS temperatures, RCS pressure and pressurizer level were maintained at nominal steady-state values. Axial shape index determined from COLSS was within 0.005 of the predicted equilibrium shape index and had not changed greater than 0.01 in the 4 hours prior to beginning the test.

Core performance data was collected from the incore detector system and stored in a computer data file for later retrieval. Coincident with incore data acquisition, CPC and CEAC data were collected from the plant computer and from the CFC operator modules.

The incore detector data file was next transported to an on-site computer system where it was transmitted to Combustion Engineering's CDC 7600. Under user control, this data was used as input to the CECOR computer code.

The CECOR computer code provided the means to synthesize detailed full-core radial and axial power distributions from the 56 x 5 array of incore detector readings. CECOR used data from 2-D multi-group diffusion theory calculations to convert the detector readings to local box powers. Planar power distributions at each level were then obtained through the use of coupling coefficients that relate the power in instrumented assemblies to the power in uninstrumented neighboring assemblies. The axial power distributions were generated by a Fourier fit to the box powers at each detector level. Subsequently, CECOR determined peak pin powers from pre-calculated pin-to-box factors. This data was formatted and presented to the user as a set of tabular, map and printer-plot edits.

After completing execution of the CECOR code at the CE computer facility, user specified output data was transmitted to the Waterford 3 site and printed. Output data files containing essential power distribution data were also created and stored for later access.

Analysis of the core performance data consisted of comparing measured power distribution parameters (synthesized by CECOR) to predictions or, in the shape annealing matrix screening, to CPC generated information. The data reduction details and associated acceptance criteria are explained below.

At the 20% test plateau, the CECOR synthesized axial power distribution data was used to perform the shape annealing matrix/boundary point power correlation coefficient (SAM/BPPCC) screening test. The 51 node CECOR axial power distribution was collapsed into a 20 node axial power distribution to allow direct comparison to the 20 node CPC axial power distribution. This data was recorded for each CPC channel concurrent with the incore data acquisition. For each CPC channel, a root-mean-square (RMS) value was calculated for the percent difference between the CPC and CECOR nodal powers as follows:

$$\text{RMS} = \sqrt{\frac{\sum_{i=4}^{17} (\text{Error}_i)^2}{14}}$$

where

$$\text{ERROR}_i = \frac{[\text{CPC Power}_i - \text{CECOR Power}_i]}{\text{CECOR Power}_i}$$

Nodes 1-3 and 18-20 were omitted from the calculation due to large boundary point power measurement uncertainty.

If the RMS for each CPC channel was less than 0.05 (i.e. 5%) the SAM/BPPCC test could be deleted from the test program at 20% power. For those channels that failed the RMS screening criteria, an additional screening test would be performed. This test consisted of comparing both the CECOR and CPC axial peaks (i.e., the maximum value of the 20 nodal powers) and the CECOR and CPC ASIs.

This additional comparison was performed as follows:

1. An error between the CECOR and CPC axial peaks was calculated from:

$$\text{Error} = \frac{[\text{CPC Peak} - \text{CECOR Peak}]}{\text{CECOR Peak}} \times 100\%$$

2. An error between the CECOR and CPC ASI was determined from:

$$\text{Error} = \text{CPC ASI} - \text{CECOR ASI}$$

where

$$\text{ASI} = \frac{\sum_{i=1}^{10} P_i^x - \sum_{i=11}^{20} P_i^x}{\sum_{i=1}^{20} P_i^x}$$

and

P_i = Normalized axial power for node i ; $i=1, 20$
 x = CPC Channel A,B,C,D

If the error between the CECOR and CPC axial peaks was:

$$-3.0\% \leq \text{ERROR} \leq 5.0\%$$

AND the error between the CECOR and CPC ASI's was:

$$-0.03 \leq \text{ERROR} \leq 0.02$$

then this additional screening test was satisfied. If all CPC channels in question passed this test, then the SAM/BPPCC test could be deleted from the 20% test plateau. If any CPC channel failed this additional screening test, then the SAM/BPPCC test would have to be performed at 20% power.

At all major test plateaus, the measured radial power distribution values were compared to the predicted values. The root-mean-square (RMS) value was calculated for the difference between the measured and predicted relative power densities of each assembly in the core, such that:

$$\text{RMS} = \sqrt{\frac{\sum_{i=1}^{217} (100 Z_i)^2}{217}}$$

where $Z_i = \text{RPD}_i(\text{measured}) - \text{RPD}_i(\text{predicted})$

If the RMS value was less than or equal to 0.03 (i.e. 3%), the acceptance criterion was satisfied. This criterion applied only to the 50% power and above test plateaus.

Similarly, measured axial power distribution values were compared to the predicted values. The RMS was calculated for the difference between the measured and normalized nodal powers, such that:

$$\text{RMS} = \sqrt{\frac{\sum_{i=1}^{51} (100 h_i)^2}{51}}$$

where $h_i = (\text{Measured Power}_i - \text{Predicted Power}_i)$ and i refers to axial node i .

If the RMS value was less than or equal to 0.03 (i.e. 3%), the acceptance criterion was satisfied. This criterion applied only to the 50% power and above test plateaus.

The measured values for the planar radial peaking factor (F_{xy}) the integrated radial peaking factor (F_r), the core axial peaking factor (F_z), and the total peaking factor (F_q), were compared to their respective predicted values. The percent difference between predicted and measured value was calculated from:

$$\% \text{ Difference} = \frac{[\text{Measured} - \text{Predicted}]}{\text{Predicted}} \times 100\%$$

If the % difference value was within $\pm 7.5\%$, the acceptance criterion was satisfied. This criterion applied only to the 50% power and above test plateaus.

RESULTS:

The core performance test was performed at the 20%, 50%, 80%, and 100% test plateaus without significant problems. The results of each test, categorized by test parameter, are summarized below.

Shape Annealing Matrix Screening at 20%

The RMS values calculated for the CPC vs. CECOR core average nodal powers were 4.87%, 4.79%, 3.88% and 4.91% for channels A, B, C and D, respectively. A graphical comparison of CPC and CECOR power distributions is presented in Figures 6.4.1.1 through 6.4.1.4.

Peaking Factors

The peaking factor results are presented in Tables 6.4.1.1 through 6.4.1.4.

Radial Power Distributions

Core maps presenting the results of the measured vs. predicted relative power density comparison are shown in Figures 6.4.1.5 through 6.4.1.8.

Axial Power Distributions

The results of the axial power distribution comparisons are shown in Figures 6.4.1.9 through 6.4.1.12. At 50% power, the RMS value for measured vs. predicted values was 3.50%. This exceeded the specified acceptance criterion of 3.00%. However, when the measured axial power distribution was compared to the 50% SONGS-2 axial power distribution, an RMS

value of 1.49% was obtained. Since the Waterford 3 axial power distribution compared well with that of SONGS-2, power ascension to and plant operation at 80% was not precluded by failing to satisfy this acceptance criterion.

The RMS values calculated from data obtained at 80% and 100% satisfied the acceptance criterion of $\leq 3.00\%$.

CONCLUSIONS:

The steady-state performance of the Waterford 3 reactor core satisfied all design and manufacturing criteria as determined in this test. With the noted exception, all test acceptance criteria were satisfied.

TABLE 6.4.1.1
20% PEAKING FACTORS

Parameter	Measured Value	Predicted Value	% Difference
Fxy	1.4469	1.3850	4.47
Fr	1.4170	1.3658	3.75
Fz	1.2813	1.2700	0.89
Fq	1.8486	1.7312	6.78

TABLE 6.4.1.2
50% PEAKING FACTORS

Parameter	Measured Value	Predicted Value	% Difference
Fxy	1.3896	1.3568	2.42
Fr	1.3632	1.3262	2.79
Fz	1.2720	1.2470	2.00
Fq	1.7596	1.6430	7.10

TABLE 6.4.1.3
80% PEAKING FACTORS

Parameter	Measured Value	Predicted Value	% Difference
Fxy	1.4223	1.3974	1.78
Fr	1.3925	1.3788	0.99
Fz	1.3050	1.2680	2.92
Fq	1.8411	1.7414	5.73

TABLE 6.4.1.4
100% PEAKING FACTORS

Parameter	Measured Value	Predicted Value	% Difference
Fxy	1.4278	1.4264	0.10
Fr	1.4010	1.4121	-0.79
Fz	1.3079	1.2910	1.31
Fq	1.8634	1.8138	2.73

FIGURE 6.4.1.1

WATERFORD-3 SES

20% AXIAL POWER COMPARISON

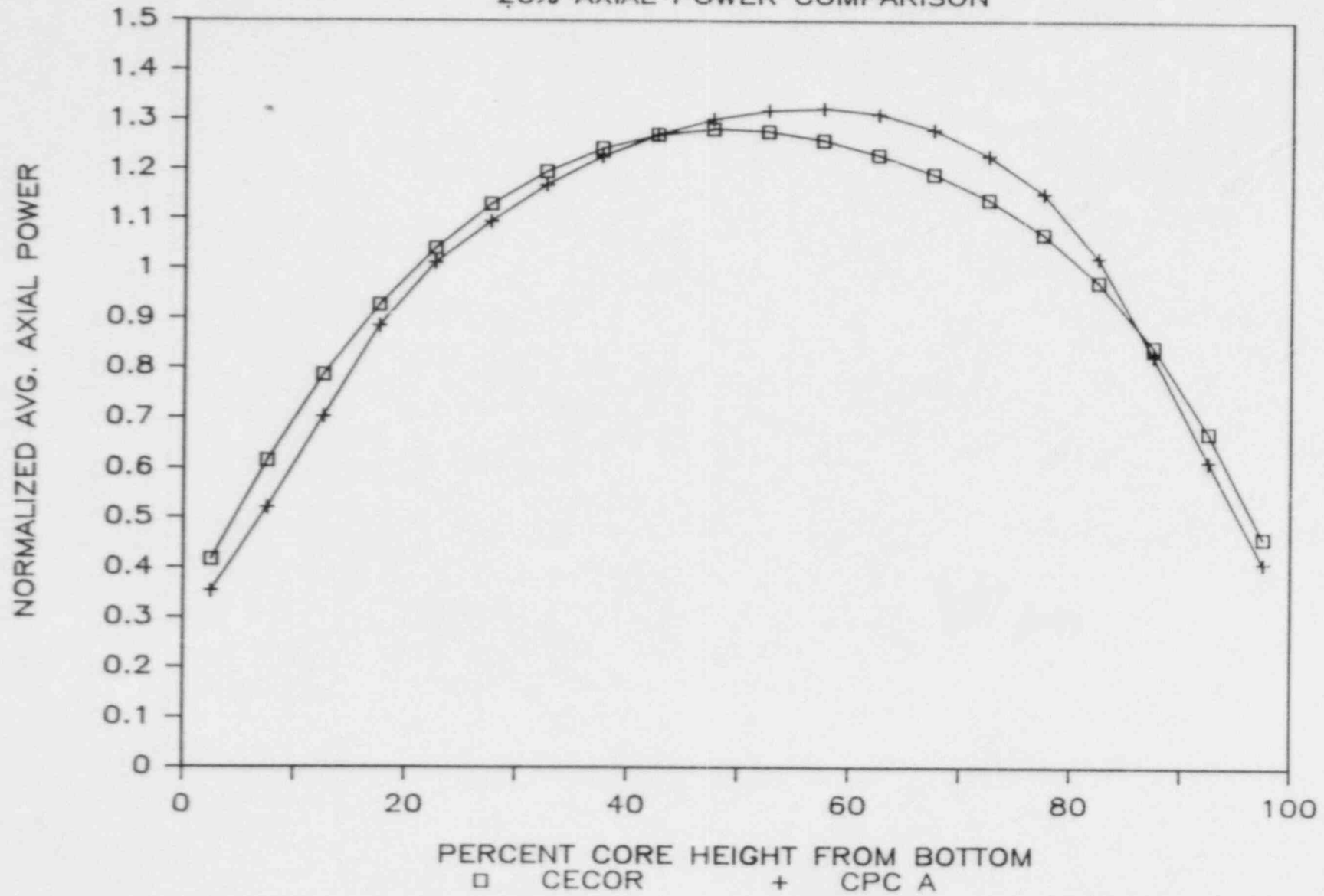


FIGURE 6.4.1.2

WATERFORD-3 SES

20% AXIAL POWER COMPARISON

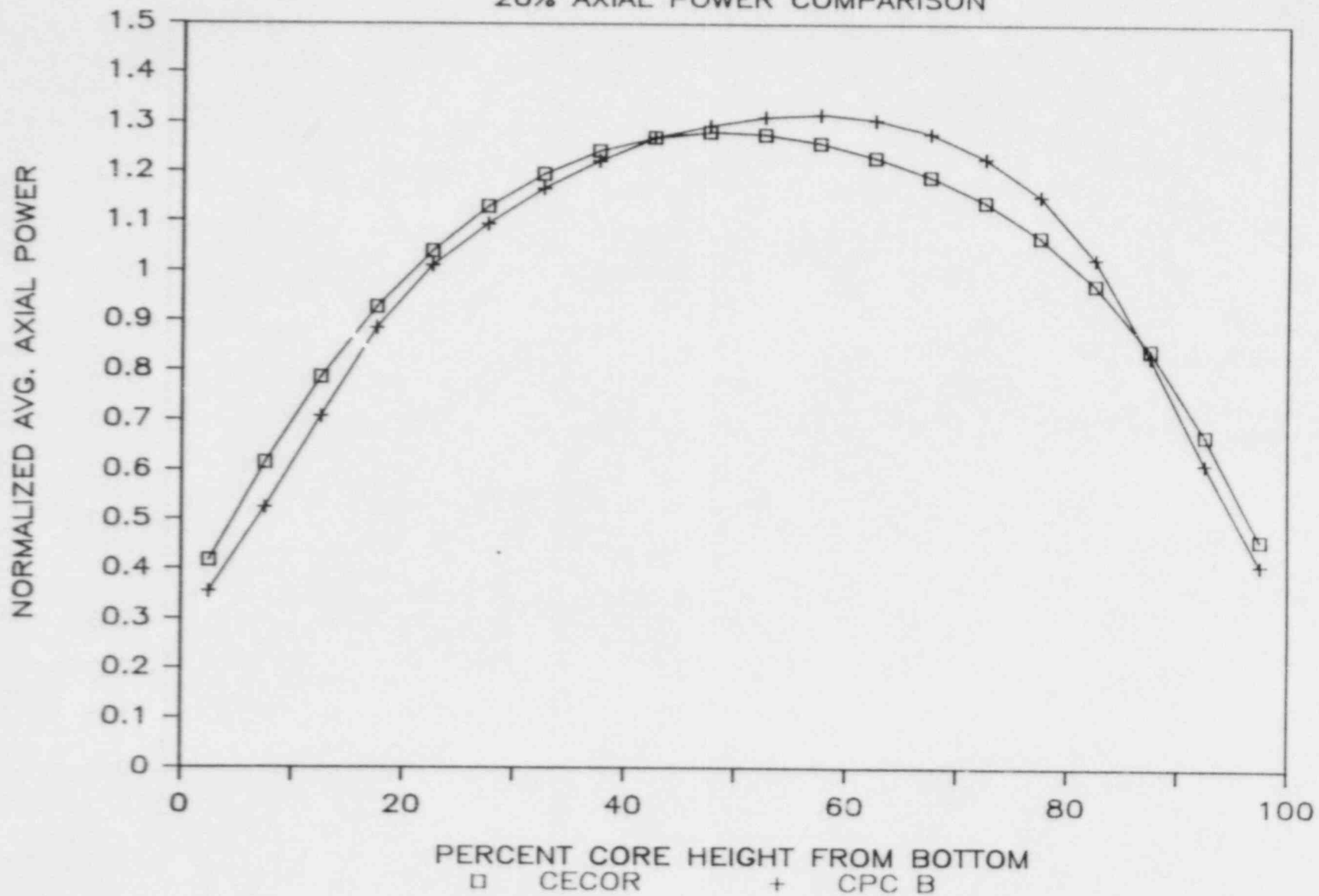


FIGURE 6.4.1.3

WATERFORD-3 SES

20% AXIAL POWER COMPARISON

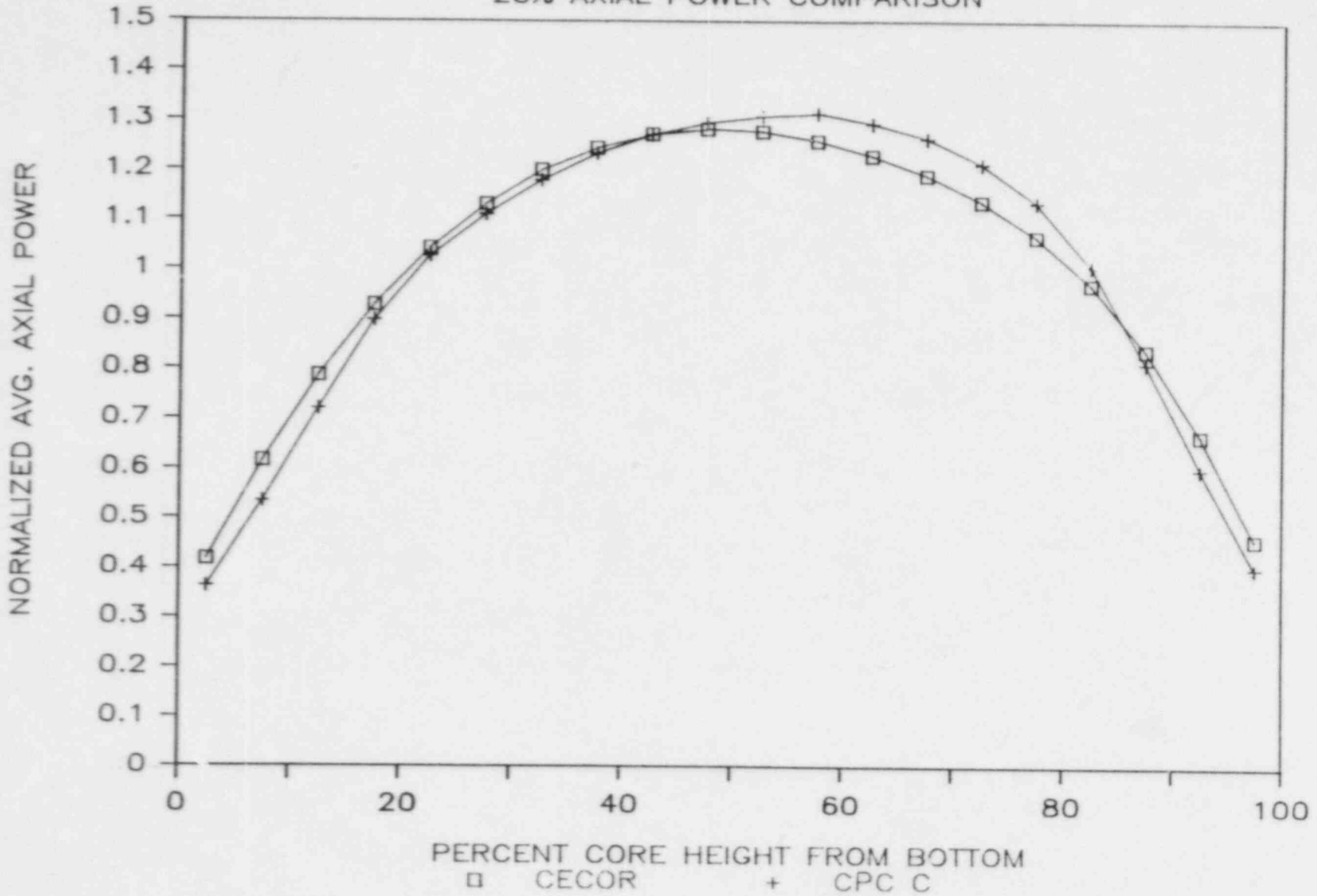


FIGURE 6.4.1.4

WATERFORD-3 SES

20% AXIAL POWER COMPARISON

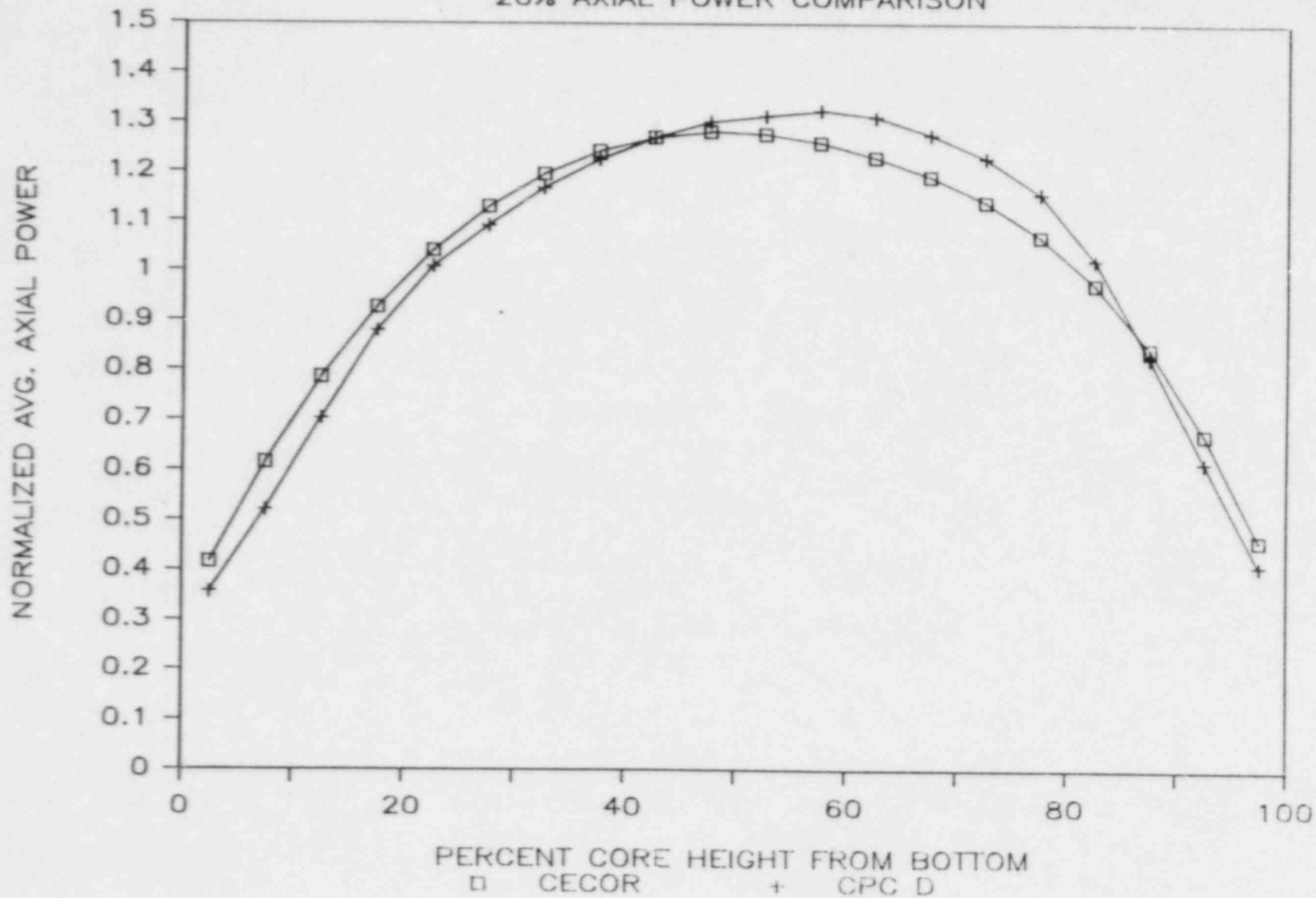
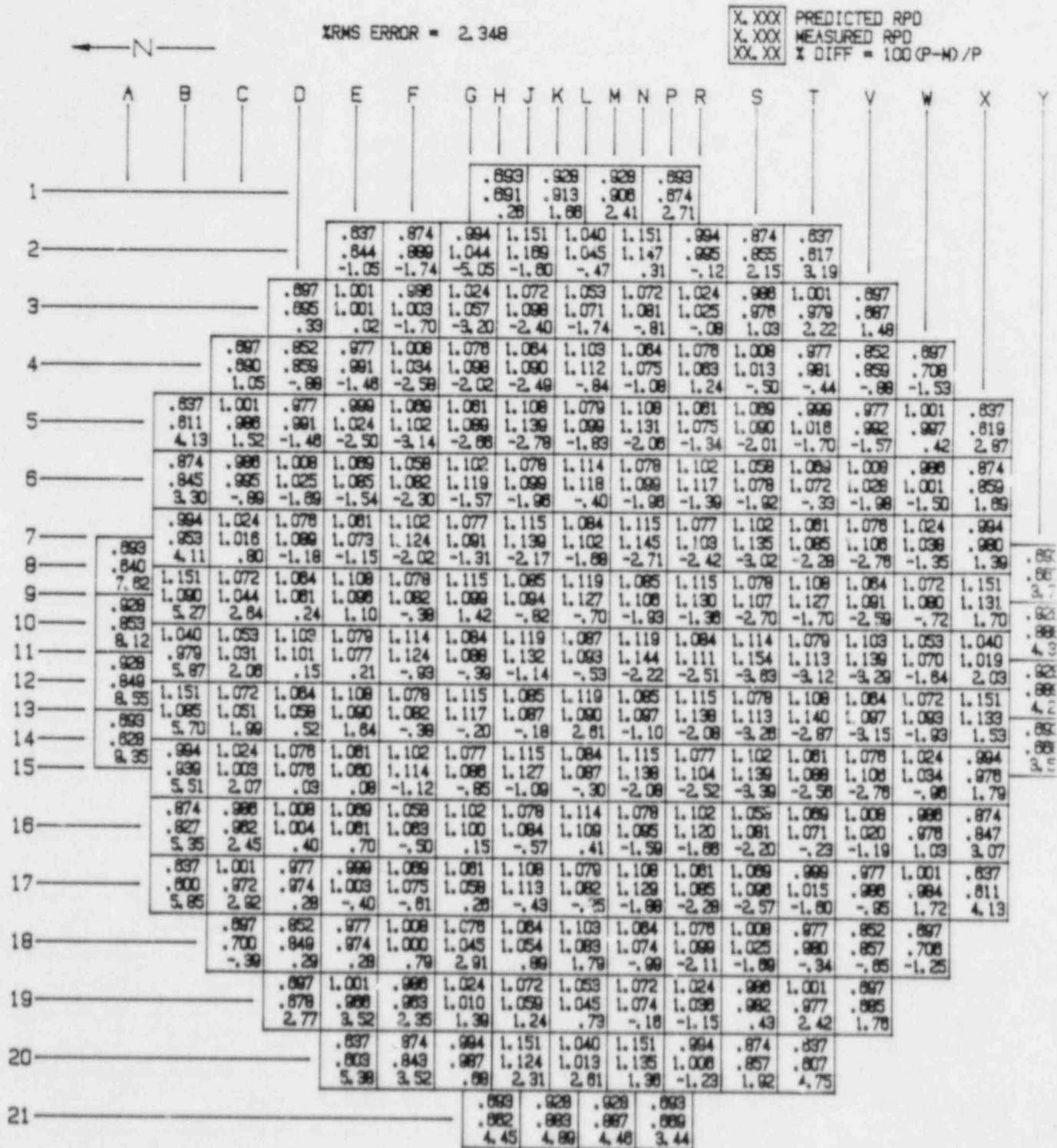


FIGURE 6.4.1.5

WATERFORD-3
 RADIAL POWER DISTRIBUTION COMPARISON
 20% RATED THERMAL POWER
 CECOR SNAPSHOT R4857ZF - 4/17/85



S/G #1

FIGURE 6.4.1.6
WATERFORD-3
 RADIAL POWER DISTRIBUTION COMPARISON
 50% RATED THERMAL POWER
 CECOR SNAPSHOT R4861GT - 4/21/85

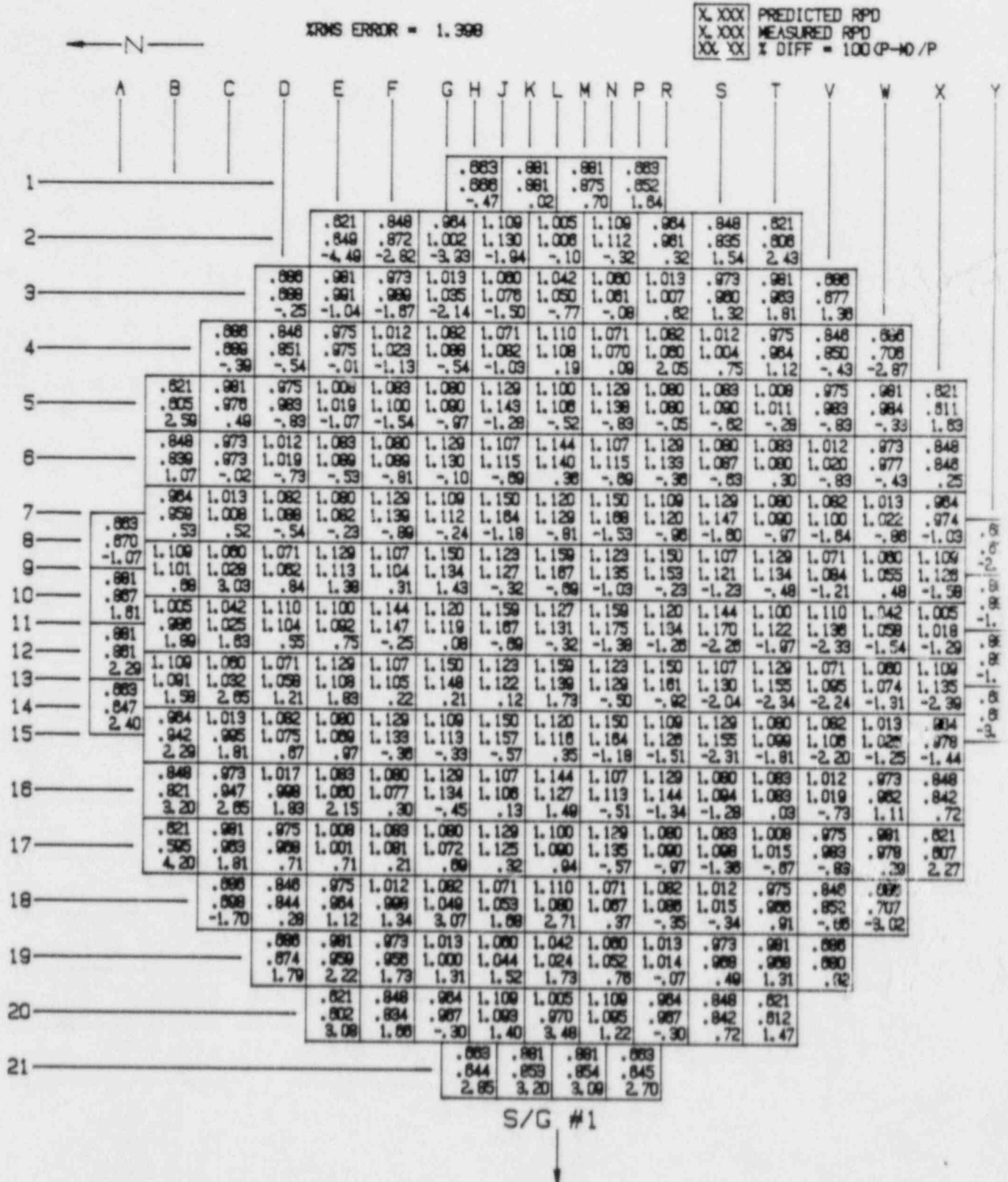


FIGURE 6.4.1.7
WATERFORD-3
 RADIAL POWER DISTRIBUTION COMPARISON
 80% RATED THERMAL POWER
 CECOR SNAPSHOT R4897MK - 5/27/85

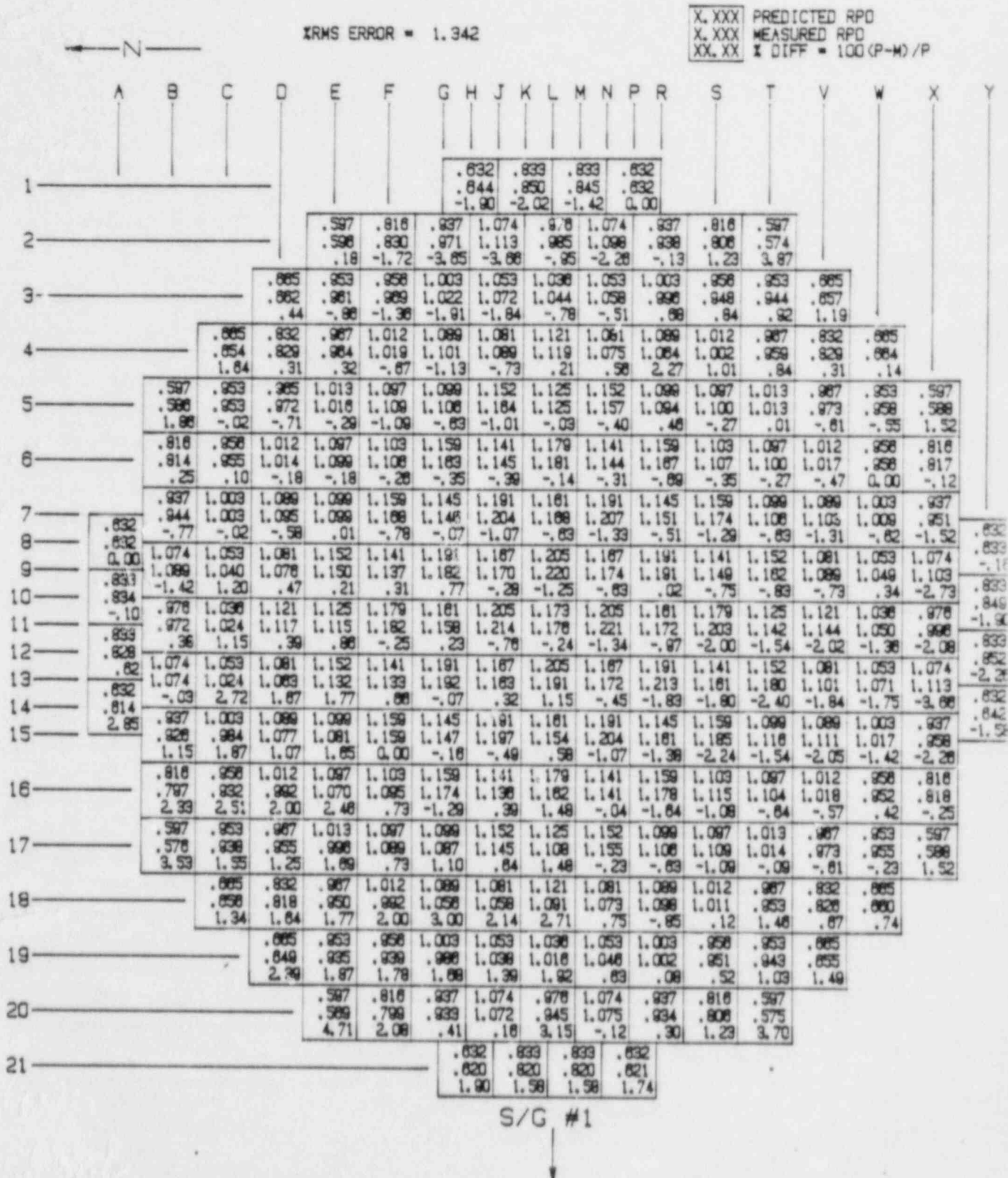


FIGURE 6.4.1.8
WATERFORD-3
 RADIAL POWER DISTRIBUTION COMPARISON
 100% RATED THERMAL POWER
 CECOR SNAPSHOT R4941L8 - 7/10/85

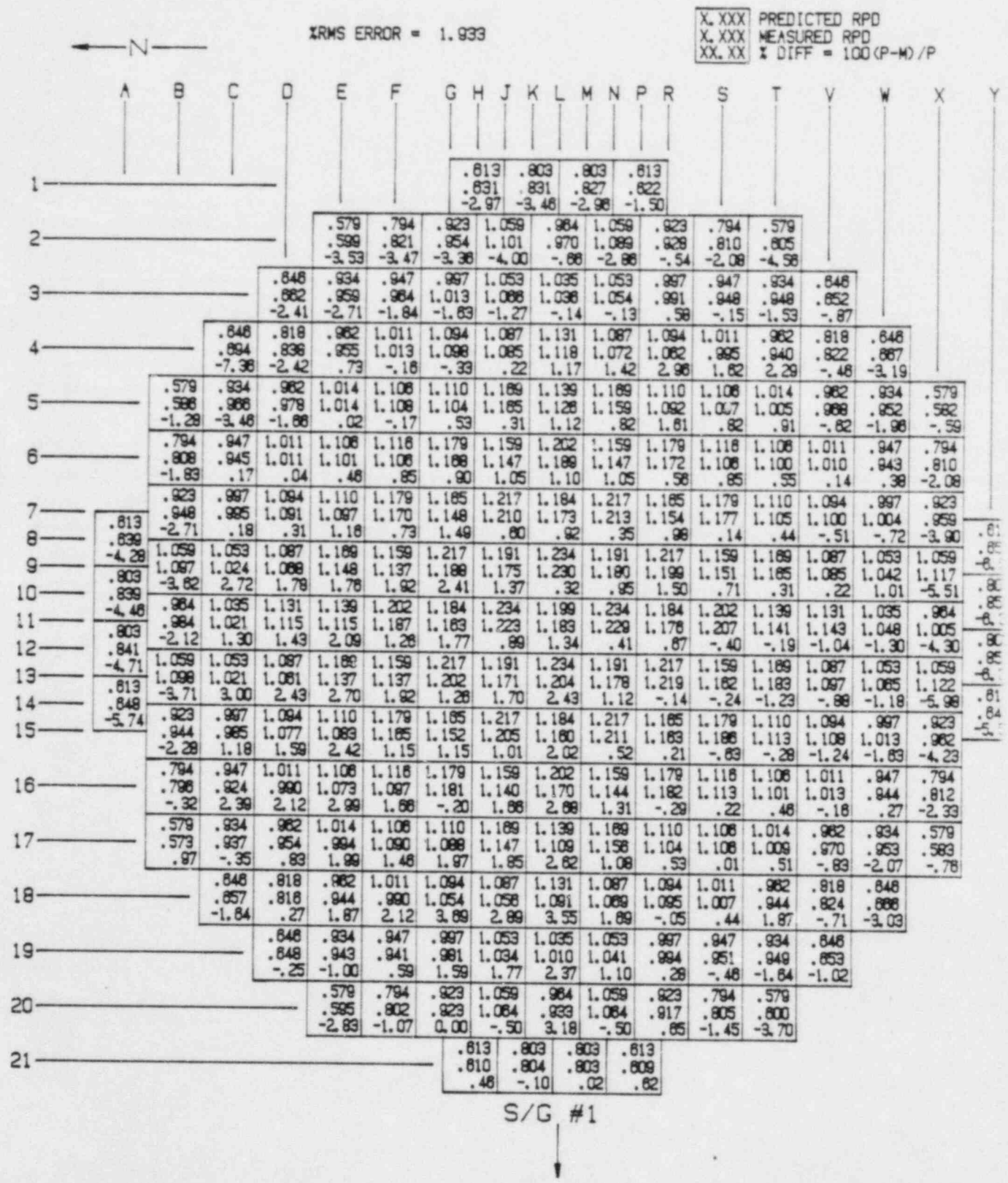


FIGURE 6.4.1.9

WATERFORD-3 SES
AXIAL POWER DISTRIBUTION COMPARISON
20% RATED THERMAL POWER
CECOR SNAPSHOT R4857ZF - 4/17/85

PREDICTED ESI = .0189
MEASURED ESI = -.0108
RMS ERROR = 3.515

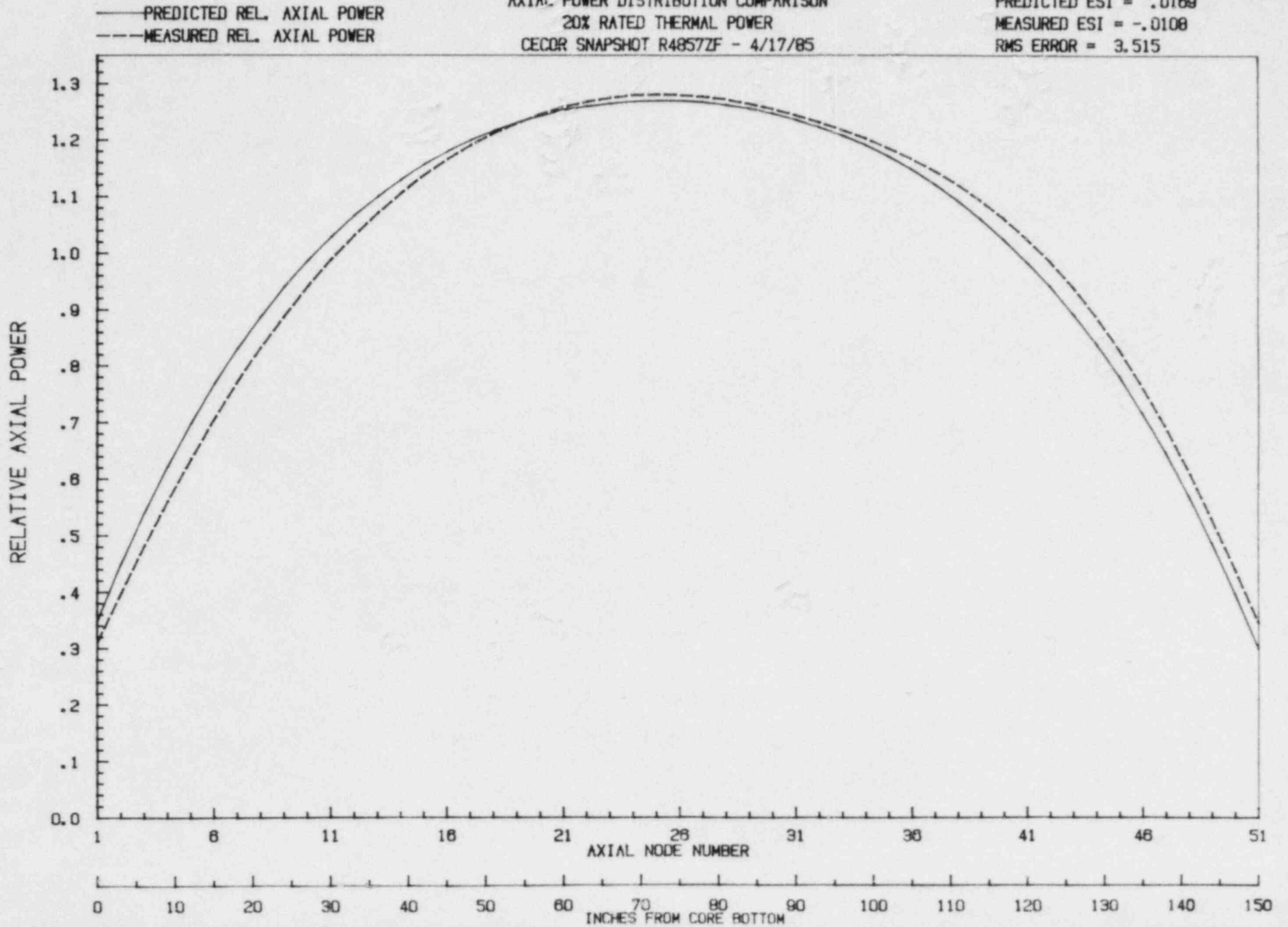


FIGURE 6.4.1.10

WATERFORD-3 SES

AXIAL POWER DISTRIBUTION COMPARISON

50% RATED THERMAL POWER

CECOR SNAPSHOT R4861GT - 4/21/85

PREDICTED ESTI = .0400

MEASURED ESTI = .0165

RMS ERROR = 3.500

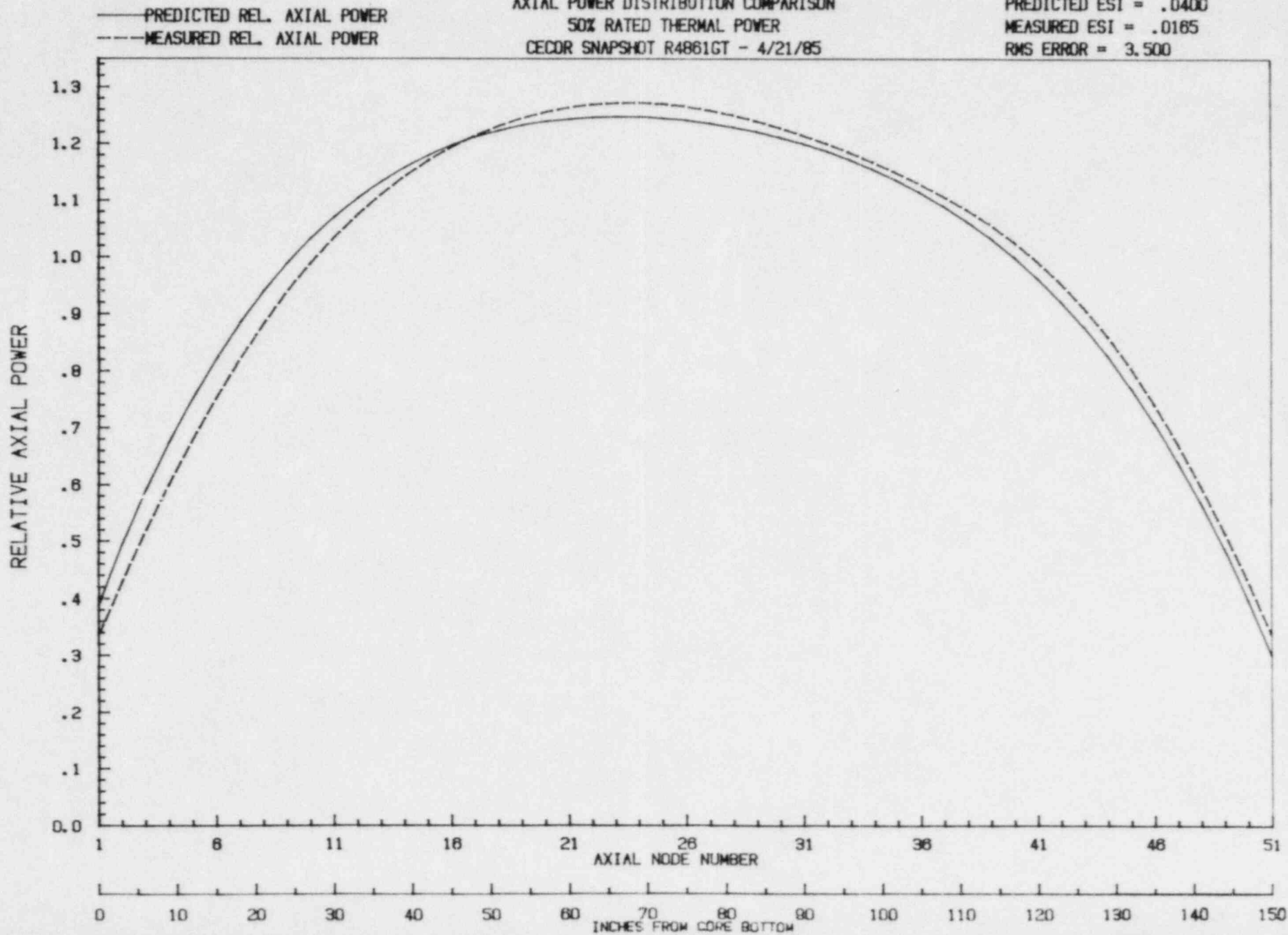


FIGURE 6.4.1.11

WATERFORD-3 SES
AXIAL POWER DISTRIBUTION COMPARISON
80% RATED THERMAL POWER
CECOR SNAPSHOT R4897MK - 5/27/85

PREDICTED ESTI = .0595
MEASURED ESTI = .0480
RMS ERROR = 2.837

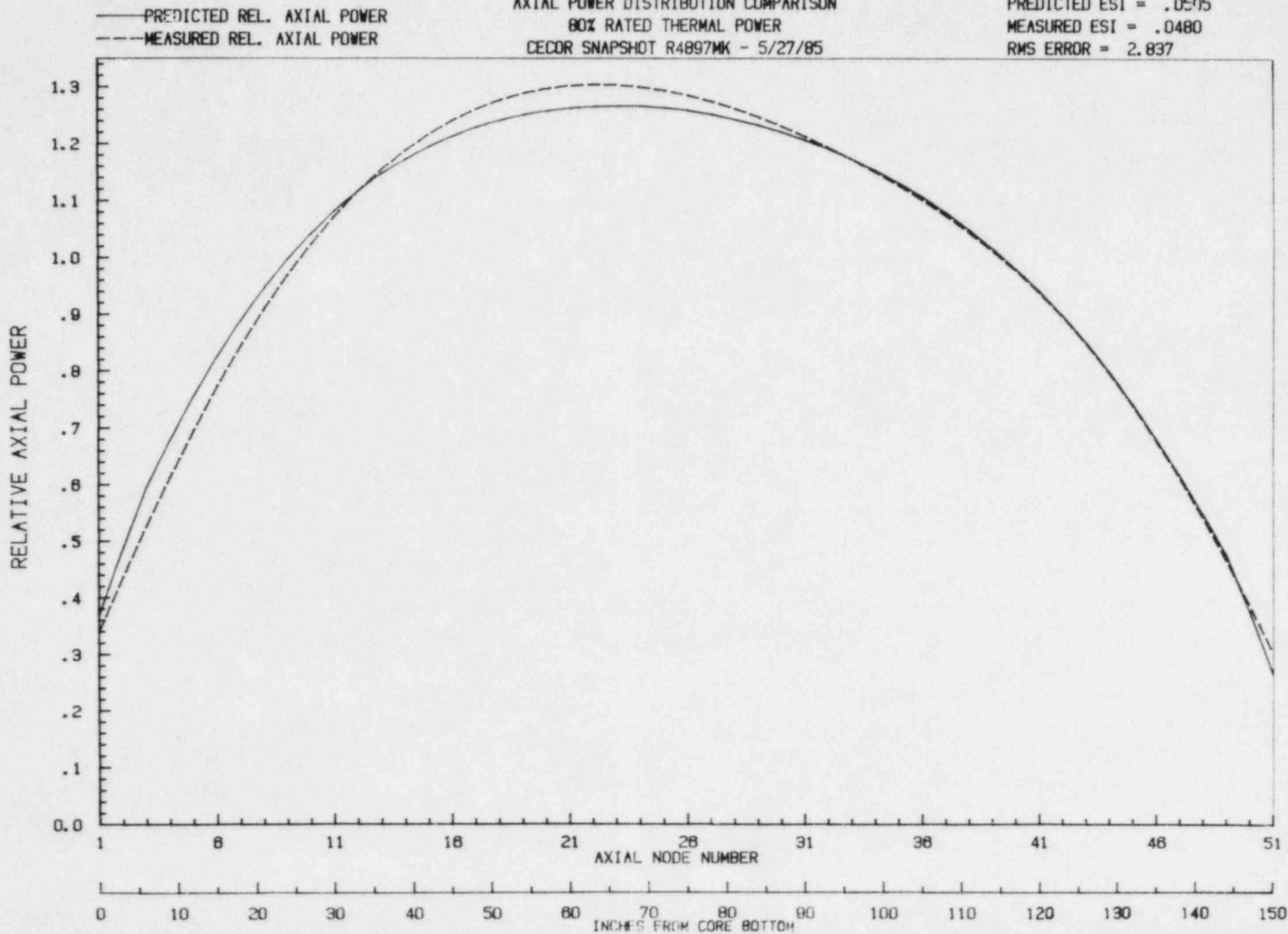
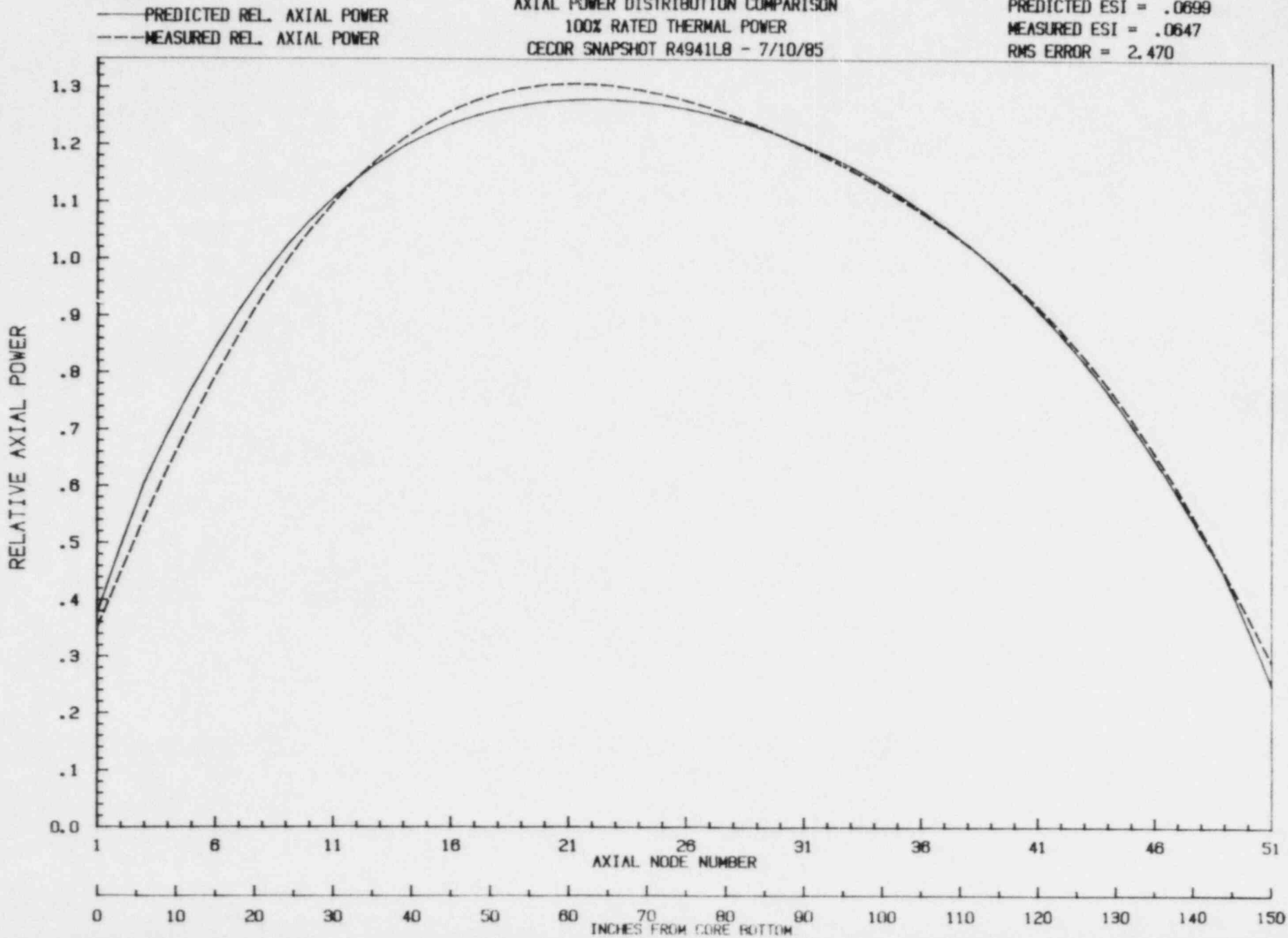


FIGURE 6.4.1.12

WATERFORD-3 SES
AXIAL POWER DISTRIBUTION COMPARISON
100% RATED THERMAL POWER
CECOR SNAPSHOT R4941L8 - 7/10/85

PREDICTED ESI = .0699
MEASURED ESI = .0647
RMS ERROR = 2.470



6.4.2 Variable Tavg Test (SIT-TP-718)

PURPOSE:

The variable Tavg test was performed to measure the isothermal temperature coefficient (ITC), moderator temperature coefficient (MTC) and power coefficient (PC). The measured MTC was subsequently verified to be within Technical Specification limits. The measured ITC and PC were confirmed to agree with corresponding predictions within specified tolerances derived from experimental and prediction error.

This test satisfied the commitments of FSAR section 14.2.12.3.26.

METHOD:

The ITC was determined by tests based upon two different methods. One method assumed the power coefficient was known from prediction and did not require CEA movement. The second method assumed that the CEA group 6 integral reactivity worth was known from prediction and required CEA movement. Similarly, the PC measurement was performed with CEA movement assuming that the CEA group 6 integral reactivity worth was known from prediction. These tests are described in more detail below.

ITC/MTC Measurement Without CEA Movement

Steady-state initial conditions were established with the reactor at the test power level, equilibrium xenon and CEA group 6 approximately 120" withdrawn. The RCS, pressurizer and VCT boron concentrations were initially within 10 ppm of their mean boron concentration to minimize undesired reactivity changes resulting from a mismatch in concentrations.

Reactor coolant cold leg temperature was increased approximately 4°F by rapidly decreasing turbine load. The negative reactivity addition from increased moderator and fuel temperature was counterbalanced by a positive reactivity addition resulting from a decrease in reactor power. Stable reactor conditions were established at the new power and temperature by making small adjustments to turbine load. Data was obtained while maintaining the reactor at steady-state. Upon completion of data collection, reactor coolant cold leg temperature was decreased approximately 8°F by rapidly increasing turbine load. This temperature decrease caused reactor power to increase until the secondary power demand was satisfied. Steady-state reactor conditions were maintained until data was collected. Next, cold leg temperature was increased approximately 8°F with power decreasing until the reactivity addition from the temperature change equalled that from the power change. This cycle was repeated three additional times while test data was collected at each steady-state power/temperature plateau. Plant conditions were finally returned to those existing prior to the initial temperature change. Figure 6.4.2.1 presents a graphic depiction of the test sequence.

Determining the ITC from test data was an iterative process. ΔT_{avg} and $\Delta power$ were calculated for successive cycle beginning and end points. Assuming a power and temperature coefficient, the magnitude of the unknown reactivity contribution (due to changing Xe and Sm concentration) for each half cycle was calculated. These values were used with the predicted power coefficient to determine the ITC for each half cycle. The resulting ITCs were averaged and used with the predicted PC to compute a new value for the unknown reactivity contribution in each half cycle. This value of the unknown contribution was in turn used to compute a new value of the ITC. The calculation sequence was iterated until the ITC converged to within $0.005 \times 10^{-4} \Delta k/k/^{\circ}F$ of the preceding value.

ITC/MTC Measurement With CEA Movement

Steady-state initial conditions were established with the reactor at the test power level, equilibrium xenon and CEA group 6 approximately 120" withdrawn. Turbine load was rapidly decreased to obtain an approximately 4°F increase in reactor coolant cold leg temperature. The reactivity feedback from increasing reactor coolant average temperature was matched by withdrawal of CEA group 6, thus maintaining reactor power constant. Upon stabilizing reactor coolant temperature and power, data was collected and the procedure reversed to decrease reactor coolant cold leg temperature approximately 8°F. After collecting data at the low temperature plateau, turbine load was decreased to obtain an approximately 8°F increase in cold leg temperature while maintaining constant reactor power with CEA withdrawal. The entire procedure was repeated 3 additional times prior to returning the reactor to those conditions that existed prior to the start of the test.

Determining the ITC from test data with CEA movement was similar to the method previously described. However, both temperature and power cycles (described in the next section) were combined and analyzed to determine the ITC.

Power Coefficient

Steady-state initial conditions were established with the reactor at the test power level, equilibrium xenon and CEA group 6 approximately 120" withdrawn. Reactor power was increased approximately 2% by withdrawing CEA group 6. The negative reactivity feedback from increasing power was matched by increasing turbine load to maintain reactor coolant average temperature constant. Upon stabilizing power and temperature, data was collected and the procedure reversed to decrease reactor power approximately 4%. After collecting data at the lower power plateau, CEA group 6 was withdrawn to increase reactor power approximately 4% while maintaining average coolant temperature constant with turbine load adjustments. The 4% power change cycle was repeated 3 times prior to returning the plant to those conditions that existed at the start of the test.

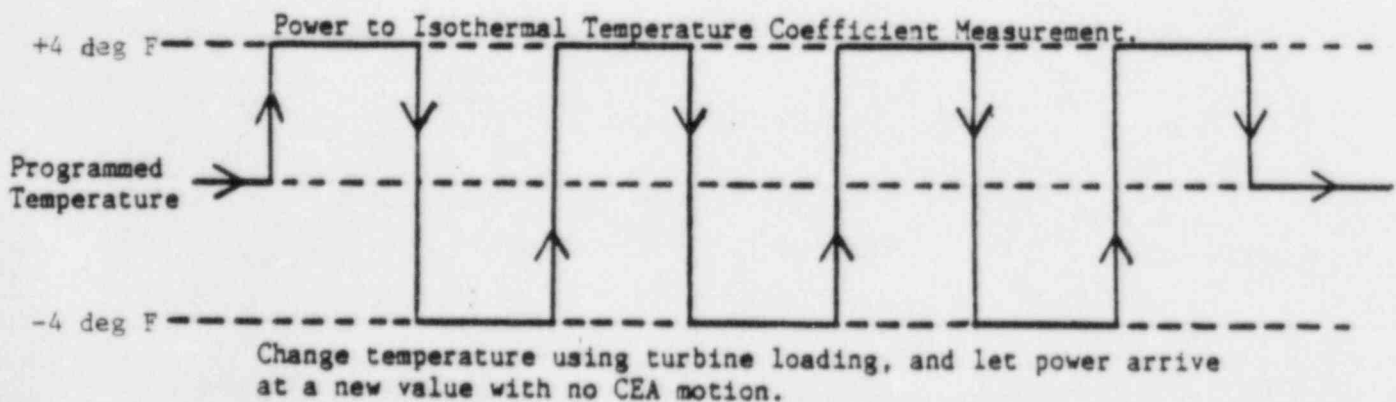
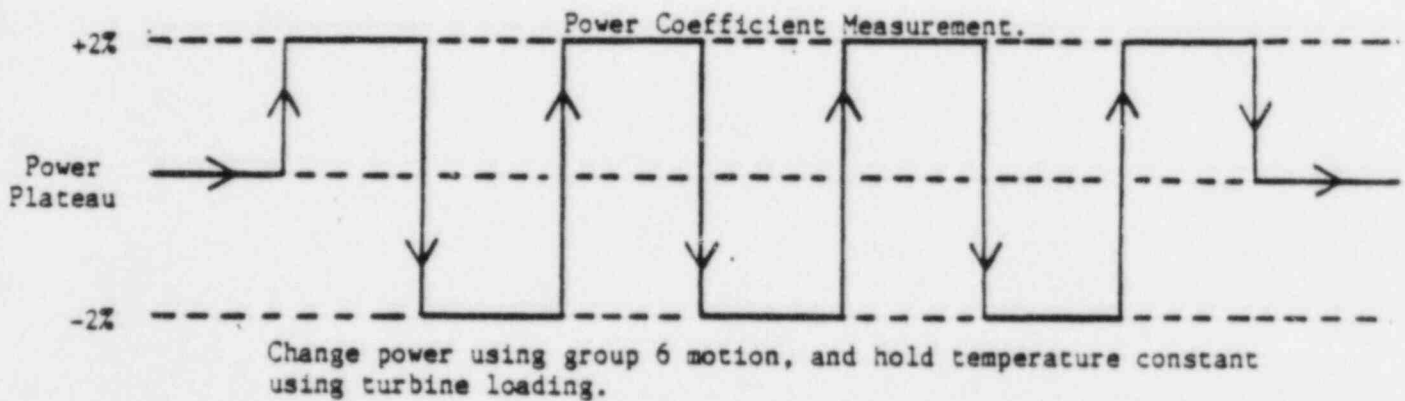
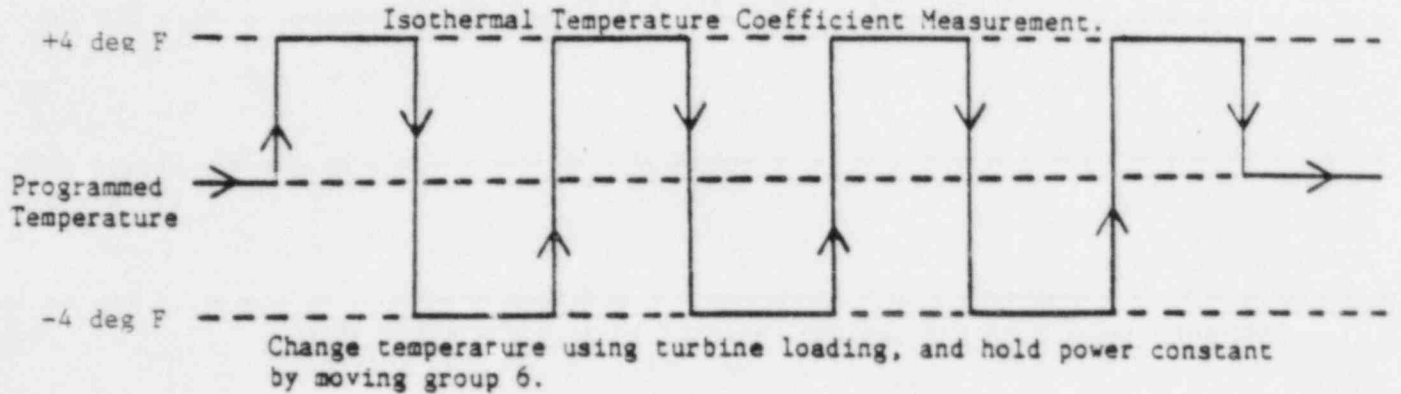
Figure 6.4.2.1 schematically shows the test sequence described above.

RESULTS:

50% Test Plateau

The ITC measurement without CEA movement commenced on April 28, 1985 at 1105 and was completed at 2025 on the same day. No unusual difficulties were encountered while performing this portion of the test.

FIGURE 6.4.2.1
VARIABLE T_{avg} TEST SEQUENCE



The ITC and PC measurements with CEA movement were started at 0330 on April 29, 1985 and were completed at 1330 on April 30, 1985. A total of 34 hours were required to complete these measurements.

While performing the temperature coefficient measurement, the plant computer failed twice. This necessitated that testing be halted until the failure was corrected and the PMC returned to normal operating status. As a result of these delays, the unknown reactivity component calculated from test data was larger than desired. Nonetheless, the resulting ITC data exhibited small variability for all temperature cycles and was acceptable.

The power coefficient measurement started at 1620 on April 29, 1985. During the subsequent power increases for the first two cycles, progressively higher CEA withdrawal was required to return the same power and temperature. Consequently, the test was stopped and initial conditions reestablished. The test was restarted at 0730 on April 30 and completed without further interruption. As with the temperature coefficient measurement, the unknown reactivity component contributing to the reactivity balance was greater than desired but the variability in individual cycle PC's was small. The data was thus acceptable.

The test results are given in Table 6.4.2.1.

100% Test Plateau

The entire variable Tavg test was performed on July 11 & 12, 1985 without significant difficulty. A delay of approximately 7 hours occurred between the end of the no-CEA-movement test and the start of the ITC measurement with CEA movement. This

time was utilized to reestablish initial conditions for the remainder of the test. Including the delay, the test was completed in just under 19 hours with acceptable results. These results are presented in Table 6.4.2.2.

CONCLUSION:

The variable T_{avg} test was successfully completed at both the 50% and 100% test plateaus with acceptable results. Based upon these results, the following conclusions were derived:

1. The MTC is less positive than $0.2 \times 10^{-4} \Delta k/k/^\circ F$ whenever thermal power is less than or equal to 70%.
2. The MTC is less positive than $0.0 \times 10^{-4} \Delta k/k/^\circ F$ whenever thermal power is greater than 70%.
3. The MTC is less negative than $-2.5 \times 10^{-4} \Delta k/k/^\circ F$ at rated thermal power.
4. The predicted ITC agreed with the measured ITC within $\pm 0.3 \times 10^{-4} \Delta k/k/^\circ F$.
5. The predicted PC agreed with the measured PC within $\pm 0.2 \times 10^{-4} \Delta k/k/\%$.

TABLE 6.4.2.1

50% VARIABLE Tavg TEST RESULTS

Parameter	Value*	Acceptance Criteria*
Measured MTC Without CEA Movement	-0.61	None
Measured MTC With CEA Movement	-0.58	Greater than -2.50
Measured ITC Without CEA Movement	-0.75	None
Measured ITC With CEA Movement	-0.72	Measured Value = -0.84 ± 0.30
Measured PC	-1.20	Measured Value = -1.02 ± 0.20
MTC Extrapolated to 70% Rated Thermal Power**	-0.68	Less than 0.20
MTC Extrapolated to 100% Rated Thermal Power**	-0.83	Less than 0.00

* All temperature coefficients reported in units of $1E-4\Delta k/k/^{\circ}F$
 All power coefficients reported in units of $1E-4\Delta k/k/\%$

** Extrapolated values based upon MTC measurement with CEA movement

TABLE 6.4.2.2

95% VARIABLE Tavg TEST RESULTS

Parameter	Value*	Acceptance Criteria*
Measured MTC Without CEA Movement	-0.79	None
Measured MTC With CEA Movement	-0.79	None
Measured ITC Without CEA Movement	-0.92	None
Measured ITC With CEA Movement	-0.92	Measured Value = -1.00 ± 0.30
Measured PC	-0.88	Measured Value = -0.88 ± 0.20
MTC Extrapolated to 100% Rated Thermal Power**	-0.81	Less than 0.00

* All temperature coefficients reported in units of $1E-4\Delta k/k/^{\circ}F$
 All power coefficients reported in units of $1E-4\Delta k/k/\%$

** Extrapolated values based upon MTC measurement with CEA movement

6.5 REACTOR COOLANT SYSTEM TESTING

6.5.1 RCS Calorimetric Flow Measurement (SIT-TP-710)

PURPOSE:

The primary purpose of this test was the determination of an accurate value of the reactor coolant system (RCS) flowrate; this measured flowrate was then used as the standard to which the COLSS and CPC calculated RCS flowrates were conservatively calibrated.

A second purpose of this test was to recalibrate the COLSS and CPC thermal powers (BDELT and BDT respectively) to secondary calorimetric power (BSCAL) following adjustment of their respective flowrates. (If no flowrate adjustments were performed, thermal power recalibration was not necessary.)

Finally, the test gathered data for use in the evaluation of the adequacy of the installed thermal power adjustment coefficients.

This test partially satisfied the commitments of FSAR section 14.2.12.3.2.

METHOD:

The performance of this test at a given plateau is illustrated by the flowchart of Figure 6.5.1.1.

DATA SET 1
 Cold leg temperatures
 Hot leg temperatures
 Pressurizer pressures
 Secondary Cal. Power
 COLSS RCS flowrates
 CPC RCS flowrates

DATA SET 2
 COLSS RCS flowrates
 CPC RCS flowrates

DATA SET 3
 Secondary Cal. Power
 CPC thermal powers
 (BDT's)

DATA SET 4
 Secondary Cal. Power
 COLSS thermal power
 (BDELT)

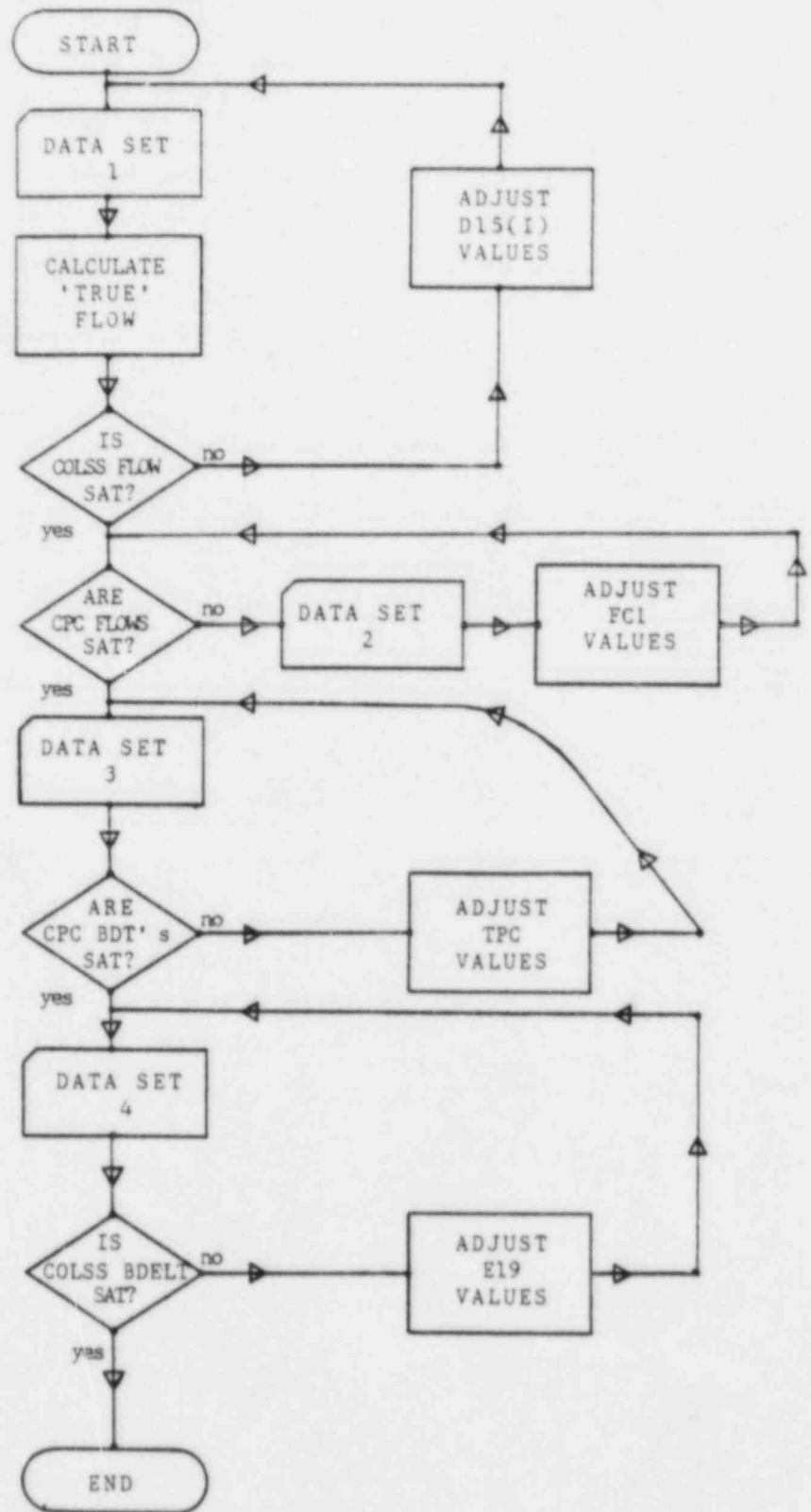


FIGURE 6.5.1.1: ADJUSTMENT FLOWCHART

The 'true' flowrate was calculated by dividing the measured enthalpy (derived from the average cold leg temperature, the average hot leg temperature, and the average pressurizer pressure of Data Set 1) into the average value of secondary calorimetric power. Comparison of the average COLSS-calculated flowrate to this value was then performed. If the COLSS flowrate was between 99.8% and 100.0% of the 'true' flowrate, it was considered satisfactory. If it was not within these bounds, adjustments were made to the D15(I) values to bring it within the specified limits.

Once the COLSS flowrate had been satisfactorily calibrated to the measured flowrate, the CPC flowrate was compared to the COLSS flowrate. Acceptability was determined by verifying that the CPC flowrate was between 99.5% and 100.0% of the average COLSS flowrate. If this was not the case, the value of FCI for each CPC channel not meeting the criteria was adjusted. (Adjustments to FCI were optional if the CPC flow was less than 99.5% of the average COLSS flow, but recommended to avoid excess conservatism from reducing the available thermal margin.) Since the COLSS flowrate was calibrated to a value less than or equal to the measured flowrate, and the CPC flowrate was subsequently adjusted to a value less than or equal to the COLSS flowrate, conservatism of the CPC flowrates was assured.

Adjustment of either the COLSS or CPC flowrate leads to a decalibration of the respective primary thermal power calculation. Hence, if adjustments to flow were performed, BDELT and BDT were recalibrated to agree with the secondary calorimetric power.

If the CPC and COLSS acceptance criteria were not initially satisfied at the 20% or 50% plateaus, adjustments were not mandatory; at 80% and 100%, however, adjustments to calibrated flow were required. The confidence in the measurement of flowrate increases with power, so attempts to calibrate flow at the lower power plateaus might have proven counterproductive.

Following completion of the flow and power adjustments at the 100% power plateau, an evaluation of the thermal power adjustment coefficients was performed. Values of CPC thermal power, adjusted to reflect the final values of FCI and TPC, were compared to BSCAL to determine the thermal power error at each power plateau. If this error were to exceed 0.5% at any plateau, then a detailed evaluation by Combustion Engineering would be required.

RESULTS:

Results from each performance of this test are summarized in Tables 6.5.1.1 through 6.5.1.5.

At the 20% power plateau, adjustments to force COLSS flow to within the necessary bounds about the 'true' flow were interrupted by RCS temperature dropping outside of the required control band (see Table 6.5.1.1). Since adjustments at this plateau were not mandatory, the initial calibration of the COLSS and CPC flow constants was left to be performed at the 50% plateau.

Adjustments at the 50% and 80% plateaus were completed satisfactorily, as shown on Tables 6.5.1.2 and 6.5.1.3.

This test was performed twice at the 100% plateau. The first performance was done to satisfy the surveillance requirements of Technical Specification 4.3.1.1, item 10 (notation 8). Results of this performance of the test are shown in Table 6.5.1.4.

Following completion of the test program, an error was discovered in the calculation of measured flow. The CPCs were adjusted conservatively with respect to COLSS, but COLSS flow was slightly greater than measured flow. An evaluation of the test data was performed, and it was determined that the CPCs were adjusted conservatively with respect to a best-estimate measured flowrate of 104.60% of design.

Data from the final performance of this test at 100% power, equilibrium xenon conditions, are summarized in Table 6.5.1.5. Conditions were sufficiently stable that, during performance of the second COLSS flow adjustment iteration, calculation of a new 'true' RCS flowrate was deemed unnecessary. The CPC flowrates were all adjusted to be approximately 0.5% conservative with respect to the COLSS flowrate, and reflect an as-left mass flowrate of 103.5% of the design value of 148×10^6 lbm/hour.

Adjustment of COLSS thermal power (BDELT) and CPC thermal powers (BDTs) was accomplished successfully at all power plateaus with the exception of 20%.

TABLE 6.5.1.1: 20% PLATEAU RESULTS
RCS CALORIMETRIC FLOW
COLSS FLOWRATE ADJUSTMENT

Measured Flowrate % design	COLSS Flowrate % design	Difference % design	Acceptable? (yes/no)
105.30	113.89	+ 8.59	no
104.40	105.37	+ 0.97	no
104.59	105.34	+ 0.75	no
-----	-----	-----	--
-----	-----	-----	--

CPC FLOWRATE ADJUSTMENT

COLSS Flowrate % design	CPC Flow (% design)				Difference (% design)				Acceptable? (yes/no)			
	A	B	C	D	A	B	C	D	A	B	C	D

AS-LEFT FLOW CONSTANT VALUES

CPC FC1				COLSS			
A	B	C	D	D15(1)	D15(2)	D15(3)	D15(4)
1.1213	1.1212	1.1218	1.1209	9184.6	8071.3	9344.5	9283.0

TABLE 6.5.1.2: 50% PLATEAU RESULTS
RCS CALORIMETRIC FLOW
COLSS FLOWRATE ADJUSTMENT

Measured Flowrate % design	COLSS Flowrate % design	Difference % design	Acceptable? (yes/no)
106.41	103.48	- 2.93	no
106.23	106.60	+ 0.37	no
105.26	106.82	+ 1.56	no
105.16	105.04	- 0.12	yes
-----	-----	-----	---

CPC FLOWRATE ADJUSTMENT

COLSS Flowrate % design	CPC Flow (% design)				Difference (% design)				Acceptable? (yes/no)			
	A	B	C	D	A	B	C	D	A	B	C	D
106.2	113.9	114.0	114.0	113.9	+7.7	+7.8	+7.8	+7.7	no	no	no	no
106.3	106.1	106.1	106.2	106.2	-0.2	-0.2	-0.1	-0.1	yes	yes	yes	yes
-----	-----	-----	-----	-----	-----	-----	-----	-----	-----	-----	-----	-----

AS-LEFT FLOW CONSTANT VALUES

CPC FCI				COLSS			
A	B	C	D	D15(1)	D15(2)	D15(3)	D15(4)
1.0438	1.0432	1.0435	1.0440	8198.9	7082.8	8354.0	8291.3

TABLE 6.5.1.3: 80% PLATEAU RESULTS
RCS CALORIMETRIC FLOW

COLSS FLOWRATE ADJUSTMENT

Measured Flowrate % design	COLSS Flowrate % design	Difference % design	Acceptable? (yes/no)
105.95	105.34	- 0.61	no
104.50	105.88	+ 1.38	no
105.20	104.31	- 0.89	no
104.83	104.94	+ 0.11	no
104.71	104.71	- 0.005	yes

CPC FLOWRATE ADJUSTMENT

COLSS Flowrate % design	CPC Flow (% design)				Difference (% design)				Acceptable? (yes/no)			
	A	B	C	D	A	B	C	D	A	B	C	D
105.95	105.6	105.5	105.6	105.6	-.31	-.44	-.34	-.35	yes	yes	yes	yes
-----	-----	-----	-----	-----	-----	-----	-----	-----	-----	-----	-----	-----
-----	-----	-----	-----	-----	-----	-----	-----	-----	-----	-----	-----	-----

AS-LEFT FLOW CONSTANT VALUES

CPC FC1				COLSS			
A	B	C	D	D15(1)	D15(2)	D15(3)	D15(4)
1.0438	1.0432	1.0435	1.0440	8191.4	7080.4	8352.6	8287.5

TABLE 6.5.1.4: 100% PLATEAU (FIRST RUN) RESULTS
RCS CALORIMETRIC FLOW
COLSS FLOWRATE ADJUSTMENT

Measured Flowrate % design	COLSS Flowrate % design	Difference % design	Acceptable? (yes/no)
104.05	104.24	+ 0.19	no
103.37	104.50	+1.13	see text
-----	-----	-----	---
-----	-----	-----	---
-----	-----	-----	---

CPC FLOWRATE ADJUSTMENT

COLSS Flowrate % design	CPC Flow (% design)				Difference (% design)				Acceptable? (yes/no)			
	A	B	C	D	A	B	C	D	A	B	C	D
104.39	104.5	104.4	104.5	104.5	+ .13	- .01	+ .10	+ .06	no	yes	no	no
105.22 *	104.3	104.3	104.3	104.3	- .91	- .91	- .92	- .93	yes	yes	yes	yes
-----	-----	-----	-----	-----	-----	-----	-----	-----	-----	-----	-----	-----

* see text

AS-LEFT FLOW CONSTANT VALUES

CPC FC1				COLSS			
A	B	C	D	D15(1)	D15(2)	D15(3)	D15(4)
1.0409	1.0418	1.0409	1.0418	8525.4	7419.2	8691.0	8622.7

TABLE 6.5.1.5: 100% PLATEAU (SECOND RUN) RESULTS
RCS CALORIMETRIC FLOW
COLSS FLOWRATE ADJUSTMENT

Measured Flowrate % design	COLSS Flowrate % design	Difference % design	Acceptable? (yes/no)
103.78	104.70	+ 0.92	no
103.78	103.58	- 0.20	yes
-----	-----	-----	---
-----	-----	-----	---
-----	-----	-----	---

CPC FLOWRATE ADJUSTMENT

COLSS Flowrate % design	CPC Flow (% design)				Difference (% design)				Acceptable? (yes/no)			
	A	B	C	D	A	B	C	D	A	B	C	D
103.70	104.5	104.4	104.4	104.4	+0.75	+0.73	+0.74	+0.71	no	no	no	no
103.97	103.5	103.5	103.5	103.5	-0.47	-0.46	-0.46	-0.47	yes	yes	yes	yes
-----	-----	-----	-----	-----	-----	-----	-----	-----	-----	-----	-----	-----

AS-LEFT FLOW CONSERVATION VALUES

CPC FCI				COLSS			
A	B	C	D	D15(1)	D15(2)	D15(3)	D15(4)
1.0319	1.0330	1.0320	1.0332	9581.8	8493.5	9764.4	9689.6

The final objective of this test was the determination of the adequacy or inadequacy of the CPC algorithms used to correct thermal power (BDT) for non-systematic, power-dependent errors. Calculation of these thermal power error values initially led to the conclusion that the CPC thermal power adjustment coefficients were inadequate. However, an evaluation of the test results, performed by Combustion Engineering, revealed that problems with the RTDs (discussed extensively in section 6.2.2 of this report) prevented an accurate assessment of the adequacy of the coefficients.

Additional data are to be taken for further evaluation; additional penalty factors are installed in COLSS and the CPCs to assure conservative operation of the plant, until the problem RTDs are replaced.

CONCLUSIONS:

All objectives and acceptance criteria of this test, with the exception of completing the final adequacy determination of the thermal power coefficients installed in the CPCs, were met.

The COLSS RCS flowrate was adjusted to ensure conservatism with respect to the measured RCS flowrate at all power plateaus except 20%. The CPC RCS flowrates were also adjusted to ensure conservatism with respect to the COLSS flowrate, again at all plateaus except 20%. COLSS and CPC thermal powers were recalibrated to BSCAL to within specified tolerances following each adjustment to flow.

Evaluation of the CPC thermal power adjustment coefficients is continuing.

6.5.2 Natural Circulation Demonstration Testing (SIT-TP-755)

PURPOSE:

The purpose of this test was to provide the operators with training in operating the plant under various natural circulation conditions. In addition, data was collected during this test to show that natural circulation flow conditions and heat removal capability are in accordance with design. The natural circulation conditions demonstrated during this test were:

- a) initiation
- b) steady state
- c) reduced reactor coolant system (RCS) pressure
- d) isolated steam generator
- e) recovery

This test satisfied the requirements of FSAR section 14.2.12.3.25.

METHOD:

Natural circulation was initiated on May 28, 1985, per SIT-TP-727, 80% Total Loss of Flow Trip/Natural Circulation Test (see Section 6.6.4), by simultaneously tripping all four reactor coolant pumps (RCPs) with the plant operating at 80% power. Following completion of a power-to-flow ratio determination per SIT-TP-727, steady state natural circulation conditions were maintained for approximately one hour. During this period, and throughout the testing, operator actions were observed and recorded by test personnel while plant data was collected utilizing the plant monitoring computer (PMC) and Test Data Acquisition System (TDAS).

Following the steady-state demonstration, all pressurizer heaters were secured, allowing RCS pressure to slowly decrease. Once the depressurization rate with no heaters on had been determined, pressure was further reduced utilizing auxiliary spray. (Note that auxiliary spray supplied by charging pumps must be used during natural circulation since there is insufficient driving head to produce normal spray flow with the RCPs deenergized). Natural circulation flow conditions were observed during this period of time at reduced pressure. This test was used to demonstrate that natural circulation can be maintained at reduced system pressures and that proper loop subcooling can be maintained. At the conclusion of the reduced pressure natural circulation demonstration, the pressurizer heaters were selectively reenergized to return RCS pressure to approximately 2250 psia.

A demonstration of natural circulation with reduced heat removal capacity was performed next. This test was used to demonstrate that natural circulation can be maintained with one steam generator isolated. Since pressure in the isolated steam generator (Steam Generator #2 during the test) would eventually rise to the saturation pressure for T_{hot} existing at that time, a cooldown was initiated to initially lower T_{cold} below 518°F, to ensure that the secondary safety valve setpoint would not be reached during the test. Once cold leg temperature had been lowered, the secondary side of steam generator #2 was isolated by closing its atmospheric dump valve (ADV), main steam isolation valve (MSIV) and securing feedwater to that generator. In this mode, cold leg temperature in the isolated steam generator rose toward hot leg temperature as heat removal in the isolated loop decreased. Adjustments to temperature were made by steaming through the ADV in the unisolated steam generator. Natural circulation conditions were observed in this configuration and maintained for 30 minutes. MSIV #2 was then reopened, unisolating steam generator #2.

Following the reduced heat removal test, steady state natural circulation was reestablished and verified and the RCPs restarted, thereby ending natural circulation testing.

RESULTS:

Prior to initiation of natural circulation, the reactor had operated at approximately 60% power for 4 days and at 80% for the last three days in the week leading up to the trip. This power history provided sufficient decay heat for the test and resulted in a core ΔT ($T_{\text{hot}} - T_{\text{cold}}$) of approximately 15°F during the six and one half hours of natural circulation testing (Normal full power ΔT is 58.2°F). In addition, the Qualified Safety Parameters Display System (QSPDS), which calculates saturation margin based on hot leg temperatures, Core Exit Thermocouple (CET) temperatures, and upper head temperature, showed that approximately 100°F of subcooling was maintained in each of the monitored regions throughout testing. Natural circulation flow was therefore shown to be able to adequately remove decay heat in each of the modes demonstrated in this test.

During the reduced RCS pressure portion of the test, primary pressure decreased at a rate of approximately 1.4 psia/minute. Auxiliary spray was used to further decrease pressure, and a minimum pressure of 2132 psia was attained during the test. Saturation margin (based on hot leg temperature) was 100.7°F at that time. Both banks of pressurizer proportional heaters were then energized, slowly returning the RCS to normal pressure.

The RCS was then cooled down to approximately 506°F cold leg temperature in preparation for isolating the secondary side of steam generator #2. Once the isolation was initiated, steam

generator pressure and cold leg temperature in the isolated loop increased. Hot leg temperatures remained essentially equal and constant in both loops. Opening MSIV #2 quickly equalized cold leg temperatures and steam generator pressures. The initiation and recovery from isolated steam generator conditions was accomplished smoothly.

The following plots (Figures 6.2.5.1 through 6.5.2.3) show key plant parameters during the natural circulation demonstrations. Time "zero" is 1515 (CDT) on May 28, 1985, two and one half hours after the total loss of flow trip per SIT-TP-727. The duration of the test was approximately 4½ hours (255 minutes); after this time the RCP's were restarted and normal hot standby conditions reestablished in accordance with plant operating procedures.

Throughout the demonstrations, hot leg temperatures were always greater than cold leg temperature. This demonstrated satisfactorily that natural circulation flow remained in the normal direction, from cold leg to hot leg in the reactor vessel, to the steam generators, and returning to the vessel through the cold legs.

CONCLUSION:

This test demonstrated that Waterford 3 performs per design in the following natural circulation conditions:

- a) initiation;
- b) steady state;
- c) reduced RCS pressure;
- d) isolated steam generator;
- e) and recovery.

The plant was easily controlled and recovered from each of these conditions with no difficulty. All licensed plant operators designated by the Plant Operations Superintendent to participate in the control and/or observation of the plant in natural circulation conditions satisfactorily partook in this test. All test acceptance criteria were met.

FIGURE 6.5.2.1

NATURAL CIRCULATION DEMONSTRATION
REACTOR COOLANT HOT AND COLD LEG TEMPERATURES

* TCOLD 1A
o TCOLD 2B
△ THOT 1
□ THOT 2

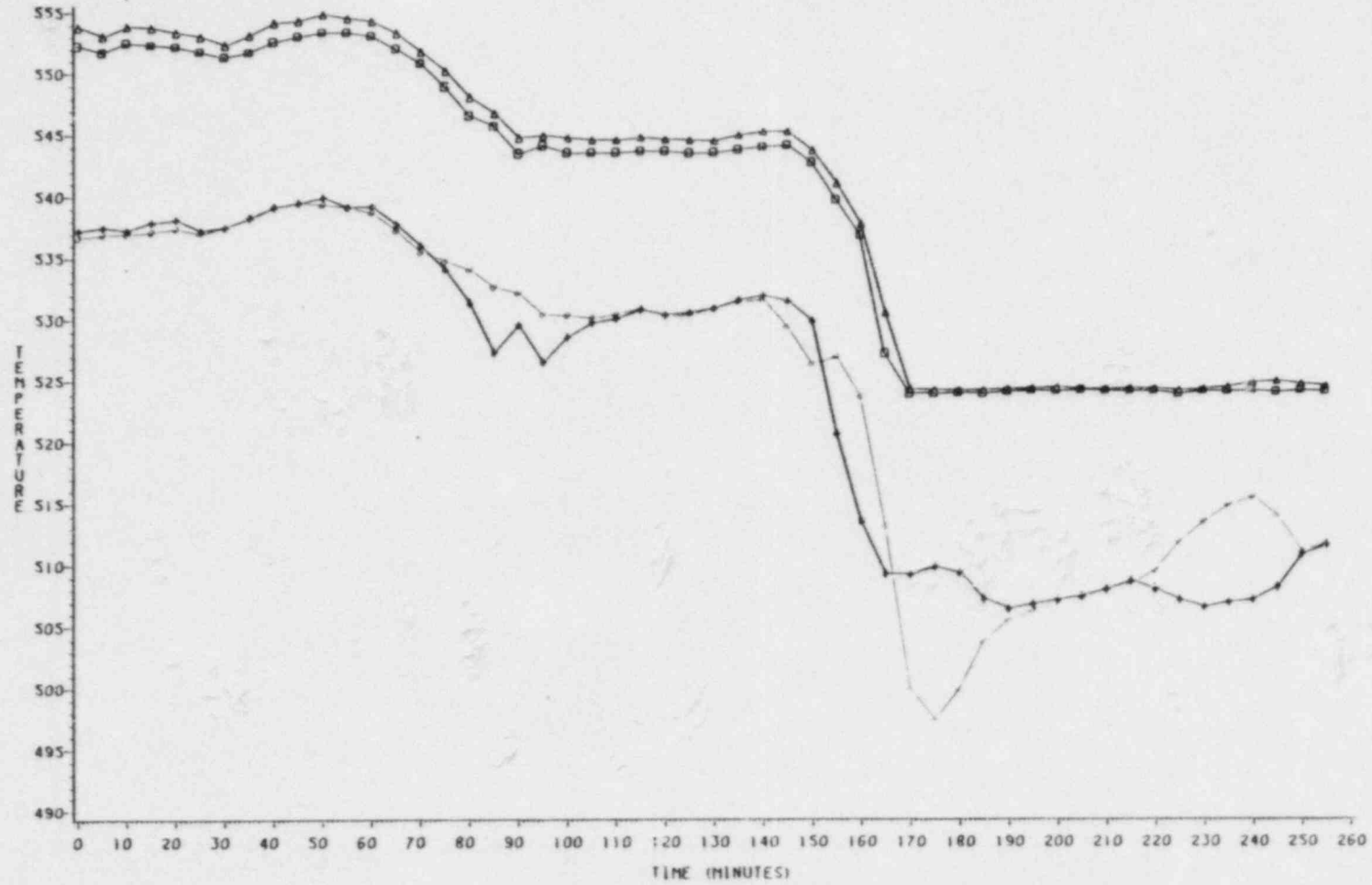


FIGURE 6.5.2.2

NATURAL CIRCULATION DEMONSTRATION
STEAM GENERATOR PRESSURES

⊕ - S/G 1
□ - S/G 2

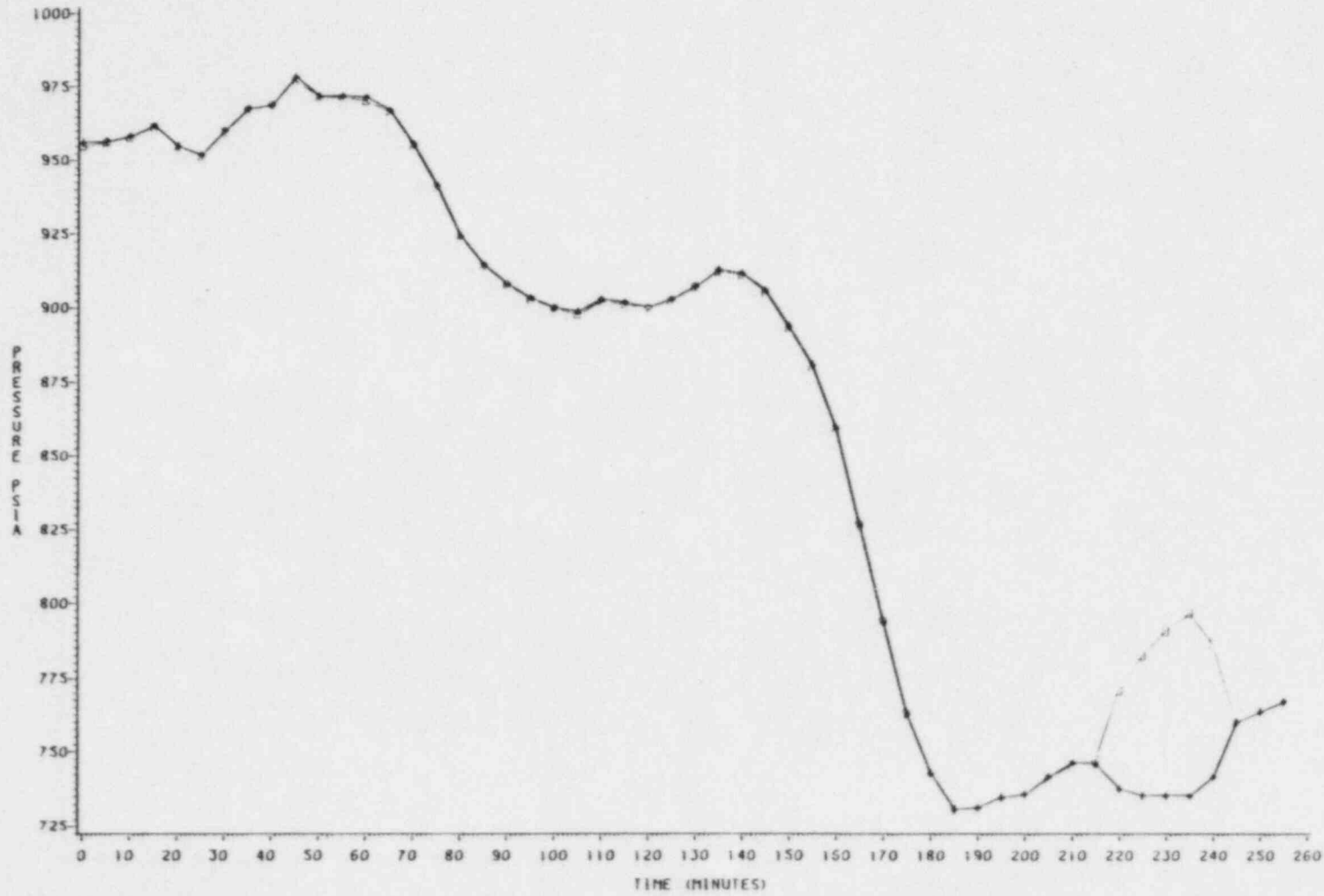
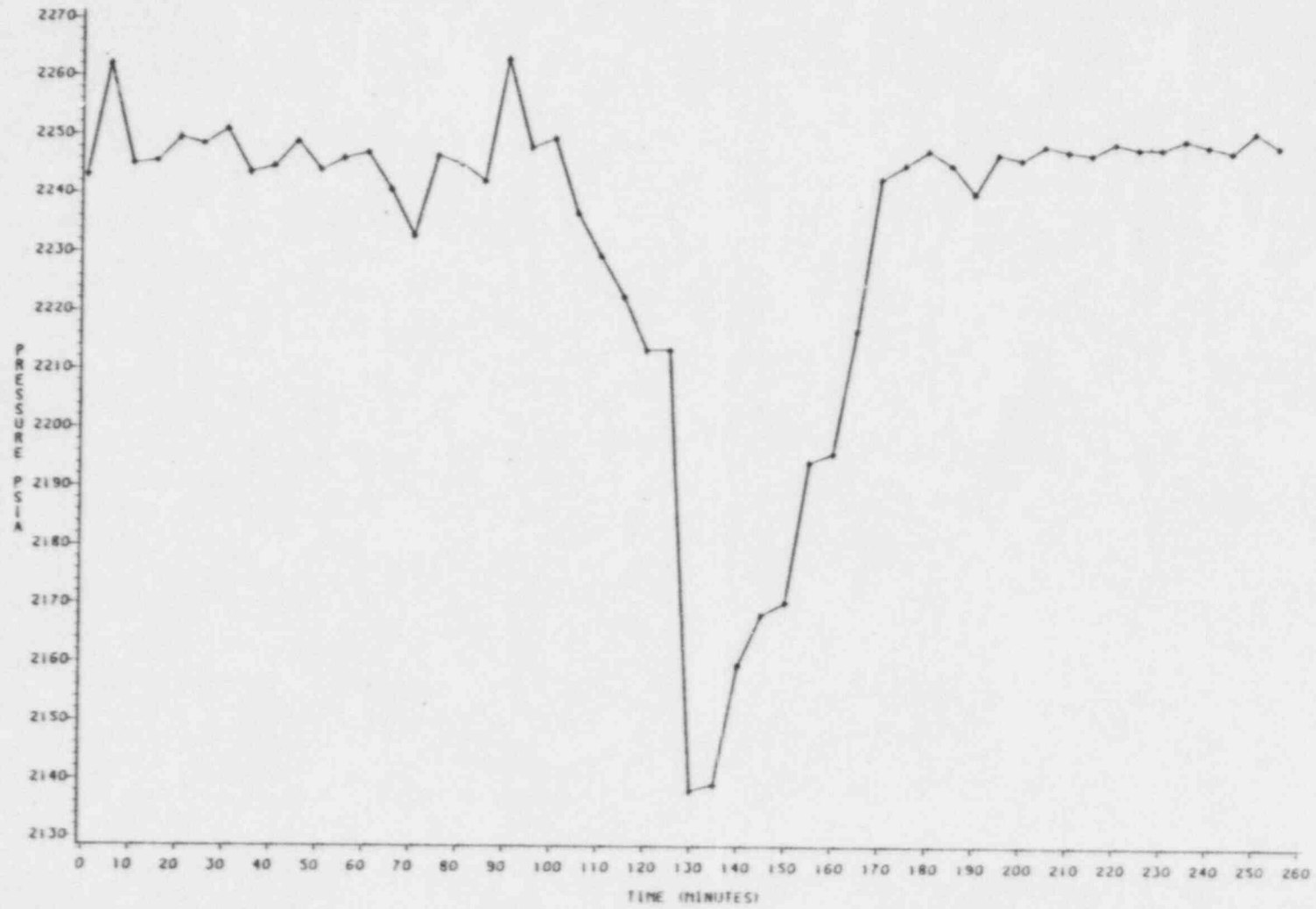


FIGURE 6.5.2.3

NATURAL CIRCULATION DEMONSTRATION
PRESSURIZER PRESSURE



6.6 TRANSIENT TESTING

6.6.1 Remote Reactor Trip with Subsequent Remote Cooldown (SIT-TP-726)

PURPOSE:

The purpose of this procedure was the demonstration of the following:

- 1) There was equipment provided at appropriate locations outside the control room which had the capability to trip the reactor.
- 2) There were adequate instrumentation and controls outside the control room to maintain the plant in a hot standby condition.
- 3) Cold shutdown of the reactor from outside the control room was achievable.
- 4) The plant operating procedures used in performing the remote shutdown and cooldown were sufficiently clear and comprehensive, and the operating personnel were familiar with their application.
- 5) The minimum required shift complement was sufficient to perform the actions required for the remote shutdown and the maintenance of hot standby.
- 6) No design deficiencies or potential hazards to plant equipment or personnel existed during a remote reactor trip and subsequent remote plant cooldown.

This test satisfied the commitments of FSAR section 14.2.12.3.33.

METHOD:

Prior to performance of this test, it had been decided to perform the remote reactor trip and the remote reactor cooldown portions of the test separately. The reactor trip portion was performed on 5/2/85; the cooldown portion was performed on 5/12/85.

Plant conditions were stabilized at a reactor power level of approximately 20% on the morning of 5/2/85, in preparation for the performance of the reactor trip portion of this test. The night shift operations personnel were held over so two complete crews of licensed operators were available for the test; one crew (the standby crew) remained in the control room throughout the evolution while the second crew (the operating crew) performed the test from remote locations.

Two dry runs of the procedure were performed so that each member of the operating crew was familiar with his responsibilities during the test. Approximately five minutes prior to the trip, the operating crew simulated an evacuation of the control room; the standby crew remained to maintain control of the plant. Upon reaching the 'B' switchgear room and verifying with the shift supervisor that all personnel were at their assigned locations, the operating crew control room supervisor tripped the reactor by opening the reactor trip circuit breakers. Control was then transferred from the control room to the remote shutdown panel (LCP-43) located at the +21' elevation of the reactor auxiliary building.

Present at the remote shutdown panel were the operating crew shift supervisor and primary nuclear plant operator. They performed the immediate and follow-up actions of plant operating procedure OP-901-004, Evacuation of Control Room and Subsequent Plant Shutdown. Communications had been established with the secondary nuclear plant operator, who was directed to perform various steps within the turbine-generator building.

From these remote locations, the operating crew established hot shutdown conditions and maintained them for the specified thirty minutes. At that time, control was transferred back to the control room, and the standby crew resumed performance of their normal duties.

The remote cooldown portion of the procedure was initiated on the afternoon of 5/12/85. With the standby crew stationed in the control room, the operating crew transferred control of the reactor to LCP-43. A controlled cooldown was initiated to bring the RCS to the temperature at which the shutdown cooling system could be placed in service. Once shutdown cooling had been established, the RCS was cooled an additional 50°F. Control was then returned to the standby crew in the control room.

RESULTS:

All objectives of this procedure were satisfactorily achieved. All acceptance criteria were satisfied. The emergency operating procedures utilized during the performance of the remote trip and cooldown were evaluated by the Nuclear Engineer and the Operations Superintendent, and were found to be adequate. Plant design, as it related to the ability to control the plant from the remote locations, was also deemed adequate.

Performance of the remote reactor trip and maintenance of hot standby conditions for thirty minutes was completed satisfactorily by the operating crew, with no intervention by the standby crew in the control room. Verification that all CEAs were fully inserted and that the turbine had tripped was performed by the standby crew shift supervisor.

Figures 6.6.1.1 through 6.6.1.6 illustrate the behavior of key plant parameters following the reactor trip. These parameters were maintained within the bands specified by the test procedure with one exception: steam generator levels were not maintained at 68%. The main feedwater pumps had been tripped by the secondary nuclear plant operator, and it was not desired to use the emergency feedwater system unless it became necessary; the low decay heat level and subsequent slow steam-down rate of the steam generators resulted in more than adequate secondary water inventory. Verification of the ability to control steam generator levels was satisfactorily demonstrated during the remote cooldown portion of the test, when use of the emergency feedwater system was required.

Performance of the cooldown to shutdown cooling conditions (and 50°F beyond that) was also satisfactorily completed without intervention by the control room crew.

CONCLUSION:

The ability to shutdown the reactor and maintain the plant in a hot standby condition from outside the control room was satisfactorily demonstrated. The ability to perform a cooldown of the reactor coolant system to shutdown cooling conditions from remote locations was also satisfactorily demonstrated.

WSES-3 REMOTE REACTOR TRIP

RCS COLD LEG TEMPERATURES

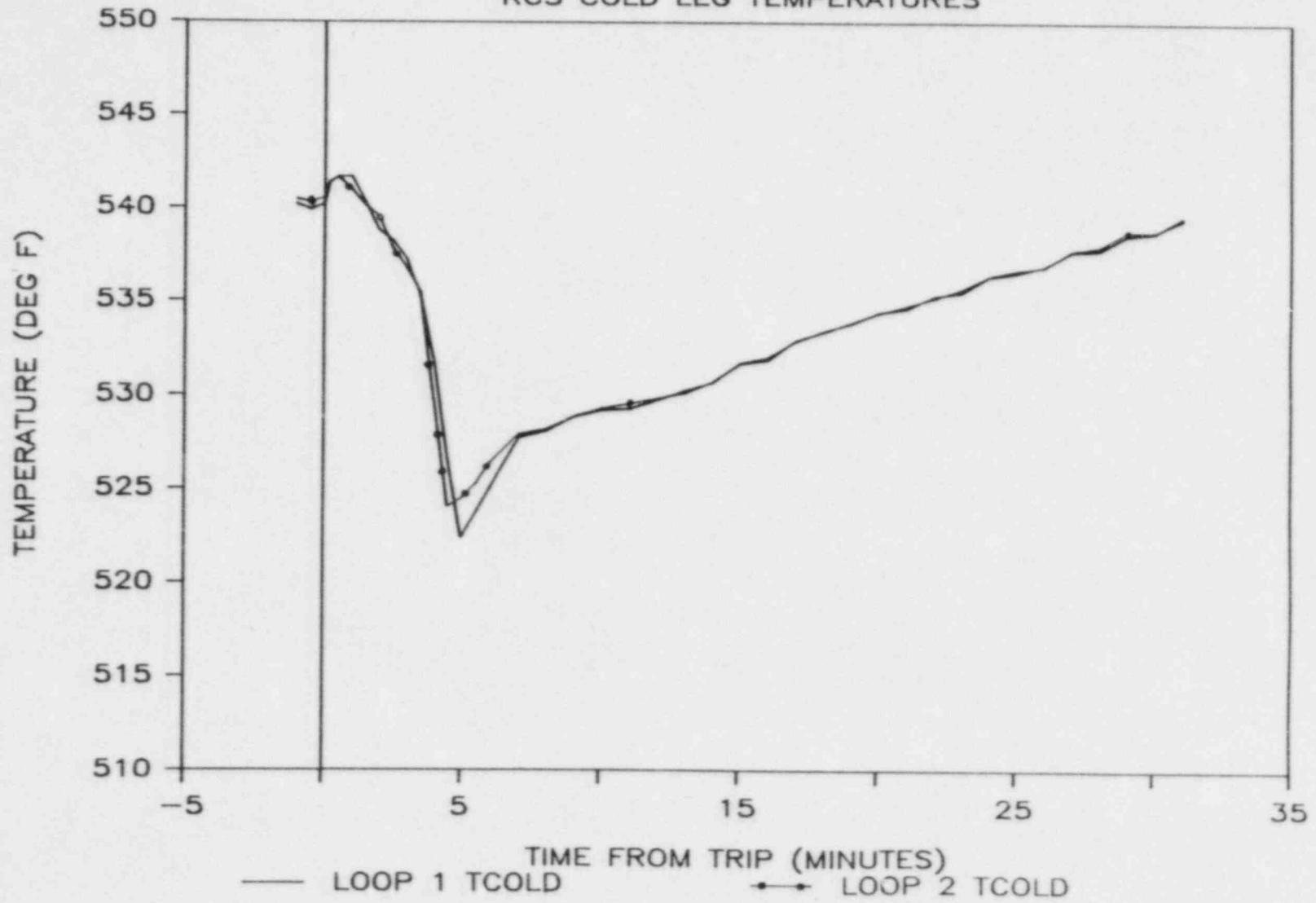


FIGURE 6.6.1.1

WSES-3 REMOTE REACTOR TRIP

RCS HOT LEG TEMPERATURES

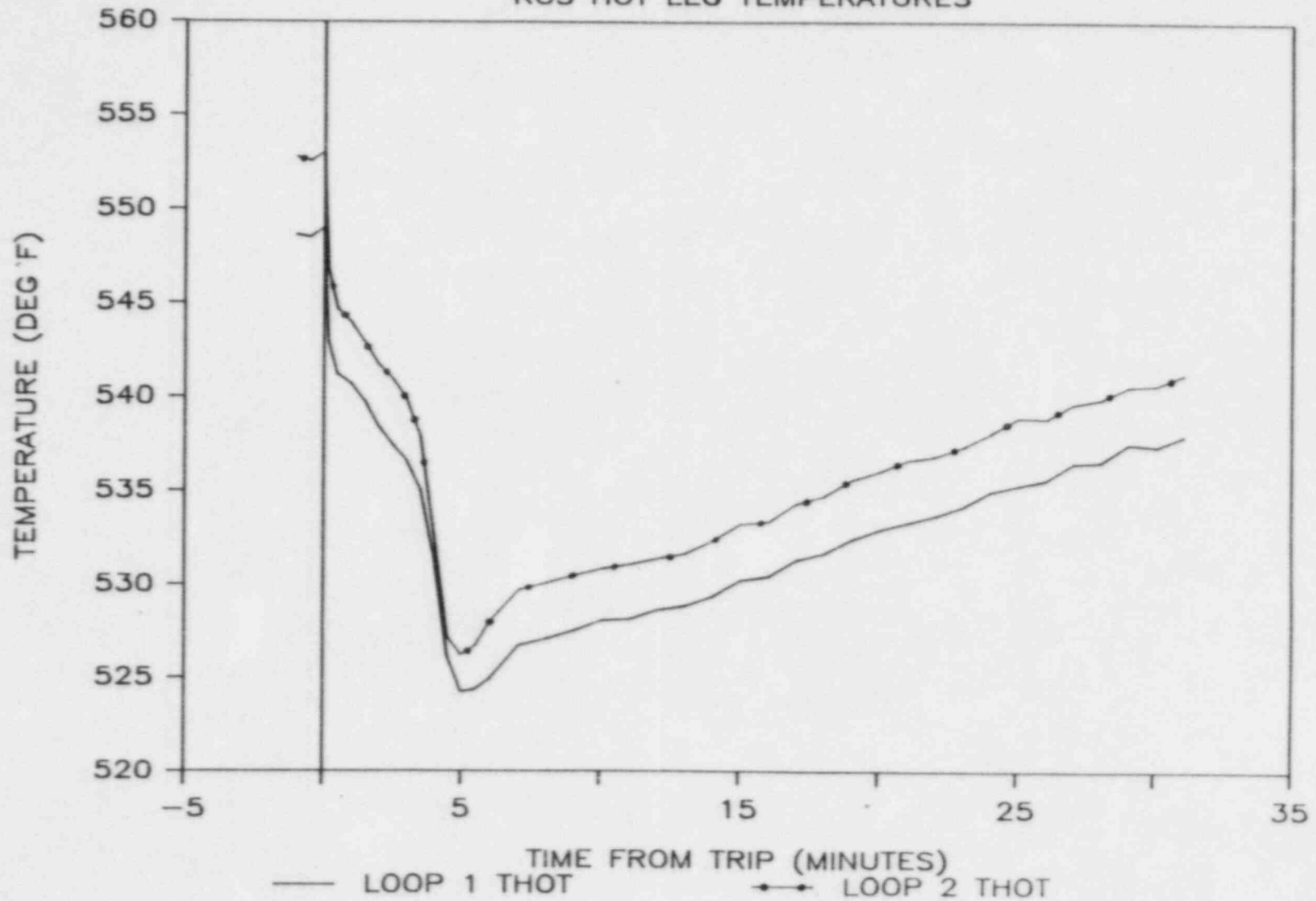


FIGURE 6.6.1.2

WSES-3 REMOTE REACTOR TRIP

PRESSURIZER PRESSURE

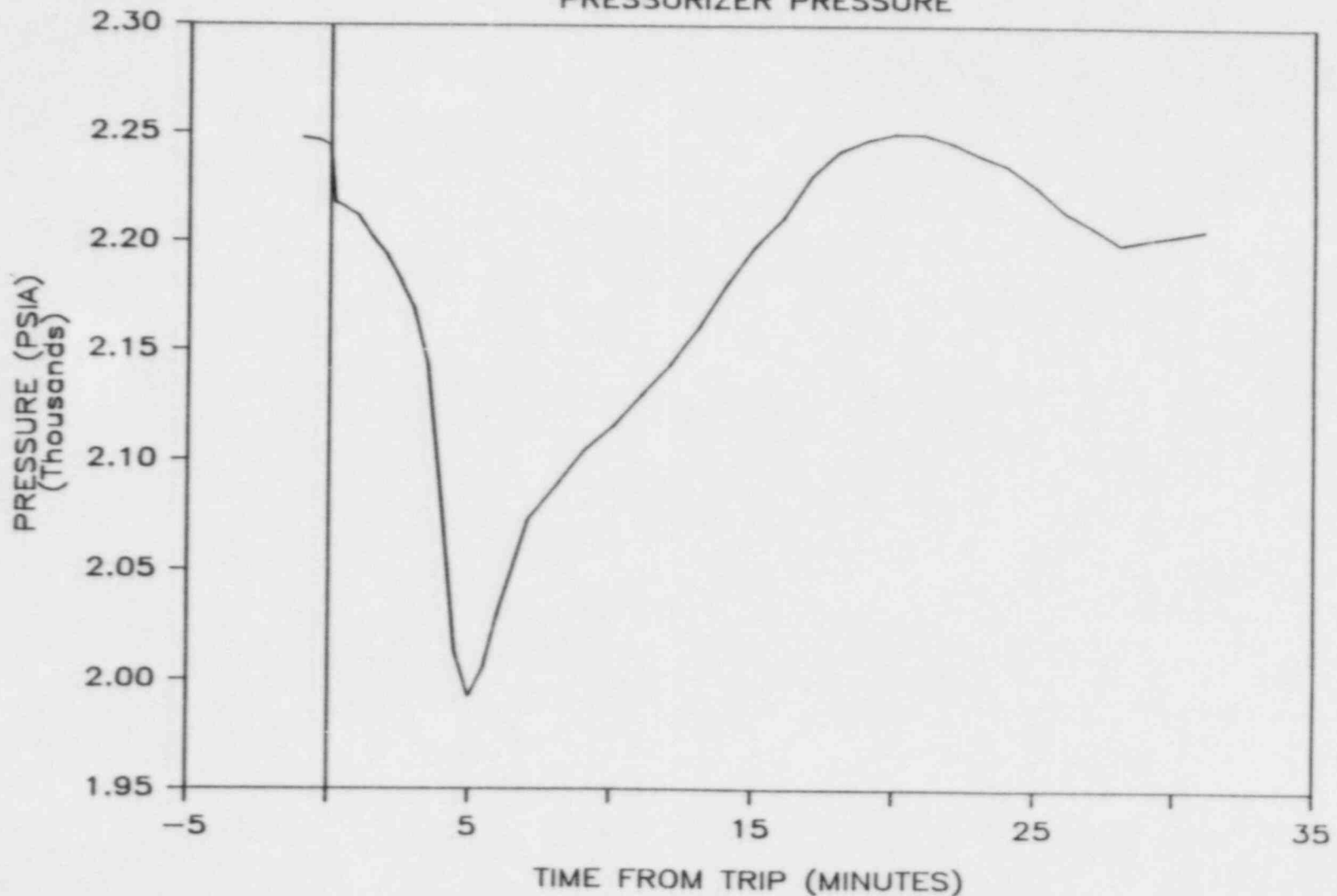


FIGURE 6.6.1.3

WSES-3 REMOTE REACTOR TRIP

PRESSURIZER LEVEL

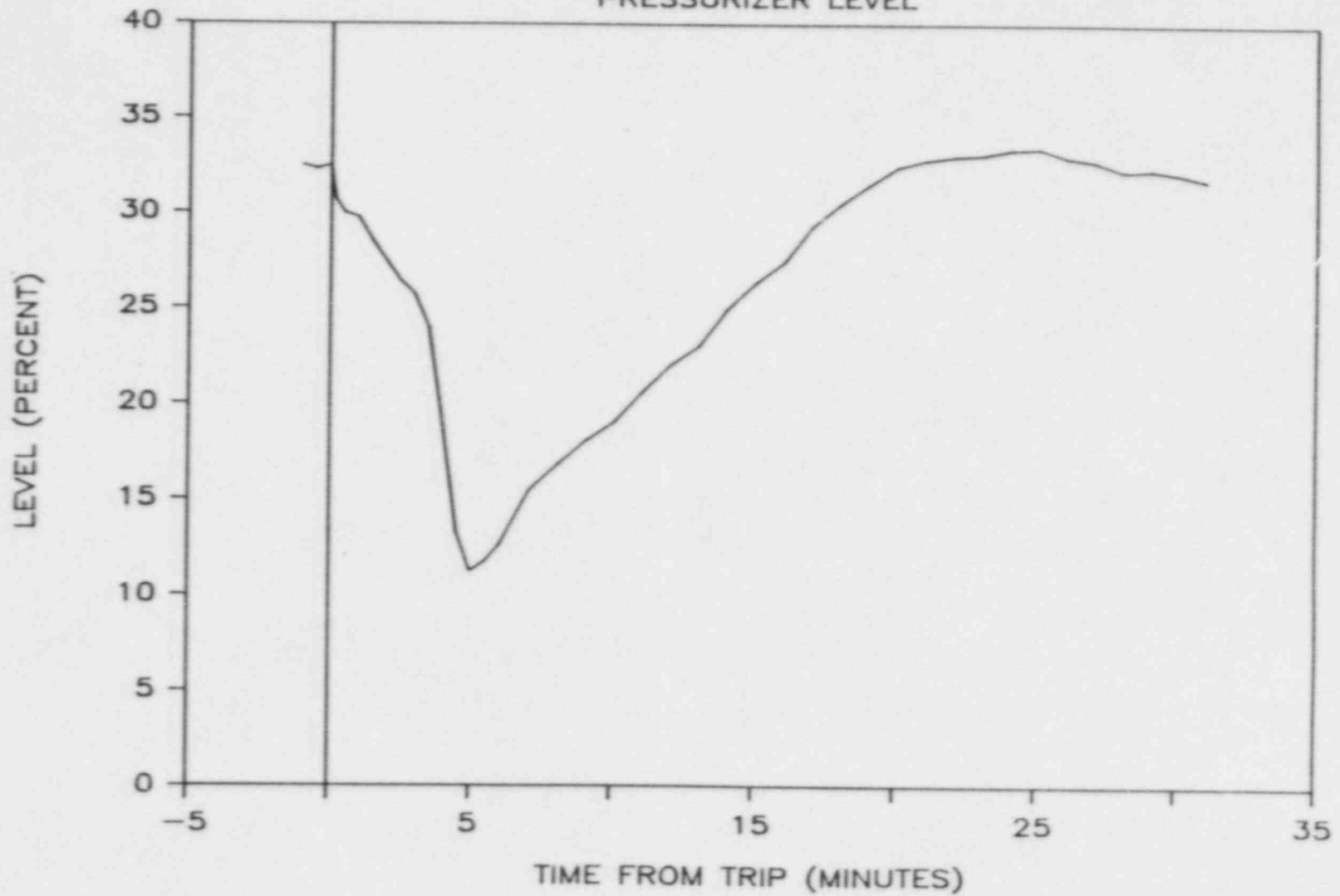


FIGURE 6.6.1.4

WSES-3 REMOTE REACTOR TRIP STEAM GENERATOR PRESSURES

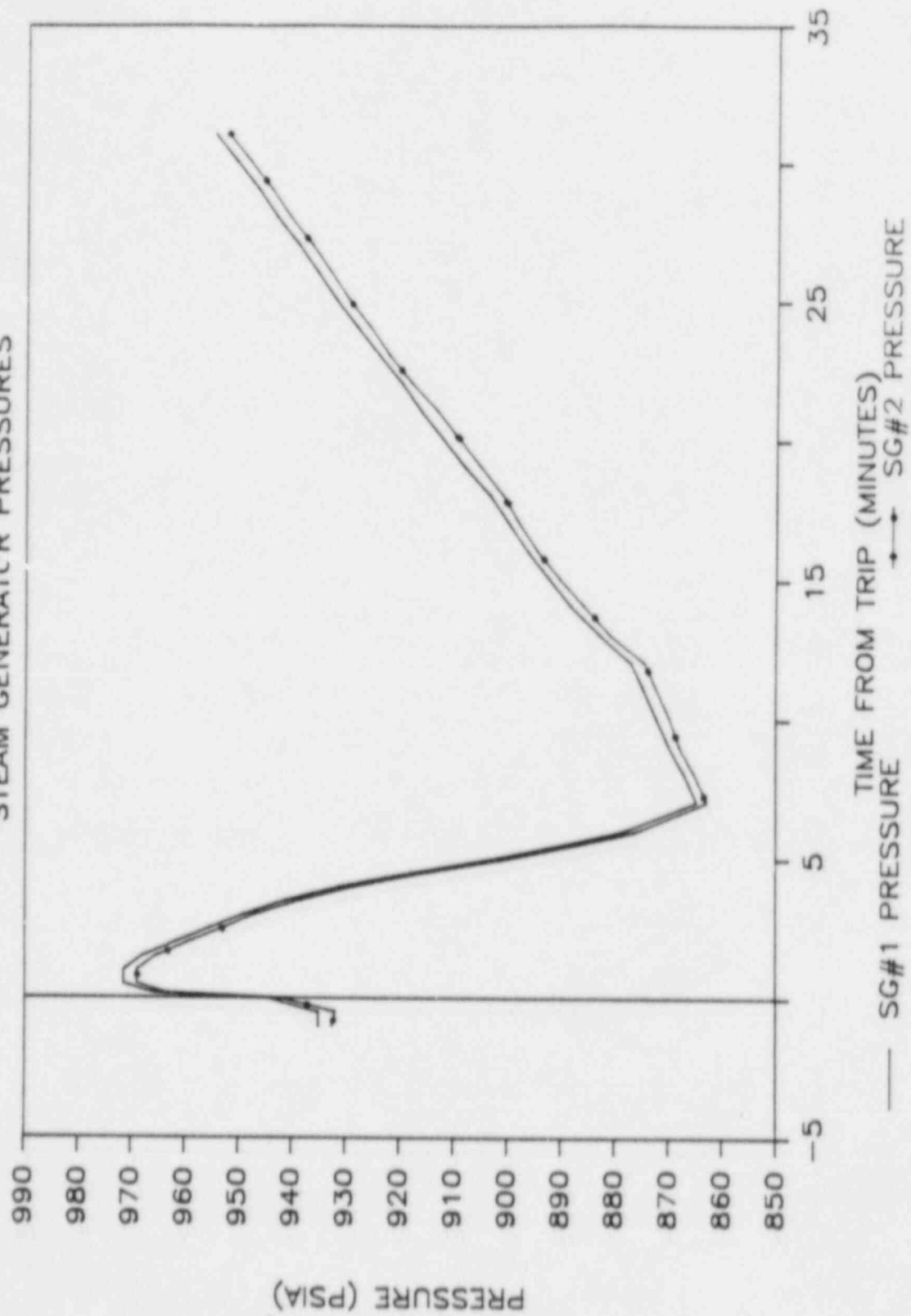


FIGURE 6.6.1.5

WSES-3 REMOTE REACTOR TRIP

STEAM GENERATOR LEVELS

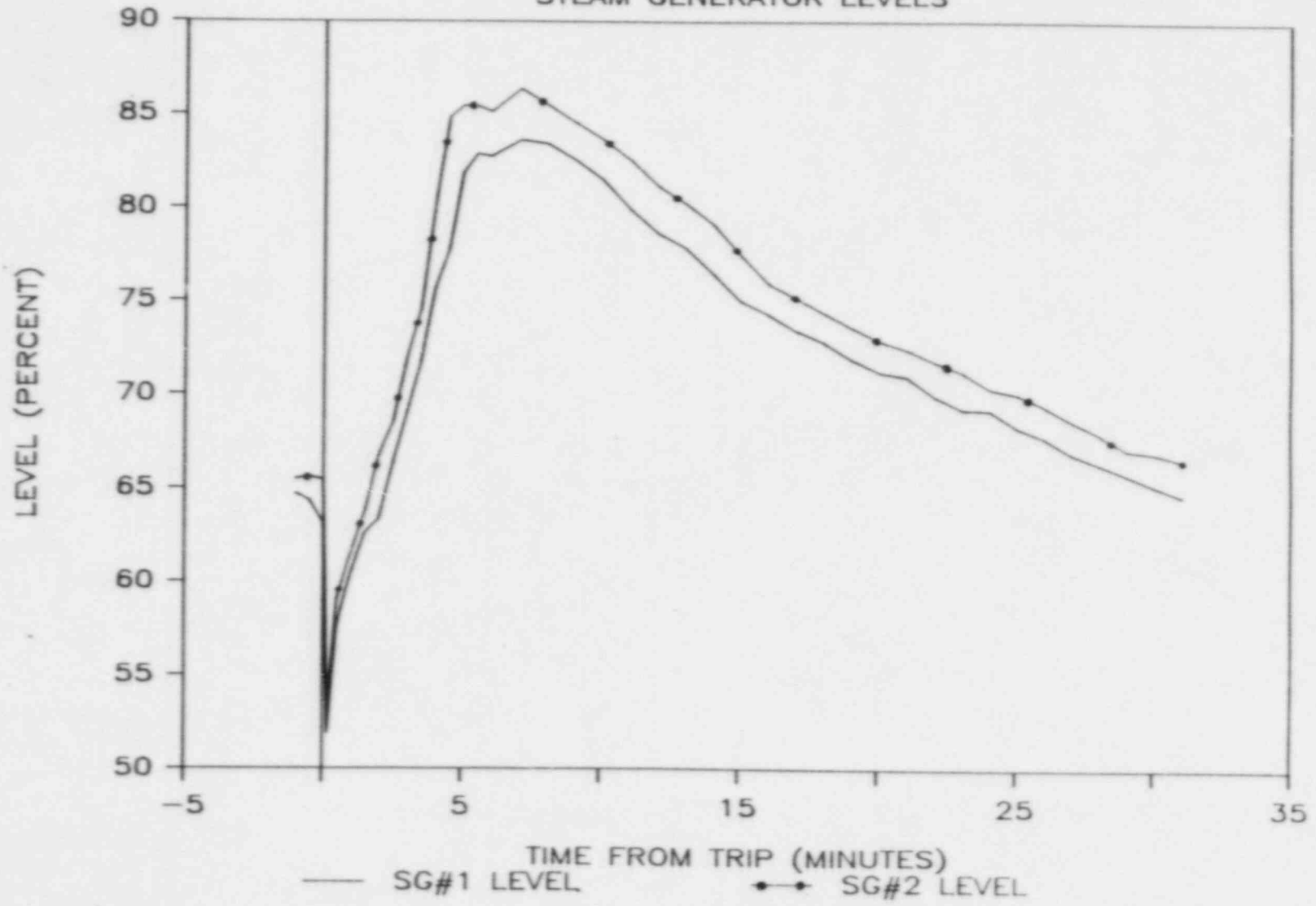


FIGURE 6.6.1.6

Plant design, as it related to the ability to control the plant from the remote locations, was found to be adequate. Plant emergency operating procedures governing a remote trip and cooldown were also deemed adequate.

The minimum required shift complement was sufficient to perform the remote reactor trip and subsequent stabilization at hot standby conditions.

6.6.2 Load Changes (SIT-TP-721)

PURPOSE:

The purpose of this test was to demonstrate that the integrated plant control systems operate satisfactorily in automatic to maintain plant parameters within specific limits.

If during performance of this test plant parameters were not maintained within or restored to specific operating bands, new setpoints were to be determined for the affected control system(s) and the test repeated to verify proper system operation.

This test satisfied in part the commitments of FSAR section 14.2.12.3.39 (see also section 6.2.7).

METHOD:

The satisfactory completion of the individual system and integrated system automatic steady state operation checkouts (see section 6.2.5) at 100% power was a prerequisite for the performance of this test.

Plant conditions were stabilized at approximately 95% power with the steam bypass control system (SBCS) the feedwater control system (FWCS), the reactor regulating system (RRS), the pressurizer level control system (PLCS), the pressurizer pressure control system (PPCS) and the digital-electro-hydraulic (DEH) system in automatic, and the control element drive mechanism control system (CEDMCS) in manual sequential (MS) with the CEAs fully withdrawn. T_{avg} was maintained within $\pm 0.5^{\circ}\text{F}$ of T_{ref} .

The test was initiated by decreasing the turbine load at a rate of 0.5% per minute to 90% using the DEH control to create a $T_{avg} - T_{ref}$ mismatch. The RRS was verified to respond immediately by inserting CEAs to restore T_{avg} to the new T_{ref} . The remaining control systems were verified as operating adequately by monitoring reactor power, reactor coolant system temperatures, pressurizer pressure and level, and steam generator levels and pressures to be within acceptable ranges during the transient. After a brief power stabilization at 90% power, power was returned to 95% at 0.5% per minute using the DEH control, while the behavior of the control systems and the response of their respective parameters were monitored for adequacy during the power increase.

RESULTS:

This test was performed as required, except that the "A" main feed pump was operated in the manual instead of automatic mode. This did not affect the test adversely because the speed of the pump was set, but the modulation of the flow control valve was able to respond to the feed demand such that the necessary flow was provided at all times. This allowed to satisfactorily demonstrate that the integrated control systems adequately control the plant during load transients. No setpoint adjustments to any of the control systems were required.

CONCLUSION:

The plant was satisfactorily shown to be able to withstand and control load changes as designed. The installed setpoints were verified acceptable and did not require any changes. All test objectives and acceptance criteria were met.

6.6.3 Loss of Offsite Power Trip (SIT-TP-728)

PURPOSE:

This test was performed to demonstrate plant performance under a total loss of AC power as well as provide operator training during loss of AC power conditions. Initially, this test verified that the reactor can be shutdown and hot standby conditions can be achieved and maintained using engineered safety features (ESF) power (4160 volt emergency diesel generators). Additionally, by simulating a total loss of onsite AC power, this test demonstrated the ability to remove decay heat with natural circulation flow in the reactor coolant system and with secondary feed from the steam-driven emergency feedwater pump.

METHOD:

At two minutes prior to the transient initiation, the unit start-up transformer disconnects were opened, isolating alternate power to the station. The transient was then initiated by tripping the main turbine from the control room, which subsequently resulted in a generator trip, causing the OCBs to open and initiating a loss of offsite power.

The reactor then tripped from approximately 20% power due to low flow projected DNBR as calculated by the CPCs. A short while after the reactor trip steady hot standby conditions were achieved. These conditions were maintained for at least 30 minutes. After satisfactorily achieving and maintaining hot standby conditions the following systems were secured to simulate a loss of onsite AC power:

- Charging and letdown
- Electric EFW pumps
- HPSI & LPSI
- PZR Heaters

With a loss of onsite power simulated, the steam driven EFW pump was brought on line to feed the steam generators to remove decay heat in conjunction with the natural circulation established in the RCS.

For the next 20 to 30 minutes the plant was maintained in this configuration.

Following adequate demonstration and operator training with the plant in natural circulation, systems were restored to a normal hot standby mode in accordance with plant operating procedures.

RESULTS:

All testing was performed according to the procedure. No difficulties or unexpected events occurred. All systems performed their function as designed. The following is a brief sequence of events:

- T = -2 min.: The unit start-up disconnects were opened.
- T = 0: The turbine was tripped (transient was started)
- T = +40 sec.: Generator tripped on reverse power; reactor tripped
- T = +10 min.: Hot standby conditions established
- T = +54 min.: Loss of onsite power was simulated
- T = +58 min.: EFW Pump A/B started
- T = +80 min.: Testing was secured; plant was returned to normal electrical line-up

Figures 6.6.3.1 and 6.6.3.2 illustrate trends of reactor coolant hot and cold leg temperature and steam generator levels with time. Time is measured in minutes from the turbine trip.

Figure 6.6.3.1 shows the initial rise in temperatures due to the load rejection followed by a collapse in delta-T due to the reactor trip. Core delta-T increased as flow coasted down to natural circulation conditions. Stable conditions were achieved at approximately +8 minutes. With the MSIV's open, the plant slowly cooled down until the MSIV's were shut at +33 minutes. Afterward, the plant continued to heat up even after the steam-driven emergency feedwater pump was started at +58 minutes. At this point, with a larger steam load, core delta-T increased.

Figure 6.6.3.2 depicts steam generator levels which stabilized at about 10 minutes into the event. A steady level decrease was observed until the MSIV's were shut at +33 minutes. Levels remained steady until +58 minutes, when the steam-driven emergency feedwater pump was started, resulting in declining levels.

Minimum RCS pressure was 2171 psia shortly after the trip. This was restored to 2250 psia. During the simulated loss of onsite power, pressure remained above 2200 psia.

CONCLUSION:

This test satisfactorily demonstrated that WSES-3 can be shutdown and maintained in a stable condition following a loss of offsite power with no compromise of safety features.

FIGURE 6.6.3.1
LOSS OF OFF-SITE POWER TEST
 REACTOR COOLANT HOT AND COLD LEG TEMPERATURES

◻ - THOT
 ◊ - TCOLD
 TIME - 0.33 MINUTES MSIVS WERE SHUT
 TIME - 0.58 MIN START FFW PUMP A/B
 SIMULATED LOSS OF ON SITE PWR

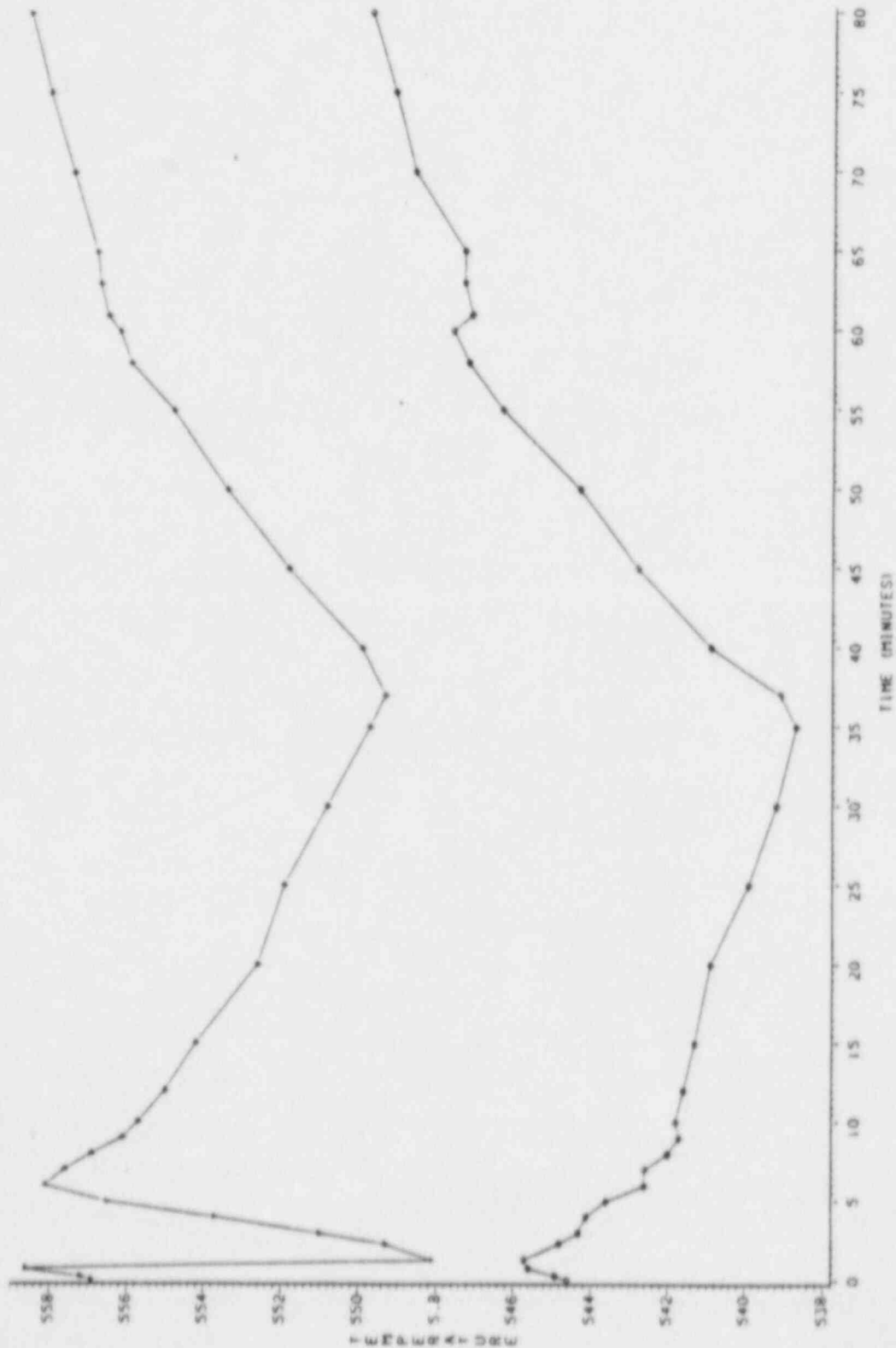
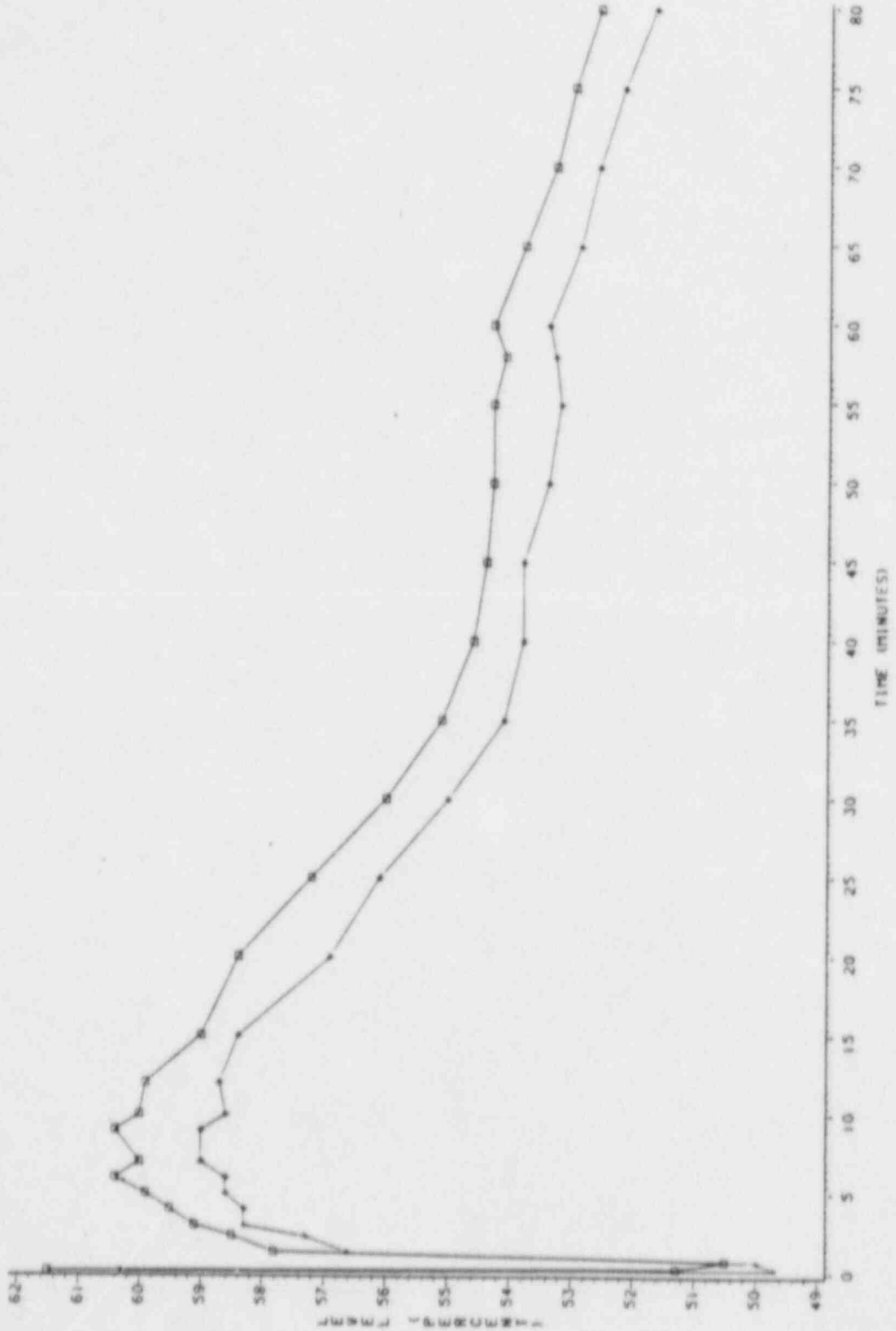


FIGURE 6.6.3.2
LOSS OF OFF-SITE POWER TEST
 STEAM GENERATOR LEVELS

□ = S/G 1
 ○ = S/G 2
 TIME = 033 MINUTES MSIVS WERE SHUT
 TIME = 058 MIN. START CFM PUMP A/B
 SIMULATED LOSS OF ON SITE PWR



Furthermore, under a combined condition of loss of offsite power and degraded onsite AC power, the plant can be controlled and decay heat rejected via natural circulation and steam driven EFW.

Operator training was also satisfactorily accomplished.

6.6.4 80% Total Loss of Flow/Natural Circulation (SIT-TP-727)

PURPOSE:

The Loss of Flow Trip was performed to demonstrate that the dynamic response of the Waterford III power plant to a total loss of forced reactor coolant flow following sustained power operation is in accordance with design and that stable natural circulation can be established to maintain adequate core cooling. FSAR section 15.3.2.1 describes a total loss of forced reactor coolant flow as an infrequent incident which is postulated to occur as a result of a loss of the main generator. No credit is taken for transfer to offsite power. The testing requirements of FSAR section 14.2.12.3.34.1 verify the proper design of the Waterford III plant and were satisfied by performing the following:

- 1) Recording plant response to the transient using strip chart recorders and a high speed digital data acquisition computer (TDAS). The plant response was then compared to the pretest computer predictions generated by the Combustion Engineering System Excursion Code (CESEC) in order to verify the code for future transient analysis. Key RCS parameters were compared to Single Value Acceptance Criteria (SVAC) numbers generated by CESEC.
- 2) Operations, Phase III test personnel and Combustion Engineering performing a complete evaluation of the test results to verify that no design deficiencies or potential personnel safety hazards exist.
- 3) Recording control system response to the transient to verify satisfactory operation.

- 4) Measuring the Core Protection Calculator (CPC) generated reactor trip response time to determine the need for calculational uncertainty factors to be used in the Core Operating Limit Supervisory System (COLSS) program.
- 5) Demonstrating that natural circulation can be initiated.
- 6) Demonstrating that the natural circulation flow rate is adequate to maintain core cooling (power to flow ratio less than 1.0).

Additional natural circulation operations training and plant maneuvering was performed in conjunction with this test as detailed in section 6.5.2 of this report.

METHOD:

The loss of flow-natural circulation testing was performed on May 28, 1985 after operating of 80% Reactor Power for approximately 65 hours. Extended high power operation prior to the trip was required so that sufficient decay heat would be present to allow the extended natural circulation operation that was required for operations training and plant maneuvering. Prior to initiating the transient all data recording instrumentation was started to collect baseline plant parameters and control system outputs. Special test equipment was installed to measure the response time from initiation of the pump trip to generation of the CPC trip signal in order to collect data to determine the COLSS EPOL1 penalty factor. To allow power ascension to 80%, an additional uncertainty penalty had been installed based on uncertainty of the shape of the 4-RCP coastdown curve as measured during post-core hot

functional testing (see also section 3.2.1). If the measured CPC response time to the loss of flow transient was within the 1611 msec acceptance criteria then this uncertainty penalty factor could be removed, or at least decreased.

The loss of forced flow was initiated by simultaneously tripping all four reactor coolant pumps using a key operated test switch wired to the DC control power for all four pump breakers. Once the transient was initiated the plant was allowed to respond with no operator action for 60 seconds. Plant response during this 60 second period was used to verify the CESEC code. Appropriate plant operating and emergency procedures were then used to stabilize the plant in hot standby conditions and establish natural circulation.

At hot standby, natural circulation conditions, RCS decay heat and flow rate were measured to determine the power to flow ratio. Decay heat was measured by isolating feedwater to both steam generators and allowing levels to decrease approximately 12%. Using the volume of water removed and the latent heat of vaporization, the core decay heat power was calculated. RCS flow was calculated using this core power and the difference between hot and cold leg temperatures. The power to flow ratio is a comparison of natural circulation power and flow to power and flow at rated thermal power and is an indication of core cooling. To have adequate core cooling the following condition must be satisfied;

$$\frac{\text{Power}}{\text{Flow}}_{nc} < \frac{\text{Power}}{\text{Flow}}_{rtp}$$

where: nc - refers to conditions under natural circulation

rtp - refers to conditions at rated thermal power
and full RCS flow.

The more commonly used power to flow ratio is expressed as follows:

$$\frac{\frac{\text{Power nc}}{\text{Power rtp}}}{\frac{\text{Flow nc}}{\text{Flow rtp}}} < 1.0$$

Satisfying this condition assures that the temperature rise across the core during natural circulation does not exceed the full power temperature rise. Following the steam down and measurement of core power, normal feedwater flow was restored and S/G levels were increased.

Operations training and plant maneuvering under natural circulation conditions continued as detailed in section 6.5.2 of this report. At the completion of this training all four reactor coolant pumps were started and normal mode 3 conditions established.

RESULTS:

The Initial Transient (CESEC Verification):

Figures 6.6.4.1 through 6.6.4.4 show the response of several key plant parameters for the first 60 seconds of the transient, and Figures 6.6.4.5 through 6.6.4.8 show the response for 10 minutes. At time zero the four reactor coolant pumps

were tripped which generated a reactor trip within 950 msec. Response of each CPC was as follows:

<u>Channel</u>	<u>Response Time</u>	<u>Type of Trip</u>
A	650 msec	Low DNBR
B	550 msec	Low DNBR
C	1550 msec	90% RCP Speed
D	950 msec	Low DNBR

Initial predictions were that all four channels would generate a low DNBR trip but further analysis by Combustion Engineering verified that with the installed addressable constants at the time of the transient Channel C would trip on 90% RCP speed just prior to the low DNBR trip. These response times were within the 1611 msec acceptance criterion, thus allowing the penalty factor previously installed into COLSS uncertainty factor EPOL1 to be removed.

Plant response during the initial 60 seconds of the transient was used to verify the CESEC code. During this time period in a transient, the plant undergoes significant changes, therefore the SVAC were used to determine acceptability of predictions. The SVAC were specified maximums or minimums for certain key plant parameters. Table 6.6.4.1 lists the SVAC and the actual plant values achieved during the transient. All the CESEC SVAC parameters behaved as predicted and met their appropriate acceptance criteria.

Following the reactor trip and the subsequent turbine trip, the rapid closure of the turbine control valves reduced the steam load causing the increase in steam generator pressures. The steam bypass control system (SBCS) valves quick opened to provide heat removal capability from the secondary plant and the resulting drop in S/G pressures. The

TABLE 6.6.4.1

CESEC SINGLE VALUE ACCEPTANCE CRITERIA PARAMETERS DURING THE FIRST 60 SECONDS FOLLOWING LOSS OF FLOW.

Parameter	Max (or Min) Value	Acceptance Criteria(SVAC)
Pressurizer Pressure	2247.07 psia	\leq 2330 psia
Pressurizer Level	15.23%	\geq 22.5%
RCS Hot Leg 1 Temp.	595.7°F	\leq 610°F
RCS Hot Leg 2 Temp.	599.6°F	\leq 610°F
Steam Generator 1 Pressure	965.0 psia	\leq 1020 psia
Steam Generator 2 Pressure	972.7 psia	\leq 1020 psia

rapid insertion of negative reactivity from the control rods dropping into the core caused the rapid reduction in reactor power and the resulting drop in hot leg temperatures. The dropping temperatures caused an RCS volume reduction and reduced pressurizer level and pressure. The outsurge of pressurizer water into hot leg #1 caused these temperatures to be slightly higher than hot leg #2.

The decreasing trend in temperature and pressure continued until the SBCS valves began to modulate closed. At about 90 seconds into the transient S/G pressures were stabilized, then gradually returned to no load values of 995 psia. During the S/G refilling, S/G #2 was overfed causing the main feedwater isolation valve to close. This excess cooling accounted for the drop in loop #2 cold leg temperatures at approximately 400 seconds into the transient.

Natural circulation was verified by stable RCS hot and cold leg temperatures with the ΔT slowly decreasing over time. This trend is clear over the long period of time during natural circulation training as shown in Figure 6.6.4.9.

Power To Flow Ratio:

Following the establishment of stable natural circulation, decay heat power was calculated by isolating feedwater to the S/Gs and allowing levels to steam down approximately 12%. This process took about 30 minutes. Care was taken during the steam-down time period to isolate or quantify any means of RCS heat addition or removal. RCS and pressurizer steam space sampling were secured and pressurizer heaters were operated in manual while logging the time in service.

Results of the steam-down, which took place from 32 minutes to 61 minutes after the reactor trip, calculated a core power of 26.21 MWth or .77% of rated thermal power. The RCS flow rate calculated using the enthalpy rise from cold to hot leg temperature was 2.4% of normal RCS flow. Combining the two gives a power to flow ratio of 0.32, thus satisfying the acceptance criterion of < 1.0 .

CONCLUSIONS:

In the unlikely event of a total loss of forced reactor coolant system flow in the Waterford III power plant, the system will operate within design limitations so as not to exceed any limits of the safety analysis. Automatic control systems respond to trip the reactor and maintain plant parameters within normal operating limits thus precluding any Engineered Safety Features Actuation. Stable natural circulation can be established to allow operators to bring the plant to cold shutdown in a controlled manner while maintaining adequate core cooling.

FIGURE 6.6.4.1

W3 LOSS OF FLOW TEST

STEAM GENERATOR AVERAGE PRESSURE
TDAS CHANNEL 10 = SG1 = †
TDAS CHANNEL 11 = SG1 = *
TDAS CHANNEL 12 = SG2 = X
TDAS CHANNEL 13 = SG2 = Y

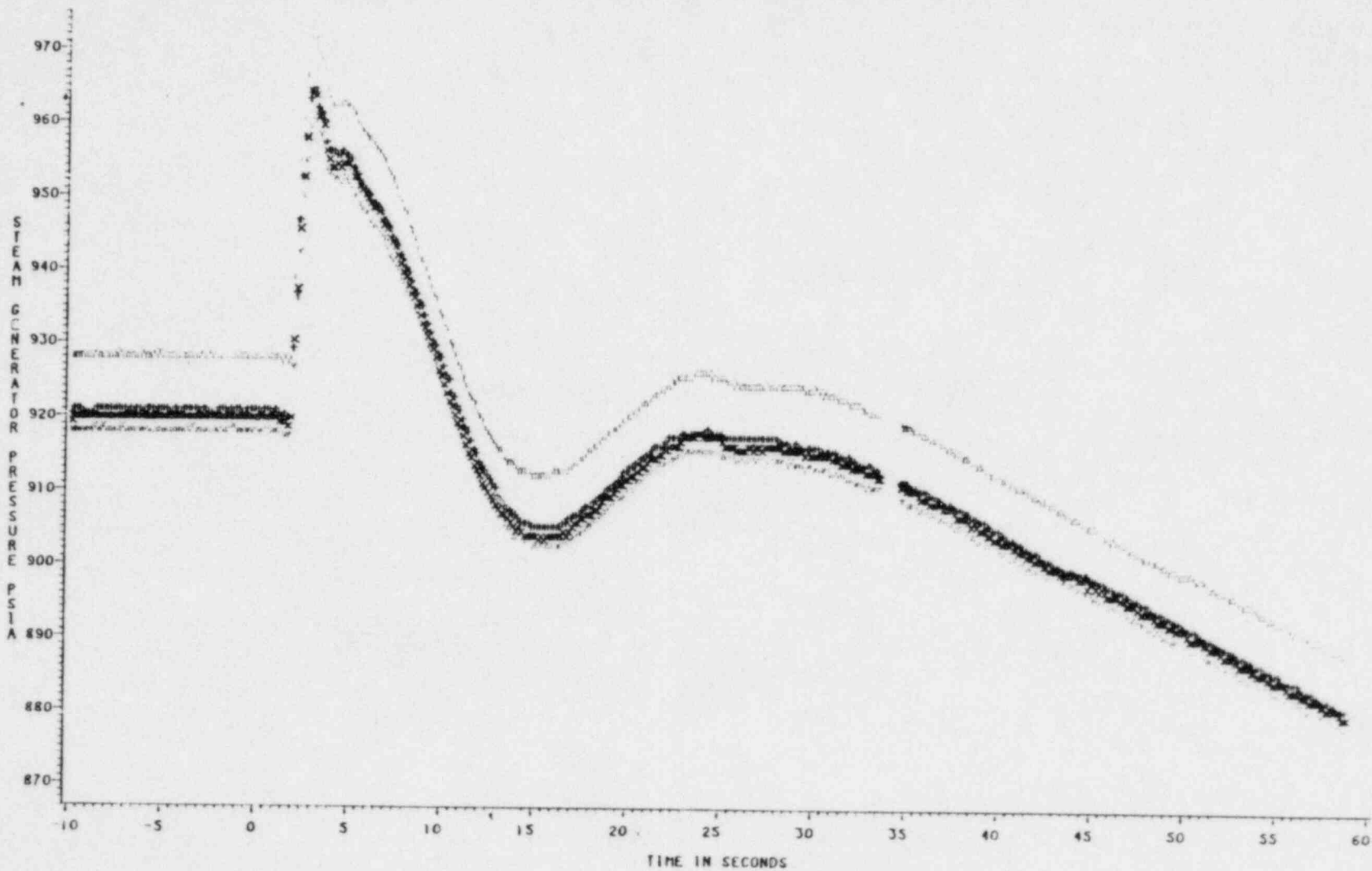


FIGURE 6.6.4.2
W3 LOSS OF FLOW TEST
RCS TEMPERATURES

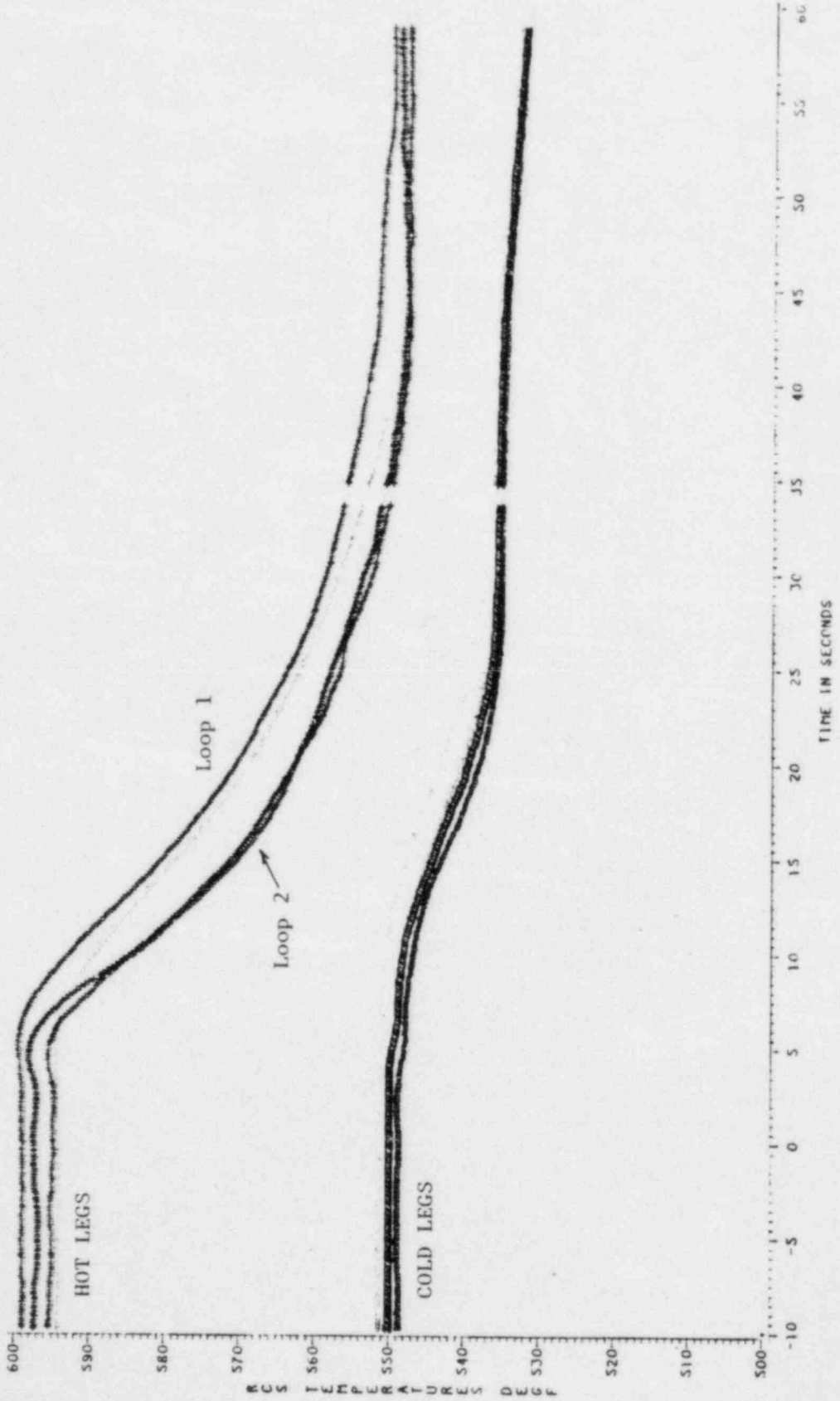


FIGURE 6.6.4.3

W3 LOSS OF FLOW TEST
PRESSURIZER PRESSURE

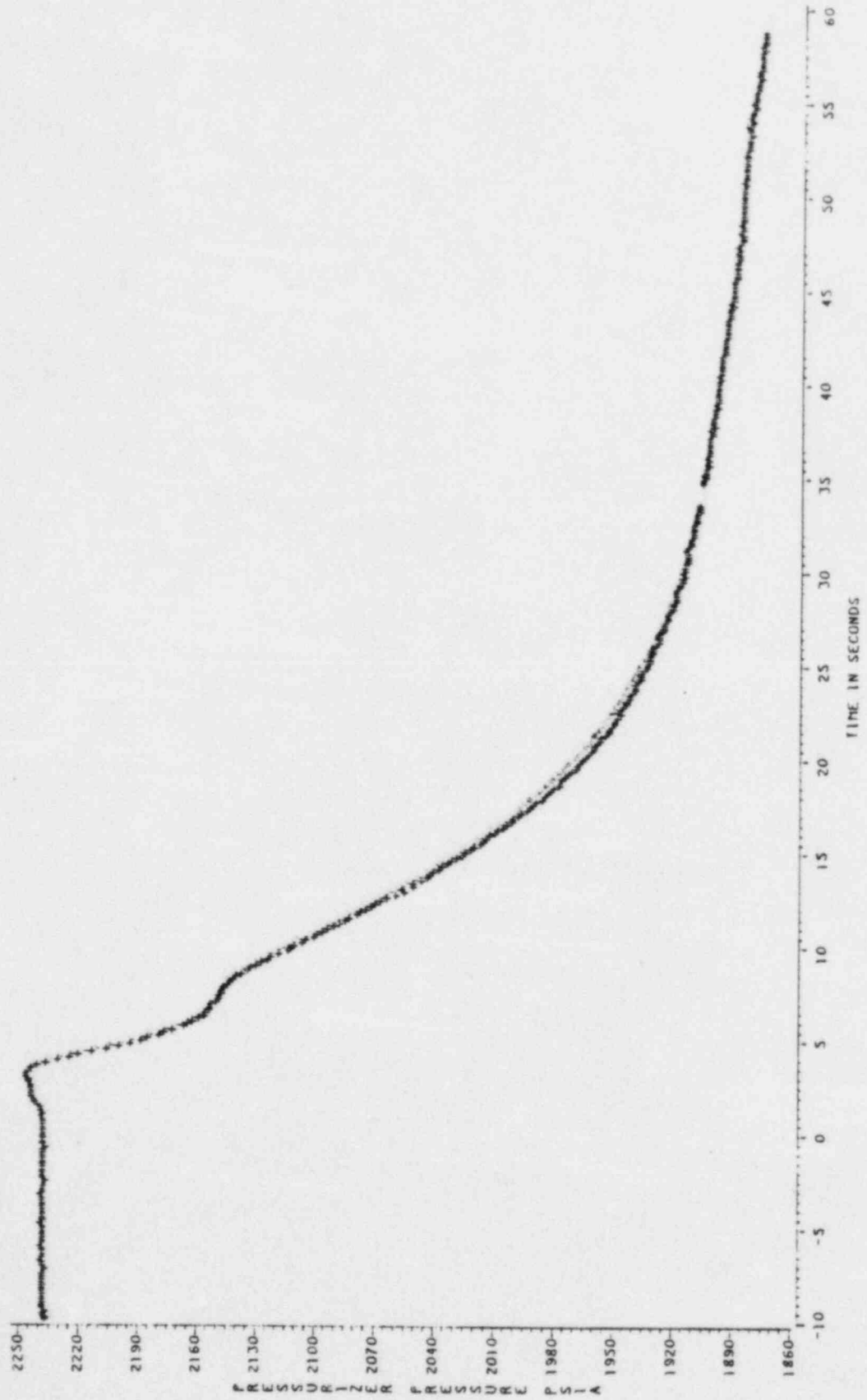


FIGURE 6.6.4.4
W3 LOSS OF FLOW TEST
PRESSURIZER LEVEL

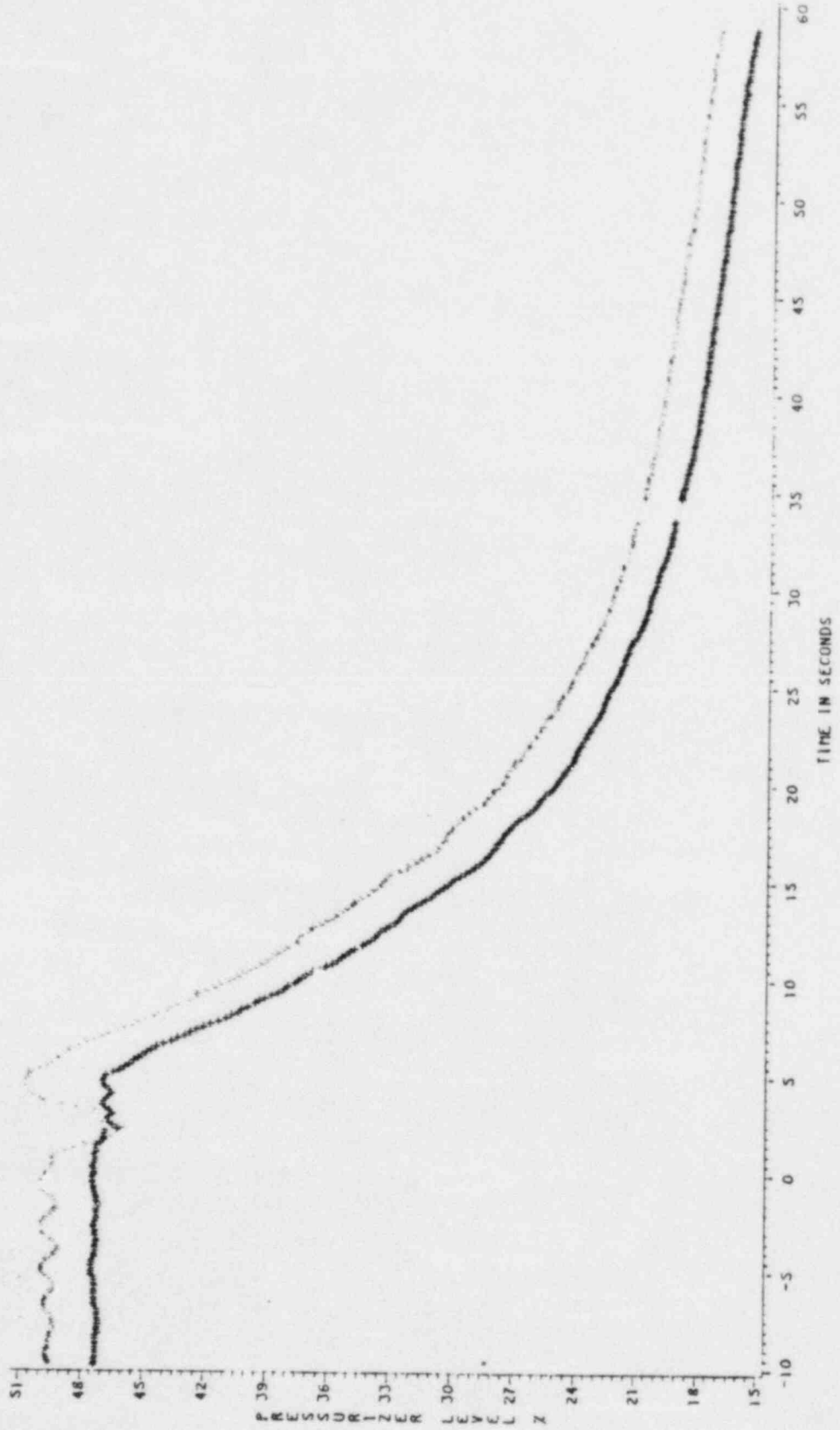


FIGURE 6.6.4.5

W3 LOSS OF FLOW TEST

STEAM GENERATOR AVERAGE PRESSURE
TDAS CHANNEL 10 = SG1 = +
TDAS CHANNEL 11 = SG1 = *
TDAS CHANNEL 12 = SG2 = X
TDAS CHANNEL 13 = SG2 = Y

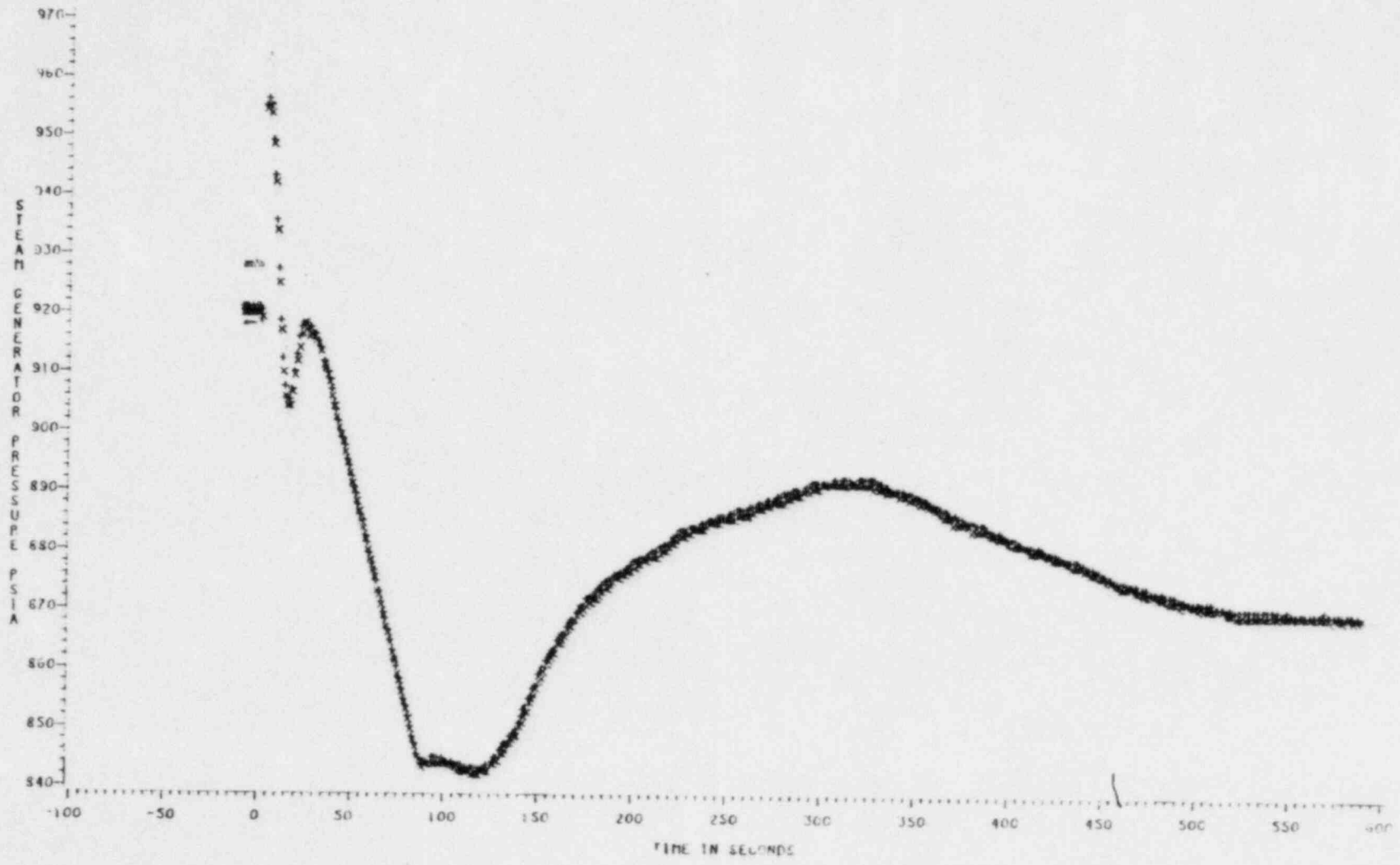


FIGURE 6.6.4.6
W3 LOSS OF FLOW TEST
RCS TEMPERATURES

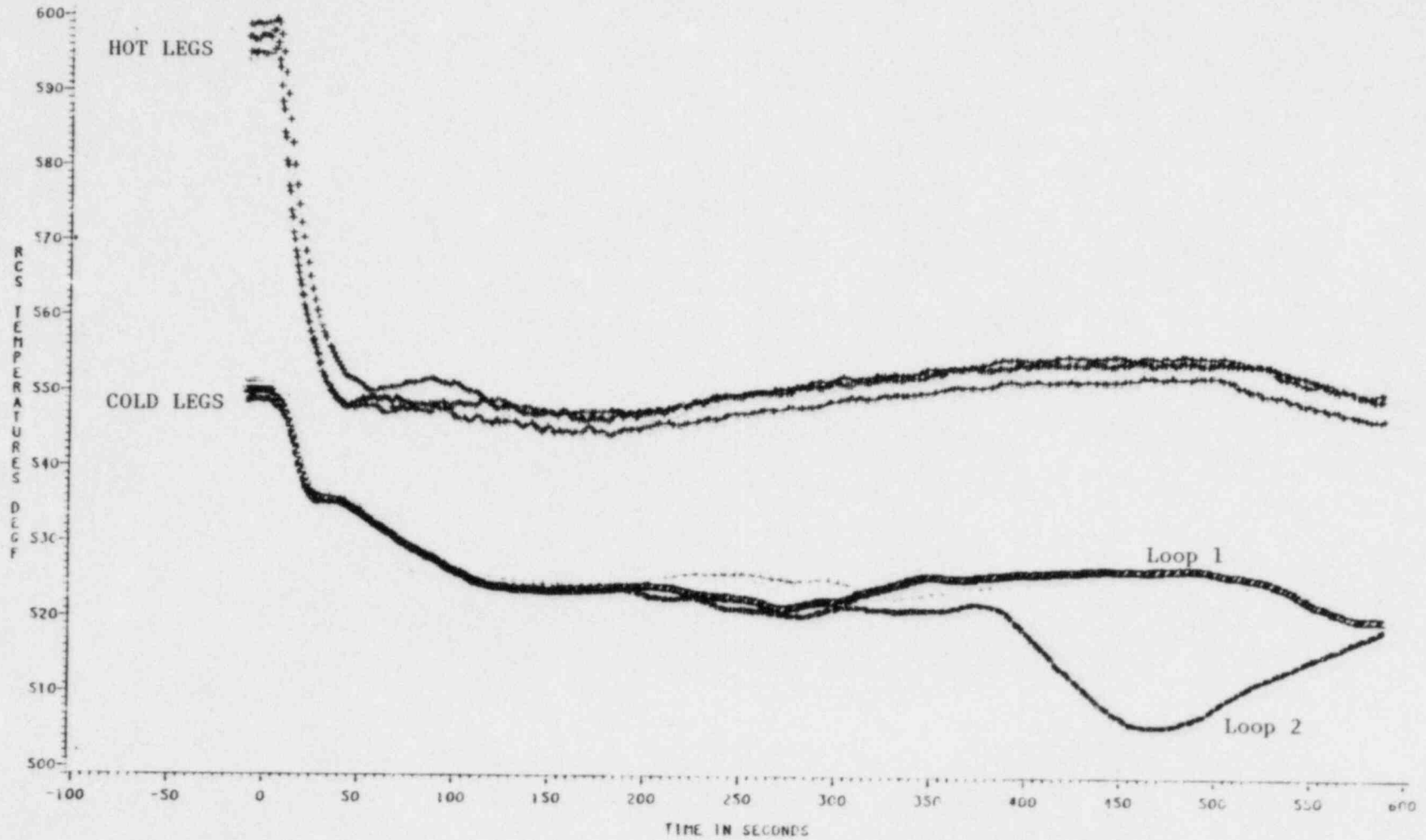


FIGURE 6.6.4.7

W3 LOSS OF FLOW TEST
PRESSURIZER PRESSURE

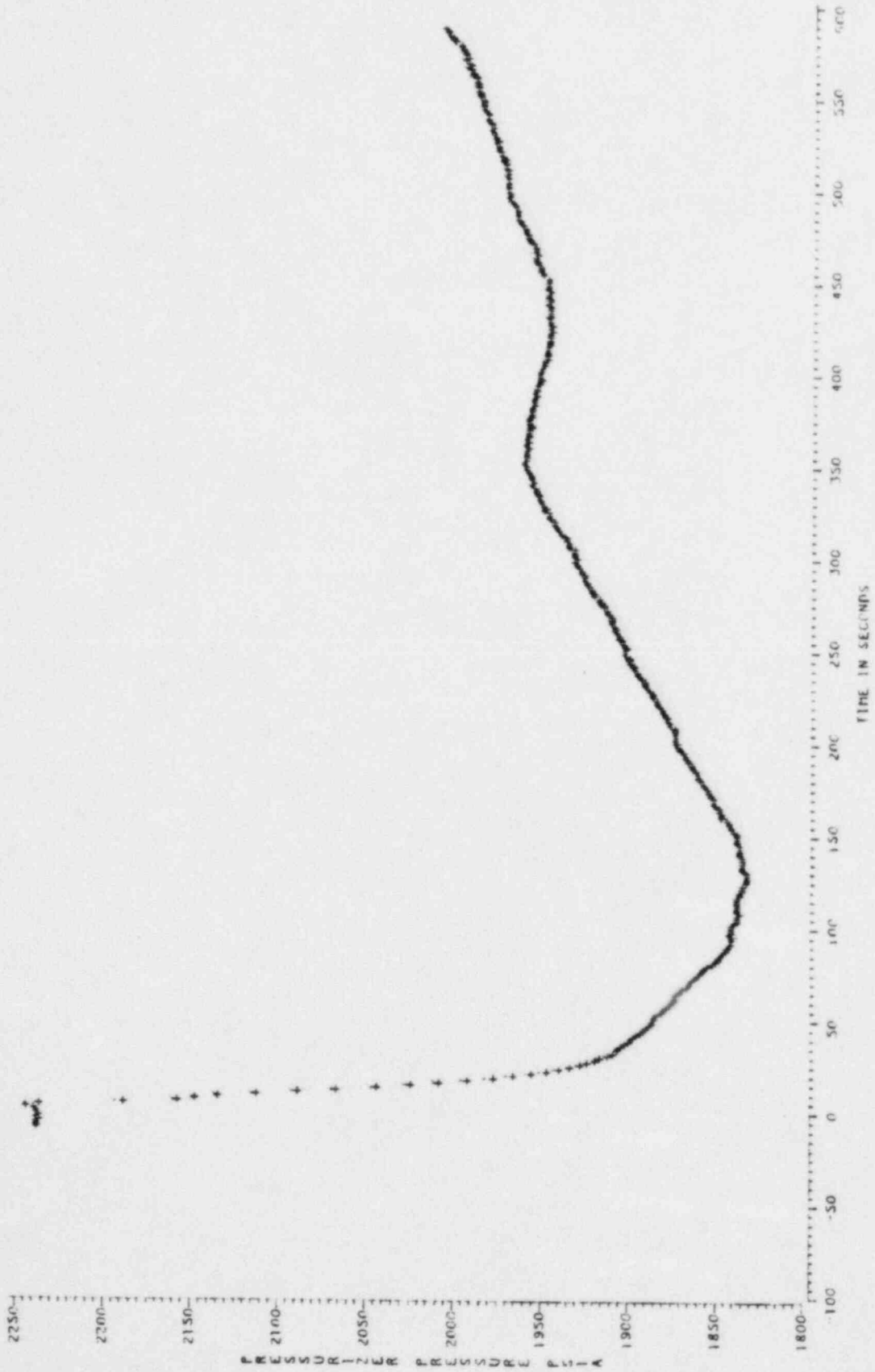


FIGURE 6.6.4.8
W3 LOSS OF FLOW TEST
PRESSURIZER LEVEL

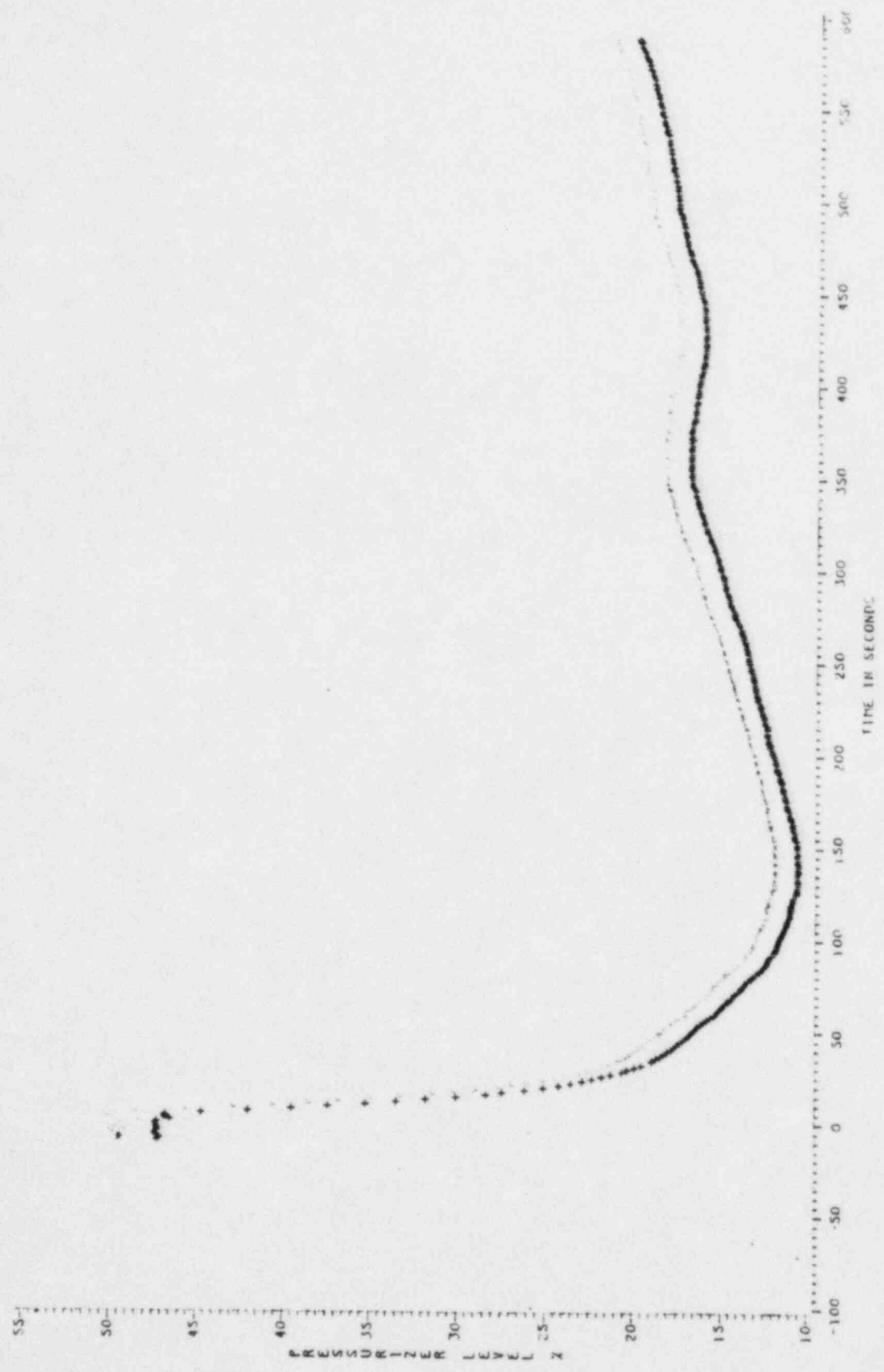
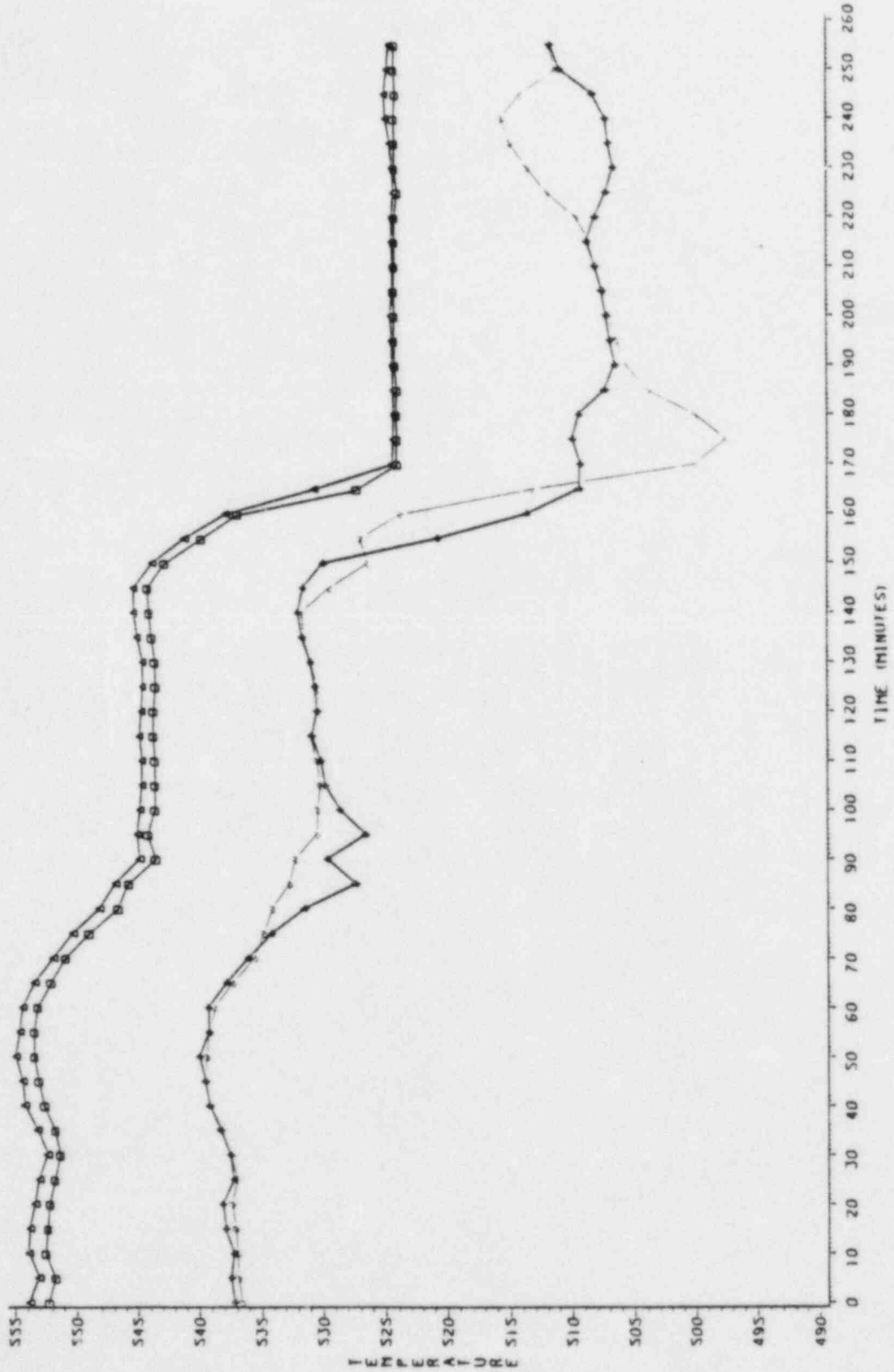


FIGURE 6.6.4.9
NATURAL CIRCULATION DEMONSTRATION
 REACTOR COOLANT HOT AND COLD LEG TEMPERATURES

■ ICOLD 1A
 ○ ICOLD 2B
 △ THOT 1
 □ THOT 2



6.6.5 100% Turbine Trip (SIT-TP-740)

PURPOSE:

This test is performed to demonstrate that the plant design is adequate to respond to a 100% power turbine trip and that plant systems respond in accordance with design. The data collected on plant response is used to verify the computer code predictions of CESEC, which is used for modeling plant transients. This test fulfills the requirements of Section 14.2.12.3.37 of the FSAR.

Additionally, the dynamic response of the main steam piping during the turbine trip was monitored in order to demonstrate the acceptability of the main steam piping design.

METHOD:

The reactor was stable with NSSS control systems (SBCS, RRS, Pressurizer Level and Pressure Control) in automatic. Data collection was accomplished by using plant computer collect logs, strip chart recorders and the test data acquisition system (TDAS). The turbine was manually tripped and no operator actions were to take place for the first 60 seconds. After 60 seconds, the operators took control of the plant using plant emergency operating procedures (EOP's).

To verify the acceptance criteria, the actual values of plant parameters were compared to the single value acceptance criteria (SVAC) which were determined from predictions utilizing the CESEC transient code.

The test procedure was originally written to perform the turbine trip at 100% power, however, provisions were made to collect the data during unplanned trips. The latter method was used.

Vibration analysis was to be accomplished by using accelerometers to measure the response of the main steam piping during the transient. Data would be acquired, stored and analyzed using a microcomputer based data acquisition system.

RESULTS:

During the ascension to 100% power (approximately 88% power), a fire occurred in the insulation of one main feedwater pump. This feed pump was immediately tripped. Since it was apparent that the plant would eventually trip on low steam generator level, data collection was initiated on the strip chart recorders and the TDAS and the turbine was manually tripped. Collected data was forwarded to Combustion Engineering to determine acceptability. Due to the fact that power was at 84% at the time of the trip (vice 100% as originally planned), the trip scenario used in the CESEC predictions had to be revised to reflect actual initial conditions and new single value acceptance criteria (SVAC's) were determined. New SVAC's and test results for the test are presented in Table 6.6.5.1. The limiting test value was the maximum or minimum value observed for the plant parameters during the first 60 seconds following the trip.

Data was not collected on SBCS valve position since this recorder was in the turbine building and could not be started before the turbine was tripped. However, valve demand was obtained on one of the control room recorders. Based on the

TABLE 6.6.5.1

TURBINE TRIP SINGLE VALUE ACCEPTANCE CRITERIA

<u>Parameter</u>	<u>Original SVAC Value</u>	<u>Updated SVAC Value</u>	<u>Limiting Test Value</u>
Pressurizer Pressure (psia)	≤ 2316	≤ 2318	2271 (max.)
Pressurizer Water Level (% indicated level)	≥ 14.4	≥ 18.4	21.6 (min.)
RCS Hot Leg 1 & 2 Temperature	≤ 613	≤ 604	602 (max.)
Steam Generator 1 Pressure (psia)	≤ 1044	≤ 1088	1036 (max.)
Steam Generator 2 Pressure (psia)	≤ 1044	≤ 1086	1035 (max.)

performance of the SBCS in other tests, it was concluded that valve demand was an acceptable method of inferring valve position. Valve demand data indicates that three valves quick-opened and the remaining three valves modulated open at a relatively slow speed. Figures 6.6.5.1 through 6.6.5.4 illustrate plant performance for reactor coolant system hot leg temperatures, pressurizer pressure, pressurizer level and steam generator pressures respectively. Time zero represents the time of the turbine trip. Several other data points are provided before the trip to depict plant conditions prior to the trip.

The vibration data was not acquired during the transient. An alternate method of demonstrating design acceptability was pursued. This consisted of post-trip piping inspections and detailed computer modeling of the dynamics of the appropriate piping sections. Preliminary results of the analyses indicate that the piping stresses are acceptable.

CONCLUSIONS:

The revised CESEC single value acceptance criteria were satisfied using the data from the unplanned trip. Good agreement was achieved between the CESEC best estimate analysis and the plant data, indicating that the plant responded as designed. Preliminary results of the main steam line vibration analyses indicate that main steam piping stresses are acceptable.

FIGURE 6.6.5.1

W3 TURBINE TRIP TEST - HOT LEG TEMPERATURES

TDAS CHANNEL 37 - -
TDAS CHANNEL 38 - -
TDAS CHANNEL 39 - X
TDAS CHANNEL 40 - Y

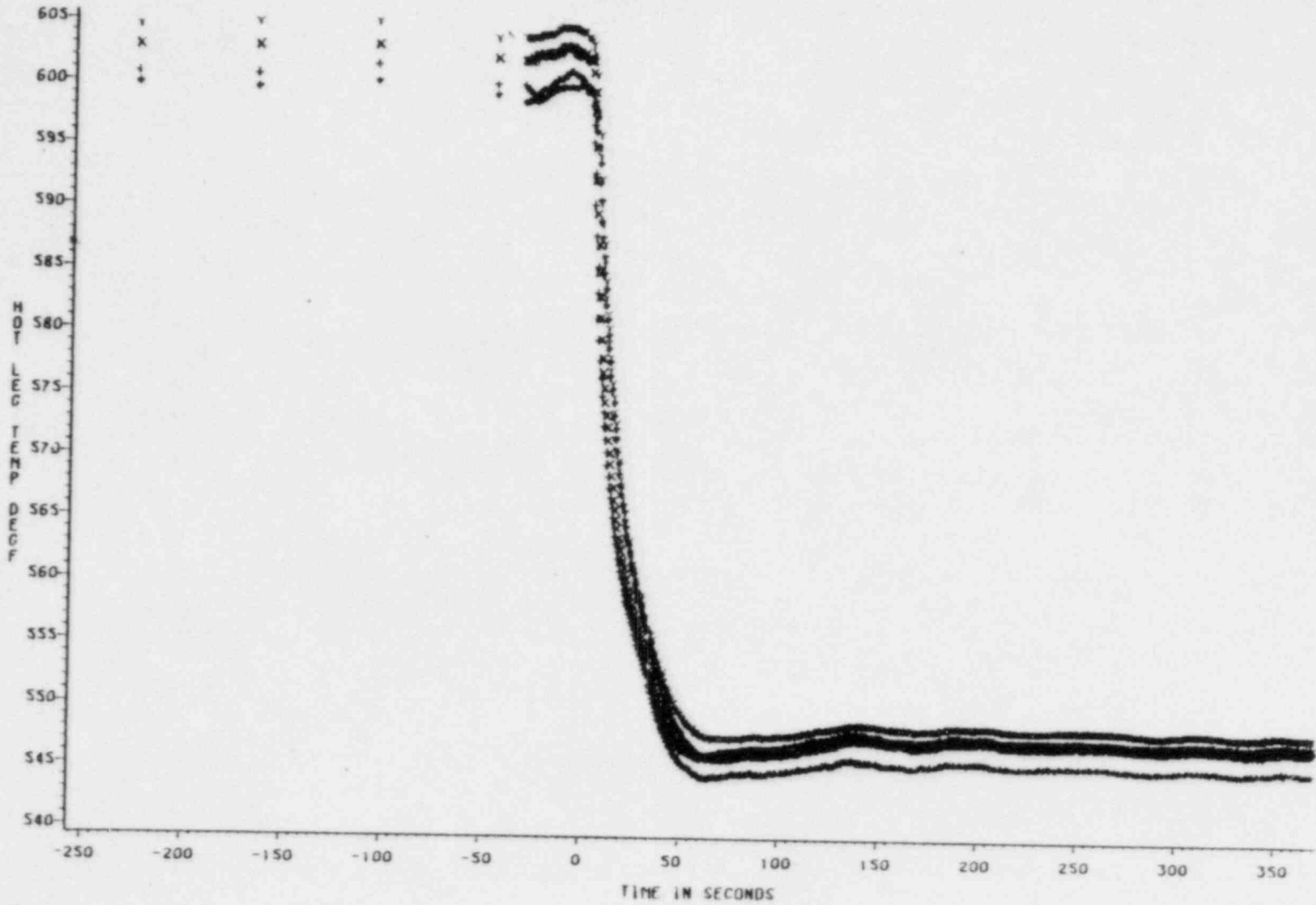


FIGURE 6.6.5.2
W3 TURBINE TRIP TEST - PRESSURIZER PRESSURES
IDAS CHANNEL 43 - -
IDAS CHANNEL 44 - -

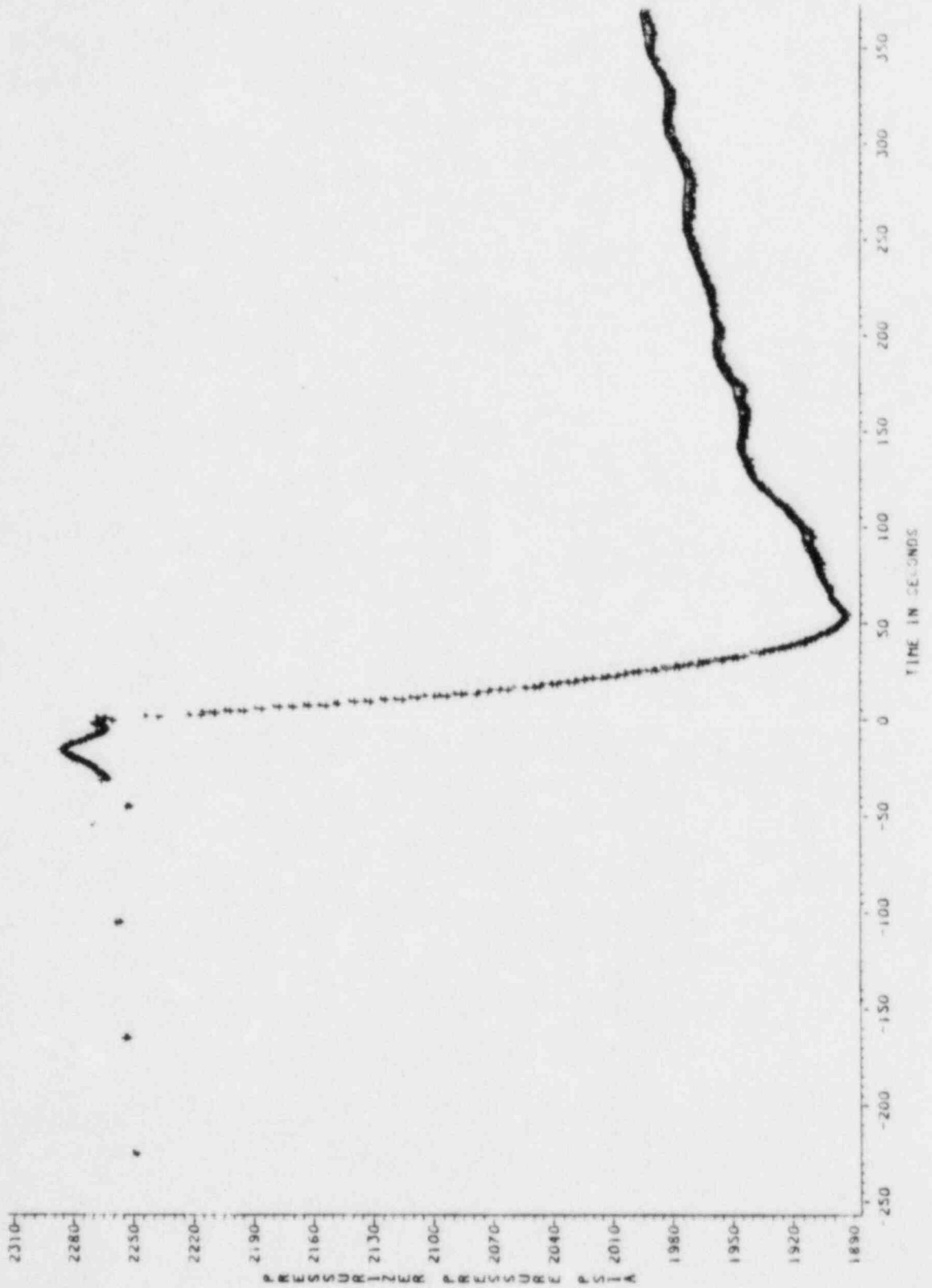


FIGURE 6.6.5.3

W3 TURBINE TRIP TEST - PRESSURIZER LEVELS

TDAS CHANNEL 45 - -
TDAS CHANNEL 46 - -

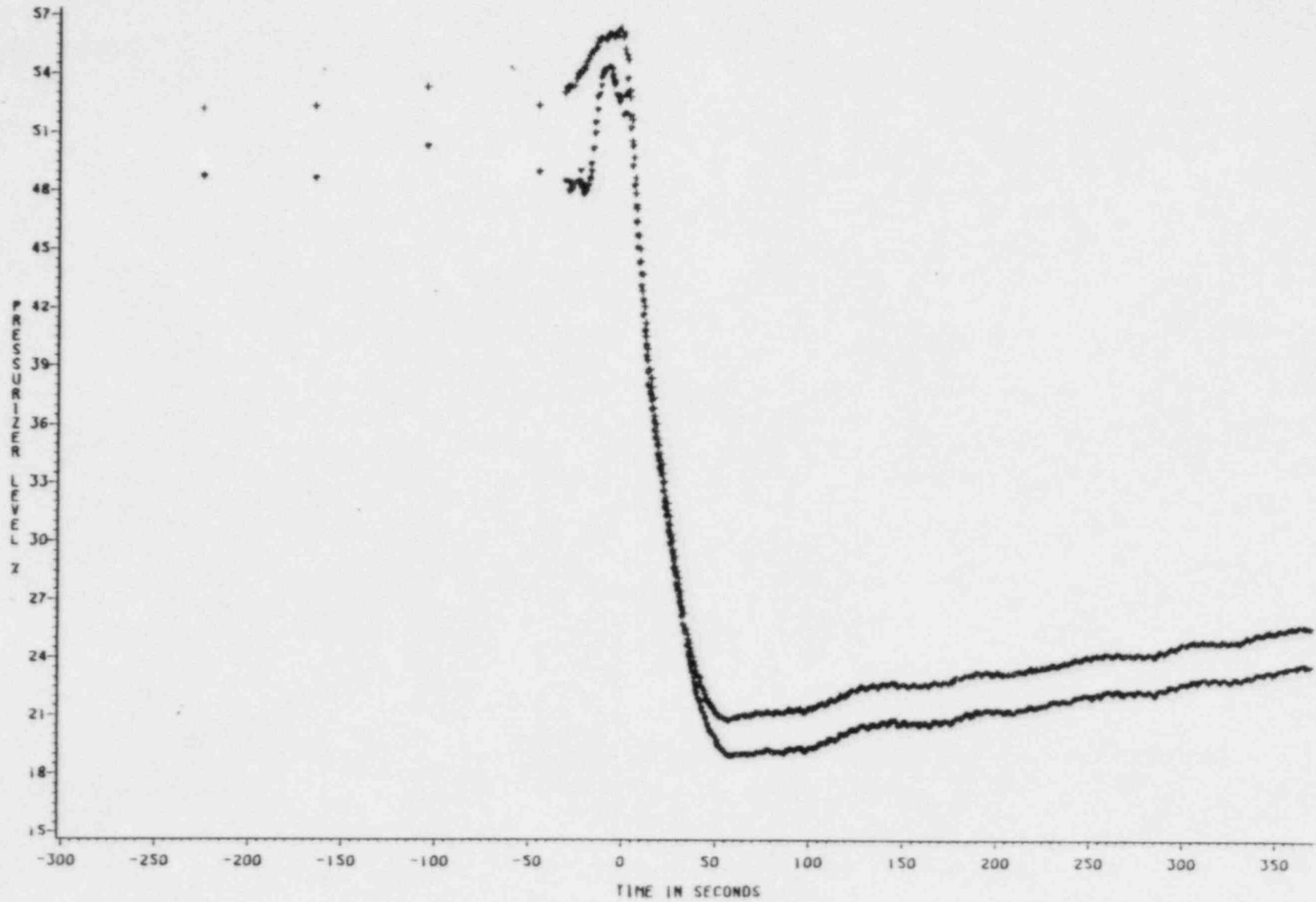
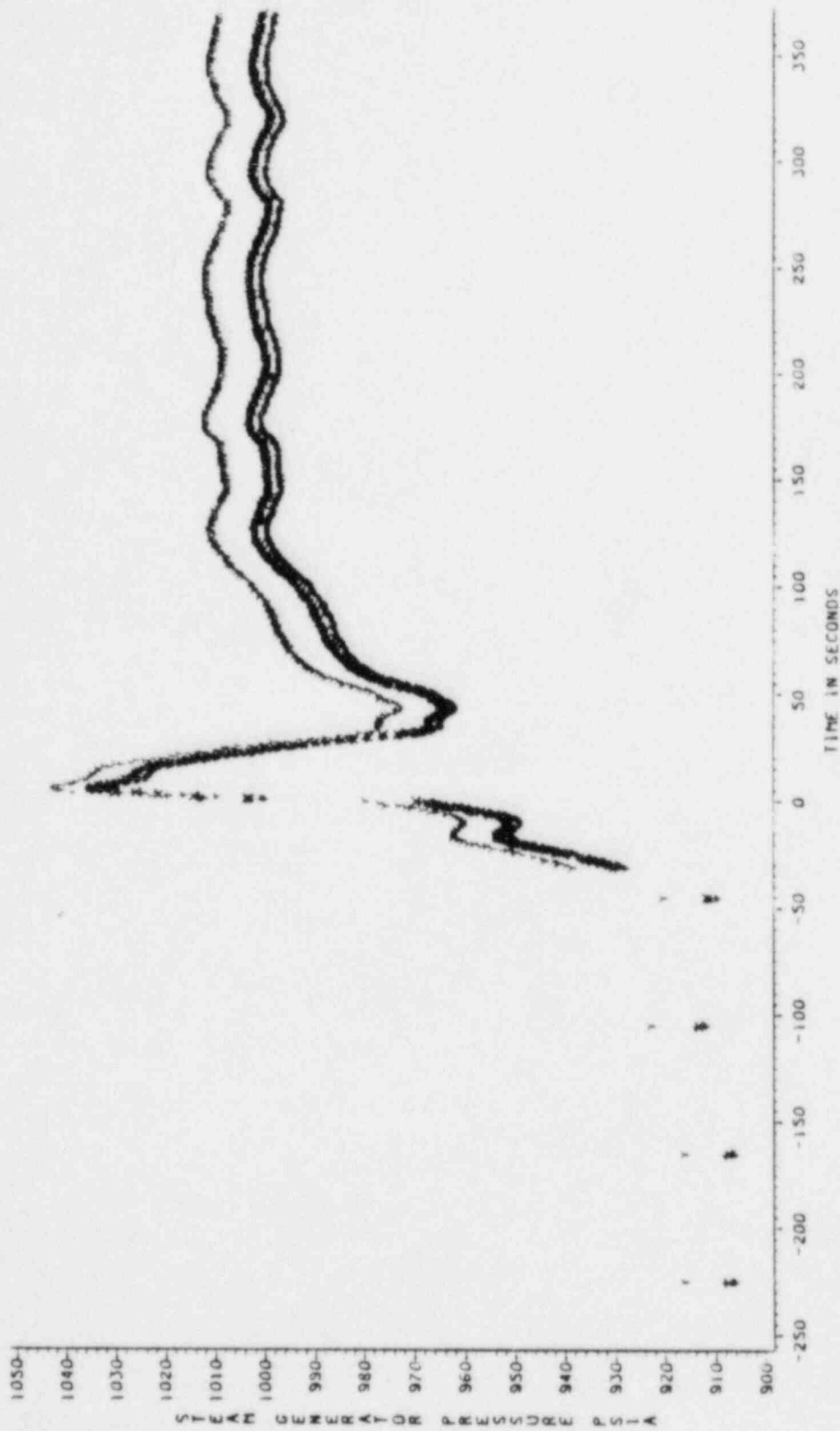


FIGURE 6.6.5.4
W3 TURBINE TRIP TEST - STEAM GENERATOR PRESSURES
TDAS CHANNEL 10 - SG1 - -
TDAS CHANNEL 11 - SG1 - -
TDAS CHANNEL 12 - SG2 - X
TDAS CHANNEL 13 - SG2 - Y



6.7 PLANT TESTING

6.7.1 NSSS Plant Data Record (SIT-TP-701)

PURPOSE:

The purpose of this test was to provide a permanent baseline data record of plant parameter indications from zero power to full power operation, during steady state operation.

METHOD:

Data collection commenced with the plant at hot zero power (i.e., the reactor at approximately 545°F, 2250 psia and $10^{-3}\%$ power) at approximately 8 hours intervals and consisted of the following:

- Reactor power and operating limits data per computer snapshot
- RCS (pressure, temperature, boron, etc.) data per computer snapshot
- RCS differential pressure data per computer snapshot
- Core exit thermocouple and heated junction thermocouple data per computer snapshot
- Secondary plant data per computer snapshot
- Incore instrumentation data per computer CECOR snapshot
- CEA data per computer CEAC Report
- CPC data per CPC Report and from the operators module
- COLSS data per COLSS Power and Operating Limits Report
- Turbine-generator data
- Plant chemistry data

Data collection was terminated upon completion of power ascension testing (see also section 3.3.1).

RESULTS:

The required data was gathered at the specified intervals.

CONCLUSION:

A substantial data base of significant plant parameters was established for plant conditions corresponding to reactor power ranging from about $10^{-3}\%$ (Mode 2) to 100% (Mode 1). This data complemented that collected during post-core hot functional testing (see section 3.3.1) to provide a full spectrum of plant baseline data from cold shutdown to full power operation conditions. The data was placed in the plant historical file for future reference. All test objectives and acceptance criteria were satisfactorily met.

6.7.2 Transient Data Record (SIT-TP-702)

PURPOSE:

The transient data record provided a means for establishing a plant baseline data record during the slow initial power increases of the Waterford 3 plant. The data provides an overview of primary and secondary plant loads and operating conditions and how they change during power increases.

METHOD:

Power ascension began on March 16, 1985 and was completed upon reaching 100% power on July 1, 1985. One hour prior to each planned power increase to a power level not yet previously achieved, data collection was initiated. Data for the following categories of plant parameters was collected.

- Plant Power
- RCS Temperature
- Reactor Power Distribution
- Operating Margin
- CEA Positions
- Turbine Load
- SBCS Steam Loads
- Steam Generator Energies

Data collection was secured one hour after stabilizing at each new power level.

RESULTS:

Data collection was performed during each power increase. A portion of the plant computer data was lost due to computer malfunctions. The data that was collected provides a good plant baseline record for future reference.

CONCLUSIONS:

Representative baseline data was collected during all initial power increases from zero to 100% full power. The data is representative of the plant performance during power increases, and plant operation is not adversely affected by the loss of some of the computer data.

6.7.3 Biological Shield Effectiveness Survey (SIT-TP-715)

PURPOSE:

The purpose of this test was to obtain baseline radiation levels in order to trend radiation level buildup with operation; to measure and document radiation levels in locations outside of the biological shield while at power; to establish the adequacy of the biological shield and to identify high-radiation zones.

METHOD:

Portable neutron and gamma survey equipment was used in performing all phases of the biological shield survey.

RESULTS:

Overall, the radiation levels in the RCB were lower than design basis estimates in the FSAR by factors ranging from 2 to 12. Maximum neutron dose rates (extrapolated to 100% power) of 10 rem/hr were observed at the south side of the refueling cavity, with a gamma dose rate of 1.25 rem/hr. Neutron dose rates ranged from 100 to 2100 mrem/hr on +46', with corresponding gamma doses of 14 to 300 mrem/hr. On +35', dose rates ranged from 20-300 mrem/hr neutron and 2-5 mrem/hr gamma. Neutron doses of 5-540 mrem/hr were found on +21', with gamma doses of 2-90 mrem/hr. On -4', general area dose rates ranged from 8-100 mrem/hr for neutrons and 4-100 mrem/hr for gammas. Dose rates at the four blowout areas adjacent to the secondary shield wall at each RCP bay were significantly higher than the rest of -4'. Neutron doses of 350-450 mrem/hr and gamma doses of 180-200 mrem/hr were found at these locations at 100% power.

System deficiencies that were identified during testing and are in the process of being corrected are as follows:

1. Radiation levels in the +21' electrical equipment room were greater than the Zone I criteria as specified in the FSAR, Zone map 12.3-4b. This problem is being corrected by a station modification that will provide additional shielding to reduce the radiation levels to those acceptable by the FSAR.
2. Radiation levels in the -4' RAB hallway are greater than the Zone II criteria as specified in the FSAR, Zone map 12.3-1b. The radiation levels in the area are due to the sample lines for the CVCS radiation monitor in the hallway. This problem was recognized prior to initial criticality and a station modification to relocate the radiation monitor was generated to correct the problem.
3. Radiation levels in the RCB on the -4' near the four RCP "blowout areas" exceed the Zone IV criteria as specified in FSAR Figure 12.3-5. For several reasons, it is felt that no station modifications are warranted; therefore, this deficiency will be corrected by means of a revision to FSAR Figure 12.3-5.
4. Radiation levels near the personnel hatch in the -4' RCB are greater than the design basis estimate in FSAR Figure 12.3-5. This deficiency is considered to be minor and is being corrected by means of a revision to FSAR Figure 12.3-5.

5. Radiation levels in the -4 wing area were found to be in excess of those specified in the FSAR, Zone Map 12.3-5. The dose rate in the area is due to shine coming from an overhead pipe chase that contains the letdown line. This deficiency is considered to be minor and is being corrected by means of a revision to FSAR Figure 12.3-5.

CONCLUSION:

The shielding survey successfully achieved its objectives. Of the five outstanding deficiencies, three will be eliminated upon completion of a revision to FSAR Figure 12.3-5 and two will be eliminated upon retest following completion of station modifications, thereby satisfying all the acceptance criteria of this test.

6.7.4 Power Ascension Testing Ventilation Capability (SIT-TP-743)

PURPOSE:

To verify that various heating, ventilation and air conditioning (HVAC) systems for the containment, annulus, areas housing engineered safety features (ESF) and areas housing ESF support systems were able to maintain design temperatures while the plant was operated at or near specified power levels (50% and 100%), and during a plant cooldown and a loss of offsite power condition.

METHOD:

The required environmental data was taken in part via plant monitoring computer (PMC) snapshots fed by permanent plant sensors. Additionally, local temperature and humidity recordings were taken where permanent plant instrumentation was not available.

Upon completion of data acquisition, in areas where multiple data points were available (e.g., the containment), the data was averaged to produce a representative temperature profile.

The resultant data was then compared against acceptance criteria values based upon FSAR Chapter 9.4, Table 9.4-1, in order to verify adequate HVAC performance.

Data was collected at the following test plateaus and/or plant conditions:

- 0% NOP/NOT

- during loss of offsite power (LOOP) testing following a reactor trip from 20% power
- 50% power
- 100% power
- during a plant cooldown

RESULTS:

The results of individual HVAC test plateaus are summarized in Table 6.7.4.1 below.

During the LOOP test, average containment air temperatures were calculated to exceed the 120°F acceptance criteria. The containment ambient air temperature sensors and/or their associated computer points were subsequently evaluated. Two computer points, one for the temperature above the quench tank, (at +46') and the second for the temperature adjacent to steam generator #1 (at +95.6') were found to be erroneously high. These high readings caused the average containment air temperature to exceed the required 120°F by 0.7°F. When these erroneous values were eliminated from the calculation of containment average air temperature, the average was 120.0°F. This temperature was acceptable, although it was equal to the maximum allowable limit.

During testing at 100% power, containment ambient air temperatures and reactor cavity temperatures were found to exceed their acceptance criteria of 120°F by 2.8°F and 1.8°F respectively. A project evaluation/information request (PEIR)

was generated to evaluate this deficiency. It should be noted, however, that at no time during this test program was the Station Technical Specification limit of 120°F containment fan cooler inlet temperature exceeded.

CONCLUSION:

The HVAC systems, as an integrated unit, performed as designed, with the exception of the containment fan coolers and the reactor cavity cooling system. These portions of the HVAC system did not meet the acceptance criteria at 100% power, as discussed above. The performance of these systems continues to be evaluated via PEIR 70494. Although not all acceptance criteria were met, the test was satisfactorily completed, and Station Technical Specification limits were shown not to be exceeded at full power operation.

TABLE 6.7.4.1

SUMMARY OF HVAC TEST RESULTS

MEASUREMENT LOCATIONS	PLANT CONDITIONS				
	0% Power	50% Power	LOOP Test	100% Power	
Containment Area Average Temperatures	116.0	119.3	120.0	122.8	
Reactor Cavity Ambient Average Temperatures	114.4	NA	NA	121.8	
Annulus Average Temperatures	91.8	105.4	105.6	107.0	
Switchgear Area Average Temperatures	69.0	76.5	70.7	76.1	
CEDMCS Area Average Temperatures	69.4	79.0	73.9	78.6	Remote Cooldown
ECCS Area (A, A/B) Average Temperatures	63.0	73.0	65.8	69.6	66.3
ECCS Area (B) Average Temperatures	60.5	67.7	64.4	69.2	67.2
Diesel Generator A Average Temperatures	69.5	86.2	80.3	90.7	
Diesel Generator B Average Temperatures	75.1	82.2	83.9	88.0	
Control Room Area Average Temperatures	75.0	73.6	71.2	71.4	

6.7.5 Atmospheric Steam Dump and Turbine Bypass Valve Capacity Checks
(SIT-TP-707)

PURPOSE:

The purpose of this test was to verify that the steam flow capacities of the two atmosphere dump valves (ADV) and of the six turbine bypass valve (TBVs) are in accordance with design requirements and safety analysis assumptions within the WSES-3 FSAR, as described below:

1. Verify that the maximum capacity of each TBV is less than that assumed in the analysis of the most severe excess heat removal accident, as described in FSAR section 15.1.1.3.
2. Verify that the maximum capacity of each ADV is less than that assumed in the analysis of the inadvertent opening of an ADV accident, as described in FSAR section 15.1.1.4.
3. Verify that the minimum capacity of each ADV is greater than that assumed in the post-LOCA long-term decay heat removal analysis, as described in FSAR section 6.3.3.4.
4. Verify that the total capacity of all six turbine bypass valves is greater than or equal to the design capacity specified in FSAR section 10.3.3.

This test satisfied the requirements of FSAR section 14.2.12.3.39.

METHOD:

Performance of this test began on 5/21/85, and continued intermittently through 5/25/85. The test was completed on 6/24/85, during the return to power following an extensive generator-related outage.

Reactor power was initially stabilized at 57%, with all six TBVs and both ADVs fully closed. An initial set of data was taken, consisting of the following parameters trended over a five minute interval:

- feedwater flow to each steam generator
- main steam flow to each feedwater pump turbine
- reheat steam flow to each feedwater pump turbine
- blowdown flow from each steam generator
- steam generator pressures
- reactor power
- TBV valve inlet pressure (local indication)

During preparations for the test, it was discovered that the flow transmitters providing reheat steam flow indication to the plant computer were temporarily inoperable. The reheat steam flow to the feedwater pump turbines was subsequently isolated; this guaranteed that changes in steam flow to the feedwater pump turbines would be accurately reflected by the change in main steam flow to the turbines.

To start the test, a dilution of the RCS was initiated. The resultant increase in RCS temperatures led to increasing steam generator pressures, which were closely monitored. Once steam generator pressures had increased by approximately 5 psia, MS-320A was stroked open a small amount. This had the effect of reducing steam generator pressures while increasing reactor power. As the dilution continued, nearly

constant steam generator pressures were maintained by periodically opening MS-320A a small amount. This process continued until MS-320A was fully opened; CEA motion was then used to stabilize primary plant conditions. Steam flow to the main turbine was maintained nearly constant throughout the opening of the valve. With MS-320A fully opened and plant conditions stabilized, the data set described above was taken again.

Once the data were recorded, testing of the next TBV was initiated. MS-319B was slowly opened as MS-320A was modulated closed, again in a controlled manner aimed at maintaining steam generator pressures constant. During the performance of this evolution, condensate pump 'B' had to be secured because of a failed weld in its recirculation line. The flow provided by only two condensate pumps was inadequate to maintain steam generator levels at the reactor power level of 70%, so power was reduced and both TBVs closed. Plant conditions were stabilized at 50% power with all TBVs and both ADVs fully closed.

MS-319B was then tested in the manner outlined for MS-320A. From an initial power level of 51%, a dilution was initiated and MS-319A modulated open slowly to maintain constant steam generator pressures. Data were recorded both with the valve fully closed and fully opened. The reactor was stabilized at 63% power in preparation for trading the opening of MS-320C with the closing of MS-319B. MS-320C failed, however, to open more than 10% when the trading with MS-319B was attempted. The decision was made to return power to approximately 50%, close MS-319B, and stabilize conditions in preparation for testing the remaining TBVs, while initiating corrective action on MS-320C.

Additional problems were then encountered with MS-319A, MS-320B, and MS-319C. These valves experienced difficulty in stroking open past approximately 10%. (The first 10% of travel on the turbine bypass valves opens a small pilot valve only; this is designed to equalize pressure on both sides of the valve plug). Troubleshooting of these problems continued through the evening of 5/21/85.

Plant conditions were stabilized at approximately 53% power early on 5/22/85. All prerequisites and initial conditions were reverified, and the initial set of data was taken. A dilution was initiated, and MS-319C was successfully modulated to 100% open. Data were taken with the valve fully opened, with the reactor at a new power level. MS-319C was then slowly modulated closed while MS-320B was stroked open, with steam generator pressures maintained nearly constant. MS-320B opened fully without any problems. A data set was taken in this configuration, with reactor power still constant at about 65%.

Attempts to stroke MS-319A were again unsuccessful. Corrective action on the valve was initiated while plant conditions were established to support testing of the two atmospheric dump valves.

The plant was stabilized at a new power level of 60%, with all TBV's and both ADV's fully closed. Prerequisites and initial conditions for ADV testing were verified. Initial data were taken once plant conditions were satisfactorily stabilized. A dilution was initiated and MS-116A was slowly modulated open. When MS-116A reached approximately 50% open, it became apparent that the condenser hotwell makeup system would be unable to keep up with the the subsequent loss of inventory if the ADV were opened much further. Concern over

a possible condensate pump trip (due to low hotwell level) led to the closing of MS-116A; an alternate means of testing the valve was required.

It was decided to reduce reactor power to about 55%, then open a TBV while increasing reactor power via dilution. Once the TBV has reached approximately 50% open, MS-116A would be opened and the TBV closed, with steam generator pressures held nearly constant throughout. Plant conditions would then be stabilized at a new power level with MS-116A opened fully. This technique offered the advantage of minimizing the amount of time spent with an ADV open. MS-116A was successfully tested in this manner; data were taken with the valve fully opened, and testing of MS-116B took place next. The two valves were traded against each other, MS-116B slowly opened while MS-116A was modulated closed. No problems were encountered during the performance of these steps.

Troubleshooting of MS-320C and MS-319A continued over the next two days. A turbine trip occurred on 5/23/85, and plant conditions necessary to support TBV testing were not reached until 5/25/85. MS-320C was successfully tested on 5/25/85; however, attempts to open MS-319A beyond approximately 85% open were unsuccessful. This valve was not successfully tested until 6/24/85 because of an extended generator-related outage following the loss-of-offsite-power trip test on 5/29/85.

Once data for a given valve became available, calculation of valve capacities was performed. A minimum, nominal, and maximum capacity for each ADV was determined, while only the nominal and maximum capacities were required for the turbine bypass valves. The primary component of a valve's capacity, whether minimum, nominal, or maximum, was the change in measured feedwater flow between the data set taken with the

valve fully opened and that taken with the valve fully closed. If steam flow to the main turbine is held approximately constant, as it was during the performance of this test, the additional feedwater flow can go only to three locations - to the condenser via the TBV (or atmosphere via the ADV), to the blowdown system via steam generator blowdown, or to the feedwater pump turbines via the main steam lines. Thus, the capacity of a TBV (or ADV, as appropriate) is nominally equal to the change in feedwater flow adjusted for the change in blowdown flow and steam flow to the feed pump turbines.

Since the minimum ADV capacity requirement and the maximum ADV and TBV capacity criteria were safety-related, uncertainties in the determination of these values had to be included in the calculations. As feedwater flow was dominant in the calculation of capacity, the uncertainty in its measurement comprised the major element of inaccuracy in the calculations. Also, since steam flow to the feedwater pump turbines always increased as the valve being tested was opened, credit was not taken for this effect in the maximum capacity calculations.

A final consideration regarding the calculation of valve capacity involved the effect of pressure on the calculations. The test was performed under plant conditions that were different from the conditions assumed in the FSAR accident analyses upon which the acceptance criteria were based. Therefore, correction of the capacities to the reference pressure conditions was necessary. Conservative assumptions regarding the nature of the pressure drop in the main steam line to the TBVs were made, and equations relating the capacity at the test conditions to the capacity if the reference conditions had been present were developed. It was subsequently determined that, because of an underestimate of

the pressure drop to an open TBV, these equations were unnecessarily conservative. Procedure changes were made, based upon an analysis of the main steam line pressure losses, which removed the excess conservatism.

In summary, a given valve's capacity is calculated as the change in feedwater flow with the valve opened versus closed, adjusted for the change in blowdown flow and the change in steam flow to the feed pump turbines under the same conditions. This nominal capacity is then adjusted for feedwater flow measurement uncertainty and corrected to the appropriate reference pressure as given in the FSAR, for comparison to the minimum (as applicable) and maximum capacity acceptance criteria.

RESULTS:

All procedure-specified acceptance criteria were satisfied. Minimum, nominal, and maximum capacities for all eight valves are given in Table 6.7.5.1.

Post-test calibration of the pressure gauges utilized to monitor TBV valve inlet pressure revealed that some gauges were inaccurate beyond specified tolerances. An analysis was subsequently performed to determine the impact of the erroneous pressure indications on the test results. This analysis also considered the effects of valves not opening to their full-stroke position. The results of the analysis indicated that no acceptance criteria were adversely impacted by these problems. A summary of the analysis has been included for documentation in the official procedure package for this test, and retained in the plant historical file.

TABLE 6.7.5.1: MEASURED ADV AND TBV CAPACITIES^(a)

Valve Number :	MS-116A	MS-116B	MS-319A	MS-319B	MS-319C	MS-320A	MS-320B	MS-320C
Valve Type :	-- Atmospheric Dumps --		----- Turbine Bypass Valves -----					
Minimum Capacity (b) :	704.07	736.79	(c)	(c)	(c)	(c)	(c)	(c)
Nominal Capacity (d,e) :	792.03	827.74	1553.11	1705.74	1607.39	1702.66	1618.04	1493.75
Maximum Capacity (f,g) :	871.93	904.57	1597.10	1758.56	1661.93	1751.06	1674.32	1533.38

***** NOTES *****

- (a) All values are given in units of klbm/hour.
- (b) The ADV minimum capacity values are corrected to a valve inlet pressure of 900 psia. The acceptance criterion specifies that each ADV's minimum capacity must be greater than or equal to 583.20 klbm/hour.
- (c) There is no minimum capacity acceptance criterion for individual turbine bypass valves; hence these values were not calculated.
- (d) The ADV nominal capacities are not pressure-corrected, and are provided for information only.
- (e) The TBV nominal capacities are corrected to a steam generator pressure of 978 psia. The total TBV combined capacity must exceed the design requirement of 9,496 klbm/hour to satisfy the acceptance criterion; the measured capacity was 9,680.69 klbm/hour.
- (f) The ADV maximum capacity values are corrected to a valve inlet pressure of 865 psia. The acceptance criterion specifies that each ADV's maximum capacity must be less than or equal to 934.00 klbm/hour.
- (g) The TBV maximum capacity values are corrected to a steam generator pressure of 949 psia. The acceptance criterion specifies that each TBV's maximum capacity must be less than or equal to 2,034.00 klbm/hour.

CONCLUSIONS:

The atmospheric dump valves and the turbine bypass valves met their respective minimum (where applicable), nominal, and maximum capacity acceptance criteria, confirming assumptions made within the relevant FSAR accident and design analyses. Problems encountered with modulation of the turbine bypass valves were resolved sufficiently to satisfactorily complete capacity testing. All test objectives were met.

6.7.6 Initial Turbine Startup (SIT-TP-708)

PURPOSE:

The purpose of this test was to verify proper operation of the turbine and generator by accelerating the turbine to operating speed, synchronizing the unit and loading the unit to 100% of rated load. In addition, various turbine protective devices were tested for proper operation. Finally, a baseline record of turbine operation was established. There was no specific FSAR chapter 14 commitment for performance of this test.

METHOD:

The turbine was placed on turning gear, latched and accelerated to 1800 rpm at which time the main generator was synchronized to the grid and loaded to 100% of rated load in an orderly fashion. Testing occurred at various speed/load combinations.

RESULTS:

1. Tests While on Turning Gear

While the unit was on turning gear, tests were performed on the bearing oil pump (BOP) and the emergency oil pump (EOP) to verify proper actuation. Local and remote tests showed that the BOP actuated at the proper lube oil pressure of 12 psig, however, the EOP did not. The EOP was reworked and successfully retested, actuating at an oil pressure of 15 psig. Additionally, the proper operation of the throttle, governor, interceptor and reheat

valve controllers was verified from the control room. All valves operated as expected. Finally, mechanical solenoid trip test were performed to verify turbine trips due to bearing low oil pressure, low vacuum or thrust bearing failure. The bearing low oil pressure trip test was acceptable at 6 psig. The low vacuum and thrust bearing test were not acceptable. These systems were reworked and successfully retested, with the low vacuum trip occurring at 20.5 inches of mercury and the thrust bearing trip occurring at 78 psig. While on turning gear, baseline data was acquired from computer collect logs and through field measurements and recordings.

2. 520 RPM Testing

The turbine was latched and accelerated to 520 RPM. A turbine trip was performed by moving the overspeed trip hand lever at the turbine pedestal. The unit tripped successfully. Following the trip test, the unit was relatched and returned to 520 RPM. Baseline data was collected as before.

3. 1800 RPM Testing

The unit was accelerated to 1800 RPM. A crip mechanism solenoid test was performed three times. (This test was performed while holding the test lever at the H.P. turbine pedestal in the "Test" position, which permitted trip testing without an actual trip.) The trip actuated at an unacceptably low pressure of 25 psig. The system was reworked and successfully retested, with trip actuation at 42 psig. Baseline data was also collected.

4. 10% Load Testing

The generator field breaker was closed and the unit synchronized to the grid on March 18, 1985. At that time the megawatt feedback loop was found to be operating incorrectly. As the loop had no affect upon load testing, as per discussions with the turbine vendor, loading was continued. (This problem was resolved on 3-22-85.) When the unit was synchronized, approximately 5% load was picked up. This load was maintained for approximately ten hours, following which the load increased to 10%. The 10% load was held for about four hours, during which baseline data was collected as before. Subsequently, load was reduced to 0% and an actual overspeed trip test was performed. The trip was unsuccessful and repeated, again with unacceptable results. The trip weights were adjusted and on the third attempt the trip was successfully accomplished, within the overspeed trip acceptance criterion range of 1998 RPM $\pm 1\%$.

5. 20% - 100% Load Testing

The turbine was loaded in 10% increments, in conjunction with the power ascension test program directions. At each load plateau, i.e., ~20, ~30, ~40, ~50, ~60, ~70, ~80, ~90 and ~100%, baseline data was collected as before. With the exception of the retesting noted above, no other testing was performed. All retests were successful.

CONCLUSION:

The turbine and generator operated as expected. The turbine protective devices performed as designed. A baseline data record of the initial turbine startup has been created, and all acceptance criteria were met.

6.7.7 Balance of Plant (BOP) Data Record (SIT-TP-748)

PURPOSE:

The purpose of this test was to collect data relative to secondary plant systems and components in order to establish an initial data base to be used for future performance comparisons and analyses.

METHOD:

Steady state conditions as specified in the Power Ascension Test Controlling Document, SIT-TP-700, were verified to exist at the given testing plateau. Additionally, reactor power was maintained constant $\pm 0.5\%$ and steam generator level was kept constant $\pm 5\%$. Special conditions which affected plant performance were noted in the chronological log for future reference during data analysis.

Data collection was accomplished by demanding snapshots of pre-established groups of data from the plant monitoring computer (PMC). In addition, feedwater heater drain flow data and MSR shell drain tank flow data was obtained utilizing a portable ultrasonic flow meter.

The groups of data collected were assembled from the following systems/components:

- Extraction Steam
- Main Steam

- Primary System (for the purpose of relating primary plant conditions to secondary side performance)
- Steam Generator Feedwater Pump Turbine
- Gland Sealing Steam
- Feedwater Heater Drains
- Main Condenser
- Main Turbine/Generator
- Steam Generators
- Condensate System
- Feedwater System

RESULTS:

Data collection was accomplished at the 15%, 20%, 40%, 50%, 60%, 70%, 80%, 90%, and 100% test plateaus. Feedwater heater drain and MSR shell drain tank drain data was collected where possible with the portable ultrasonic flowmeter.

CONCLUSION:

A substantial quantity of data relative to the secondary plant was collected at all test plateaus of interest ranging from 15% through 100% reactor power. This data was reviewed and subsequently placed into the plant historical file for future reference in plant performance analysis. All test objectives and acceptance criteria were satisfactorily met.

6.7.8 Level 2 Piping Vibration Testing (SPO-99P-004)

PURPOSE:

The purpose of this test was to verify by measurement and/or observation that vibration amplitudes were acceptable for piping systems or portions thereof whose configuration and/or support locations were changed after completion of vibration testing performed in accordance with procedure SPO-99P-001.

METHOD:

The system or portions thereof subject to retest under this procedure were identified by engineering. Systems to be tested were walked down to ascertain that the as built conditions of piping and supports conformed to those assumed in the analysis. The visual observation was made for the portion(s) of the piping systems with allowable vibration amplitude greater than 20 mils. The points with the allowable vibration amplitude less than 20 mils were marked on stress isometrics and actual vibration amplitudes were measured at those locations with hand held vibration meters.

RESULTS:

All vibration amplitudes observed and measured for the piping systems or portion(s) thereof subject to retest, were less than the maximum allowable vibration amplitude established by analysis and found to be acceptable.

CONCLUSION:

The vibration testing performed in accordance with procedures SPO-99P-004 and SPO-99P-001 satisfactorily demonstrated that vibration amplitude of piping systems during various modes of operation were within allowable limits.

6.7.9 Pipe Whip Restraint Monitoring (SIT-TP-900)

PURPOSE:

The purpose of this test was to verify by measurement and/or observation that all pipe whip restraints, both soft ('U' - bar type) and hard (rigid restraint), cleared all piping, piping insulation and piping components during cold and normal operating condition. The clearances between pipe and whip restraints have to be within specified tolerances, in order to perform their intended design function as described in FSAR Chapter 3. Section 3.6, "Protection Against Dynamic Effects Associated With the Postulated Rupture of Piping".

The test satisfied the commitments of FSAR section 14.2.12.3.17.

METHOD:

All soft whip restraints ('U' - bar type) were monitored for pipe clearances and end gaps. All rigid type whip restraints were monitored for interferences only (clearances on rigid type pipe whip restraints were measured during pre-core hot function testing).

Prior to beginning post-core hot functional testing all pipe whip restraints were walked down to verify their location and proper installation. All soft whip restraints clearances were measured at ambient temperature to establish base line data.

During post-core hot functional testing, all whip restraints were visually checked at intermediate plateaus for interferences. Interferences observed during testing were identified and corrective action implemented before proceeding. All soft whip restraint piping clearances and temperature were measured at maximum achieved temperature. Because of heat losses, actual operating temperatures were less than design operating temperatures. Results, however, were accepted based on interpolation between actual and maximum operating temperature values.

RESULTS:

All rigid type whip restraints cleared their associated piping and piping components and all soft whip restraints satisfied the design requirements for end gaps at design operating temperature. Deficiencies were noted and corrective action implemented.

CONCLUSION:

The monitoring of pipe whip restraints, performed in accordance with procedure SIT-TP-900, demonstrated that pipe whip restraints were installed such that they will perform their intended design function without interfering with piping components.

6.7.10 Inspection of Mechanical Snubbers and Spring Supports (STP-36)

PURPOSE:

The purpose of this test was to verify by measurements and/or observation that mechanical snubbers and spring supports were properly installed and responding correctly to design criteria during plant heat-up, cooldown and normal operating conditions as committed in FSAR Chapter 14, Section 14.2.12.3.17, "Piping Thermal Growth, Vibration and Shock", and Section 14.2.12.2.95, "Snubber Thermal Motion".

METHOD:

All snubber supports and spring supports were walked down before taking cold data. Preset pins from constant and variable spring supports were removed and cold load settings recorded by using a built in scale. All snubber supports were visually checked for location, orientation, installation and adequate swing clearance, and cold settings were measured using a built in scale. Prior to hot functional testing all deficiencies were identified to engineering and corrective action was implemented.

All snubber supports and spring supports with thermal movement of $\frac{1}{4}$ " or more were monitored during hot functional and power ascension testing. Systems which did not operate during testing were not monitored for hot settings. (e.g., high pressure safety injection system, containment spray system, etc.) Piping temperatures were measured using hand held digital pyrometers and thermocouple probes.

RESULTS:

Snubber supports and spring supports were accepted based on the following criteria.

- (1) Snubber supports had adequate swing clearance to allow snubber movement.
- (2) Snubber operated in the mid-range of its travel, not the first or last half-inch unless otherwise accepted by engineering.
- (3) Spring support actual cold load settings were within 10% of design cold load settings and actual hot settings were within 20% of design hot load settings.
- (4) When actual piping temperatures were less than maximum operating temperature, actual hot loads or hot settings were determined acceptable based on extrapolated values between actual and maximum operating temperatures.

All snubber supports were found to be acceptable based on the above criteria. All spring supports on safety related piping systems were acceptable. On heater drain and extraction steam systems some spring support hot load settings were out of tolerance due to excessive vibration on piping systems. The problems were identified to engineering and corrective action will be implemented per Station Modification #895. After completion of work, these spring support load settings will be adjusted.

CONCLUSION:

Inspection of mechanical snubbers and spring supports was performed in accordance with procedure STP-36, and demonstrated that all mechanical snubbers and spring supports respond correctly to design criteria.

SECTION 7.0

APPENDIX A

LIST OF ACRONYMS

APPENDIX A
Part 1 of 4

LIST OF ACRONYMS

AOO	anticipated operational occurrence
ARI	all rods inserted
ARO	all rods out
ASI	axial shape index
ASME	American Society of Mechanical Engineers
BAMT	boric acid makeup tanks
BOC	beginning of cycle
BOL	beginning of life
BOP	balance of plant
BPPCC	boundary point power correlation constant
CCWS	component cooling water system
CE	Combustion Engineering
CEA	control element assembly
CEAC	control element assembly calculator
CEDM	control element drive mechanism
CEDMCS	control element drive mechanism control system
CESEC	Combustion Engineering System Excursion Code
CET	core exit thermocouple
CIAS	containment isolation actuation signal
CIS	containment isolation system
CIWA	condition identification and work authorization
COLSS	core operating limits supervisory system
CPC	core protection calculator
CPS	counts per second
CSAS	containment spray actuation signal
CSB	core support barrel
CSP	condensate storage pool
CST	central standard time

APPENDIX A

(continued)

Part 2 of 4

LIST OF ACRONYMS

CVCS	chemical and volume control system
DEH	digital electro-hydraulic
DNB	departure from nucleate boiling
DNBR	departure from nucleate boiling ratio
DRC	digital reactivity computer
EARO	essentially all rods out
ECBC	estimated critical boron concentration
EFAS	emergency feedwater actuation signal
EFPD	effective full power days
EFWCS	emergency feedwater control system
EFWS	emergency feedwater system
EOC	end of cycle
ESF	engineered safety feature
ESFAS	engineered safety feature actuation system
FHB	fuel handling building
FLCEA	full length control element assembly
FSAR	final safety analysis report
FTC	fuel temperature coefficient
FWCS	feedwater control system
HPSI	high pressure safety injection
HVAC	heating, ventilation, air-conditioning
HZP	hot zero power
ICI	in-core instrumentation
ILRT	integrated leak rate test
ITC	isothermal temperature coefficient
LCO	limiting condition for operation
LOOP	loss-of-offsite-power
LPD	local power density
LPSI	low pressure safety injection
LTOP	low temperature overpressure protection
M&TE	measuring and test equipment

APPENDIX A
(continued)
Part 3 of 4

LIST OF ACRONYMS

MG	manual group
MI	manual individual
MICDS	moveable in-core detector system
MS	manual sequential
MSIS	main steam isolation signal
MSIV	main steam isolation valve
MTC	moderator temperature coefficient
MWE	megawatt electric
MWTh	megawatt thermal
NRC	nuclear regulatory commission
NSSS	nuclear steam supply system
OL	operating license
OOS	out of sequence
PAT	power ascension testing
PCHFT	post-core hot functional testing
PDIL	power dependent insertion limit
PEIR	project evaluation/information request
PLCEA	part length control element assembly
PMC	plant monitoring computer
PMU	primary make-up
PORC	plant operations review committee
PORV	power operated relief valve
PPDIL	pre-power dependent insertion limit
PPS	plant protection system
PWR	pressurized water reactor
PZR	pressurizer
QSPDS	qualified safety parameter display system
RAB	reactor auxiliary building
RCP	reactor coolant pump
RCS	reactor coolant system
RM	refueling machine

APPENDIX A
(continued)
Part 4 of 4

LIST OF ACRONYMS

RMS	root mean square
RPCS	reactor power cutback system
RPF	radial peaking factor
RRS	reactor regulating system
RSPT	reed switch position transmitter
RTD	resistance temperature detector
RV	reactor vessel
RWSP	refueling water storage pool
SAM	shape annealing matrix
SBCS	steam bypass control system
SER	safety evaluation report
SFHM	spent fuel handling machine
SFP	spent fuel pool
SG	steam generator
SIAS	safety injection actuation system
SIS	safety injection system
SIT	safety injection tank
SONGS	San Onofre Nuclear Generating Station
TLOF	total loss of flow
UGS	upper guide structure
VCT	volume control tank
VLPMS	vibration and loose parts monitoring system
WSES	Waterford Steam Electric Station